THE PERFORMANCE OF DENSITY FUNCTIONALS WITH RESPECT TO THE CORRELATION CONSISTENT BASIS SETS

Xuelin Wang, B.S., M.S

Dissertation Prepared for the Degree of

DOCTOR OF PHILOSOPHY

UNIVERSITY OF NORTH TEXAS

August 2005

APPROVED:

Angela K. Wilson, Major Professor
Martin Schwartz, Committee Member
Thomas R. Cundari, Committee Member
Teresa D. Golden, Committee Member
Ruthanne D. Thomas, Chair of the Department of Chemistry
Sandra L. Terrell, Dean of the Robert B.Toulouse School of Graduates Studies

Wang, Xuelin, The performance of density functional theory with the correlation consistent basis sets. Doctor of Philosophy (Chemistry), August 2005, 216 pp., 49 tables, 12 illustrations, 165 references.

Density functional theory has been used in combination with the correlation consistent and polarization consistent basis sets to investigate the structures and energetics for a series of first-row closed shell and several second-row molecules of potential importance in atmospheric chemistry. The impact of basis set choice upon molecular description has been examined, and irregular convergence of molecular properties with respect to increasing basis set size for several functionals and molecules has been observed. The possible reasons and solutions for this unexpected behavior including the effect of contraction and uncontraction, of the basis set diffuse *sp* basis functions, basis set superposition error (BSSE) and core-valence sets also have been examined.

ACKNOWLEDGEMENTS

I would like to thank my advisor Dr. Angela K. Wilson for allowing me to join and grow in her research group. It is her effort that directs me to walk into the kingdom of computational chemistry. Without her, this dissertation would not have been possible. I thank her for her patience and encouragement that help me go through difficult times, for her valuable insight and suggestions that contribute greatly to my dissertation, and for her generously supporting me to take part in numerous academic meetings. To the members of my committee: I thank Professor Martin Schwartz, Professor Thomas Cundari, Professor Teresa Golden, and Professor Kirk A. Peterson for their patience, valuable feedback to my research, and their kind recommendations.

I also want to thank the guys in our research group- Scott, Brian, Ben, and Pankaj *et al*., who have helped me go through the English for my dissertation. Thank you for the wonderful time we have spent together.

TABLE OF CONTENTS

LIST OF TABLES

LIST OF ILLUSTRATIONS

CHAPTER 1

INTRODUCTION

Density functional theory (DFT) has become a widely used tool for describing the electronic structure of a wide range of systems. In DFT, the ground state energy of a system of interacting electrons can be expressed as a function of the electron density. The complexity of DFT is to find an "exact" link (functional) between the electron density and the kinetic and potential energies. Early DFT approaches such as the Thomas-Fermi model involved numerous theoretical difficulties, and the predicted molecular properties obtained using this early approach were not satisfying.[1, 2] Thus, DFT was not at all widely used in the chemistry community until many years later and until methodologies evolved further. Key to widespread use was the introduction of the Kohn-Sham approach to DFT.[3] Kohn and Sham used a non-interacting reference system, where no interactions between electrons were considered, to represent an interacting system (a full molecule), and also introduced the use of orbitals into density functional theory. These developments helped to enable an improved description of the kinetic energy and the potential energy arising from nucleus-electron and electron-electron interactions. However, further improvement in the kinetic energy is needed, and this remaining not-yet-described energy can be merged with residual corrections arising from the use of a non-interacting system into another energy term, -*exchange-correlation* energy-, which has to be treated approximately, and typically is treated in two different terms – an exchange term and a

correlation term. Much effort has been focused upon developing an approach to describe this exchange-correlation energy. In fact, DFT has experienced several generations of developments to accomplish this goal.

One of the simplest Kohn-Sham approaches is called the local density approximation (LDA) and is based on the uniform electron gas. The exchange-correlation energy density of a uniform electron gas is used to approximately represent that of a real inhomogeneous system. The exchange-correlation energy per particle of a uniform electron gas can be calculated accurately from quantum Monte Carlo calculations. In the early stages of DFT use, this simple approximation was remarkablely successful in many applications. Even presently, the LDA is still active in the simulation of solid state systems. One of the most popular LDA methods is SVWN, which uses Slater exchange (S)[4] and Vosko, Wilk, and Nusair 1980 correlation functionals (VWN).[5] However, the LDA methods have some cumbersome deficiencies, where the LDA is not adequate to describe systems such as those which are highly inhomogeneous (the uniform gas approximation works well for systems in which the electron density changes slowly throughout the system).

Since the LDA is often not adequate to provide reasonable accuracy for many systems, attempts to go beyond the LDA are necessary. One natural extension of the LDA is the improvement of the description of the exchange-correlation functional by including the gradient of the electron density. The functionals coined in this approach are the so-called general gradient approximation (GGA) methods, which are constructed to retain the correct features of LDA, while making further improvements. GGA methods consider the correction arising from electron gradient for both exchange and correlation functionals. However, due to the dominant exchange effect in the exchange-correlation functional, only the correction to exchange functional is

addressed here. The common procedure to form GGA exchange functionals is to multiply the LDA functional by F_x, a function of the density gradient. Varied GGA exchange functionals have different F_x, which were originally obtained numerically in order for the exchange functional to obey physicalcriteria. For example, Becke's B88 (B) exchange[6] uses Equation(1-1) as F_x,

$$F_x(s) = 1 + \frac{\beta s^2}{1 + \gamma s^2} \qquad \text{Equation (1-1)}$$

where s is proportional to $\nabla\rho(r)/\rho(r)$ where $\rho(r)$ is the electron density at distance r.The parameters β and γ are constants, which were fit to the exchange energies of a large number of atoms. This form satisfies the observation that when the density gradient becomes large, gradient corrections are insignificant. Many modifications to exchange functionals have been proposed, and further details about these developments can be found in the literature. For example, the current study utilized three pure GGA methods including BLYP,[6] [7] BPW91[8]and BP86.[9]

At present, one of the most widely used DFT functional is B3LYP.[10] It is a typical hybrid functional. The so-called hybrid means a mixing of Hartree-Fock exchange energy and pure DFT exchange energy (including local and gradient correction) weighted by several empirical parameters, which were obtained based on empirical calibration procedures. B3LYP has achieved great success for many chemical problems such as in the prediction of geometries, thermodynamics properties, and the understanding of chemical reactions. Although new functionals and mechanisms continue to be developed, B3LYP is still used widely due to its well-established performance. Examples of hybrid functionals include B3PW91, B3P86, and BHandHLYP. In this study, B3LYP, B3PW91, and B3P86are investigated.

To date, DFT [3, 11] has become one of the most prominent tools in describing the electronic structure of molecules due to its low cost and consideration of electron correlation. With its N^3 scaling (N is the number of basis functions), DFT has a similar computational cost as compared with the Hartree-Fock (HF) approach. However, DFT accounts for more of the electron correlation than does HF. Although DFT has many advantages, a range of problems still exist such as self-interaction error [12] (the error resulting from an inability for the coulomb and exchange interactions of an electron with itself to cancel out), poor predictions of dispersion forces, [13, 14] and lack of correct asymptotic decay of potential. A variety of density functionals have been proposed, and the development of new functionals continues to be an active area of research. With the availability of a variety of functionals, a question arises: How can the "best" functional be chosen for a given scientific problem?

A hierarchy of the performance arising from the use of density functionals has not been established due to the lack of a systematic way of improving the wavefunctions, especially the exchange-correlation potential. As a result, correct electronic structure of molecules cannot be achieved in a stepwise, well-defined manner. To better understand the successes and failures of DFT, a general and effective means to evaluate the performance of different functionals is needed. One possible means is the use of the correlation consistent basis sets,[15] cc-pV*x*Z (*x*=D(2), T(3), Q(4) and 5), which have been used extensively with *ab initio* methods. The correlation consistent basis sets are based on a detailed analysis of correlation energy in an atom. The main advantage of the correlation consistent basis sets is that they are built to systematically recover the correlation energy. The results obtained from a series of calculations with the correlation consistent basis sets can be extrapolated to the complete basis set (CBS) limit, where the remaining error arises from the method used to approximate the electronic Schrödinger

equation. Using this approach, the performance of various theoretical approaches can be assessed.

A number of studies have proven the usefulness of the correlation consistent basis sets with high accuracy *ab initio* methods.[16-20] However, it is not clear whether the correlation consistent basis sets can be applied to assess the performance of density functionals since they are optimized using the configuration interaction plus single and double excitation (CISD) method. In this study, our goal is to evaluate and compare the performance of various functionals with the correlation consistent basis sets by carrying out a series of benchmark calculations. We explore the possibility of using the correlation consistent basis sets as an effective means to assess the reliability of density functionals.

In this study, benchmark calculations were carried out for a set of 17 closed shell first-row molecules by using several density functionals with the correlation consistent basis sets. The accuracy and precision of the various density functionals were analyzed, along with the convergence of atomization energy with respect to increasing basis set size. The performance of the systematically developed polarization consistent basis set -designed especially for DFT – were also investigated. Following these benchmark studies, other factors including basis set uncontraction, basis set superposition error, diffuse basis functions, and core-valence functions, which may affect the convergence of molecular properties with respect to correlation consistent basis sets, were also examined.

Additonal work has included the use of DFT methods in combination with the newly developed tight *d*-augmented correlation consistent basis sets to study several second-row molecules including SO_2, CCl, ClO_2, HSO, and HOS. The tight *d*-augmented sets include a tight *d* function at each basis set level (as well as modifications to the standard set of *d* functions), and

were developed to reduce the deficiencies noted in the standard basis sets for second-row atoms, especially for sulfur. In previous studies, it has shown that the effect of tight *d* functions is quite substantial, particularly at the double- and triple-zeta levels for the sulfur species. The molecules mentioned above have a strong basis set dependence. The calculations with small basis sets (cc-pVDZ and cc-pVTZ) result in large errors in atomization energy for SO_2, CCl, ClO_2 and an incorrect prediction of the relative stability of HSO and HOS isomers. In this study, the effect of the tight *d*-augmented sets on the structures, frequencies, and energies of these molecules is discussed in detail. In addition to these properties, the effect of tight *d* on the enthalpies of formation of HSO and the reaction barrier of HSO/HOS isomerization reaction are also investigated.

CHAPTER 2

THE PERFORMANCE OF DENSITY FUNCTIONALS WITH RESPECT TO BASIS SET: CORRELATION CONSISTENT BASIS SETS

2.1 Introduction

The early success of density functional theory is based on the local density approximation (LDA), where the exchange-correlation energy generally consists of the Slater exchange energy[4] and the Vosko-Wilk-Nusair correlation energy.[5] However, LDA exhibits deficiencies in the calculation of thermochemical properties. The deficiencies are improved significantly by generalized gradient approximation (GGA) methods like BLYP[6, 7] and BPW91[21], where the gradient of electron density is included in the exchange-correlation functional. Later, even better performance was obtained for so-called hybrid density functionals that include the exact Hartree-Fock exchange energy. A typical example, B3LYP,[10] is constructed by a linear combination of local density approximation, Becke's gradient correction, and the Hartree-Fock exchange energy. The linear coefficients were determined by a fitting of the heats of formation of 55 molecules. Since the advent of B3LYP, hybrid density functionals have been extensively used in describing thermochemical properties, structures, and harmonic frequencies of a large range of molecules, and yields superior results to prior LDA and GGA methods. Recently, another type of approximation to exchange-correlation functional was

proposed. This approximation, called the meta-GGA,[22] requires the second derivative of electron density and kinetic energy densities as additional variables in the exchange-correlation functional. Although meta-GGA owns many of the known properties of the exact exchange and correlation energy, it is not clear whether new functionals can surpass B3LYP in popularity due to too few benchmark studies of functional performance.

Such a wide choice of functionals brings DFT users to a question: which functional is the best for a scientific problem of interest? As addressed in Chapter 1, a possible key to answer this question is to extend the basis set to the complete basis sets limit (or Kohn-Sham limit in the case of DFT), where no further improvement to the basis set is possible, and the remaining error is due to the method alone. At this point, the success and failure of density functionals may be assessed. However, systematic studies of the dependence of density functionals upon increasing basis set size are limited.[23-28] Several previous studies on basis set convergence for density functional theory are discussed below.

Martin evaluated basis set convergence in density functional theory by comparing a series of *ab initio* and DFT benchmark studies.[29] Basis set convergence in DFT calculations is similar to that at the HF level, and is faster than in *ab initio* correlation calculations like MP2 and CCSD(T). Strong basis set dependence at the SCF level is also observed in DFT calculations like for the description of hydrogen bonds. For most properties, results near convergence to the basis set limit can generally be achieved using a basis set with *spdf* functions augmented with diffuse functions.

Gill, Johnson, and Pople examined the performance of BLYP with a variety of Pople basis sets,[30] 6-31G(d),6-31+G(d), 6-311+G(2df,p), and 6-311+G(3df, 2p). They found that the BLYP predicts the atomization energy, ionization potential and proton affinity well for the

extended G2 data set, even when BLYP is used in combination with the smallest basis set. The mean absolute deviation in the energy with respect to experiment decreases with increasing basis set size. When the "high-level correction" used in G2 theory was added to the BLYP results, the overall mean absolute error with 6-31G(d) is reduced from 6.45 kcal/mol to 4.18 kcal/mol.

The above studies focus only upon both low-level basis sets and non-systematically developed basis sets. A number of studies have utilized higher-level basis sets. Martin compared the performance of B3LYP and CCSD(T) used with the correlation consistent basis sets for geometries and frequencies of a series of molecules including several large species such as furan and pyrrole.[26] At the double zeta level, B3LYP geometries are more accurate than the CCSD(T) results. B3LYP/cc-pVTZ predicts geometries to within 0.002 Å of the experiment. However, unlike the case for CCSD(T), increasing basis set size to cc-pVQZ only made small improvement in the geometry over B3LYP/cc-pVDZ. Similar basis set convergence can also be found for harmonic frequency, with the exception of several cases where frequency has strong basis set dependence. B3LYP in combination with the cc-pV*x*Z basis set were also applied to determine the geometries and frequencies for a large range of small inorganics and their ions by Raymond and Wheeler.[31] The Kohn-Sham limit was obtained by extrapolating the cc-pV*x*Z results (*x*=D, T and Q), and was compared with experiment.

Denis and Ventura calculated the enthalpy of formation of several species important in atmospheric chemistry using B3LYP and B3PW91 with the correlation consistent basis sets.[32] The predicted properties agree well with previous multireference configuration interaction (MRCI) results. The heats of hydrogenation for a few nitrogen compounds were calculated by Sekusak and Frenking[33] using the pure density functionals BLYP and BP86, as well as the hybrid functionals B3LYP, B3PW91, and B3P86. They employed several basis sets including

cc-pV*x*Z and aug-cc-pV*x*Z (*x*=D, T, Q). It was observed that B3LYP heats of reactions did not converge as the basis set size increased for both the cc-pV*x*Z and aug-cc-pV*x*Z families of basis sets. The irregular convergence was attributed to the possibility that the correlation consistent basis sets, which are optimized for *ab initio* methods, are not necessarily optimal for use with density functional theory.

The goal of this chapter is to study the systematic convergence behavior of DFT with respect to the correlation consistent basis sets. Structures and energies were determined using several popular functionals on a set of closed-shell first-row molecules, which were derived from preceding work by Martell and Goddard.[27] Several statistical methods including normal distribution and mean absolute deviation were utilized to assess the accuracy and precision of the calculated atomization energies. Two extrapolation schemes were used to estimate the Kohn-Sham limits.

2.2 Methodology

In this study, two exchange density functionals, B (B88)[6] and B3[34] (a three-parameter adiabatic connection exchange term), were used with three correlation functionals, Lee-Yang-Parr (LYP),[7] Perdew 1986 (P86),[9] and Perdew-Wang 1991 (PW91).[8] Combining these functionals produce six gradient corrected functionals: BLYP, BPW91, BP86, B3LYP, B3PW91, and B3P86. The numerical grid (75, 302) was used to evaluate the integral in exchange-correlation functionals. It includes 75 radial shells and 302 angular points per shell, resulting in approximately 7000 quadrature points per atom. This grid is specified as “finegrid” in the Gaussian 98 software package,[35] which was used throughout this study. Larger grids were also evaluated, but no impact was observed upon the molecular properties studied.

Standard and augmented correlation consistent basis sets (cc-pV*x*Z and aug-cc-pV*x*Z where *x* = D(2), T(3), Q(4) and 5) were employed to determine the structures and atomization energies of O_3, H_2, H_2O, HF, HCN, CO, N_2, HNO, H_2O_2, HOF, F_2, CO_2, H_2CO, CH_3NH_2, CH_3OH, N_2H_4, and CH_3F. Geometry optimizations and frequency calculations were performed for each method/basis set combination. The atomization energy includes the zero-point energy correction, which was taken directly from the frequency calculations. For energy calculations on the atoms, the tight convergence criterion (10^{-8}) on density was requested to keep the same level of accuracy between atoms and molecules. When this option is not used, the default convergence criterion (10^{-4}) is used, and, as a result, very unusual convergence behavior is observed. Typically, this unusual behavior is expressed as an energy fluctuation with respect to increasing basis set size.

Two popular empirical extrapolation schemes were used to obtain the complete basis set (CBS) limit, or Kohn-Sham (KS) limit, in the case of DFT. One is Feller's exponential scheme,[36] which is used frequently in *ab initio* methods for the correlation consistent basis sets.

$$D_e(x) = D_e(\infty) + Ae^{-Bx} \qquad (2\text{-}1)$$

x is the cardinal number of the basis set (i.e. for cc-pVDZ, *x* = 2; for cc-pVTZ, *x* = 3), $D_e(x)$ represents some property at the "*x*" level, and $D_e(\infty)$ represents the extrapolated KS limit. The parameters A and B are determined in the curve fit. At least three points are needed in the nonlinear fitting scheme.

Another extrapolation scheme is the two-point extrapolation by Halkier et al,[37] given below:

$$D_e(\infty) = \frac{\left(D_e(x) \times x^3\right) - \left(D_e(x-1) \times (x-1)^3\right)}{x^3 - (x-1)^3} \qquad (2\text{-}2)$$

The advantage of this scheme over Feller's exponential extrapolation is that only two points are necessary.

2.3 Discussion and Results

2.3.1 Geometry

The structures of 17 molecules were optimized using the six outlined methods and the correlation consistent basis sets, and are reported in Table 2.1. Overall, the structures converge quickly with respect to increasing basis set size, and are nearly converged at the triple zeta level. Increasing the basis set size beyond the triple zeta level only provides a minor improvement to the geometries. The bond lengths are within 0.015 Å of experiments at the triple zeta level. However, several exceptions were noted: the H-N bond in HNO for all hybrid functionals; the O-O bond in H_2O_2 for B3PW91, B3P86, and BLYP; the O-F bond in HOF for B3PW91 and B3P86; the F-F bond in F_2 for B3PW91 and B3P86; the N-N bond in N_2H_4 for B3PW91 and B3P86; and the C-F bond in CH_3F for BLYP. These bond lengths differ from experiment by 0.025-0.035 Å. Most bond angles are within 2^o of experiment with the exceptions of the H-N-C angle in CH_3NH_2 and the H-N-N angle in N_2H_4 for all pure functionals, which differ from experiment by 2.5^o-3.0^o. The convergence of the dihedral angle of H-O-O-H is achieved at the

cc-pVQZ level, rather than at the cc-pVTZ level, while this is not true for the augmented correlation consistent basis sets where the dihedral angle is nearly converged with aug-cc-pVTZ.

Table 2.1 Optimized bond lengths and angles. Bond lengths are given in angstroms, and bond angles are given in degrees.

Molecules, Experiment	Basis set	B3LYP	B3PW91	B3P86	BLYP	BPW91	BP86
O_3							
r(OO) =	cc-pVDZ	1.2597	1.2508	1.2500	1.2953	1.2815	1.2836
1.278 Å[a]	cc-pVTZ	1.2563	1.2474	1.2464	1.2919	1.2780	1.2798
	cc-pVQZ	1.2531	1.2448	1.2438	1.2881	1.2749	1.2767
	cc-pV5Z	1.2524	1.2442	1.2431	1.2873	1.2741	1.2756
	aug-cc-pVDZ	1.2565	1.2479	1.2471	1.2908	1.2774	1.2793
	aug-cc-pVTZ	1.2549	1.2464	1.2454	1.2901	1.2767	1.2785
	aug-cc-pVQZ	1.2522	1.2440	1.2430	1.2868	1.2737	1.2755
	aug-cc-pV5Z	1.2520	1.2436	1.2427	1.2866	1.2735	1.2752
a(OOO) =	cc-pVDZ	117.95	118.07	118.04	117.90	118.00	117.97
116.8°[a]	cc-pVTZ	118.14	118.23	118.19	118.00	118.11	118.05
	cc-pVQZ	118.26	118.31	118.28	118.10	118.21	118.16
	cc-pV5Z	118.30	118.34	118.31	118.11	118.22	118.16
	aug-cc-pVDZ	118.07	118.10	118.07	117.97	118.02	117.98
	aug-cc-pVTZ	118.28	118.34	118.30	118.14	118.24	118.20
	aug-cc-pVQZ	118.35	118.40	118.36	118.20	118.29	118.24
	aug-cc-pV5Z	118.35	118.38	118.35	118.19	118.28	118.23
H_2							
r(HH) =	cc-pVDZ	0.7617	0.7609	0.7604	0.7674	0.7657	0.7681
0.741 Å[b]	cc-pVTZ	0.7429	0.7444	0.7441	0.7468	0.7481	0.7506
	cc-pVQZ	0.7420	0.7436	0.7433	0.7457	0.7473	0.7498
	cc-pV5Z	0.7418	0.7434	0.7432	0.7455	0.7471	0.7496
	aug-cc-pVDZ	0.7609	0.7600	0.7598	0.7662	0.7647	0.7672
	aug-cc-pVTZ	0.7429	0.7444	0.7441	0.7468	0.7481	0.7506
	aug-cc-pVQZ	0.7420	0.7436	0.7434	0.7458	0.7473	0.7498
	aug-cc-pV5Z	0.7418	0.7434	0.7432	0.7455	0.7471	0.7496
H_2O							

-continue-

-continue-

Molecules, Experiment	Basis set	B3LYP	B3PW91	B3P86	BLYP	BPW91	BP86
r(HO) =	cc-pVDZ	0.9687	0.9663	0.9659	0.9798	0.9762	0.9779
0.956 Å[a]	cc-pVTZ	0.9614	0.9596	0.9594	0.9715	0.9687	0.9707
	cc-pVQZ	0.9603	0.9587	0.9584	0.9703	0.9677	0.9697
	cc-pV5Z	0.9603	0.9587	0.9584	0.9703	0.9677	0.9697
	aug-cc-pVDZ	0.9649	0.9631	0.9629	0.9751	0.9724	0.9744
	aug-cc-pVTZ	0.9621	0.9601	0.9599	0.9719	0.9692	0.9712
	aug-cc-pVQZ	0.9606	0.9590	0.9587	0.9707	0.9680	0.9700
	aug-cc-pV5Z	0.9604	0.9588	0.9586	0.9705	0.9679	0.9698
a(HOH) =	cc-pVDZ	102.74	102.68	102.74	101.77	101.78	101.74
105.2°[a]	cc-pVTZ	104.50	104.34	104.38	103.75	103.60	103.57
	cc-pVQZ	104.88	104.66	104.70	104.20	103.97	103.94
	cc-pV5Z	105.10	104.84	104.87	104.48	104.18	104.16
	aug-cc-pVDZ	104.76	104.42	104.44	104.16	103.80	103.81
	aug-cc-pVTZ	104.95	104.83	104.86	104.48	104.17	104.15
	aug-cc-pVQZ	105.12	104.86	104.88	104.52	104.20	104.19
	aug-cc-pV5Z	105.13	104.87	104.90	104.54	104.22	104.21
HF							
r(HF) =	cc-pVDZ	0.9268	0.9244	0.9241	0.9384	0.9344	0.9358
0.917 Å[b]	cc-pVTZ	0.9225	0.9198	0.9197	0.9330	0.9293	0.9311
	cc-pVQZ	0.9214	0.9189	0.9189	0.9320	0.9282	0.9302
	cc-pV5Z	0.9220	0.9192	0.9191	0.9325	0.9288	0.9306
	aug-cc-pVDZ	0.9256	0.9235	0.9232	0.9367	0.9333	0.9349
	aug-cc-pVTZ	0.9242	0.9216	0.9216	0.9350	0.9311	0.9329
	aug-cc-pVQZ	0.9224	0.9196	0.9195	0.9330	0.9293	0.9311
	aug-cc-pV5Z	0.9222	0.9194	0.9193	0.9328	0.9290	0.9308
HCN							
r(HC) =	cc-pVDZ	1.0772	1.0775	1.0769	1.0836	1.0833	1.0852
1.064 Å[a]	cc-pVTZ	1.0654	1.0672	1.0663	1.0711	1.0729	1.0744
	cc-pVQZ	1.0655	1.0673	1.0664	1.0712	1.0730	1.0746
	cc-pV5Z	1.0656	1.0673	1.0665	1.0714	1.0731	1.0747
	aug-cc-pVDZ	1.0744	1.0752	1.0746	1.0808	1.0811	1.0831
	aug-cc-pVTZ	1.0656	1.0674	1.0665	1.0714	1.0730	1.0746
	aug-cc-pVQZ	1.0656	1.0673	1.0665	1.0713	1.0731	1.0747
	aug-cc-pV5Z	1.0656	1.0673	1.0665	1.0714	1.0732	1.0747

-continue-

-continue-

Molecules, Experiment	Basis set	B3LYP	B3PW91	B3P86	BLYP	BPW91	BP86
r(CN) =	cc-pVDZ	1.1579	1.1578	1.1571	1.1697	1.1692	1.1703
1.156 Å[a]	cc-pVTZ	1.1462	1.1468	1.1459	1.1575	1.1576	1.1585
	cc-pVQZ	1.1450	1.1455	1.1446	1.1565	1.1565	1.1574
	cc-pV5Z	1.1450	1.1454	1.1445	1.1565	1.1564	1.1573
	aug-cc-pVDZ	1.1568	1.1569	1.1561	1.1684	1.1680	1.1691
	aug-cc-pVTZ	1.1460	1.1464	1.1455	1.1573	1.1573	1.1582
	aug-cc-pVQZ	1.1451	1.1456	1.1447	1.1566	1.1566	1.1575
	aug-cc-pV5Z	1.1450	1.1454	1.1445	1.1565	1.1564	1.1573
CO							
r(CO) =	cc-pVDZ	1.1345	1.1340	1.1334	1.1471	1.1459	1.1469
1.128 Å[b]	cc-pVTZ	1.1262	1.1260	1.1253	1.1379	1.1373	1.1382
	cc-pVQZ	1.1237	1.1236	1.1229	1.1355	1.1349	1.1358
	cc-pV5Z	1.1236	1.1235	1.1227	1.1354	1.1347	1.1356
	aug-cc-pVDZ	1.1340	1.1337	1.1330	1.1463	1.1453	1.1463
	aug-cc-pVTZ	1.1258	1.1257	1.1249	1.1376	1.1369	1.1378
	aug-cc-pVQZ	1.1238	1.1237	1.1230	1.1356	1.1350	1.1359
	aug-cc-pV5Z	1.1236	1.1235	1.1227	1.1354	1.1347	1.1356
N_2							
r(NN) =	cc-pVDZ	1.1044	1.1036	1.1032	1.1172	1.1154	1.1166
1.098 Å[b]	cc-pVTZ	1.0914	1.0912	1.0906	1.1032	1.1025	1.1034
	cc-pVQZ	1.0902	1.0901	1.0895	1.1022	1.1016	1.1025
	cc-pV5Z	1.0900	1.0899	1.0892	1.1019	1.1013	1.1022
	aug-cc-pVDZ	1.1044	1.1036	1.1032	1.1168	1.1152	1.1163
	aug-cc-pVTZ	1.0912	1.0910	1.0904	1.1030	1.1023	1.1032
	aug-cc-pVQZ	1.0901	1.0901	1.0894	1.1021	1.1015	1.1024
	aug-cc-pV5Z	1.0899	1.0898	1.0892	1.1019	1.1012	1.1021
HNO							
r(HN) =	cc-pVDZ	1.0776	1.0758	1.0746	1.1002	1.0967	1.0997
1.09 Å[c]	cc-pVTZ	1.0628	1.0630	1.0620	1.0813	1.0805	1.0829
	cc-pVQZ	1.0613	1.0619	1.0610	1.0792	1.0793	1.0815
	cc-pV5Z	1.0607	1.0614	1.0605	1.0781	1.0783	1.0808
	aug-cc-pVDZ	1.0674	1.0673	1.0664	1.0855	1.0845	1.0871
	aug-cc-pVTZ	1.0613	1.0618	1.0610	1.0786	1.0785	1.0810
	aug-cc-pVQZ	1.0610	1.0616	1.0607	1.0783	1.0784	1.0810
	aug-cc-pV5Z	1.0608	1.0615	1.0606	1.0781	1.0783	1.0809

-continue-

-continue-

Molecules, Experiment	Basis set	B3LYP	B3PW91	B3P86	BLYP	BPW91	BP86
r(NO) =	cc-pVDZ	1.2028	1.1985	1.1983	1.2193	1.2130	1.2145
1.209 Å[c]	cc-pVTZ	1.1984	1.1945	1.1939	1.2153	1.2091	1.2106
	cc-pVQZ	1.1970	1.1932	1.1926	1.2139	1.2081	1.2093
	cc-pV5Z	1.1966	1.1927	1.1922	1.2137	1.2078	1.2092
	aug-cc-pVDZ	1.2051	1.2006	1.2002	1.2221	1.2155	1.2172
	aug-cc-pVTZ	1.1978	1.1939	1.1934	1.2149	1.2088	1.2103
	aug-cc-pVQZ	1.1964	1.1926	1.1921	1.2135	1.2076	1.2090
	aug-cc-pV5Z	1.1962	1.1924	1.1918	1.2133	1.2074	1.2088
a(HNO) =	cc-pVDZ	108.35	108.36	108.32	108.30	108.29	108.28
108.047°[c]	cc-pVTZ	108.68	108.67	108.65	108.55	108.53	108.50
	cc-pVQZ	108.81	108.79	108.77	108.68	108.68	108.63
	cc-pV5Z	108.87	108.85	108.83	108.73	108.72	108.70
	aug-cc-pVDZ	108.65	108.61	108.57	108.53	108.52	108.48
	aug-cc-pVTZ	108.86	108.84	108.82	108.74	108.72	108.69
	aug-cc-pVQZ	108.92	108.89	108.87	108.81	108.78	108.75
	aug-cc-pV5Z	108.92	108.89	108.87	108.80	108.78	108.75
H_2O_2							
r(HO) =	cc-pVDZ	0.9734	0.9714	0.9710	0.9853	0.9823	0.9840
0.965 Å[d]	cc-pVTZ	0.9659	0.9642	0.9640	0.9773	0.9748	0.9766
	cc-pVQZ	0.9650	0.9633	0.9631	0.9763	0.9740	0.9759
	cc-pV5Z	0.9654	0.9634	0.9631	0.9764	0.9739	0.9759
	aug-cc-pVDZ	0.9700	0.9683	0.9682	0.9817	0.9789	0.9809
	aug-cc-pVTZ	0.9667	0.9649	0.9647	0.9781	0.9753	0.9774
	aug-cc-pVQZ	0.9654	0.9637	0.9634	0.9767	0.9741	0.9763
	aug-cc-pV5Z	0.9652	0.9635	0.9633	0.9766	0.9740	0.9760
r(OO) =	cc-pVDZ	1.4525	1.4392	1.4375	1.4915	1.4713	1.4735
1.464 Å[d]	cc-pVTZ	1.4517	1.4373	1.4355	1.4920	1.4701	1.4721
	cc-pVQZ	1.4489	1.4343	1.4324	1.4891	1.4672	1.4693
	cc-pV5Z	1.4489	1.4334	1.4316	1.4888	1.4664	1.4688
	aug-cc-pVDZ	1.4507	1.4362	1.4345	1.4897	1.4687	1.4710
	aug-cc-pVTZ	1.4512	1.4364	1.4346	1.4916	1.4695	1.4719
	aug-cc-pVQZ	1.4483	1.4333	1.4315	1.4885	1.4667	1.4686
	aug-cc-pV5Z	1.4480	1.4330	1.4312	1.4883	1.466	1.4684

-continue-

-continue-

Molecules, Experiment	Basis set	B3LYP	B3PW91	B3P86	BLYP	BPW91	BP86
a(HOO) = 99.4°[d]	cc-pVDZ	99.87	100.13	100.14	98.60	99.03	98.97
	cc-pVTZ	100.43	100.68	100.69	99.19	99.53	99.54
	cc-pVQZ	100.69	100.92	100.94	99.50	99.81	99.81
	cc-pV5Z	100.78	101.02	101.03	99.63	99.97	99.92
	aug-cc-pVDZ	100.79	100.93	100.94	99.71	99.95	99.93
	aug-cc-pVTZ	100.74	100.95	100.96	99.59	99.91	99.87
	aug-cc-pVQZ	100.81	101.05	101.06	99.68	100.01	99.97
	aug-cc-pV5Z	100.81	101.06	101.06	99.69	100.02	99.97
d(HOOH) = 111.8°[d]	cc-pVDZ	117.68	116.07	116.24	119.37	116.84	117.00
	cc-pVTZ	113.91	112.44	112.47	115.04	112.87	113.05
	cc-pVQZ	113.00	111.67	111.69	113.89	112.01	112.21
	cc-pV5Z	113.35	111.94	111.95	114.49	112.50	112.58
	aug-cc-pVDZ	113.23	111.59	111.75	114.29	112.34	112.42
	aug-cc-pVTZ	113.39	111.85	111.83	114.28	112.34	112.46
	aug-cc-pVQZ	113.37	111.84	111.81	114.42	112.37	112.27
	aug-cc-pV5Z	113.43	111.91	111.89	114.44	112.44	112.46
HOF							
r(HO) = 0.96 Å[e]	cc-pVDZ	0.9775	0.9754	0.9751	0.9898	0.9864	0.9883
	cc-pVTZ	0.9700	0.9685	0.9683	0.9817	0.9790	0.9811
	cc-pVQZ	0.9693	0.9677	0.9676	0.9809	0.9782	0.9803
	cc-pV5Z	0.9694	0.9679	0.9677	0.9811	0.9783	0.9804
	aug-cc-pVDZ	0.9747	0.9725	0.9726	0.9866	0.9836	0.9857
	aug-cc-pVTZ	0.9715	0.9694	0.9692	0.9829	0.9799	0.9820
	aug-cc-pVQZ	0.9698	0.9682	0.968	0.9819	0.9786	0.9808
	aug-cc-pV5Z	0.9696	0.968	0.9678	0.9814	0.9785	0.9806
r(OF) = 1.442 Å[e]	cc-pVDZ	1.4349	1.4240	1.4219	1.4706	1.4543	1.4551
	cc-pVTZ	1.4301	1.4164	1.4145	1.4675	1.4480	1.4489
	cc-pVQZ	1.4291	1.4152	1.4132	1.4669	1.4475	1.4487
	cc-pV5Z	1.4286	1.4146	1.4126	1.4667	1.4471	1.4483
	aug-cc-pVDZ	1.4328	1.4196	1.4179	1.4699	1.4516	1.4526
	aug-cc-pVTZ	1.4310	1.4166	1.4147	1.4684	1.4489	1.4502
	aug-cc-pVQZ	1.4288	1.4148	1.4127	1.4668	1.4473	1.4484
	aug-cc-pV5Z	1.4284	1.4144	1.4124	1.4666	1.4469	1.4481

-continue-

-continue-

Molecules, Experiment	Basis set	B3LYP	B3PW91	B3P86	BLYP	BPW91	BP86
a(HOF) = 97.2 Å[e]	cc-pVDZ	97.87	97.99	98.00	96.96	97.13	97.11
	cc-pVTZ	98.48	98.68	98.68	97.43	97.67	97.64
	cc-pVQZ	98.63	98.80	98.81	97.58	97.89	97.85
	cc-pV5Z	98.71	98.88	98.88	97.68	97.97	97.93
	aug-cc-pVDZ	98.56	98.76	98.67	97.65	97.85	97.83
	aug-cc-pVTZ	98.59	98.84	98.84	97.68	97.95	97.91
	aug-cc-pVQZ	98.72	98.90	98.90	97.66	98.00	97.96
	aug-cc-pV5Z	98.74	98.91	98.91	97.73	98.01	97.97
F_2							
r(FF) = 1.412 Å[b]	cc-pVDZ	1.4102	1.4004	1.3981	1.4435	1.4303	1.4302
	cc-pVTZ	1.3976	1.3855	1.3835	1.433	1.4163	1.4167
	cc-pVQZ	1.3968	1.3846	1.3825	1.4328	1.4159	1.4161
	cc-pV5Z	1.3962	1.3840	1.3818	1.4326	1.4154	1.4157
	aug-cc-pVDZ	1.4034	1.3922	1.3899	1.4386	1.4230	1.4230
	aug-cc-pVTZ	1.3971	1.3849	1.3829	1.4331	1.4161	1.4164
	aug-cc-pVQZ	1.3961	1.3839	1.3817	1.4324	1.4154	1.4155
	aug-cc-pV5Z	1.3957	1.3836	1.3814	1.4320	1.4150	1.4153
CO_2							
r(CO) = 1.162 Å[a]	cc-pVDZ	1.1673	1.1656	1.1650	1.1815	1.1784	1.1797
	cc-pVTZ	1.1604	1.1592	1.1584	1.1736	1.1714	1.1725
	cc-pVQZ	1.1588	1.1576	1.1568	1.1720	1.1699	1.1710
	cc-pV5Z	1.1587	1.1575	1.1567	1.1721	1.1699	1.1709
	aug-cc-pVDZ	1.1673	1.1659	1.1652	1.1811	1.1783	1.1795
	aug-cc-pVTZ	1.1605	1.1592	1.1585	1.1737	1.1715	1.1725
	aug-cc-pVQZ	1.1589	1.1577	1.1569	1.1722	1.1700	1.1711
	aug-cc-pV5Z	1.1587	1.1575	1.1568	1.1721	1.1699	1.1709
H_2CO							
r(CO) = 1.205 Å[a]	cc-pVDZ	1.2040	1.2022	1.2017	1.2156	1.2129	1.2140
	cc-pVTZ	1.1992	1.1976	1.1969	1.2105	1.2082	1.2095
	cc-pVQZ	1.1982	1.1963	1.1956	1.2096	1.2070	1.2084
	cc-pV5Z	1.1984	1.1964	1.1957	1.2102	1.2075	1.2085
	aug-cc-pVDZ	1.2073	1.2051	1.2045	1.2196	1.2160	1.2172
	aug-cc-pVTZ	1.2004	1.1984	1.1977	1.2122	1.2092	1.2102
	aug-cc-pVQZ	1.1987	1.1967	1.1960	1.2106	1.2078	1.2088
	aug-cc-pV5Z	1.1985	1.1965	1.1958	1.2103	1.2076	1.2085

-continue-

-continue-

Molecules, Experiment	Basis set	B3LYP	B3PW91	B3P86	BLYP	BPW91	BP86
r(CH) = 1.111 Å[a]	cc-pVDZ	1.1203	1.1196	1.1188	1.1309	1.1293	1.1317
	cc-pVTZ	1.1065	1.1080	1.1068	1.1155	1.1167	1.1181
	cc-pVQZ	1.1056	1.1073	1.1062	1.1145	1.1160	1.1174
	cc-pV5Z	1.1053	1.1071	1.1059	1.1141	1.1153	1.1171
	aug-cc-pVDZ	1.1139	1.1145	1.1137	1.1228	1.1231	1.1253
	aug-cc-pVTZ	1.1057	1.1073	1.1062	1.1143	1.1156	1.1174
	aug-cc-pVQZ	1.1054	1.1072	1.1060	1.1141	1.1154	1.1172
	aug-cc-pV5Z	1.1053	1.1070	1.1059	1.1141	1.1153	1.1173
a(HCO) = 121.9°[a]	cc-pVDZ	122.47	122.44	122.40	122.66	122.62	122.61
	cc-pVTZ	122.10	122.08	122.04	122.19	122.22	122.11
	cc-pVQZ	122.01	122.00	121.97	122.09	122.14	122.03
	cc-pV5Z	121.95	121.95	121.92	122.06	122.01	121.99
	aug-cc-pVDZ	121.84	121.88	121.84	122.00	121.98	121.95
	aug-cc-pVTZ	121.93	121.93	121.90	122.03	122.01	121.98
	aug-cc-pVQZ	121.94	121.94	121.92	122.04	122.00	121.98
	aug-cc-pV5Z	121.94	121.94	121.92	122.04	122.00	122.01
CH_3NH_2							
r(HC) = 1.093 Å[a]	cc-pVDZ	1.1120	1.1111	1.1103	1.1207	1.1194	1.1213
	cc-pVTZ	1.0980	1.0989	1.0980	1.1053	1.1060	1.1081
	cc-pVQZ	1.0968	1.0981	1.0970	1.1039	1.1050	1.1069
	cc-pV5Z	1.0964	1.0978	1.0968	1.1036	1.1047	1.1064
	aug-cc-pVDZ	1.1057	1.1057	1.1048	1.1130	1.1128	1.1149
	aug-cc-pVTZ	1.0970	1.0983	1.0973	1.1040	1.1051	1.1069
	aug-cc-pVQZ	1.0966	1.0979	1.0968	1.1035	1.1047	1.1066
	aug-cc-pV5Z	1.0965	1.0978	1.0968	1.1033	1.1043	1.1063
r(NH) = 1.011 Å[a]	cc-pVDZ	1.0228	1.0213	1.0208	1.0327	1.0297	1.0322
	cc-pVTZ	1.0127	1.0122	1.0117	1.0216	1.0202	1.0221
	cc-pVQZ	1.0116	1.0112	1.0107	1.0203	1.0189	1.0211
	cc-pV5Z	1.0114	1.0109	1.0104	1.0203	1.0191	1.0211
	aug-cc-pVDZ	1.0175	1.0166	1.0161	1.0259	1.0246	1.0268
	aug-cc-pVTZ	1.0122	1.0117	1.0112	1.0206	1.0194	1.0216
	aug-cc-pVQZ	1.0113	1.0111	1.0106	1.0199	1.0188	1.0209
	aug-cc-pV5Z	1.0112	1.0109	1.0106	1.0200	1.0189	1.0207

-continue-

-continue-

Molecules, Experiment	Basis set	B3LYP	B3PW91	B3P86	BLYP	BPW91	BP86
r(CN) = 1.474 Å[a]	cc-pVDZ	1.4640	1.4578	1.4563	1.4779	1.4681	1.4705
	cc-pVTZ	1.4641	1.4584	1.4560	1.4793	1.4693	1.4705
	cc-pVQZ	1.4634	1.4569	1.4550	1.4783	1.4679	1.4696
	cc-pV5Z	1.4635	1.4566	1.4545	1.4788	1.4684	1.4702
	aug-cc-pVDZ	1.4669	1.4609	1.4593	1.4818	1.4720	1.4739
	aug-cc-pVTZ	1.4645	1.4578	1.4559	1.4796	1.4690	1.4712
	aug-cc-pVQZ	1.4632	1.4568	1.4549	1.4786	1.4681	1.4697
	aug-cc-pV5Z	1.4631	1.4566	1.4549	1.4790	1.4690	1.4698
a(HNC) = 112.1°[a]	cc-pVDZ	109.34	109.30	109.32	108.67	108.79	108.66
	cc-pVTZ	110.37	110.24	110.32	109.73	109.71	109.73
	cc-pVQZ	110.69	110.58	110.65	110.13	110.10	110.08
	cc-pV5Z	110.91	110.88	110.88	110.37	110.26	110.26
	aug-cc-pVDZ	110.84	110.57	110.60	110.38	110.16	110.15
	aug-cc-pVTZ	110.96	110.82	110.88	110.51	110.37	110.33
	aug-cc-pVQZ	111.04	110.87	110.93	110.55	110.42	110.41
	aug-cc-pV5Z	111.03	110.88	110.93	110.53	110.35	110.41
CH_3OH r(OH) = 0.956 Å[a]	cc-pVDZ	0.9677	0.9656	0.9653	0.9788	0.9757	0.9776
	cc-pVTZ	0.9606	0.9589	0.9587	0.9712	0.9685	0.9705
	cc-pVQZ	0.9594	0.9578	0.9576	0.9699	0.9673	0.9693
	cc-pV5Z	0.9593	0.9578	0.9576	0.9697	0.9672	0.9692
	aug-cc-pVDZ	0.9639	0.9623	0.9620	0.9747	0.9718	0.9737
	aug-cc-pVTZ	0.9608	0.9591	0.9589	0.9714	0.9686	0.9706
	aug-cc-pVQZ	0.9596	0.9580	0.9577	0.9701	0.9674	0.9695
	aug-cc-pV5Z	0.9596	0.9578	0.9577	0.9694	0.9670	0.9695
a(HOC) = 108.87°[a]	cc-pVDZ	107.49	107.39	107.43	106.79	106.62	106.59
	cc-pVTZ	108.51	108.32	108.38	107.77	107.58	107.61
	cc-pVQZ	108.86	108.63	108.70	108.17	107.92	107.95
	cc-pV5Z	109.01	108.63	108.70	108.42	108.10	108.13
	aug-cc-pVDZ	108.89	108.63	108.68	108.27	108.02	108.03
	aug-cc-pVTZ	109.01	108.74	108.80	108.35	108.08	108.10
	aug-cc-pVQZ	109.05	108.79	108.85	108.41	108.13	108.15
	aug-cc-pV5Z	109.05	108.80	108.83	108.49	108.18	108.33

-continue-

-continue-

Molecules, Experiment	Basis set	B3LYP	B3PW91	B3P86	BLYP	BPW91	BP86
N_2H_4							
r(HN) =	cc-pVDZ	1.0266	1.0249	1.0244	1.0378	1.0349	1.0371
1.016 Å[f]	cc-pVTZ	1.0152	1.0147	1.0141	1.0249	1.0236	1.0256
	cc-pVQZ	1.0140	1.0137	1.0131	1.0235	1.0225	1.0245
	cc-pV5Z	1.0137	1.0135	1.0129	1.0232	1.0223	1.0243
	aug-cc-pVDZ	1.0202	1.0196	1.0191	1.0299	1.0285	1.0306
	aug-cc-pVTZ	1.0145	1.0142	1.0137	1.0239	1.0229	1.0249
	aug-cc-pVQZ	1.0138	1.0136	1.0131	1.0233	1.0223	1.0244
	aug-cc-pV5Z	1.0137	1.0135	1.0129	1.0233	1.0223	1.0242
r(NN) =	cc-pVDZ	1.4356	1.4247	1.4232	1.4613	1.4439	1.4474
1.446 Å[f]	cc-pVTZ	1.4357	1.4249	1.4230	1.4625	1.4452	1.4484
	cc-pVQZ	1.4327	1.4224	1.4205	1.4585	1.4420	1.4451
	cc-pV5Z	1.4313	1.4212	1.4193	1.4567	1.4406	1.4436
	aug-cc-pVDZ	1.4355	1.4252	1.4237	1.4606	1.4441	1.4474
	aug-cc-pVTZ	1.4334	1.4231	1.4213	1.4594	1.4428	1.4461
	aug-cc-pVQZ	1.4311	1.4210	1.4192	1.4561	1.4402	1.4433
	aug-cc-pV5Z	1.4309	1.4208	1.4190	1.4561	1.4402	1.4428
a(HNN) =	cc-pVDZ	106.67	106.95	106.99	105.48	105.97	105.82
108.85°[f]	cc-pVTZ	107.42	107.64	107.71	106.23	106.67	106.55
	cc-pVQZ	107.74	107.92	107.99	106.61	106.99	106.89
	cc-pV5Z	107.97	108.11	108.17	106.89	107.21	107.12
	aug-cc-pVDZ	107.66	107.75	107.81	106.66	106.89	106.80
	aug-cc-pVTZ	107.92	108.05	108.10	106.84	107.16	107.04
	aug-cc-pVQZ	108.04	108.16	108.21	106.99	107.29	107.19
	aug-cc-pV5Z	108.05	108.17	108.22	106.99	107.29	107.16
CH_3F							
r(HC) =	cc-pVDZ	1.1037	1.1026	1.1018	1.1119	1.1104	1.1126
1.087 Å[g]	cc-pVTZ	1.0903	1.0916	1.0906	1.0971	1.0979	1.0998
	cc-pVQZ	1.0892	1.0907	1.0897	1.0958	1.0968	1.0988
	cc-pV5Z	1.0889	1.0905	1.0895	1.0954	1.0967	1.0985
	aug-cc-pVDZ	1.0979	1.0980	1.0973	1.1048	1.1047	1.1069
	aug-cc-pVTZ	1.0895	1.0910	1.0900	1.0959	1.0972	1.0989
	aug-cc-pVQZ	1.0890	1.0906	1.0896	1.0953	1.0967	1.0986
	aug-cc-pV5Z	1.0889	1.0905	1.0895	1.0953	1.0966	1.0986

-continue-

-continue-

Molecules, Experiment	Basis set	B3LYP	B3PW91	B3P86	BLYP	BPW91	BP86
r(CF) = 1.383 Å[g]	cc-pVDZ	1.3847	1.3788	1.3773	1.4001	1.3919	1.3926
	cc-pVTZ	1.3865	1.3791	1.3775	1.4050	1.3953	1.3964
	cc-pVQZ	1.3884	1.3801	1.3785	1.4071	1.3970	1.3981
	cc-pV5Z	1.3898	1.3810	1.3792	1.4092	1.3983	1.3993
	aug-cc-pVDZ	1.4014	1.3942	1.3925	1.4223	1.4095	1.4105
	aug-cc-pVTZ	1.3921	1.3831	1.3813	1.4119	1.4003	1.4014
	aug-cc-pVQZ	1.3906	1.3817	1.3798	1.4102	1.3991	1.4000
	aug-cc-pV5Z	1.3902	1.3813	1.3794	1.4098	1.3987	1.4000
a(HCF) = 108.73°[g]	cc-pVDZ	109.55	109.57	109.56	109.69	109.73	109.75
	cc-pVTZ	109.07	109.20	109.19	108.99	109.14	109.12
	cc-pVQZ	108.90	109.08	109.07	108.82	108.96	108.94
	cc-pV5Z	108.77	108.99	108.98	108.66	108.82	108.80
	aug-cc-pVDZ	108.43	108.55	108.54	108.20	108.47	108.46
	aug-cc-pVTZ	108.68	108.90	108.90	108.55	108.73	108.75
	aug-cc-pVQZ	108.73	108.95	108.95	108.60	108.78	108.76
	aug-cc-pV5Z	108.73	108.96	108.96	108.60	108.78	108.76

[a] Ref. [38]
[b] Ref. [39]
[c] Ref. [40]
[d] Ref. [41]
[e] Ref. [42]
[f] Ref. [43]
[g] Ref. [44]

2.3.2. Atomic Energy

Total energies for hydrogen and four first-row atoms are presented in Table 2.2 and compared with accurate Davidson's atomic energies.[45] As shown in the table, the total energies decrease with respect to increasing basis set size. For methods with the same correlation

functional, the atomic energy obtained when the B3 exchange functional is used is lower than that from the B exchange functional. On the other hand, for the B3LYP, B3PW91, and B3P86 functionals, the sequence of atomic energy is given as follows: B3PW91 > B3LYP > B3P86. This trend is true for all of the atoms, with the exception of hydrogen. However, no general trend is observed for BLYP, BPW91, and BP86 functionals. Overall, at the quintuple zeta level, BLYP gives the best agreement with the Davidson energies, with differences of 0.002 hartree, 0.004 hartree, and 0.003 hartree for H, C, and N, respectively. The best atomic energies for other atoms are obtained with B3PW91, with differences of 0.002 hartree for O and 0.003 hartree for F.

2.3.3 Atomization Energy

Generally, the atomization energies from DFT converge rapidly as the basis set size increases, as shown in Table 2.3. In fact, unlike geometries, atomization energies are nearly converged at the quadruple zeta level. For B3LYP and B3PW91, most of the atomization energies are underestimated when the low-level basis sets are used. With increasing basis set size, the energies approach the experimental energies. However, for the other four functionals,

Table 2.2 Total energies for atoms in hartrees.

Atoms Exact.[a]	Basis set	B3LYP	B3PW91	B3P86	BLYP	BPW91	BP86
H	cc-pVDZ	-0.501258	-0.503232	-0.517800	-0.496403	-0.503029	-0.499131
-0.5000	cc-pVTZ	-0.502156	-0.503979	-0.518516	-0.497555	-0.503928	-0.500026
	cc-pVQZ	-0.502346	-0.504154	-0.518681	-0.497781	-0.504127	-0.500220
	cc-pV5Z	-0.502428	-0.504230	-0.518745	-0.497889	-0.504222	-0.500305
	aug-cc-pVDZ	-0.501657	-0.503546	-0.518053	-0.497007	-0.503481	-0.499564
	aug-cc-pVTZ	-0.502260	-0.504068	-0.518578	-0.497722	-0.504063	-0.500146
	aug-cc-pVQZ	-0.502392	-0.504194	-0.518708	-0.497860	-0.504192	-0.500278
	aug-cc-pV5Z	-0.502436	-0.504238	-0.518751	-0.497905	-0.504236	-0.500319
C	cc-pVDZ	-37.851975	-37.831115	-37.947726	-37.837836	-37.838906	-37.839115
-37.8450	cc-pVTZ	-37.858575	-37.836831	-37.953414	-37.845501	-37.845158	-37.845500
	cc-pVQZ	-37.860592	-37.838843	-37.955405	-37.847806	-37.847432	-37.847767
	cc-pV5Z	-37.861508	-37.839647	-37.956171	-37.849077	-37.848519	-37.848815
	aug-cc-pVDZ	-37.854196	-37.832790	-37.949301	-37.840848	-37.841057	-37.841347
	aug-cc-pVTZ	-37.859061	-37.837199	-37.953710	-37.845313	-37.845684	-37.846001
	aug-cc-pVQZ	-37.860785	-37.839022	-37.955532	-37.848135	-37.847721	-37.848012
	aug-cc-pV5Z	-37.861541	-37.839682	-37.956195	-37.849140	-37.848581	-37.848868
N	cc-pVDZ	-54.589136	-54.569045	-54.706717	-54.572571	-54.579225	-54.578063
-54.5893	cc-pVTZ	-54.601781	-54.580425	-54.718013	-54.586935	-54.591632	-54.590617
	cc-pVQZ	-54.605328	-54.583875	-54.721438	-54.590896	-54.595425	-54.594424
	cc-pV5Z	-54.606704	-54.585109	-54.722633	-54.592689	-54.596984	-54.595951
	aug-cc-pVDZ	-54.593843	-54.572754	-54.710301	-54.578765	-54.583922	-54.582907

-continue-

-continue-

Atoms Exact.[a]	Basis set	B3LYP	B3PW91	B3P86	BLYP	BPW91	BP86
	aug-cc-pVTZ	-54.602891	-54.581280	-54.718765	-54.588525	-54.592807	-54.591765
	aug-cc-pVQZ	-54.605735	-54.584222	-54.721709	-54.591546	-54.595955	-54.594897
	aug-cc-pV5Z	-54.606773	-54.585175	-54.722681	-54.592811	-54.597092	-54.596047
O	cc-pVDZ	-75.068499	-75.039479	-75.202793	-75.054526	-75.055672	-75.058322
-75.067	cc-pVTZ	-75.091864	-75.061252	-75.224296	-75.080286	-75.078956	-75.081617
	cc-pVQZ	-75.098201	-75.067414	-75.230377	-75.087251	-75.085609	-75.088249
	cc-pV5Z	-75.100485	-75.069519	-75.232426	-75.090069	-75.088122	-75.090729
	aug-cc-pVDZ	-75.077164	-75.046591	-75.209636	-75.065596	-75.064389	-75.067160
	aug-cc-pVTZ	-75.094180	-75.063128	-75.226007	-75.083421	-75.081375	-75.083994
	aug-cc-pVQZ	-75.099049	-75.068125	-75.230973	-75.088511	-75.086619	-75.089179
	aug-cc-pV5Z	-75.100614	-75.069647	-75.232520	-75.090288	-75.088324	-75.090901
F	cc-pVDZ	-99.726602	-99.691439	-99.880126	-99.713359	-99.712549	-99.717987
-99.734	cc-pVTZ	-99.762867	-99.725500	-99.913775	-99.752932	-99.748808	-99.754142
	cc-pVQZ	-99.772527	-99.734856	-99.922991	-99.763470	-99.758830	-99.764091
	cc-pV5Z	-99.775818	-99.737929	-99.926007	-99.767416	-99.762394	-99.767624
	aug-cc-pVDZ	-99.739496	-99.702133	-99.890454	-99.729776	-99.725693	-99.731208
	aug-cc-pVTZ	-99.766141	-99.728127	-99.916206	-99.757394	-99.752240	-99.757522
	aug-cc-pVQZ	-99.773645	-99.735763	-99.923766	-99.765151	-99.760138	-99.765306
	aug-cc-pV5Z	-99.775969	-99.738073	-99.926116	-99.767680	-99.762631	-99.767828

[a] Davidson estimates of the atomic energies, which are from ref. [45]

the atomization energies are overestimated for a number of molecules, even with the low-level basis sets. Further, atomization energies become further from experiment as the basis set size increases. Typical examples are O_3, HCN, F_2, CO_2, and H_2CO.

Interestingly, the atomization energies for a number of molecules do not converge with increasing basis set size. This is particularly evident when pure density functionals are utilized, and there are two types of irregular convergence patterns have been observed. Generally, a slight energy dip occurs at the quintuple zeta level. The dip is small (< 0.5 kcal/mol), and the most pronounced example is CO_2 with a dip of 0.9 kcal/mol at the BLYP/cc-pV5Z level. This type of convergence pattern occurs for most of the molecules. Another irregular convergence pattern is for F_2 and O_3. The convergence of F_2 is very irregular, even for B3LYP and B3PW91. The maximum value of the F_2 atomization energy occurs at the triple zeta level. For O_3, using BLYP with the correlation consistent basis sets results in a fluctuation in energy: 168.32 kcal/mol for cc-pVDZ, 166.96 kcal/mol for cc-pVTZ, 167.28 kcal/mol for cc-pVQZ, and 166.79 kcal/mol for cc-pV5Z.

The augmented correlation consistent basis sets can help remedy the irregular convergence problem, but not for all cases. The dip still occurs at the aug-cc-pV5Z level for HF, F_2, HOF, and CO_2, but is less pronounced (< 0.2 kcal/mol). Additionally, the diffuse functions in the augmented correlation consistent basis sets cannot improve the convergence behavior of the atomization energies for F_2 and O_3.

2.3.4. Statistical Analysis

The mean error, mean absolute error (MAE), and normal distribution were utilized to compare the performance of the density functionals when used with the correlation consistent

basis sets. The mean energies are listed in Table 2.4 and normal distributions are plotted in Figs. 2.1 and 2.2. In terms of the mean errors, atomization energies are underestimated by B3LYP and B3PW91, whereas they are overestimated by the other four functionals. The best result is obtained using B3LYP and aug-cc-pV5Z, with a MAE of 2.19 kcal/mol. For B3P86, BLYP, BPW91, and BP86, the results nearest to experiment are achieved at the double zeta level. The MAE gets larger when the basis set size increases.

Based on the normal distributions of the atomization energies of DFT with the correlation consistent basis sets, the hybrid density functionals B3LYP and B3PW91 perform much better than other density functionals. As the basis set size increases, both the accuracy (represented by the location of the peak) and precision (represented by the width of peak) improve. The curves become narrower and move towards experiment. For the pure functionals, improvement of accuracy and precision seem not to occur as the basis set size increases. The curves are not sensitive to the increase in the size of the basis set, and a broad error distribution remains for all levels of basis sets. The normal distribution curve of B3P86 at the double zeta level is similar to that of B3LYP and B3PW91 at the double zeta level. However, as the basis set size increases, the curves broaden and migrate away from the experiment.

Table 2.3 Calculated atomization energies in kcal/mol. The errors in the calculated atomization energies, as compared with experiment are provided in parenthesis.

Molecules, Expt.[a]	Basis set	B3LYP	B3PW91	B3P86	BLYP	BPW91	BP86
O_3	cc-pVDZ	133.76 (-8.64)	134.11 (-8.29)	143.72 (1.32)	168.32 (25.92)	169.28 (26.88)	177.67 (35.27)
142.4	cc-pVTZ	135.68 (-6.72)	137.72 (-4.68)	147.50 (5.10)	166.96 (24.56)	170.11 (27.71)	178.39 (35.99)
	cc-pVQZ	136.58 (-5.82)	138.79 (-3.61)	148.67 (6.27)	167.28 (24.88)	170.74 (28.34)	179.05 (36.65)
	cc-pV5Z	136.45 (-5.95)	138.73 (-3.67)	148.69 (6.29)	166.79 (24.39)	170.41 (28.01)	178.76 (36.36)
	aug-cc-pVDZ	134.41 (-7.99)	136.41 (-5.99)	146.30 (3.90)	165.88 (23.48)	169.12 (26.72)	177.46 (35.06)
	aug-cc-pVTZ	135.39 (-7.01)	137.75 (-4.65)	147.73 (5.33)	165.82 (23.42)	169.52 (27.12)	177.91 (35.51)
	aug-cc-pVQZ	136.67 (-5.73)	138.92 (-3.48)	148.93 (6.53)	166.98 (24.58)	170.56 (28.16)	178.97 (36.57)
	aug-cc-pV5Z	136.70 (-5.70)	138.92 (-3.48)	148.91 (6.51)	166.98 (24.58)	170.54 (28.14)	178.93 (36.53)
H_2	cc-pVDZ	101.11 (-2.19)	98.83 (-4.47)	103.43 (0.13)	100.17 (-3.13)	97.34 (-5.96)	103.06 (-0.24)
103.3	cc-pVTZ	103.93 (0.63)	100.98 (-2.32)	105.70 (2.40)	103.27 (-0.03)	99.61 (-3.69)	105.42 (2.12)
	cc-pVQZ	104.03 (0.73)	101.07 (-2.23)	105.82 (2.52)	103.35 (0.05)	99.67 (-3.63)	105.50 (2.20)
	cc-pV5Z	104.02 (0.72)	101.07 (-2.23)	105.83 (2.53)	103.31 (0.01)	99.64 (-3.66)	105.48 (2.18)
	aug-cc-pVDZ	100.90 (-2.40)	98.61 (-4.69)	103.27 (-0.03)	99.86 (-3.44)	97.05 (-6.25)	102.77 (-0.53)
	aug-cc-pVTZ	103.82 (0.52)	100.89 (-2.41)	105.65 (2.35)	103.08 (-0.22)	99.46 (-3.84)	105.29 (1.99)
	aug-cc-pVQZ	103.98 (0.68)	101.03 (-2.27)	105.79 (2.49)	103.25 (-0.05)	99.60 (-3.70)	105.44 (2.14)
	aug-cc-pV5Z	104.01 (0.71)	101.06 (-2.24)	105.82 (2.52)	103.29 (-0.01)	99.63 (-3.67)	105.47 (2.17)
H_2O	cc-pVDZ	206.14 (-13.26)	205.40 (-14.00)	214.10 (-5.30)	207.84 (-11.56)	207.40 (-12.00)	215.95 (-3.45)
219.4	cc-pVTZ	214.85 (-4.55)	213.37 (-6.03)	222.22 (2.82)	216.81 (-2.59)	215.59 (-3.81)	224.29 (4.89)

-continue-

-continue-

Molecules, Expt.[a]	Basis set	B3LYP	B3PW91	B3P86	BLYP	BPW91	BP86
	cc-pVQZ	216.78 (-2.62)	215.02 (-4.38)	223.87 (4.47)	218.91 (-0.49)	217.33 (-2.07)	226.08 (6.68)
	cc-pV5Z	217.57 (-1.83)	215.66 (-3.74)	224.51 (5.11)	219.81 (0.41)	218.03 (-1.37)	226.81 (7.41)
	aug-cc-pVDZ	215.20 (-4.20)	213.56 (-5.84)	222.36 (2.96)	217.53 (-1.87)	215.99 (-3.41)	224.74 (5.34)
	aug-cc-pVTZ	217.29 (-2.11)	215.47 (-3.93)	224.31 (4.91)	219.59 (0.19)	217.91 (-1.49)	226.69 (7.29)
	aug-cc-pVQZ	217.83 (-1.57)	215.89 (-3.51)	224.73 (5.33)	220.17 (0.77)	218.34 (-1.06)	227.12 (7.72)
	aug-cc-pV5Z	217.86 (-1.54)	215.91 (-3.49)	224.74 (5.34)	220.20 (0.80)	218.35 (-1.05)	227.12 (7.72)
HF	cc-pVDZ	124.58 (-10.82)	124.61 (-10.79)	129.11 (-6.29)	126.08 (-9.32)	126.34 (-9.06)	130.60 (-4.80)
135.4	cc-pVTZ	131.30 (-4.10)	130.80 (-4.60)	135.35 (-0.05)	133.07 (-2.33)	132.76 (-2.64)	137.11 (1.71)
	cc-pVQZ	132.78 (-2.62)	132.06 (-3.34)	136.59 (1.19)	134.74 (-0.66)	134.13 (-1.27)	138.49 (3.09)
	cc-pV5Z	133.37 (-2.03)	132.53 (-2.87)	137.04 (1.64)	135.43 (0.03)	134.68 (-0.72)	139.04 (3.64)
	aug-cc-pVDZ	132.00 (-3.40)	131.35 (-4.05)	135.82 (.42)	134.17 (-1.23)	133.57 (-1.83)	137.89 (2.49)
	aug-cc-pVTZ	133.28 (-2.12)	132.52 (-2.88)	137.04 (1.64)	135.41 (0.01)	134.73 (-0.67)	139.10 (3.70)
	aug-cc-pVQZ	133.57 (-1.83)	132.72 (-2.68)	137.22 (1.82)	135.72 (0.32)	134.93 (-0.47)	139.30 (3.90)
	aug-cc-pV5Z	133.56 (-1.84)	132.70 (-2.70)	137.20 (1.80)	135.71 (0.31)	134.91 (-0.49)	139.27 (3.87)
HCN	cc-pVDZ	295.79 (-6.71)	294.45 (-8.05)	303.84 (1.34)	303.84 (1.34)	303.43 (0.93)	311.77 (9.27)
302.5	cc-pVTZ	302.78 (0.28)	300.73 (-1.77)	310.36 (7.86)	310.36 (7.86)	309.19 (6.69)	317.62 (15.12)
	cc-pVQZ	303.74 (1.24)	301.65 (-0.85)	311.29 (8.79)	311.21 (8.71)	309.99 (7.49)	318.42 (15.92)
	cc-pV5Z	303.63 (1.13)	301.59 (-0.91)	311.26 (8.76)	310.92 (8.42)	309.80 (7.30)	318.25 (15.75)
	aug-cc-pVDZ	295.68 (-6.82)	294.42 (-8.08)	303.92 (1.42)	303.12 (0.62)	302.88 (0.38)	311.19 (8.69)
	aug-cc-pVTZ	302.60 (0.10)	300.68 (-1.82)	310.39 (7.89)	310.46 (7.96)	308.93 (6.43)	317.40 (14.9)

-continue-

-continue-

Molecules, Expt.[a]	Basis set	B3LYP	B3PW91	B3P86	BLYP	BPW91	BP86
	aug-cc-pVQZ	303.58 (1.08)	301.51 (-0.99)	311.22 (8.72)	310.89 (8.39)	309.73 (7.23)	318.21 (15.71)
	aug-cc-pV5Z	303.60 (1.10)	301.58 (-0.92)	311.25 (8.75)	310.85 (8.35)	309.73 (7.23)	318.20 (15.70)
CO	cc-pVDZ	248.42 (-7.78)	248.77 (-7.43)	254.18 (-2.02)	256.35 (0.15)	257.70 (1.50)	261.90 (5.70)
256.2	cc-pVTZ	252.12 (-4.08)	252.23 (-3.97)	257.84 (1.64)	259.25 (3.05)	260.43 (4.23)	264.71 (8.51)
	cc-pVQZ	252.84 (-3.36)	252.97 (-3.23)	258.61 (2.41)	259.76 (3.56)	260.99 (4.79)	265.25 (9.05)
	cc-pV5Z	252.56 (-3.64)	252.76 (-3.44)	258.43 (2.23)	259.26 (3.06)	260.63 (4.43)	264.90 (8.70)
	aug-cc-pVDZ	247.20 (-9.00)	247.79 (-8.41)	253.33 (-2.87)	254.29 (-1.91)	256.05 (-0.15)	260.22 (4.02)
	aug-cc-pVTZ	251.36 (-4.84)	251.68 (-4.52)	257.36 (1.16)	258.66 (2.46)	259.60 (3.40)	263.88 (7.68)
	aug-cc-pVQZ	252.47 (-3.73)	252.66 (-3.54)	258.36 (2.16)	259.16 (2.96)	260.51 (4.31)	264.81 (8.61)
	aug-cc-pV5Z	252.53 (-3.67)	252.73 (-3.47)	258.42 (2.22)	259.19 (2.99)	260.55 (4.35)	264.85 (8.65)
N_2	cc-pVDZ	219.32 (-5.78)	215.60 (-9.50)	223.51 (-1.59)	231.22 (6.12)	228.07 (2.97)	235.22 (10.12)
225.1	cc-pVTZ	225.45 (0.35)	221.50 (-3.60)	229.52 (4.42)	236.49 (11.39)	233.12 (8.02)	240.24 (15.14)
	cc-pVQZ	226.38 (1.28)	222.40 (-2.70)	230.46 (5.36)	237.27 (12.17)	233.87 (8.77)	241.03 (15.93)
	cc-pV5Z	226.43 (1.33)	222.46 (-2.64)	230.55 (5.45)	237.19 (12.09)	233.83 (8.73)	241.00 (15.90)
	aug-cc-pVDZ	219.36 (-5.74)	215.88 (-9.22)	223.84 (-1.26)	230.53 (5.43)	227.71 (2.61)	234.80 (9.70)
	aug-cc-pVTZ	225.42 (0.32)	221.48 (-3.62)	229.58 (4.48)	236.25 (11.15)	232.93 (7.83)	240.10 (15.00)
	aug-cc-pVQZ	226.52 (1.42)	222.50 (-2.60)	230.60 (5.50)	237.33 (12.23)	233.90 (8.80)	241.08 (15.98)
	aug-cc-pV5Z	226.60 (1.50)	222.60 (-2.50)	230.68 (5.58)	237.38 (12.28)	233.98 (8.88)	241.14 (16.04)
HNO	cc-pVDZ	192.98 (-3.92)	190.78 (-6.12)	200.74 (3.84)	206.22 (9.32)	204.55 (7.65)	213.96 (17.06)
196.9	cc-pVTZ	196.94 (0.04)	194.78 (-2.12)	204.91 (8.01)	209.05 (12.15)	207.57 (10.67)	217.00 (20.10)

-continue-

-continue-

Molecules, Expt.[a]	Basis set	B3LYP	B3PW91	B3P86	BLYP	BPW91	BP86
	cc-pVQZ	198.00 (1.10)	195.78 (-1.12)	205.94 (9.04)	209.98 (13.08)	208.47 (11.57)	217.91 (21.01)
	cc-pV5Z	198.13 (1.23)	195.92 (-0.98)	206.11 (9.21)	209.96 (13.06)	208.49 (11.59)	217.95 (21.05)
	aug-cc-pVDZ	194.64 (-2.26)	192.76 (-4.14)	202.86 (5.96)	206.87 (9.97)	205.69 (8.79)	215.10 (18.20)
	aug-cc-pVTZ	197.27 (0.37)	195.17 (-1.73)	205.37 (8.47)	209.08 (12.18)	207.73 (10.83)	217.22 (20.32)
	aug-cc-pVQZ	198.26 (1.36)	196.04 (-0.86)	206.24 (9.34)	210.12 (13.22)	208.62 (11.72)	218.11 (21.21)
	aug-cc-pV5Z	198.29 (1.39)	196.07 (-0.83)	206.26 (9.36)	210.14 (13.24)	208.63 (11.73)	218.11 (21.21)
H_2O_2	cc-pVDZ	241.65 (-10.65)	240.09 (-12.21)	252.58 (0.28)	252.29 (-0.01)	250.97 (-1.33)	262.93 (10.63)
252.3	cc-pVTZ	249.23 (-3.07)	247.67 (-4.63)	260.33 (8.03)	259.28 (6.98)	258.08 (5.78)	270.12 (17.82)
	cc-pVQZ	250.48 (-1.82)	248.78 (-3.52)	261.47 (9.17)	260.51 (8.21)	259.15 (6.85)	271.21 (18.91)
	cc-pV5Z	250.74 (-1.56)	248.98 (-3.32)	261.70 (9.40)	260.72 (8.42)	259.29 (6.99)	271.38 (19.08)
	aug-cc-pVDZ	247.65 (-4.65)	246.06 (-6.24)	258.75 (6.45)	258.02 (5.72)	256.71 (4.41)	268.80 (16.5)
	aug-cc-pVTZ	250.16 (-2.14)	248.56 (-3.74)	261.31 (9.01)	260.14 (7.84)	258.92 (6.62)	271.04 (18.74)
	aug-cc-pVQZ	250.87 (-1.43)	249.11 (-3.19)	261.85 (9.55)	260.89 (8.59)	259.45 (7.15)	271.56 (19.26)
	aug-cc-pV5Z	250.89 (-1.41)	249.11 (-3.19)	261.83 (9.53)	260.89 (8.59)	259.42 (7.12)	271.53 (19.23)
HOF	cc-pVDZ	144.19 (-7.41)	142.49 (-9.11)	150.51 (-1.09)	156.42 (4.82)	154.70 (3.10)	162.29 (10.69)
151.6	cc-pVTZ	148.35 (-3.25)	147.16 (-4.44)	155.33 (3.73)	159.55 (7.95)	158.52 (6.92)	166.15 (14.55)
	cc-pVQZ	148.77 (-2.83)	147.59 (-4.01)	155.80 (4.20)	159.85 (8.25)	158.85 (7.25)	166.49 (14.89)
	cc-pV5Z	148.75 (-2.85)	147.57 (-4.03)	155.81 (4.21)	159.73 (8.13)	158.72 (7.12)	166.39 (14.79)
	aug-cc-pVDZ	146.71 (-4.89)	145.52 (-6.08)	153.73 (2.13)	158.10 (6.50)	157.05 (5.45)	164.70 (13.10)
	aug-cc-pVTZ	148.50 (-3.10)	147.42 (-4.18)	155.68 (4.08)	159.44 (7.84)	158.58 (6.98)	166.27 (14.67)

-continue-

-continue-

Molecules, Expt.[a]	Basis set	B3LYP	B3PW91	B3P86	BLYP	BPW91	BP86
	aug-cc-pVQZ	148.83 (-2.77)	147.66 (-3.94)	155.92 (4.32)	159.80 (8.20)	158.81 (7.21)	166.50 (14.90)
	aug-cc-pV5Z	148.82 (-2.78)	147.63 (-3.97)	155.88 (4.28)	159.79 (8.19)	158.77 (7.17)	166.45 (14.85)
F_2	cc-pVDZ	36.32 (-0.58)	34.69 (-2.21)	38.16 (1.26)	50.67 (13.77)	48.76 (11.86)	51.96 (15.06)
36.9	cc-pVTZ	36.54 (-0.36)	36.10 (-0.80)	39.71 (2.81)	49.21 (12.31)	48.74 (11.84)	51.91 (15.01)
	cc-pVQZ	36.04 (-0.86)	35.82 (-1.08)	39.48 (2.58)	48.41 (11.51)	48.24 (11.34)	51.42 (14.52)
	cc-pV5Z	35.63 (-1.27)	35.49 (-1.41)	39.21 (2.31)	47.78 (10.88)	47.73 (10.83)	50.94 (14.04)
	aug-cc-pVDZ	33.94 (-2.96)	33.46 (-3.44)	37.15 (0.25)	46.70 (9.80)	46.29 (9.39)	49.49 (12.59)
	aug-cc-pVTZ	35.59 (-1.31)	35.48 (-1.42)	39.21 (2.31)	47.68 (10.78)	47.69 (10.79)	50.91 (14.01)
	aug-cc-pVQZ	35.68 (-1.22)	35.55 (-1.35)	39.28 (2.38)	47.77 (10.87)	47.75 (10.85)	50.97 (14.07)
	aug-cc-pV5Z	35.68 (-1.22)	35.54 (-1.36)	39.27 (2.37)	47.77 (10.87)	47.72 (10.82)	50.94 (14.04)
CO_2	cc-pVDZ	375.18 (-6.72)	378.49 (-3.41)	387.69 (5.79)	390.46 (8.56)	395.87 (13.97)	402.33 (20.43)
381.9	cc-pVTZ	380.63 (-1.27)	383.85 (1.95)	393.37 (11.47)	394.00 (12.10)	399.60 (17.70)	406.14 (24.24)
	cc-pVQZ	381.49 (-0.41)	384.74 (2.84)	394.30 (12.40)	394.46 (12.56)	400.18 (18.28)	406.67 (24.77)
	cc-pV5Z	380.95 (-0.95)	384.34 (2.44)	393.98 (12.08)	393.52 (11.62)	399.48 (17.58)	406.02 (24.12)
	aug-cc-pVDZ	372.82 (-9.08)	376.99 (-4.91)	386.43 (4.53)	386.01 (4.11)	392.80 (10.9)	399.17 (17.27)
	aug-cc-pVTZ	379.21 (-2.69)	382.80 (0.90)	392.49 (10.59)	392.31 (10.41)	397.98 (16.08)	404.55 (22.65)
	aug-cc-pVQZ	380.85 (-1.05)	384.22 (2.32)	393.92 (12.02)	393.38 (11.48)	399.33 (17.43)	405.92 (24.02)
	aug-cc-pV5Z	380.86 (-1.04)	384.25 (2.35)	393.92 (12.02)	393.32 (11.42)	399.30 (17.40)	405.88 (23.98)
H_2CO	cc-pVDZ	350.33 (-6.97)	350.80 (-6.50)	362.09 (4.79)	356.37 (-0.93)	357.96 (0.66)	368.18 (10.88)
357.3	cc-pVTZ	356.51 (-0.79)	356.30 (-1.00)	367.97 (10.67)	361.85 (4.55)	362.77 (5.47)	373.21 (15.91)

-continue-

-continue-

Molecules, Expt.[a]	Basis set	B3LYP	B3PW91	B3P86	BLYP	BPW91	BP86
	cc-pVQZ	357.47 (0.17)	357.18 (-0.12)	368.91 (11.61)	362.64 (5.34)	363.51 (6.21)	373.96 (16.66)
	cc-pV5Z	357.38 (0.08)	357.16 (-0.14)	368.92 (11.62)	362.31 (5.01)	363.30 (6.00)	373.79 (16.49)
	aug-cc-pVDZ	351.05 (-6.25)	351.71 (-5.59)	363.23 (5.93)	356.16 (-1.14)	358.11 (0.81)	368.36 (11.06)
	aug-cc-pVTZ	356.36 (-0.94)	356.29 (-1.01)	368.10 (10.80)	361.83 (4.53)	362.45 (5.15)	372.96 (15.66)
	aug-cc-pVQZ	357.34 (0.04)	357.10 (-0.20)	368.90 (11.60)	362.27 (4.97)	363.24 (5.94)	373.76 (16.46)
	aug-cc-pV5Z	357.37 (0.07)	357.14 (-0.16)	368.93 (11.63)	362.25 (4.95)	363.24 (5.94)	373.75 (16.45)
CH_3NH_2	cc-pVDZ	531.57 (-11.13)	530.63 (-12.07)	552.18 (9.48)	530.87 (-11.83)	531.08 (-11.62)	552.24 (9.54)
542.5	cc-pVTZ	542.83 (0.13)	540.56 (-2.14)	562.62 (19.92)	542.14 (-0.56)	540.87 (-1.83)	562.38 (19.68)
	cc-pVQZ	544.51 (1.81)	542.07 (-0.63)	564.18 (21.48)	543.79 (1.09)	542.33 (-0.37)	563.87 (21.17)
	cc-pV5Z	544.87 (2.17)	542.39 (-0.31)	564.55 (21.85)	543.98 (1.28)	542.50 (-0.20)	564.11 (21.41)
	aug-cc-pVDZ	535.91 (-6.79)	534.47 (-8.23)	556.38 (13.68)	535.02 (-7.68)	534.64 (-8.06)	556.03 (13.33)
	aug-cc-pVTZ	543.68 (0.98)	541.38 (-1.32)	563.59 (20.89)	543.33 (0.63)	541.51 (-1.19)	563.14 (20.44)
	aug-cc-pVQZ	544.91 (2.21)	542.39 (-0.31)	564.57 (21.87)	544.08 (1.38)	542.55 (-0.15)	564.16 (21.46)
	aug-cc-pV5Z	544.98 (2.28)	542.46 (-0.24)	564.63 (21.93)	544.06 (1.36)	542.57 (-0.13)	564.18 (21.48)
CH_3OH	cc-pVDZ	468.45 (-12.35)	468.87 (-11.93)	486.45 (5.65)	469.32 (-11.48)	470.91 (-9.89)	487.75 (6.95)
480.9	cc-pVTZ	478.25 (-2.55)	477.65 (-3.15)	495.70 (14.90)	478.88 (-1.92)	479.39 (-1.41)	496.56 (15.76)
	cc-pVQZ	479.76 (-1.04)	478.97 (-1.83)	497.08 (16.28)	480.34 (-0.46)	480.64 (-0.16)	497.86 (17.06)
	cc-pV5Z	480.00 (-0.80)	479.18 (-1.62)	497.35 (16.55)	480.40 (-0.40)	480.71 (-0.09)	497.98 (17.18)
	aug-cc-pVDZ	472.85 (-7.95)	473.02 (-7.78)	490.91 (10.11)	473.36 (-7.44)	474.69 (-6.11)	491.70 (10.90)
	aug-cc-pVTZ	479.08 (-1.72)	478.46 (-2.34)	496.67 (15.87)	480.04 (-0.76)	480.02 (-0.78)	497.31 (16.51)

-continue-

-continue-

Molecules, Expt.[a]	Basis set	B3LYP	B3PW91	B3P86	BLYP	BPW91	BP86
	aug-cc-pVQZ	480.06 (-0.74)	479.23 (-1.57)	497.42 (16.62)	480.53 (-0.27)	480.80 (0.00)	498.09 (17.29)
	aug-cc-pV5Z	480.10 (-0.70)	479.26 (-1.54)	497.45 (16.65)	480.51 (-0.29)	480.78 (-0.02)	498.06 (17.26)
N_2H_4	cc-pVDZ	395.93 (-9.57)	392.02 (-13.48)	412.65 (7.15)	400.79 (-4.71)	397.30 (-8.20)	417.79 (12.29)
405.5	cc-pVTZ	408.17 (2.67)	403.37 (-2.13)	424.32 (18.82)	412.83 (7.33)	408.45 (2.95)	429.14 (23.64)
	cc-pVQZ	410.57 (5.07)	405.51 (0.01)	426.49 (20.99)	415.28 (9.78)	410.62 (5.12)	431.34 (25.84)
	cc-pV5Z	411.31 (5.81)	406.15 (0.65)	427.14 (21.64)	415.96 (10.46)	411.18 (5.68)	431.96 (26.46)
	aug-cc-pVDZ	404.08 (-1.42)	399.46 (-6.04)	420.38 (14.88)	408.98 (3.48)	404.66 (-0.84)	425.42 (19.92)
	aug-cc-pVTZ	410.10 (4.60)	405.11 (-0.39)	426.13 (20.63)	414.72 (9.22)	410.15 (4.65)	430.94 (25.44)
	aug-cc-pVQZ	411.42 (5.92)	406.23 (0.73)	427.23 (21.73)	416.15 (10.65)	411.31 (5.81)	432.09 (26.59)
	aug-cc-pV5Z	411.49 (5.99)	406.30 (0.80)	427.28 (21.78)	416.17 (10.67)	411.35 (5.85)	432.10 (26.60)
CH_3F	cc-pVDZ	389.44 (-12.96)	389.70 (-12.7)	402.92 (0.52)	390.93 (-11.47)	392.09 (-10.31)	404.57 (2.17)
402.4	cc-pVTZ	397.11 (-5.29)	396.65 (-5.75)	410.36 (7.96)	398.04 (-4.36)	398.43 (-3.97)	411.25 (8.85)
	cc-pVQZ	397.95 (-4.45)	397.40 (-5.00)	411.18 (8.78)	398.75 (-3.65)	399.06 (-3.34)	411.94 (9.54)
	cc-pV5Z	397.99 (-4.41)	397.46 (-4.94)	411.29 (8.89)	398.56 (-3.84)	398.95 (-3.45)	411.86 (9.46)
	aug-cc-pVDZ	391.51 (-10.89)	391.92 (-10.48)	405.41 (3.01)	392.24 (-10.16)	393.63 (-8.77)	406.22 (3.82)
	aug-cc-pVTZ	397.45 (-4.95)	397.08 (-5.32)	410.95 (8.55)	398.58 (-3.82)	398.58 (-3.82)	411.51 (9.11)
	aug-cc-pVQZ	398.04 (-4.36)	397.50 (-4.90)	411.36 (8.96)	398.65 (-3.75)	399.01 (-3.39)	411.95 (9.55)
	aug-cc-pV5Z	398.05 (-4.35)	397.50 (-4.90)	411.34 (8.94)	398.60 (-3.80)	398.96 (-3.44)	411.89 (9.49)

[a] Experimental values are from Ref.[46]

2.3.5. Kohn-Sham Limit

The atomization energies have been extrapolated to obtain the Kohn-Sham limits for B3LYP and B3PW91, since these two functionals gave the smallest MAEs compared with experiments. Three extrapolation schemes have been used: an exponential extrapolation using double, triple, and quadruple zeta results marked as KS_{DTQ}; the two-point scheme using double and triple zeta results KS_{DT}; and the two-point scheme using triple and quadruple zeta results KS_{TQ}. The results are summarized in Table 2.5 and 2.6. For KS_{DTQ} and KS_{TQ} with the cc-pVxZ basis sets, F_2 is not included due to its irregular convergence behavior.

Table 2.4 Mean absolute errors (MAE) and mean errors (ME) for the atomization energies in kcal/mol.

Basis set	B3LYP	B3PW91	B3P86	BLYP	BPW91	BP86
MAE						
cc-pVDZ	8.09	8.96	3.40	7.91	8.11	10.86
cc-pVTZ	2.36	3.24	7.68	7.18	7.37	15.24
cc-pVQZ	2.19	2.38	8.68	7.32	7.46	16.11
cc-pV5Z	2.22	2.31	8.81	7.15	7.28	16.12
aug-cc-pVDZ	5.69	6.42	4.69	6.12	6.17	11.91
aug-cc-pVTZ	2.34	2.72	8.17	6.67	6.92	15.51
aug-cc-pVQZ	2.19	2.26	8.88	7.22	7.26	16.20
aug-cc-pV5Z	2.19	2.24	8.90	7.22	7.26	16.19
ME						
cc-pVDZ	-8.09	-8.96	1.49	0.33	0.07	9.86
cc-pVTZ	-1.88	-3.01	7.68	5.79	5.33	15.24
cc-pVQZ	-0.85	-2.05	8.68	6.70	6.19	16.11
cc-pV5Z	-0.76	-1.95	8.81	6.65	6.16	16.12
aug-cc-pVDZ	-5.69	-6.42	4.20	2.01	2.00	11.85
aug-cc-pVTZ	-1.53	-2.61	8.17	6.11	5.53	15.51
aug-cc-pVQZ	-0.69	-1.90	8.88	6.74	6.23	16.20
aug-cc-pV5Z	-0.66	-1.87	8.90	6.73	6.23	16.19

When the results are extrapolated to the KS limit, the atomization energies are improved slightly. Overall, extrapolation does not provide a substantial improvement in accuracy for B3LYP. Among all extrapolation schemes, KS_{DT} performs the worst. However, extrapolation leads to a substantial improvement for B3PW91 in particular for KS_{DT}, which yields a MAE of 1.87 kcal/mol. This may be interpreted by the fact that B3LYP overestimates the extrapolations of the atomization energy for almost half of the molecules, while for B3PW91, this is the case for only three molecules.

2.4 Conclusions

In summary, both structures and atomization energies converge rapidly with respect to increasing basis set size. Structures are nearly converged at the triple zeta level, while the atomization energies are nearly converged at the quadruple zeta level. B3LYP and B3PW91 with aug-cc-pV5Z give the best atomization energies, showing deviations of 2.19 and 2.24 kcal/mol, respectively. For B3LYP and B3PW91, both the accuracy and the precision of the atomization energies are improved as the basis set size is increased. In contrast, the accuracy and precision of the atomization energies are not sensitive to the size of the basis set for B3P86, BLYP, BPW91, and BP86.

The atomization energies for a number of molecules do not converge with increasing the size of the standard correlation consistent basis sets. This is especially true when these basis sets are used with the pure density functionals BLYP, BPW91, and BP86. Generally, this irregular convergence appears as a slight energy dip at the quintuple zeta level. The augmented correlation consistent basis sets can alleviate these irregular convergence problems, but not for all cases.

Table 2.5 Kohn-Sham atomization energy limits for B3LYP using the cc-pV*x*Z and aug-cc-pV*x*Z basis sets, and utilizing several different extrapolation schemes. Additionally, the mean absolute error resulting from the use of each extrapolation scheme and basis set is reported. The energies are reported in kcal/mol.

Molecule	KS_{DTQ} cc-pV*x*Z	aug-cc-pV*x*Z	KS_{DT} cc-pV*x*Z	aug-cc-pV*x*Z	KS_{TQ} cc-pV*x*Z	aug-cc-pV*x*Z	Experiment[a]
O_3 [b]	137.39	136.70	136.48	135.80	137.24	137.61	142.4
H_2	104.04	103.99	105.11	105.04	104.11	104.10	103.3
H_2O	217.33	218.01	218.52	218.17	218.19	218.22	219.4
HF	133.20	133.65	134.13	133.82	133.86	133.77	135.4
HCN	303.89	303.74	305.72	305.51	304.43	304.30	302.5
CO	253.02	252.87	253.68	253.11	253.37	253.27	256.2
N_2	226.54	226.76	228.04	227.97	227.05	227.32	225.1
HNO	198.38	198.86	198.61	198.38	198.77	198.98	196.9
H_2O_2	250.72	251.15	252.42	251.22	251.39	251.39	252.3
HOF	148.81	148.90	150.10	149.25	149.07	149.07	151.6
F_2 [c]	-	35.68	36.64	36.29	-	35.73	36.9
CO_2	381.65	381.41	382.93	381.90	382.11	382.04	381.9
H_2CO	357.64	357.56	359.11	358.59	358.17	358.05	357.3
CH_3NH_2	544.61	544.94	547.37	546.75	545.54	545.60	542.5
CH_3OH	480.13	480.35	482.48	481.80	480.96	480.89	480.9
N_2H_4	411.15	411.79	413.33	412.64	412.31	412.39	405.5
CH_3F	398.06	398.11	400.34	399.95	398.57	398.47	402.4
MAE	2.21[d]	2.18 (2.24[d])	2.43 (2.57[d])	2.45 (2.57[d])	2.22[d]	2.17 (2.23[d])	

[a] Experimental values are from Ref.[46] . [b] Due to the near-linear convergence of O_3 as the augmented basis set size is increased from aug-cc-pVDZ through aug-cc-pVQZ, the three-point extrapolations included the aug-cc-pVTZ, aug-cc-pVQZ, and aug-cc-pV5Z results. [c] Due to the unusual behavior of F_2 atomization energies beyond the triple zeta level for the cc-pV*x*Z series, the KS_{DTQ} and KS_{TQ} extrapolations were not performed. [d] MAE was obtained omitting F_2.

Table 2.6 Kohn-Sham atomization energy limits for B3PW91 using the cc-pV*x*Z and aug-cc-pV*x*Z basis sets, and utilizing several different extrapolation schemes. Additionally, the mean absolute error resulting from the use of each extrapolation scheme and basis set is reported. The energies are reported in kcal/mol.

Molecule	KS_{DTQ}		KS_{DT}		KS_{TQ}		Experiment[a]
	cc-pV*x*Z	aug-cc-pV*x*Z	cc-pV*x*Z	aug-cc-pV*x*Z	cc-pV*x*Z	aug-cc-pV*x*Z	
O_3 [b]	139.24	138.92	139.24	138.32	139.57	139.78	142.4
H_2	101.08	101.04	101.89	101.85	101.14	101.13	103.3
H_2O	215.45	216.01	216.73	216.27	216.22	216.20	219.4
HF	132.38	132.75	133.41	133.01	132.97	132.86	135.4
HCN	301.80	301.64	303.38	303.31	302.31	302.12	302.5
CO	253.18	252.99	253.68	253.32	253.52	253.38	256.2
N_2	222.56	222.73	223.98	223.84	223.05	223.24	225.1
HNO	196.12	196.53	196.47	196.19	196.51	196.67	196.9
H_2O_2	248.97	249.26	250.86	249.62	249.59	249.51	252.3
HOF	147.64	147.69	149.12	148.23	147.91	147.83	151.6
F_2 [c]	-	35.55	36.69	36.33	-	35.59	36.9
CO_2	384.92	384.69	386.10	385.24	385.39	385.26	381.9
H_2CO	357.35	357.27	358.61	358.22	357.83	357.69	357.3
CH_3NH_2	542.13	542.36	544.54	544.09	542.96	542.92	542.5
CH_3OH	479.30	479.45	481.45	480.85	480.03	479.89	480.9
N_2H_4	406.01	406.51	408.15	407.49	407.08	407.05	405.5
CH_3F	397.50	397.54	399.57	399.25	397.96	397.81	402.4
MAE	2.32[d]	2.19 (2.24[d])	1.87 (1.98[d])	2.02 (2.11[d])	2.11[d]	2.06 (2.11[d])	

[a] Experimental values are from Ref.[46]. [b] Due to the near-linear convergence of O_3 as the augmented basis set size is increased from aug-cc-pVDZ through aug-cc-pVQZ, the three-point extrapolations included the aug-cc-pVTZ, aug-cc-pVQZ, and aug-cc-pV5Z results. [c] Due to the unusual behavior of F_2 atomization energies beyond the triple zeta level for the cc-pV*x*Z series, the KS_{DTQ} and KS_{TQ} extrapolations were not performed. [d] MAE was obtained omitting F_2.

Figure 2.1 Normal distribution of the errors in the atomization energies with respect to experiment (the "0") for the hybrid functionals B3LYP (a and b), B3P86 (c and d), and B3PW91 (e and f) with the cc-pV*x*Z and aug-cc-pV*x*Z basis sets.

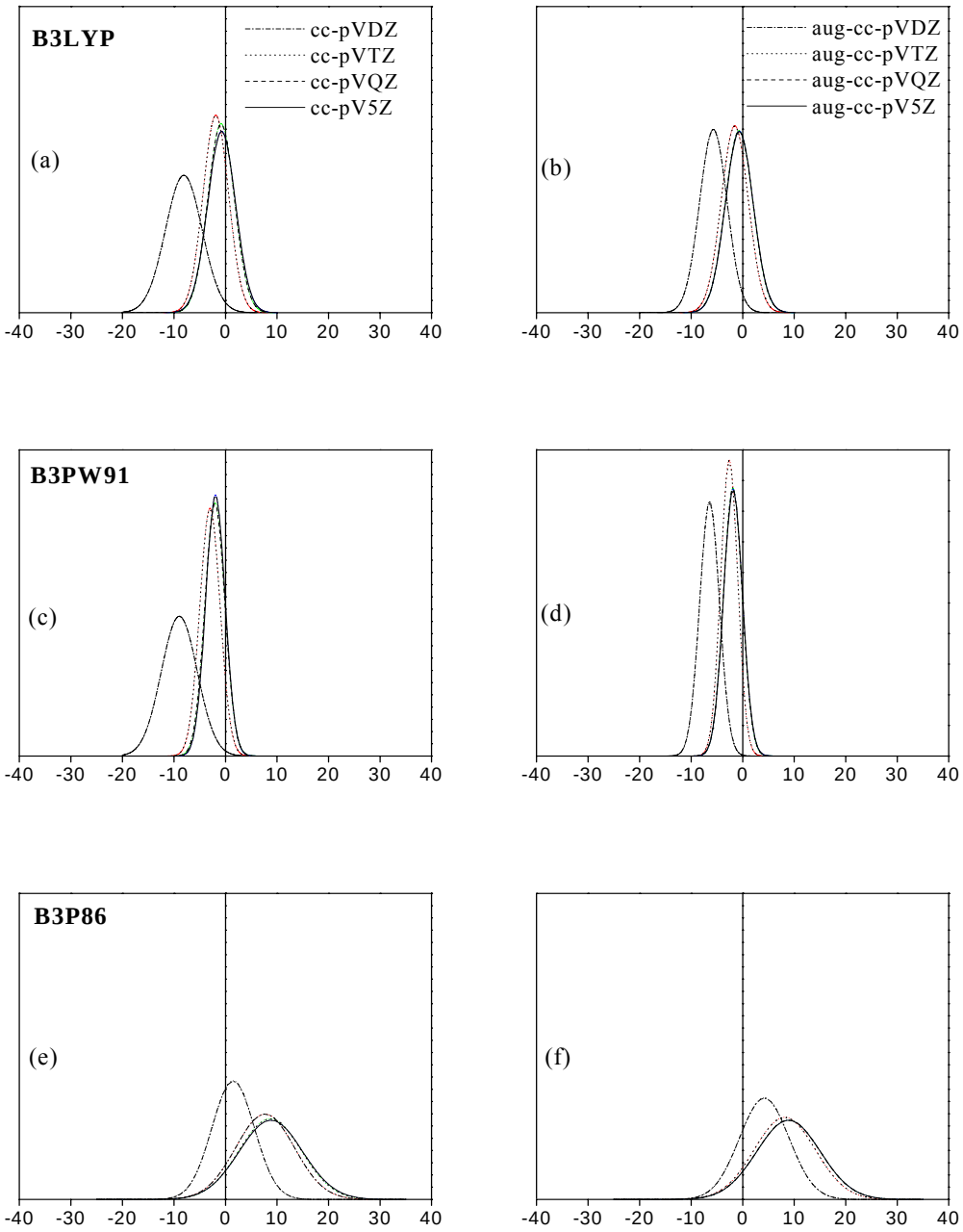

Figure 2.2 Normal distribution of the errors in the atomization energies with respect to experiment (the "0") for the pure functionals BLYP (a and b), BP86 (c and d), and BPW91 (e and f) with the cc-pV*x*Z and aug-cc-pV*x*Z basis sets.

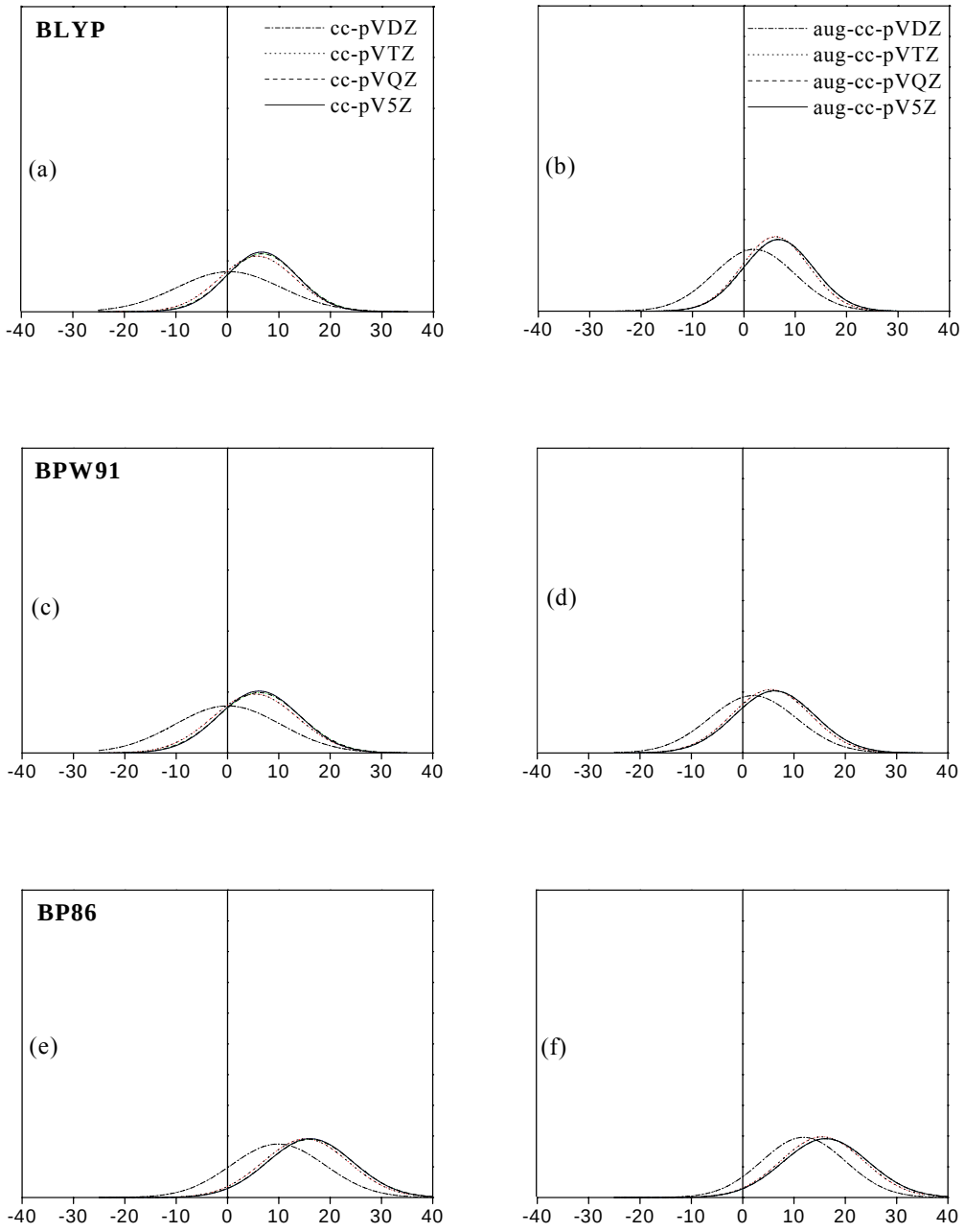

CHAPTER 3

THE PERFORMANCE OF DENSITY FUNCTIONALS WITH RESPECT TO BASIS SET: POLARIZATION CONSISTENT BASIS SETS

3.1 Introduction

As addressed in the last chapter, a simple and effective means to assess the performance of density functionals is needed. Such a means already exists for *ab initio* methods. The correlation consistent basis sets developed by Dunning and co-workers [15, 47-55] have proven to be an efficient tool in estimating the complete basis sets (CBS) limit, and then assessing the reliability of various theoretical approaches, as demonstrated by thousands of *ab initio* studies. However, the question is whether or not the correlation consistent basis sets can be used effectively when combined with density functional theory (DFT). In last chapter, we investigated the structures and energies of a series of molecules with potential importance in atmospheric chemistry using several popular density functionals and the correlation consistent basis sets. Unexpected convergence behavior in the atomization energies was observed for some functionals, however, the reason is not clear.

In this section, the performance of DFT with another type of systematically developed basis sets, the polarization consistent basis sets,[56] is examined. By comparing and analyzing the compositions and performance of these two types of basis sets, we try to understand the

reason for the unexpected convergence problem. A systematic sequence of basis sets, the polarization consistent basis sets pc-X (X=0, 1, 2, 3, 4), were developed by Jensen.[56] These basis sets were developed expressly for DFT via an analysis of the convergence of the total energy, using criteria similar to that used to develop the correlation consistent basis set. However, in contrast to the correlation consistent basis sets,[15] molecules were used as a target to optimize the exponents of the polarization functions since the polarization functions are not greatly dependent on the atomic DFT calculation. So far, the polarization consistent basis sets have been expanded to include the first-row and second-row atoms. In addition, a set of diffuse functions has been developed for the polarization consistent basis sets.[56-61]

Despite the fact that the polarization consistent basis sets were optimized for BLYP, it is not clear whether they can be applied to other density functionals in a systematic way. In this project, the convergence behavior of the polarization consistent basis sets, in combination with several popular functionals including BLYP,[6, 7] BPW91,[8] and BP86,[9] as well as B3LYP,[10] B3PW91, and B3P86, is investigated. To compare with the correlation consistent basis sets, we examine the structures and energies for the same set of molecules derived from Martell and Goddard's work[27] and discussed in Chapter 2 of this dissertation. Also, a full statistical error analysis is performed to understand the accuracy and the precision of structures and energies with respect to increasing basis set size.

3.2. Methodology

The basis sets used throughout the current project are the polarization consistent basis sets including pc-X (X=1, 2, 3, 4). pc-1 was compared with cc-pVDZ because they have the same highest angular momentum; likewise pc-2 was compared with cc-pVTZ, etc. The pc-0

basis set was excluded because it is a single-zeta level basis set, and there is no single-zeta basis set for the correlation consistent basis set series. The density functionals include three pure functionals: BLYP, BPW91, and BP86, as well as three hybrid functionals: B3LYP, B3PW91, and B3P86. Geometry optimization and frequency calculations were carried out for each combination of the polarization consistent basis sets and density functionals. Zero point corrections were obtained from frequency calculations and are included in the atomization energies. All calculations were performed using the Gaussian 98 software package.[35] The default numerical grid (75, 302) was used to evaluate the exchange-correlation integral, and a tight convergence criterion on density was requested when calculating the total energies for the atoms. Two empirical extrapolation schemes, an exponential and a two-point extrapolation scheme, were utilized to extrapolate the Kohn-Sham (KS) limit. Both schemes were discussed in the "Methodology" section of the last chapter.

3.3 Results and Discussions

3.3.1. Geometry

Overall, the convergence of geometries, listed in Table 3.1, is fast with increasing basis set size, and the geometries reach near convergence at the pc-2 level. The bond lengths are within 0.02Å of experiment, while the bond angles are within 2^{o} of experiment at the pc-2 level. The exceptions in bond length include: the O-O bond in O_3 and the H-N bond in HNO for all hybrid functionals; the O-O bond in H_2O_2, the O-F bond in HOF, and the F-F bond in F_2 for B3PW91, B3P86, and BLYP; the H-O bond in HOF for all pure functionals; the N-N bond in

Table 3.1 Optimized bond lengths and angles. Bond lengths are given in angstroms, and bond angles are given in degrees.

Molecules	B3LYP	B3PW91	B3P86	BLYP	BPW91	BP86	Expt.[a]
O_3, r(OO)							1.2780 Å[a]
pc-1	1.2636	1.2543	1.2534	1.3002	1.2857	1.2879	
pc-2	1.2551	1.2465	1.2454	1.2903	1.2766	1.2783	
pc-3	1.2522	1.2440	1.2429	1.2870	1.2738	1.2756	
pc-4	1.2519	1.2437	1.2427	1.2867	1.2735	1.2752	
θ(OOO)							116.8°[a]
pc-1	117.84	117.93	117.91	117.72	117.81	117.77	
pc-2	118.16	118.24	118.19	118.00	118.11	118.05	
pc-3	118.32	118.35	118.32	118.12	118.23	118.19	
pc-4	118.35	118.39	118.35	118.19	118.26	118.22	
H_2, r(HH)							0.7414 Å[b]
pc-1	0.7554	0.7542	0.7539	0.7614	0.7596	0.7620	
pc-2	0.7436	0.7448	0.7446	0.7478	0.7487	0.7513	
pc-3	0.7418	0.7434	0.7432	0.7455	0.7471	0.7496	
pc-4	0.7417	0.7434	0.7431	0.7455	0.7471	0.7496	
H_2O, r(HO)							0.956 Å[a]
pc-1	0.9683	0.9662	0.9655	0.9791	0.9757	0.9776	
pc-2	0.9604	0.9586	0.9584	0.9706	0.9678	0.9698	
pc-3	0.9604	0.9587	0.9585	0.9704	0.9678	0.9698	
pc-4	0.9604	0.9587	0.9585	0.9704	0.9678	0.9698	
θ(HOH)							105.2°[a]
pc-1	104.06	103.97	104.08	103.20	103.13	103.14	
pc-2	105.19	104.94	104.97	104.58	104.27	104.27	
pc-3	105.13	104.87	104.89	104.53	104.21	104.20	
pc-4	105.13	104.87	104.89	104.54	104.22	104.20	
HF, r(HF)							0.917 Å[b]
pc-1	0.9306	0.9280	0.9279	0.9415	0.9378	0.9394	
pc-2	0.9221	0.9192	0.9192	0.9327	0.9289	0.9307	
pc-3	0.9222	0.9194	0.9193	0.9328	0.9290	0.9308	
pc-4	0.9222	0.9194	0.9193	0.9328	0.9290	0.9308	

-continue-

-continue-

Molecules	B3LYP	B3PW91	B3P86	BLYP	BPW91	BP86	Expt.[a]
HCN, *r*(HC)							1.064 Å[a]
pc-1	1.0758	1.0760	1.0755	1.0826	1.0822	1.0842	
pc-2	1.0658	1.0673	1.0665	1.0718	1.0732	1.0749	
pc-3	1.0655	1.0673	1.0664	1.0714	1.0731	1.0747	
pc-4	1.0656	1.0673	1.0665	1.0714	1.0731	1.0747	
r(CN)							1.156 Å[a]
pc-1	1.1543	1.1537	1.1531	1.1664	1.1653	1.1666	
pc-2	1.1458	1.1461	1.1452	1.1574	1.1573	1.1581	
pc-3	1.1449	1.1454	1.1445	1.1565	1.1564	1.1573	
pc-4	1.1449	1.1454	1.1445	1.1564	1.1564	1.1573	
CO, *r*(CO)							1.128 Å[b]
pc-1	1.1330	1.1317	1.1312	1.1458	1.1437	1.1449	
pc-2	1.1247	1.1245	1.1237	1.1366	1.1359	1.1368	
pc-3	1.1236	1.1235	1.1227	1.1354	1.1348	1.1355	
pc-4	1.1236	1.1234	1.1227	1.1353	1.1347	1.1356	
N_2, *r*(NN)							1.098 Å[b]
pc-1	1.1009	1.0995	1.0991	1.1139	1.1116	1.1129	
pc-2	1.0909	1.0907	1.0899	1.103	1.1023	1.1031	
pc-3	1.0899	1.0898	1.0892	1.1019	1.1013	1.1022	
pc-4	1.0899	1.0898	1.0891	1.1018	1.1012	1.1021	
HNO, *r*(HN)							1.090 Å[c]
pc-1	1.0691	1.0675	1.0665	1.0899	1.0869	1.0894	
pc-2	1.0607	1.0611	1.0603	1.0783	1.0781	1.0807	
pc-3	1.0607	1.0613	1.0605	1.0780	1.0782	1.0807	
pc-4	1.0608	1.0614	1.0605	1.0781	1.0783	1.0808	
r(NO)							1.209 Å[c]
pc-1	1.2049	1.2000	1.1997	1.2220	1.2151	1.2169	
pc-2	1.1982	1.1941	1.1935	1.2155	1.2093	1.2107	
pc-3	1.1964	1.1925	1.1920	1.2135	1.2076	1.2090	
pc-4	1.1962	1.1923	1.1918	1.2133	1.2073	1.2087	
θ(HNO)							108.047°[c]
pc-1	108.23	108.26	108.23	108.07	108.10	108.05	
pc-2	108.76	108.75	108.74	108.59	108.61	108.58	
pc-3	108.90	108.87	108.85	108.76	108.75	108.72	

-continue-

-continue-

Molecules	B3LYP	B3PW91	B3P86	BLYP	BPW91	BP86	Expt.[a]
pc-4	108.91	108.89	108.87	108.80	108.77	108.75	
H_2O_2, r(HO)							0.965 Å[d]
pc-1	0.9741	0.9723	0.9721	0.986	0.9829	0.9849	
pc-2	0.9652	0.9633	0.9631	0.9766	0.9740	0.9761	
pc-3	0.9655	0.9634	0.9632	0.9766	0.9740	0.9760	
pc-4	0.9652	0.9634	0.9632	0.9766	0.9740	0.9760	
r(OO)							1.464 Å[d]
pc-1	1.4630	1.4483	1.4466	1.5036	1.4822	1.4847	
pc-2	1.4515	1.4366	1.4348	1.4923	1.4696	1.4719	
pc-3	1.4489	1.4332	1.4314	1.4887	1.4663	1.4687	
pc-4	1.4480	1.4329	1.4311	1.4882	1.4659	1.4683	
θ(HOO)							99.4°[d]
pc-1	99.95	100.25	100.26	98.66	99.09	98.98	
pc-2	100.56	100.77	100.78	99.35	99.73	99.69	
pc-3	100.81	101.04	101.05	99.67	100.00	99.95	
pc-4	100.82	101.06	101.06	99.69	100.02	99.97	
d(HOOH)							111.8°[d]
pc-1	117.91	116.16	116.34	119.88	117.65	117.84	
pc-2	115.86	114.34	114.37	117.41	115.12	115.16	
pc-3	113.28	111.84	111.81	114.31	112.37	112.35	
pc-4	113.41	111.86	111.85	114.40	112.38	112.34	
HOF, r(HO)							0.960 Å[e]
pc-1	0.9786	0.9765	0.9764	0.9907	0.9874	0.9895	
pc-2	0.9696	0.9678	0.9676	0.9814	0.9783	0.9804	
pc-3	0.9696	0.9679	0.9677	0.9813	0.9784	0.9805	
pc-4	0.9696	0.9680	0.9677	0.9813	0.9784	0.9805	
r(OF)							1.442 Å[e]
pc-1	1.4450	1.4324	1.4305	1.4815	1.4640	1.4650	
pc-2	1.4312	1.4171	1.4150	1.4693	1.4495	1.4507	
pc-3	1.4286	1.4145	1.4125	1.4668	1.4471	1.4483	
pc-4	1.4284	1.4143	1.4123	1.4665	1.4468	1.4480	
θ(HOF)							97.2°[e]
pc-1	97.81	97.97	97.97	96.84	97.11	97.09	
pc-2	98.54	98.72	98.73	97.52	97.82	97.78	
pc-3	98.73	98.90	98.90	97.71	97.99	97.96	

-continue-

-continue-

Molecules	B3LYP	B3PW91	B3P86	BLYP	BPW91	BP86	Expt.[a]
pc-4	98.74	98.91	98.91	97.73	98.01	97.97	
F_2, *r*(FF)							1.412 Å[b]
pc-1	1.4189	1.4081	1.4056	1.4521	1.4376	1.4377	
pc-2	1.4002	1.3876	1.3854	1.4366	1.4191	1.4194	
pc-3	1.3960	1.3838	1.3816	1.4325	1.4153	1.4156	
pc-4	1.3957	1.3835	1.3813	1.4320	1.4150	1.4152	
CO_2, *r*(CO)							1.162 Å[a]
pc-1	1.1651	1.1626	1.1620	1.1791	1.1756	1.1769	
pc-2	1.1593	1.1580	1.1572	1.1727	1.1705	1.1715	
pc-3	1.1587	1.1575	1.1567	1.1721	1.1699	1.1709	
pc-4	1.1587	1.1575	1.1567	1.1721	1.1699	1.1708	
H_2CO, *r*(CO)							1.205 Å[a]
pc-1	1.2038	1.2015	1.2010	1.2156	1.2125	1.2140	
pc-2	1.1992	1.1972	1.1964	1.2110	1.2082	1.2092	
pc-3	1.1984	1.1965	1.1957	1.2103	1.2076	1.2086	
pc-4	1.1984	1.1965	1.1957	1.2103	1.2076	1.2084	
r(CH)							1.111 Å[a]
pc-1	1.1148	1.1141	1.1131	1.1252	1.1240	1.1258	
pc-2	1.1057	1.1071	1.1060	1.1148	1.1156	1.1175	
pc-3	1.1053	1.1070	1.1059	1.1141	1.1153	1.1171	
pc-4	1.1053	1.1070	1.1059	1.1141	1.1153	1.1175	
θ(HCO)							121.9°[a]
pc-1	122.23	122.17	122.12	122.32	122.33	122.23	
pc-2	121.98	121.99	121.96	122.09	122.04	122.02	
pc-3	121.94	121.95	121.92	122.04	122.00	121.98	
pc-4	121.94	121.94	121.92	122.04	122.00	122.01	
CH_3NH_2, *r*(HC)							1.093 Å[a]
pc-1	1.1066	1.1056	1.1048	1.1160	1.1144	1.1168	
pc-2	1.0972	1.0983	1.0972	1.1046	1.1053	1.1072	
pc-3	1.0965	1.0978	1.0967	1.1035	1.1046	1.1065	
pc-4	1.0965	1.0978	1.0967	1.1036	1.1048	1.1066	
r(NH)							1.011 Å[a]
pc-1	1.0196	1.0183	1.0179	1.0293	1.0267	1.0287	
pc-2	1.0114	1.0110	1.0104	1.0202	1.0189	1.0209	

-continue-

-continue-

Molecules	B3LYP	B3PW91	B3P86	BLYP	BPW91	BP86	Expt.[a]
pc-3	1.0111	1.0109	1.0104	1.0198	1.0187	1.0207	
pc-4	1.0111	1.0109	1.0104	1.0199	1.0188	1.0208	
r(CN)							1.474 Å[a]
pc-1	1.4614	1.4550	1.4536	1.4753	1.4654	1.4673	
pc-2	1.4629	1.4564	1.4544	1.4780	1.4677	1.4692	
pc-3	1.4630	1.4566	1.4547	1.4784	1.4679	1.4695	
pc-4	1.4630	1.4566	1.4547	1.4781	1.4678	1.4695	
θ(HNC)							112.1°[a]
pc-1	110.39	110.42	110.46	109.76	109.92	109.89	
pc-2	111.02	110.89	110.97	110.49	110.41	110.42	
pc-3	111.05	110.88	110.94	110.56	110.42	110.42	
pc-4	111.05	110.88	110.94	110.55	110.41	110.41	
CH_3OH, *r*(OH)							0.956 Å[a]
pc-1	0.9678	0.9659	0.9656	0.9787	0.9757	0.9777	
pc-2	0.9597	0.9579	0.9577	0.9704	0.9675	0.9696	
pc-3	0.9593	0.9577	0.9575	0.9699	0.9672	0.9693	
pc-4	0.9593	0.9577	0.9575	0.9698	0.9671	0.9692	
θ(HOC)							108.87°[a]
pc-1	108.27	108.22	108.27	107.52	107.45	107.46	
pc-2	108.91	108.68	108.74	108.23	108.00	108.02	
pc-3	109.06	108.80	108.86	108.41	108.13	108.15	
pc-4	109.06	108.80	108.86	108.42	108.12	108.14	
N_2H_4, *r*(HN)							1.016 Å[f]
pc-1	1.0229	1.0215	1.0210	1.0337	1.0312	1.0333	
pc-2	1.0140	1.0136	1.0130	1.0236	1.0224	1.0244	
pc-3	1.0136	1.0134	1.0128	1.0231	1.0221	1.0242	
pc-4	1.0137	1.0134	1.0129	1.0231	1.0222	1.0242	
r(NN)							1.446 Å[f]
pc-1	1.4313	1.4202	1.4187	1.4566	1.4387	1.4422	
pc-2	1.4306	1.4204	1.4185	1.4554	1.4393	1.4422	
pc-3	1.4309	1.4208	1.4190	1.4562	1.4401	1.4431	
pc-4	1.4309	1.4207	1.4189	1.4559	1.4399	1.4430	
θ(HNN)							108.85°[f]
pc-1	107.60	107.89	107.95	106.47	106.96	106.82	
pc-2	108.08	108.23	108.30	107.02	107.35	107.26	
pc-3	108.05	108.18	108.23	106.99	107.29	107.19	

-continue-

-continue-

Molecules	B3LYP	B3PW91	B3P86	BLYP	BPW91	BP86	Expt.[a]
pc-4	108.05	108.18	108.23	107.00	107.30	107.20	
CH_3F, r(HC)							1.087 Å[g]
pc-1	1.0972	1.0963	1.0961	1.1062	1.1047	1.1069	
pc-2	1.0894	1.0908	1.0898	1.0963	1.0971	1.0990	
pc-3	1.0889	1.0905	1.0895	1.0953	1.0966	1.0984	
pc-4	1.0889	1.0905	1.0895	1.0953	1.0966	1.0985	
r(CF)							1.383 Å[g]
pc-1	1.3896	1.3833	1.3813	1.4058	1.3962	1.3973	
pc-2	1.3908	1.3818	1.3801	1.4100	1.3989	1.4000	
pc-3	1.3901	1.3812	1.3793	1.4097	1.3986	1.3996	
pc-4	1.3901	1.3812	1.3793	1.4097	1.3986	1.3996	
θ(HCF)							108.73°[g]
pc-1	109.01	109.02	109.08	109.09	109.17	109.16	
pc-2	108.77	108.99	108.98	108.68	108.85	108.82	
pc-3	108.74	108.96	108.96	108.61	108.79	108.77	
pc-4	108.74	108.96	108.96	108.60	108.78	108.76	

[a] Ref. [38]
[b] Ref. [39]
[c] Ref. [40]
[d] Ref. [41]
[e] Ref. [42]
[f] Ref. [43]
[g] Ref. [44]

N_2H_4 for B3P86; and the C-F bond in CH_3F for BLYP. For bond angles, the exceptions include: the O-O-O angle in O_3 for all functionals; the H-O-O angle in H_2O_2 and the H-O-F angle in HOF for all hybrid functionals; the H-N-N angle in N_2H_4 for all pure functionals. Additionally, the dihedral angle converges slightly slower than the bond angles. For example, the error at the pc-2 is about 2.5-5.6° for H_2O_2, but with the larger basis set, pc-3, the error reduces to 0.5°. Thus, it appears that at least a quadruple zeta level basis set should be used to reach convergence of the dihedral angle.

3.3.2. Atomic Energy

The total energies of hydrogen and four first-row atoms are listed in Table 3.2 with their respective Davidson energies.[45] Overall, B3PW91 results in the best agreement with Davidson energies for nitrogen, oxygen, and fluorine using the pc-3, or higher basis set. Differences of about 0.004 hartree for nitrogen, about 0.002 hartree for oxygen, and about 0.004 hartree for fluorine are observed. For the hydrogen, the smallest difference is about 0.0002 hartree using BP86 with the pc-2 or higher basis sets. Both BPW91 and BP86 result in an error of no more than 0.004 hartree for the carbon when using the pc-2 or higher basis sets. Interestingly, the B3LYP errors are higher for all atoms but hydrogen.

Table 3.2 Total energies for atoms given in hartrees.

Atom, Exact[a]	B3LYP	B3PW91	B3P86	BLYP	BPW91	BP86
H, -0.5000						
Pc-1	-0.501560	-0.503318	-0.517788	-0.497025	-0.503368	-0.499435
Pc-2	-0.502373	-0.504169	-0.518686	-0.497844	-0.504173	-0.500261
Pc-3	-0.502441	-0.504242	-0.518755	-0.497912	-0.504242	-0.500325
Pc-4	-0.502443	-0.504244	-0.518757	-0.497914	-0.504244	-0.500328
C, -37.8450						
Pc-1	-37.842664	-37.820473	-37.937183	-37.830160	-37.829578	-37.830061
Pc-2	-37.860248	-37.838120	-37.954632	-37.848005	-37.847249	-37.847539
Pc-3	-37.861659	-37.839734	-37.956220	-37.849372	-37.848739	-37.848998
Pc-4	-37.861739	-37.839849	-37.956343	-37.849439	-37.848827	-37.849086
N, -54.5893						
Pc-1	-54.576861	-54.555075	-54.692822	-54.562678	-54.567218	-54.566369
Pc-2	-54.604843	-54.583046	-54.720527	-54.591030	-54.595198	-54.594114
Pc-3	-54.606938	-54.585287	-54.722771	-54.593100	-54.597324	-54.596253
Pc-4	-54.607020	-54.585398	-54.722888	-54.593169	-54.597409	-54.596340
O, -75.067						
Pc-1	-75.052487	-75.021368	-75.184645	-75.041601	-75.040106	-75.043034
Pc-2	-75.097335	-75.066156	-75.228999	-75.087154	-75.085053	-75.087594
Pc-3	-75.100740	-75.069719	-75.232573	-75.090545	-75.088514	-75.091073
Pc-4	-75.100928	-75.069937	-75.232796	-75.090722	-75.088719	-75.091276
F, -99.734						
Pc-1	-99.706282	-99.668608	-99.857178	-99.696950	-99.692973	-99.698645
pc-2	-99.771357	-99.733290	-99.921270	-99.763174	-99.758048	-99.763177
pc-3	-99.776153	-99.738221	-99.926249	-99.768001	-99.762906	-99.768088
pc-4	-99.776360	-99.738449	-99.926480	-99.768196	-99.763124	-99.768302

[a] Reference [45]

3.3.3. Atomization Energy

As shown in Table 3.3, most of the atomization energies converge with respect to increasing size of the basis set. Basis set limits are nearly reached at the pc-3 level. The atomization energies of seven molecules were overestimated by B3LYP at the pc-4 level. In fact, the largest errors for B3LYP at the pc-4 level include O_3 (-5.70 kcal/mol), CO (-3.64 kcal/mol), HOF (-2.78 kcal/mol), CH_3NH_2 (2.45 kcal/mol), N_2H_4 (5.97 kcal/mol), and CH_3F (-4.36 kcal/mol). Unlike B3LYP, only the atomization energies of two molecules are overestimated by B3PW91 at the pc-4 level. The errors are 2.43 kcal/mol for CO_2 and 0.81 kcal/mol for N_2H_4. At the pc-4 level, molecules with atomization energies that are accurate to within 1 kcal/mol include: HCN (-0.90 kcal/mol), HNO (-0.80kcal/mol), H_2CO (-0.12 kcal/mol), CH_3NH_2 (-0.02 kcal/mol), and N_2H_4 (0.81 kcal/mol)**.** B3P86, BLYP, BPW91, and BP86 overestimate the atomization energy for most of molecules. The energies of those molecules are closest to experiment at the pc-1 level, with the energy deviating further from experiment with increasing basis set size. The atomization energy of CH_3NH_2 shows the maximum error for B3P86, while the maximum error for the three pure functionals arises from the atomization energy of O_3.

The irregular convergence problem noted in the study of DFT with the correlation consistent basis sets also occurs for the polarization consistent basis sets. The atomization energies of several molecules such as HF, HOF, F_2, CO, CO_2, and H_2CO have a slight dip at the pc-4 level. The dips (<0.05 kcal/mol) are much less pronounced than those observed for the correlation consistent basis sets. Interestingly, the irregular convergence behavior of F_2 observed with the correlation consistent basis sets in the last project does not occur when using the polarization consistent basis sets. A possible reason for this may be from the scheme in developing the polarization consistent basis sets, in which F_2 was used as a target molecule to

optimize the basis functions. However, the relative size of the basis sets should be considered when making this comparison. The primitive and contracted functions of hydrogen and four first-row atoms for each level of the two basis sets are provided in Table 3.4.

For hydrogen, the polarization consistent basis sets have the same or more contracted functions than the correlation consistent basis sets. This is also the case for the uncontracted functions. The difference between uncontracted functions in both basis sets becomes more substantial in the larger basis sets. For example, the polarization consistent basis sets have one additional primitive *p* function at the pc-3 level and two additional primitive *p* functions at the pc-4 level compared with the correlation consistent basis sets. The difference in both basis sets for first-row atoms is similar to that of hydrogen, except that the difference includes not only *s* and *p* functions, but also a higher angular momentum *d* function for both contracted and uncontracted functions. Considering that the correlation consistent basis sets and the polarization consistent basis sets were developed for *ab initio* and DFT, respectively, as well as the fact that DFT converges faster than *ab initio* methods, the difference in the composition of each type of basis set is surprising. However, it is this difference in composition that leads to a slightly better convergence behavior for the polarization consistent basis sets. Although neither of the sets is necessarily ideal for DFT since a slight energy dip still exists for the polarization consistent basis sets.

Table 3.3 Calculated atomization energy in kcal/mol. The difference in the atomization energy, relative to experiment, is reported in parentheses.

Molecules Expt.[a]	Basis Set	B3LYP	B3PW91	B3P86	BLYP	BPW91	BP86
O_3, 142.4	pc-1	126.95 (-15.45)	127.88 (-14.52)	137.57 (-4.83)	160.85 (18.45)	162.49 (20.09)	170.81 (28.41)
	pc-2	134.47 (-7.93)	137.00 (-5.40)	146.91 (4.51)	165.07 (22.67)	168.88 (26.48)	177.17 (34.77)
	pc-3	136.56(-5.84)	138.86 (-3.54)	148.86 (6.46)	166.79 (24.39)	170.46 (28.06)	178.85 (36.45)
	pc-4	136.70(-5.70)	138.96 (-3.44)	148.94 (6.54)	166.97 (24.57)	170.58 (28.18)	178.95 (36.55)
H_2, 103.3	pc-1	102.25(-1.05)	99.89 (-3.41)	104.64 (1.34)	101.14 (-2.16)	98.24 (-5.06)	104.03 (0.73)
	pc-2	103.74(0.44)	100.89 (-2.41)	105.61 (2.31)	102.97 (-0.33)	99.44 (-3.86)	105.23 (1.93)
	pc-3	104.01(0.71)	101.05 (-2.25)	105.82 (2.52)	103.28 (-0.02)	99.62 (-3.68)	105.46 (2.16)
	pc-4	104.02(0.72)	101.06 (-2.24)	105.82 (2.52)	103.29 (-0.01)	99.62 (-3.68)	105.47 (2.17)
H_2O, 219.4	pc-1	208.64(-10.76)	208.05 (-11.35)	216.97 (-2.43)	209.85 (-9.55)	209.64 (-9.76)	218.37 (-1.03)
	pc-2	216.87(-2.53)	215.17 (-4.23)	224.01 (4.61)	218.93 (-0.47)	217.40 (-2.00)	226.14 (6.74)
	pc-3	217.84(-1.56)	215.91 (-3.49)	224.74 (5.34)	220.15 (0.75)	218.33 (-1.07)	227.10 (7.70)
	pc-4	217.86(-1.54)	215.93 (-3.47)	224.75 (5.35)	220.19 (0.79)	218.36 (-1.04)	227.13 (7.73)
HF, 135.4	pc-1	126.96(-8.44)	127.05 (-8.35)	131.66 (-3.74)	128.22 (-7.18)	128.60 (-6.80)	132.95 (-2.45)
	pc-2	132.92(-2.48)	132.22 (-3.18)	136.74 (1.34)	134.85 (-0.55)	134.27 (-1.13)	138.63 (3.23)
	pc-3	133.57(-1.83)	132.73 (-2.67)	137.22 (1.82)	135.70 (0.30)	134.92 (-0.48)	139.27 (3.87)
	pc-4	133.57(-1.83)	132.72 (-2.68)	137.21 (1.81)	135.71 (0.31)	134.92 (-0.48)	139.27 (3.87)

-continue-

-continue-

Molecules Expt.[a]	Basis Set	B3LYP	B3PW91	B3P86	BLYP	BPW91	BP86
HCN, 302.5	pc-1	297.75(-4.75)	296.48 (-6.02)	306.00 (3.50)	305.04 (2.54)	304.73 (2.23)	313.09 (10.59)
	pc-2	303.11(0.61)	301.28 (-1.22)	310.96 (8.46)	310.26 (7.76)	309.34 (6.84)	317.79 (15.29)
	pc-3	303.58(1.08)	301.56 (-0.94)	311.26 (8.76)	310.78 (8.28)	309.69 (7.19)	318.17 (15.67)
	pc-4	303.61(1.11)	301.60 (-0.90)	311.29 (8.79)	310.85 (8.35)	309.78 (7.28)	318.24 (15.74)
CO, 256.2	pc-1	248.67(-7.53)	249.55 (-6.65)	254.98 (-1.22)	255.74 (-0.46)	257.76 (1.56)	261.81 (5.61)
	pc-2	251.91(-4.29)	252.26 (-3.94)	257.96 (1.76)	258.57 (2.37)	260.06 (3.86)	264.36 (8.16)
	pc-3	252.56(-3.64)	252.79 (-3.41)	258.48 (2.28)	259.20 (3.00)	260.60 (4.40)	264.89 (8.69)
	pc-4	252.56(-3.64)	252.78 (-3.42)	258.47 (2.27)	259.21 (3.01)	260.62 (4.42)	264.90 (8.70)
N_2, 225.1	pc-1	218.43(-6.67)	214.80 (-10.30)	222.72 (-2.38)	229.71 (4.61)	226.66 (1.56)	233.71 (8.61)
	pc-2	225.15(0.05)	221.43 (-3.67)	229.54 (4.44)	235.78 (10.68)	232.68 (7.58)	239.85 (14.75)
	pc-3	226.46(1.36)	222.49 (-2.61)	230.60 (5.50)	237.16 (12.06)	233.80 (8.70)	240.99 (15.89)
	pc-4	226.62(1.52)	222.64 (-2.46)	230.72 (5.62)	237.39 (12.29)	234.02 (8.92)	241.18 (16.08)
HNO, 196.9	pc-1	191.63(-5.27)	189.64 (-7.26)	199.73 (2.83)	204.06 (7.16)	202.67 (5.77)	212.07 (15.17)
	pc-2	197.00(0.10)	195.03 (-1.87)	205.22 (8.32)	208.77 (11.87)	207.52 (10.62)	216.97 (20.07)
	pc-3	198.20(1.30)	196.01 (-0.89)	206.20 (9.30)	209.98 (13.08)	208.53 (11.63)	218.01 (21.11)
	pc-4	198.30(1.40)	196.10 (-0.80)	206.28 (9.38)	210.13 (13.23)	208.66 (11.76)	218.13 (21.23)
H_2O_2, 252.3	pc-1	241.80(-10.50)	240.59 (-11.71)	253.34 (1.04)	251.98 (-0.32)	251.14 (-1.16)	263.26 (10.96)
	pc-2	249.93(-2.37)	248.42 (-3.88)	261.12 (8.82)	259.80 (7.50)	258.63 (6.33)	270.69 (18.39)
	pc-3	250.88(-1.42)	249.13 (-3.17)	261.85 (9.55)	260.83 (8.53)	259.43 (7.13)	271.52 (19.22)
	pc-4	250.89(-1.41)	249.13 (-3.17)	261.84 (9.54)	260.87 (8.57)	259.44 (7.14)	271.53 (19.23)

-continue-

-continue-

Molecules Expt.[a]	Basis Set	B3LYP	B3PW91	B3P86	BLYP	BPW91	BP86
HOF, 151.6	pc-1	143.61(-7.99)	142.30(-9.30)	150.47(-1.13)	155.44(3.84)	154.23(2.63)	161.89(10.29)
	pc-2	148.20(-3.40)	147.18(-4.42)	155.39(3.79)	159.17(7.57)	158.31(6.71)	165.95(14.35)
	pc-3	148.83(-2.77)	147.66(-3.94)	155.91(4.31)	159.78(8.18)	158.80(7.20)	166.47(14.87)
	pc-4	148.82(-2.78)	147.65(-3.95)	155.89(4.29)	159.78(8.18)	158.79(7.19)	166.46(14.86)
F_2, 36.9	pc-1	33.99(-2.91)	32.82(-4.08)	36.34(-0.56)	48.04(11.14)	46.70(9.80)	49.88(12.98)
	pc-2	35.08(-1.82)	34.99(-1.91)	38.67(1.77)	47.40(10.50)	47.37(10.47)	50.54(13.64)
	pc-3	35.66(-1.24)	35.54(-1.36)	39.27(2.37)	47.75(10.85)	47.75(10.85)	50.96(14.06)
	pc-4	35.69(-1.21)	35.55(-1.35)	39.28(2.38)	47.77(10.87)	47.73(10.83)	50.95(14.05)
CO_2, 381.9	pc-1	375.57(-6.33)	379.34(-2.56)	388.60(6.70)	389.63(7.73)	395.64(13.74)	401.96(20.06)
	pc-2	380.24(-1.66)	383.87(1.97)	393.49(11.59)	392.82(10.92)	398.99(17.09)	405.51(23.61)
	pc-3	380.94(-0.96)	384.37(2.47)	394.05(12.15)	393.36(11.46)	399.40(17.50)	405.98(24.08)
	pc-4	380.90(-1.00)	384.33(2.43)	394.00(12.10)	393.36(11.46)	399.40(17.50)	405.96(24.06)
H_2CO, 357.3	pc-1	351.95(-5.35)	352.73(-4.57)	364.25(6.95)	356.92(-0.38)	358.95(1.65)	369.18(11.88)
	pc-2	356.73(-0.57)	356.76(-0.54)	368.53(11.23)	361.53(4.23)	362.80(5.50)	373.27(15.97)
	pc-3	357.38(0.08)	357.18(-0.12)	368.98(11.68)	362.23(4.93)	363.25(5.95)	373.77(16.47)
	pc-4	357.39(0.09)	357.18(-0.12)	368.97(11.67)	362.25(4.95)	363.29(5.99)	373.80(16.50)
CH_3NH_2, 542.5	pc-1	534.54(-7.96)	533.97(-8.53)	556.04(13.54)	532.47(-10.03)	533.20(-9.30)	554.59(12.09)
	pc-2	543.72(1.22)	541.64(-0.86)	563.78(21.28)	542.52(0.02)	541.48(-1.02)	563.02(20.52)
	pc-3	544.85(2.35)	542.38(-0.12)	564.57(22.07)	543.87(1.37)	542.41(-0.09)	564.03(21.53)
	pc-4	544.95(2.45)	542.48(-0.02)	564.65(22.15)	544.01(1.51)	542.56(0.06)	564.17(21.67)

-continue-

-continue-

Molecules Expt.[a]	Basis Set	B3LYP	B3PW91	B3P86	BLYP	BPW91	BP86
CH_3OH, 480.9	pc-1	470.73(-10.17)	471.56 (-9.34)	489.57 (8.67)	470.37 (-10.53)	472.53 (-8.37)	489.54 (8.64)
	pc-2	479.02(-1.88)	478.59 (-2.31)	496.73 (15.83)	479.17 (-1.73)	479.90 (-1.00)	497.11 (16.21)
	pc-3	480.07(-0.83)	479.27 (-1.63)	497.46 (16.56)	480.41 (-0.49)	480.74 (-0.16)	498.03 (17.13)
	pc-4	480.10(-0.80)	479.29 (-1.61)	497.47 (16.57)	480.47 (-0.43)	480.80 (-0.10)	498.08 (17.18)
N_2H_4, 405.5	pc-1	398.16(-7.34)	394.61 (-10.89)	415.69 (10.19)	401.74 (-3.76)	398.79 (-6.71)	419.50 (14.00)
	pc-2	409.93(4.43)	405.14 (-0.36)	426.12 (20.62)	414.26 (8.76)	409.88 (4.38)	430.61 (25.11)
	pc-3	411.34(5.84)	406.18 (0.68)	427.18 (21.68)	415.93 (10.43)	411.15 (5.65)	431.93 (26.43)
	pc-4	411.47(5.97)	406.31 (0.81)	427.29 (21.79)	416.12 (10.62)	411.34 (5.84)	432.1 (26.60)
CH_3F, 402.4	pc-1	391.69(-10.71)	392.36 (-10.04)	405.94 (3.54)	391.95 (-10.45)	393.66 (-8.74)	406.24 (3.84)
	pc-2	397.32(-5.08)	397.09 (-5.31)	410.90 (8.50)	397.69 (-4.71)	398.41 (-3.99)	411.28 (8.88)
	pc-3	398.03(-4.37)	397.52 (-4.88)	411.36 (8.96)	398.54 (-3.86)	398.95 (-3.45)	411.88 (9.48)
	pc-4	398.04 (-4.36)	397.53 (-4.87)	411.36 (8.96)	398.57 (-3.83)	398.98 (-3.42)	411.90 (9.50)

[a] Experimental data are from reference [46]

Table 3.4 A comparison of primitive and contracted basis set size for correlation consistent and polarization consistent basis sets for hydrogen and the first row atoms, boron through neon.

Basis Set	Hydrogen		First Row Atoms	
	Primitive	Contracted	Primitive	Contracted
cc-pVDZ	4*s*1*p*	2*s*1*p*	9*s*4*p*1*d*	3*s*2*p*1*d*
cc-pVTZ	5*s*2*p*1*d*	3*s*2*p*1*d*	10*s*5*p*2*d*1*f*	4*s*3*p*2*d*1*f*
cc-pVQZ	6*s*3*p*2*d*1*f*	4*s*3*p*2*d*1*f*	12*s*6*p*3*d*2*f*1*g*	5*s*4*p*3*d*2*f*1*g*
cc-pV5Z	8*s*4*p*3*d*2*f*1*g*	5*s*4*p*3*d*2*f*1*g*	14*s*8*p*4*d*3*f*2*g*1*h*	6*s*5*p*4*d*3*f*2*g*1*h*
pc-1	4*s*1*p*	2*s*1*p*	7*s*4*p*1*d*	3*s*2*p*1*d*
pc-2	6*s*2*p*1*d*	3*s*2*p*1*d*	10*s*6*p*2*d*1*f*	4*s*3*p*2*d*1*f*
pc-3	9*s*4*p*2*d*1*f*	5*s*4*p*2*d*1*f*	14*s*9*p*4*d*2*f*1*g*	6*s*5*p*4*d*2*f*1*g*
pc-4	11*s*6*p*3*d*2*f*1*g*	7*s*6*p*3*d*2*f*1*g*	18*s*11*p*6*d*3*f*2*g*1*h*	8*s*7*p*6*d*3*f*2*g*1*h*

3.3.4. Statistical Analysis

The mean errors (ME) and mean absolute errors (MAE) of the atomization energy are shown in Table 3.5. For B3LYP and B3PW91, the MAE decreases as the basis set size increases, with the smallest MAEs being 2.19 and 2.23 kcal/mol, respectively. The other four density functionals follow a reverse trend: the MAE increases as the basis set size increases. B3P86 results are in best agreement with experiments at the pc-1 level, while the MAEs worsen when a larger basis set is used. BP86 overestimates almost all atomization energies, which leads to similar MEs and MAEs for each basis set level.

The MAEs of the atomization energies for the correlation consistent basis sets are also summarized in Table 3.5 for comparison with the polarization consistent basis sets. Although the difference in composition is substantial, similar performance is achieved for both basis sets, and both basis sets converge to the same basis set limit. However, the MAEs are slightly less for the polarization consistent basis sets than for the correlation consistent basis sets. For example, the differences in MAE between pc-4 and cc-pV5Z are 0.03 kcal/mol for B3LYP and 0.08 kcal/mol for B3PW91.

The normal distributions for the atomization energy as compared with experimens are plotted in Figure 3.1 for the six density functionals with the polarization consistent basis sets. The advantage of the normal distribution is its ability to assess the precision (width of the peak) and the accuracy (location of the peak with respect to experiment) through visualization. The normal distribution curves for the polarization consistent basis sets are similar to those for the correlation consistent basis sets. For the hybrid functionals B3LYP and B3PW91, the peak narrows and moves towards to experiment as the basis set size increase. Thus, both the accuracy and the precision are improved. The normal distribution of B3P86 differs from other hybrid

functionals: the width of peak remains unchanged and the location of the peak moves further away from experiment when increasing the basis set size. Unlike B3LYP and B3PW91, the normal distributions of all pure functionals are not sensitive to basis set choice. Increasing the basis set size does not change the wide error distribution (~40 kcal/mol) and the location of the peak.

3.3.5. Kohn-Sham Limit

Since B3LYP and B3PW91 result in the smallest MAEs in the atomization energies compared with experiment at the pc-4 level, these two functionals were used to extrapolate to the KS limit. The two empirical extrapolation schemes, which were outlined in the previous project description, were used to obtain KS limits and are listed in Table 3.6 and 3.7. The notations for the different extrapolation methods are: the exponential scheme KS_{1234} using pc-1, pc-2, pc-3, and pc-4; the exponential scheme KS_{123} using pc-1, pc-2, and pc-3; the exponential scheme KS_{234} using pc-2, pc-3, and pc-4; the two-point scheme KS_{12} using pc-1 and pc-2; and the two-point scheme KS_{23} using pc-2 and pc-3.

For all extrapolation methods, KS_{23} provides the best agreement with experiment for B3LYP, with a deviation of 2.07 kcal/mol, which was only 0.12 kcal/mol less than the MAE at the pc-4 level. The KS_{12} method is the only one in which the MAE of extrapolation is higher than the pc-4 level for B3LYP. However, it does perform best for B3PW91, with an extrapolated atomization energy that is 0.47 kcal/mol lower than the MAE at the pc-4 level. Different from the two-point scheme, whose performance depends on the individual functional, the exponential schemes perform consistently. A slight improvement is always achieved for exponential methods, no matter whether B3LYP or B3PW91 is used.

Figure 3.1 Normal distribution of the errors in the atomization energies with respect to experiment (the "0") for DFT methods B3LYP (a), BLYP (b), B3PW91 (c), BPW91 (d), B3P86 (e), and BP86 (f) with the pc-X basis sets.

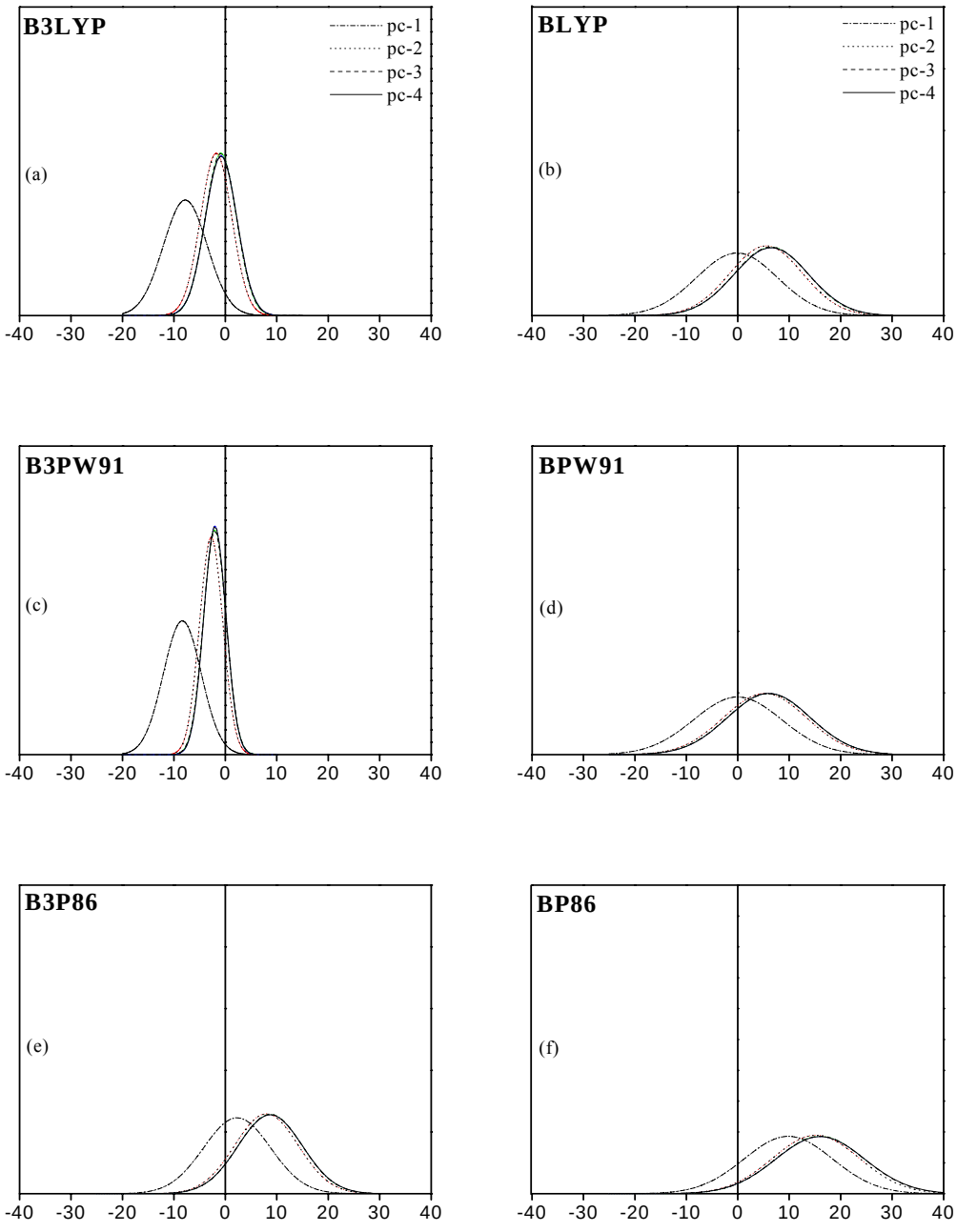

Table 3.5 Mean absolute errors (MAE) and mean errors (ME) for the atomization energies in kcal/mol.

Basis set	B3LYP	B3PW91	B3P86	BLYP	BPW91	BP86
MAE						
pc-1	7.60	8.17	4.38	6.49	6.77	10.43
pc-2	2.39	2.80	8.18	6.63	7.00	15.39
pc-3	2.17	2.25	8.89	7.16	7.25	16.16
pc-4	2.19	2.23	8.92	7.22	7.28	16.21
ME						
pc-1	-7.60	-8.17	2.46	0.03	0.18	10.02
pc-2	-1.60	-2.57	8.18	5.70	5.46	15.39
pc-3	-0.70	-1.88	8.89	6.66	6.19	16.16
pc-4	-0.65	-1.84	8.92	6.73	6.25	16.21
MAE						
cc-pVDZ	8.09	8.96	3.40	7.91	8.11	10.86
cc-pVTZ	2.36	3.24	7.68	7.18	7.37	15.24
cc-pVQZ	2.19	2.38	8.68	7.32	7.46	16.11
cc-pV5Z	2.22	2.31	8.81	7.15	7.28	16.12
ME						
cc-pVDZ	-8.09	-8.96	1.49	0.33	0.07	9.86
cc-pVTZ	-1.88	-3.01	7.68	5.79	5.33	15.24
cc-pVQZ	-0.85	-2.05	8.68	6.70	6.19	16.11
cc-pV5Z	-0.76	-1.95	8.81	6.65	6.16	16.12

3.4. Conclusions

For all density functionals studied, the geometries are nearly converged at the pc-2 level. However, a basis set of at least pc-3 should be used to reach near convergence for the atomization energy. In general, the polarization consistent basis sets have more contracted and uncontracted functions than the correlation consistent basis sets, especially for the larger basis sets. This difference helps to lead to a slightly better convergence behavior for the polarization consistent basis sets with DFT. However, an unusual convergence problem, observed in the earlier study with the correlation consistent basis sets, occurs for the polarization consistent basis

sets as well, though the energy dip at the pc-4 level is less pronounced. The B3LYP and B3PW91 functionals perform best, with a MAE of ~2 kcal/mol for atomization energies. The normal distribution of atomization energies for the six functionals shows that, for B3LYP and B3PW91, both the accuracy and the precision are improved as the basis set size increases. However, no improvement was observed for pure functionals with respect to basis set size.

Table 3.6 Kohn-Sham atomization energy limits and mean absolute errors for B3LYP determined using the pc-X basis sets and several different extrapolation schemes. The energies are reported in kcal/mol.

Molecules	KS_{1234}	KS_{123}	KS_{234}	KS_{12}	KS_{23}	Expt. [a]
O_3	136.80	137.36	136.71	137.64	138.08	142.4
H_2	104.04	104.07	104.02	104.36	104.21	103.3
H_2O	217.91	217.97	217.86	220.34	218.55	219.4
HF	133.61	133.65	133.57	135.43	134.05	135.4
HCN	303.63	303.62	303.62	305.37	303.92	302.5
CO	252.60	252.73	252.56	253.27	253.04	256.2
N_2	226.65	226.78	226.64	227.98	227.42	225.1
HNO	198.35	198.55	198.31	199.27	199.08	196.9
H_2O_2	250.93	251.00	250.89	253.36	251.56	252.3
HOF	148.86	148.92	148.82	150.14	149.28	151.6
F_2	35.72	36.32	35.69	35.53	36.08	36.9
CO_2	381.07	381.07	380.92	382.20	381.46	381.9
H_2CO	357.43	357.49	357.39	358.74	357.86	357.3
CH_3NH_2	544.79	544.81	544.76	547.39	545.48	542.5
CH_3OH	480.26	480.32	480.20	482.62	480.93	480.9
N_2H_4	411.51	411.52	411.48	414.89	412.36	405.5
CH_3F	398.09	398.14	398.04	399.69	398.56	402.4
MAE	2.17	2.10	2.19	2.48	2.07	

[a] Experimental values are from reference [46]

Table 3.7 Kohn-Sham atomization energy limits and mean absolute errors for B3PW91 determined using the pc-X basis sets and several different extrapolation schemes. The energies are reported in kcal/mol.

Molecules	KS_{1234}	KS_{123}	KS_{234}	KS_{12}	KS_{23}	Expt. [a]
O_3	139.05	139.34	138.97	140.84	140.22	142.4
H_2	101.07	101.09	101.06	101.31	101.18	103.3
H_2O	215.95	216.00	215.93	218.17	216.46	219.4
HF	132.74	132.78	132.72	134.39	133.10	135.4
HCN	301.59	301.58	301.61	303.31	301.76	302.5
CO	252.82	252.92	252.79	253.40	253.17	256.2
N_2	222.65	222.69	222.66	224.22	223.26	225.1
HNO	196.12	196.22	196.11	197.30	196.72	196.9
H_2O_2	249.15	249.20	249.13	251.72	249.64	252.3
HOF	147.68	147.72	147.66	149.23	148.02	151.6
F_2	35.59	35.73	35.55	35.90	35.94	36.9
CO_2	384.43	384.43	384.35	385.78	384.73	381.9
H_2CO	357.20	357.23	357.18	358.46	357.48	357.3
CH_3NH_2	542.26	542.26	542.29	544.67	542.72	542.5
CH_3OH	479.40	479.44	479.39	481.65	479.87	480.9
N_2H_4	406.30	406.29	406.33	409.57	406.94	405.5
CH_3F	397.53	397.56	397.53	399.08	397.83	402.4
MAE	2.21	2.16	2.22	1.76	1.93	

[a] Experimental values are from reference [46]

CHAPTER 4

THE PERFORMANCE OF DENSITY FUNCTIONALS WITH RESPECT TO BASIS SET: BASIS SET CONTRACTION AND UNCONTRACTION

4.1 Introduction

In our earlier work (Chapter 2), several density functionals in conjunction with the correlation consistent basis sets were used to determine the structures and energies of a series of 17 molecules.[62] The convergence of the atomization energies toward the Kohn-Sham limit with respect to increasing basis set size was examined. We noted irregular convergence of atomization energies as the basis set size increases for a number of widely used density functionals. A similar problem was also observed in a previous study by Sekusak and Frenking, in which reaction enthalpies of the hydrogenation reaction of N_2 were determined using several functionals.[33] A possible reason for this irregular convergence has been attributed to the construction of the correlation consistent basis sets, considering that the basis sets were optimized using CISD,[15] and it is not clear whether basis sets, derived from an *ab initio* method, are optimal for use with density functional theory. To understand this issue further, recently developed basis sets, the polarization consistent basis sets,[56, 58] have been utilized to carry out a parallel study (Chapter 3) to our correlation consistent benchmark study (Chapter 2). Analogous to the correlation consistent basis sets, the polarization consistent basis sets are

comprised of a systematically constructed series of basis sets, but they were optimized explicitly for density functional theory. As compared with the correlation consistent basis sets, the polarization consistent basis sets improve the irregular convergence problem of energetic properties with respect to increasing basis set size noted in our earlier studies, though it is not the solution for all irregular convergence cases noted previously. This improvement is partly related to the size of the polarization consistent basis sets, which have more basis functions than the correlation consistent basis sets at the triple-, quadruple-, and quintuple-zeta levels.

As addressed in the introduction to this thesis (Chapter 1), the correlation consistent basis sets may be a potential means to understand the performance of density functionals and develop a hierarchy of density functional approaches. Therefore, it is important to understand the underlying non-convergent behavior of energetics with respect to increasing size of the correlation consistent basis set. One possible reason is grid size. Inappropriate selection of grid size could result in unusual behavior of molecular properties. However, our calculations have ruled it out as a cause of the irregular convergence. Several other possibilities that could lead to the irregular convergence have been investigated. In this study, we will focus on the contraction of the basis sets.

Basis set contraction has been utilized in almost all popular basis sets. Through the contraction of some of the basis functions that are important in the description of energetic properties, but not important in the description of bonding, the efficiency of a calculation can be improved. In general, basis functions that describe core electrons are contracted, as core electrons are important in the overall energetics, but are less important in chemical bonding. The basis functions needed for the description of core electrons consist of a large number of functions, which play a critical role in describing the cusp that exists in the wavefunction near

the nucleus. However, as a consequence of contraction, the basis sets are less flexible, and there is often a slight increase in total energy.

Generally, two types of contraction schemes are used in the construction of basis sets: the general contraction scheme[63] and the segmented contraction scheme. In the general contraction scheme, each contracted basis function contains almost all the primitive functions. A typical example of a basis set, in which the general contraction scheme has been employed, is the correlation consistent basis set. In the segmented contraction scheme, the primitive functions included in the contracted function are different for each contracted basis function. A typical example is Dunning's [5s3p] basis set.[64]

In this study, we investigated the impact of basis set contraction on the convergence behavior of atomization energy. The performance of two density functionals, B3LYP and BLYP, is evaluated with respect to increasing size of the correlation consistent basis sets. Several different contraction schemes are examined.

4.2 Methodology

Two density functionals, BLYP and B3LYP, were selected based upon our previous work, and were used to investigate the effect of basis set uncontraction on convergence of atomization energies. In our previous study, irregular convergence of atomization energies with respect to increasing size of the correlation consistent basis set was observed for a number of molecules. Though irregular convergence of the atomization energies has been observed using all functionals studied to date, we narrow our focus to BLYP and B3LYP in this investigation, as they are representative examples of functional performance. As in our first and second chapters, the calculations are carried out on the same 17 closed-shell first-row molecules.

Table 4.1 The composition of primitive and contracted basis set size for correlation consistent for hydrogen and the first row atoms, boron through neon.

Basis Set	Hydrogen		First Row Atoms	
	Primitive	Contracted	Primitive	Contracted
cc-pVDZ	4*s*1*p*	2*s*1*p*	9*s*4*p*1*d*	3*s*2*p*1*d*
cc-pVTZ	5*s*2*p*1*d*	3*s*2*p*1*d*	10*s*5*p*2*d*1*f*	4*s*3*p*2*d*1*f*
cc-pVQZ	6*s*3*p*2*d*1*f*	4*s*3*p*2*d*1*f*	12*s*6*p*3*d*2*f*1*g*	5*s*4*p*3*d*2*f*1*g*
cc-pV5Z	8*s*4*p*3*d*2*f*1*g*	5*s*4*p*3*d*2*f*1*g*	14*s*8*p*4*d*3*f*2*g*1*h*	6*s*5*p*4*d*3*f*2*g*1*h*

As has been discussed in the introduction to this chapter, the general contraction scheme is used in the correlation consistent basis sets. As seen in Table 4.1, for the cc-pVDZ basis set of non-hydrogen atoms, the general contraction of the 9*s*4*p* primitive functions contracts to [2*s*1*p*] and keeps the outermost primitive *s* and *p* function uncontracted (each contracted *s* function comes from the same nine *s* primitive functions, and each contracted *p* function comes from the same four *p* primitive functions). As a result, the *sp* part of cc-pVDZ is [3*s*2*p*] and the contraction can be denoted as {9,9,1/4,1} (in this notation, before "/", two "9"s are the number of primitive *s* functions in the first and second contracted *s* functions, respectively, and "1" is the number of primitive *s* functions in the third contracted *s* function. Likewise, after "/", "4" is the number of primitive *p* functions in the first contracted *p* function and "1" is the number of *p* functions in the second contracted *p* function) for *s* and *p* functions, respectively. The primitive functions that are contracted are weighted with contraction coefficients, which are taken from the atomic orbital coefficients for the 1*s*, 2*s* and 2*p* atomic orbital at the Hartree-Fock level. The cc-pVTZ contracts 10*s*5*p* to [2*s*1*p*] and leaves the first and third outermost *s* and two outermost *p* primitive functions uncontracted, with a contraction {10,10,1,1/5,1,1},which forms a *sp* part of

[4*s*3*p*]. Likewise, the contractions for cc-pVQZ and cc-pV5Z are {12,12,1,1,1/6,1,1,1} with three outermost *s* and *p* primitive functions uncontracted and {14,14,1,1,1,1/8,1,1,1,1} with four outermost *s* and *p* primitive functions uncontracted, respectively. Finally, the polarization functions with high angular momentum (*d*, *f*, *g*, *h*), which are optimized from CISD methods, (1*d*) for cc-pVDZ, (2*d*1*f*) for cc-pVTZ, (3*d*2*f*1*g*) for cc-pVQZ, and (4*d*3*f*2*g*1*h*) for cc-pV5Z, are combined with the *sp* part to form the standard correlation consistent basis sets. The basis sets for hydrogen atom take the similar contraction scheme, with the difference in that only *s* primitive functions are contracted and all *p* functions keep uncontracted.

In this study, the standard correlation consistent basis sets are uncontracted according to several different procedures. The first type of uncontraction is a complete uncontraction of the *s* and *p* contracted functions, resulting in (9*s*4*p*1*d*) for cc-pVDZ, (10*s*5*p*2*d*1*f*) for cc-pVTZ, (12*s*6*p*3*d*2*f*1*g*) for cc-pVQZ, and (14*s*8*p*4*d*3*f*2*g*1*h*) for cc-pV5Z. A second type of uncontraction involves only the uncontraction of the *s* functions, with the contracted *p* functions unchanged. For the contracted *s* functions, the outermost primitive function was uncontracted first, and then continuing inward until the basis set is completely uncontracted. For example, the resulting contraction scheme from partially uncontracting cc-pVDZ include: {8,8,1}, {7,7,1,1}, {6,6,1,1,1}, {5,5,1,1,1,1} and so on. When the first primitive *s* function is uncontracted from cc-pVDZ, it is the exactly same uncontracted *s* function already included in the standard cc-pVDZ set. Thus, the first uncontracted function is removed from the basis set in order to avoid having multi basis functions with same exponents in the calculations, and the contraction scheme is {8,8,1} rather than {8,8,1,1}.

We performed single point energy calculations on atoms and molecules with each partially uncontracted basis set. Same to the calculations in previous chapters, all single point

energy calculations request the full convergence by setting the convergence criteria to 10^{-8} on density. The energy calculations on the molecules, which used the uncontracted basis sets, were based on the structure optimized using the standard correlation consistent basis sets since the partially uncontracted basis sets cause very little effect on the optimized geometries of the molecules. All calculations were carried out using the Gaussian 98 package.

4.3 Results and Riscussion

4.3.1 The Contraction Errors of DFT with the Correlation Consistent Basis Sets

As shown in Tables 4.2 and 4.3, atomic energies for H, C, N, O, and F, and atomization energies of several molecules (N_2, CO, O_3, H_2O, and HCN) were calculated using BLYP with the standard correlation consistent basis sets and with the basis sets uncontracted as discussed in the previous section. The molecules were chosen due to the convergence behaviors of their atomization energies with respect to increasing basis set size observed in earlier studies by Wang and Wilson.[62] For the hybrid functional B3LYP, the atomization energies of H_2O and N_2 converge smoothly as the basis set size increases, while a slight energy dip occurs at the quintuple zeta level for CO, O_3, and HCN. When the pure functional BLYP is used, irregular convergence even gets worse, with an energy dip at the quintuple zeta level for N_2, CO, and HCN and an irregular convergent behavior for O_3. The contraction errors in the energies relative to the energies calculated using the standard contracted correlation consistent basis sets are also summarized in the tables. Overall, the contraction error is generally small for both the atomic energy and the atomization energies for higher-level basis sets, but more substantial at the double and triple zeta levels. For example with the F atom, the contraction error of the atomic energy is –6.07 mH at the double zeta level, and is decresed to –0.33 mH at the quintuple zeta level. For

H_2O, the contraction error of the atomization enery is 3.74 kcal/mol at the double-zeta level, while the contraction error is reduced to zero at the quadruple zeta level. As seen in Table 4.3, the completely uncontracted basis set cannot improve the convergence behavior of the atomization energy. The only change arises for O_3. For completely uncontracted basis sets, the O_3 atomization energies at the double-zeta level is smaller than that at the triple-zeta level, whereas the atomization energy at double-zeta level is larger than that at the triple-zeta level for the standard correlation consistent basis sets.

Table 4.2 The effect of the uncontraction of the correlation consistent basis sets on the BLYP atomic energies. The atomic energies are reported in Hartree (E_h), while the change in the atomic energy arising from use of the uncontracted basis set is reported in millihartree (mE_h).

Basis Set	Composition	H	C	N	O	F
cc-pVDZ	[3*s*2*p*1*d*]	0.496403	37.837836	54.572571	75.054526	99.713359
ΔE (mE_h)	(9*s*4*p*1*d*)	-0.4045	-3.1910	-4.2740	-5.1109	-6.0698
cc-pVTZ	[4*s*3*p*2*d*1*f*]	0.497555	37.845501	54.586935	75.080286	99.752932
ΔE (mE_h)	(10*s*5*p*2*d*1*f*)	-0.0023	-1.0752	-1.1069	-1.1206	-1.1700
cc-pVQZ	[5*s*4*p*3*d*2*f*1*g*]	0.497781	37.847806	54.590896	75.087251	99.763470
ΔE (mE_h)	(12*s*6*p*3*d*2*f*1*g*)	-0.0003	-0.9532	-0.9694	-0.9689	-0.9888
cc-pV5Z	[6*s*5*p*4*d*3*f*2*g*1*h*]	0.497889	37.849077	54.592689	75.090069	99.767416
ΔE (mE_h)	(14*s*8*p*4*d*3*f*2*g*1*h*)	-0.0005	-0.2462	-0.2772	-0.3121	-0.3260

Table 4.3 The effect of the contraction of the correlation consistent basis sets on the BLYP atomization energies (in kcal/mol). Both the atomization energies and the change in atomization energy arising from the uncontraction are reported in kcal/mol

Basis Set	Composition	N_2	CO	O_3	H_2O	HCN
cc-pVDZ	[3*s*2*p*1*d*]	231.22	256.35	168.32	207.84	303.84
	{9*s*4*p*1*d*}	232.84	258.34	166.72	211.58	307.48
ΔE (kcal/mol)	{9*s*4*p*1*d*}	+1.62	+1.99	-1.60	+3.74	+3.64
cc-pVTZ	[4*s*3*p*2*d*1*f*]	236.49	259.25	166.96	216.81	310.36
	{10*s*5*p*2*d*1*f*}	236.83	259.72	167.91	216.98	310.82
ΔE (kcal/mol)	{10*s*5*p*2*d*1*f*}	+0.34	+0.47	+0.95	+0.17	+0.46
cc-pVQZ	[5*s*4*p*3*d*2*f*1*g*]	237.27	259.76	167.28	218.91	311.21
	{12*s*6*p*3*d*2*f*1*g*}	237.29	259.73	167.36	218.91	311.22
ΔE (kcal/mol)	{12*s*6*p*3*d*2*f*1*g*}	+0.02	-0.03	+0.08	0	+0.1
cc-pV5Z	[6*s*5*p*4*d*3*f*2*g*1*h*]	237.19	259.26	166.79	219.81	310.92
	{14*s*8*p*4*d*3*f*2*g*1*h*}	237.21	259.28	166.81	219.81	310.94
ΔE (kcal/mol)	{14*s*8*p*4*d*3*f*2*g*1*h*}	+0.02	+0.02	+0.02	0	+0.02

As discussed, an uncontraction of only the *s* functions was also examined, and the results for atomization energies are presented in Table 4.4. This uncontraction seems to have an effect upon the convergence behavior of the atomization energy, although the contraction error is still small. The impact is reflected as a decrease in the atomization energy at the quadruple-zeta level, while there is little change at the quintuple-zeta level. As a result, the energy dip at the quintuple-zeta level present with the contracted sets was reduced or eliminated with the uncontracted sets. For example, using BLYP in combination with the uncontracted sets results in a well-behaved convergence occurs for N_2 and a reduced energy dip for HCN. Furthermore, the irregular convergence of O_3 atomization energy is improved, although the convergence is still not smooth.

Table 4.4 The effect of the uncontraction of s functions on the BLYP atomization energy (in kcal/mol). Both the atomization energies and the change in atomization energy arising from the uncontraction are reported in kcal/mol

Basis Set	Composition	N_2	CO	O_3	H_2O	HCN
cc-pVDZ	[3*s*2*p*1*d*]	231.22	256.35	168.32	207.84	303.84
	9s2p1d	231.04	256.18	168.58	210.81	304.55
ΔE (kcal/mol)	*9s2p1d*	-0.18	-0.17	0.26	2.97	0.71
cc-pVTZ	[4*s*3*p*2*d*1*f*]	236.49	259.25	166.96	216.81	310.36
	10s3p2d1f	236.55	259.46	167.38	216.87	310.46
ΔE (kcal/mol)	*10s3p2d1f*	0.06	0.21	0.42	0.06	0.1
cc-pVQZ	[5*s*4*p*3*d*2*f*1*g*]	237.27	259.76	167.28	218.91	311.21
	12s4p3d2f1g	237.09	259.60	167.10	218.82	310.93
ΔE (kcal/mol)	*12s4p3d2f1g*	-0.18	-0.16	-0.18	-0.09	-0.28
cc-pV5Z	[6*s*5*p*4*d*3*f*2*g*1*h*]	237.19	259.26	166.79	219.81	310.92
	14s5p4d3f2g1h	237.13	259.22	166.73	219.78	310.86
ΔE (kcal/mol)	*14s5p4d3f2g1h*	-0.06	-0.04	-0.06	-0.03	-0.06

4.3.2 The Effect of Basis Set Uncontraction on the Atomic Energy

In order to better understand the impact of the uncontraction of the *s* sets on the convergence of atomization energy, the variation of atomic energy with respect to the number of uncontracted *s* functions was examined. Figure 4.1 and Figure 4.2 illustrate the total energy of N and N_2 for each partially uncontracted basis sets, respectively. For double-, triple-, and quadruple-zeta level basis sets, the total energy decreases as the first several *s* functions are uncontracted. The lowest atomic energy was observed as the fifth *s* primitive function is uncontracted. After that, the energy remains constant. In contrast to the behavior noted for the other level of basis sets, little change occurs in the atomic energy with the quintuple-zeta level basis set. As a result, there is a faster convergence of the atomic energy for the uncontracted basis set than for the standard basis sets. As a test of the convergence rate, we calculated the difference between two atomic energies calculated with two next basis set levels, and listed them in Table 4.5. The data in Table 4.5 demonstrates that acceleration of the convergence is mainly expressed at the quadruple- and quintuple-zeta levels since the atomic energy at the quintuple-zeta level is insensitive to the basis set uncontraction. Considering that the energy dip observed in earlier work occurs at the quintuple-zeta level, it indicates that uncontraction may help to remedy the irregular convergence problem. Unfortunately, this does not occur for all molecules.

Figure 4.1 The effect of the uncontraction of inner *s* functions on the total energy of the N atom. "0*s*" represents the standard cc-pVxZ basis set. "1*s*" represents the partially uncontracted basis sets with one s primitive function uncontracted and the other primitive functions contracted. "2*s*" represents the basis set with two s primitive functions uncontracted, …

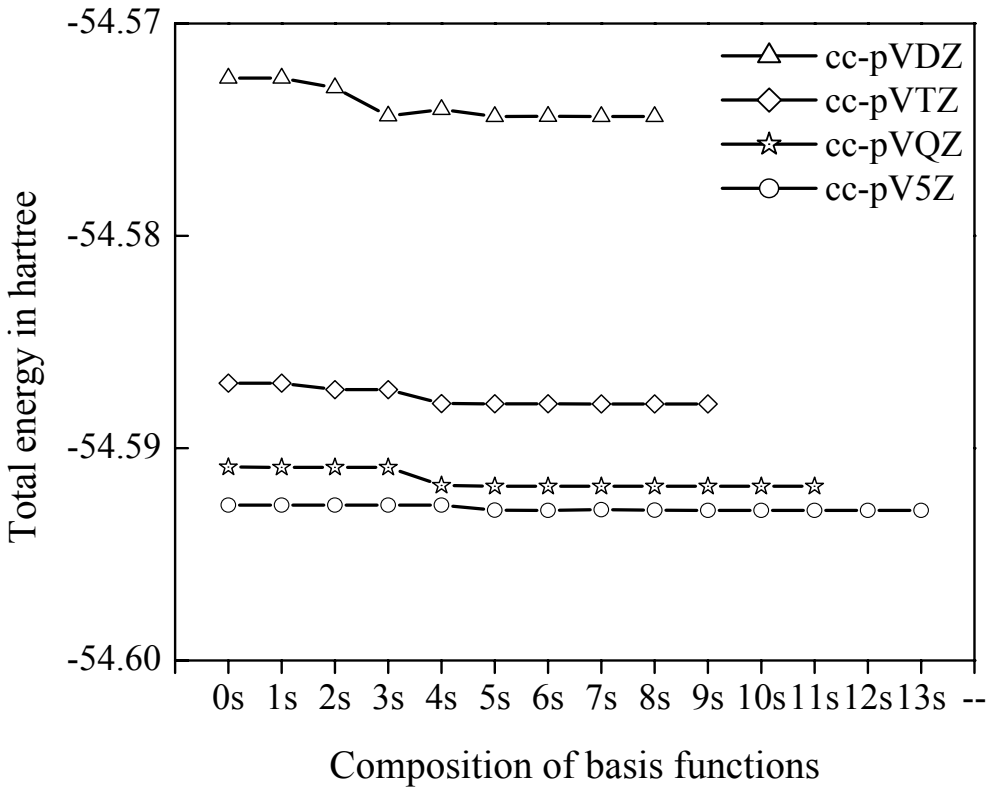

Figure 4.2 The effect of the uncontraction of inner *s* functions on the total energy of the N_2 molecule. "0*s*" represents the standard cc-pVxZ basis set. "1*s*" represents the partially uncontracted basis sets with one s primitive function uncontracted and the other primitive functions contracted. "2*s*" represents basis set with two primitive functions uncontracted, …

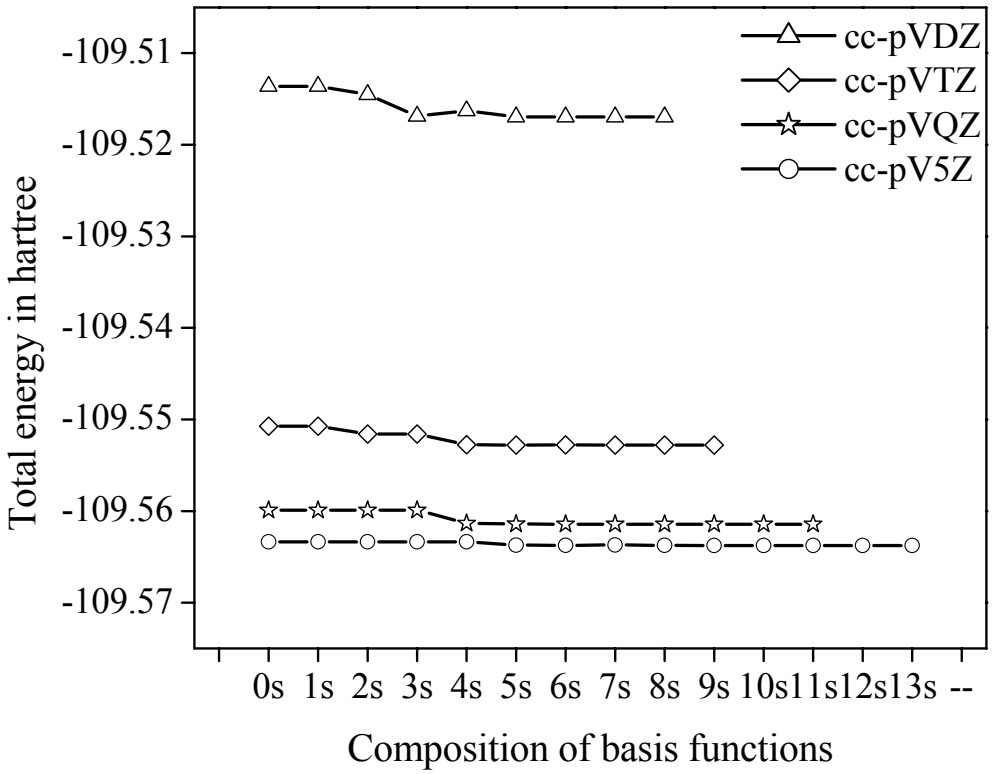

Table 4.5 The effect of contraction on the difference in total energies (kcal/mol) between the sequential levels of basis sets. DT represents the difference in energy between cc-pVDZ and cc-pVTZ, TQ represents the difference in energy between cc-pVTZ and cc-pVQZ, …

Basis Set	N_2			N			2N
	DT	TQ	Q5	DT	TQ	Q5	Q5
0s	23.29	5.75	2.17	9.01	2.49	1.13	2.25
1s	23.29	5.75	2.17	9.01	2.49	1.13	2.25
2s	23.27	5.21	2.17	8.92	2.29	1.13	2.25
3s	21.79	5.21	2.17	8.09	2.29	1.13	2.25
4s	22.90	5.37	1.28	8.70	2.42	0.59	1.17
5s	22.49	5.42	1.45	8.49	2.44	0.71	1.41
6s	22.49	5.42	1.46	8.49	2.44	0.71	1.42
7s	22.49	5.41	1.43	8.50	2.44	0.69	1.38
8s	22.50	5.42	1.45	8.50	2.44	0.71	1.41
9s		5.42	1.46		2.44	0.71	1.42
10s			1.46			0.71	1.42
11s			1.46			0.71	1.42

4.3.3 The Effect of Partially Uncontracted Basis Sets on the Convergence

Although the reason for the irregular convergence problem is not fully understood, an observation can be made that, as compared with the convergence rate of the total energy of molecules, the convergence of atomic energy is slower. It is this difference in the convergence rate that contributes to a slight energy dip at the quintuple-zeta level. The convergence rate of total energy represent the ability to recover the DFT energy. A means to accelerate the convergence of the atomic energy may reduce the observed convergence problem in the atomization energy. This idea is tested by a use of dual basis set approach, using the

uncontracted basis sets to calculate the atomic energies and standard basis sets to calculate total energies for the molecules. The equation below is proposed as a possible means to calculate the atomization energy. Indeed, we need only the partially uncontracted basis sets rather than completely uncontracted basis sets since more than five *s* primitive functions, contribute little to the atomic energy, while increasing the computational expense of the calculation. The compositions of the suggested partially uncontracted (noted uc-cc-pV*x*Z) basis sets are: uc-cc-pVDZ: 7*s*2*p*1*d*; uc-cc-pVTZ: 7*s*3*p*2*d*1*f*; uc-cc-pVQZ: 7*s*4*p*3*d*2*f*1*g*; uc-cc-pV5Z: 7*s*5*p*4*d*3*f*2*g*1*h*.

$$\Delta E = E_{AB} - (E_{ucA} + E_{ucB})$$

This dual basis set approach improves the convergence behavior of atomization energy for all molecules studied. The atomization energies of CO from the dual basis set approach are compared with those from the standard correlation consistent basis sets, as shown in Figure 4.3. The largest change are observed at the double-, triple- and quadruple-zeta basis set levels, with little difference observed at the quintuple-zeta level. The lowering of energies results in a better-behaved convergence of atomization energies.

This dual basis set approach was also applied to B3LYP. In our earlier work, the best agreement with experiment was observed for B3LYP, as was the smoothest convergence behavior. Therefore, it is important to examine whether or not the proposed approach is still useful. The mean absolute errors (MAE) of the atomization eneries obtained with the standard sets and the dual basis set approach were listed in Table 4.6, and MAE of the Kohn-Sham limits obtained by using several extrapolation schemes were also included in Table 4.6. Using this dual basis set approach improves the convergence of atomization energies for all 17 molecules. however, relative to the MAE arising from the standard sets, the dual basis set approach

increases the MAE of atomization energy, in particular at the lower-level basis sets. At the double-zeta level, the MAE arising from dual basis set approach is 10.13 kcal/mol, 2.04 kcal/mol larger than MAE from standard sets. With increasing basis set size, the difference between MAEs arsing from two basis sets gets smaller, with a 0.11 kcal/mol difference at the quintuple-zeta level. Among all extrapolation schemes used, KS_{Q5} results in the best agreement with experiments for the dual basis set approach. However, KS_{Q5} cannot be obtained for the standard sets due to the energy dip occurred at the quintuple-zeta level.

Figure 4.3 A comparison of the CO atomization energies calculated using standard and partially uncontracted correlation consistent basis sets. The atomization energy is in kcal/mol.

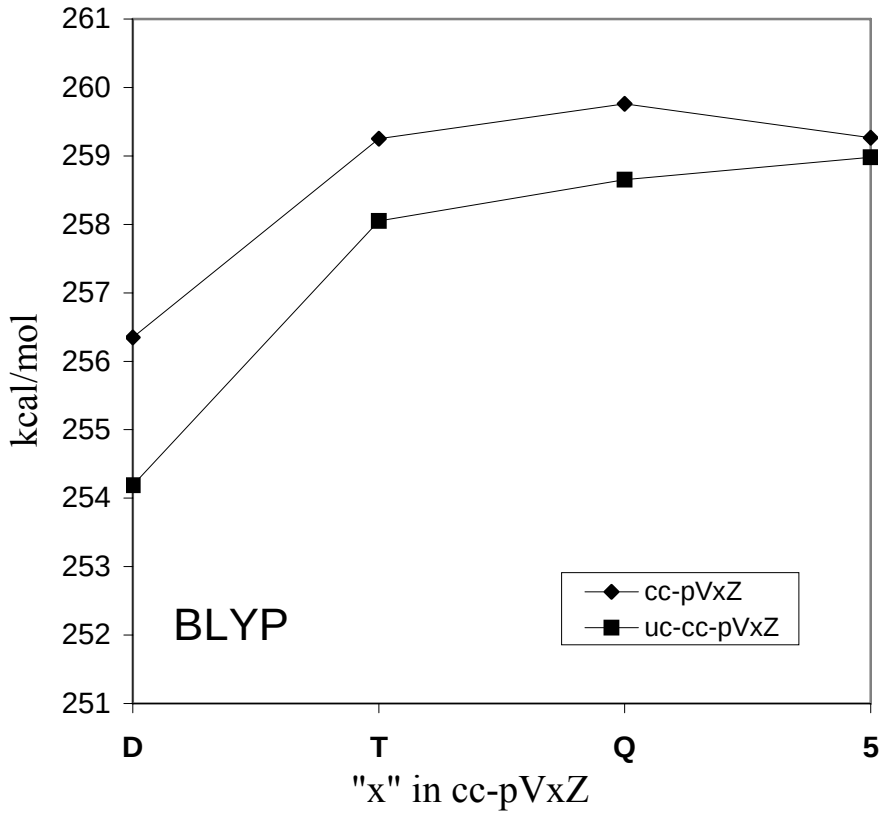

Table 4.6 Mean absolute errors of the atomization energy computed by B3LYP with partially uncontracted correlation consistent basis sets and of the Kohn-Sham atomization energy limits utilizing several different extrapolation schemes are provided. The corresponding results with the standard correlation consistent basis sets are also included for comparison. The energy is in kcal/mol.

Basis sets	D	T	Q	5	KS_{DTQ5}	KS_{DTQ}	KS_{DT}	KS_{TQ}	KS_{Q5}
cc-pV*x*Z	8.09	2.36	2.19	2.22		2.21[a]	2.43	2.45	
uc-cc-pV*x*Z	10.13	2.96	2.47	2.33	2.34		2.54	2.32	2.24

[a] MAE was obtained omitting F_2, due to its irregular convergence

4.4 Conclusions

The contraction error from DFT with the correlation consistent basis sets is small in general, and the maximum error is obtained at the double zeta level. Though the contraction error is relatively small. the uncontracting *s* functions help to reduce the previously noted convergence problem in the atomization energy with respect to increasing basis set size, but not for all molecules. Based on a analysis of the total energies of atoms and molecules, it is found that the energy dip results from the different convergence rate of total energies for atoms and molecules. The uncontraction of inner *s* functions accelerates the convergence of atomic energy. A dual basis set approach is proposed to reduce the convergence problem. Our results indicate that this approach improves the convergence behavior with slight impact on the accuracy.

CHAPTER 5

THE PERFORMANCE OF DENSITY FUNCTIONALS WITH RESPECT TO BASIS SETS: THE DIFFUSE *S* AND *P* FUNCTIONS

5.1 Introduction

In the preceding chapters we examined the convergence of molecular properties with respect to the correlation consistent basis sets[15] for a series of molecules in the context of DFT. An unexpected convergence behavior was noted, especially for the pure density functionals. Using the augmented correlation consistent basis sets (aug-cc-pV*x*Z)[54] can help reduce the convergence problem, but not for all cases. Another means to reduce the convergence problems is via an uncontraction of the basis sets, though this does not provide a solution for all molecules. In the course of these studies, we found that the convergence problem for atomization energies arises from the relatively slow convergence rate of the total energies of the atoms, as compared with that of the molecule. Based on our prior calculations and analysis, it is evident that the unusual convergence behavior may be related to the construction of the correlation consistent basis sets. However, in addressing the convergence problem in terms of basis set construction, the best means is not clear – whether or not additional polarization or diffuse functions are needed, and, whether higher or lower angular momentum functions are needed. The general observations regarding basis set performance with respect to DFT suggests that lower

angular momentum functions will be more important. This chapter examines the impact of the correlation consistent basis sets augmented with low and high angular momentum diffuse functions on the convergence of energies and structures.

For anionic systems, additional diffuse functions (functions with small exponents) are necessary for accurate calculations with *ab initio* or DFT methods.[54] Diffuse functions are required for describing molecular properties, like electron affinity, which rely on an accurate description of the wavefunction tail. Diffuse functions are included in a wide variety of basis sets such as 6-31+G[65] and DZP++[66]. The augmented correlation consistent basis sets (aug-cc-pV*x*Z) were proposed in a study by Kendall, Dunning and Harrison,[54] and are one of the most popular basis sets with diffuse functions used today. In this study, Kendall *et al*. reported electron affinities for a series of first-row atoms and molecules using the multi-reference configuration interaction with single and double excitations (MRCISD) method in combination with the augmented correlation consistent basis sets. They noted that the addition of a set of diffuse functions to the standard basis sets (a diffuse function for each angular momentum type within a standard basis set – i.e., the aug-cc-pVTZ basis set includs diffuse *s*, *p*, *d*, and *f* basis functions) was critical for accurate descriptions of the electron affinity of anions. Among the angular momentum diffuse functions (*s*, *p*, *d*, *f*, *g*, and *h*), the improvement in the description of electron affinity due to the addition of *s* and *p* functions is dominant, and the addition of other diffuse functions (*d*, *f*, *g*, and *h*) has a less substantial effect on the calculated electron affinities.

The polarization consistent basis sets,[56] designed explicitly for DFT, and discussed in an earlier chapter (Chapter 3) of this dissertation, also have an augmented form.[59] Unlike the correlation consistent basis sets, these sets, which were introduced after the current study was completed, simply include *s* and *p* diffuse functions.

A number of previous studies have shown that density functionals perform well for electron affinity predictions. [30, 67-69] For example, BLYP gave average errors of ~0.2 eV for a set of small molecules. [70] However, it is surprising that several density functionals predicted positive HOMO energies for stable bound anionic systems, [71-73] which indicates that, according to Koopmans' theorem, an anionic system is not stable and prone to loose an electron. Studies by Perdew et al. attribute this controversy to the self-interaction error, [67, 74, 75] which is the error resulting from the Coulomb and exchange interaction of an electron with itself, which can be cancelled out in the context of *ab initio*, but not in DFT. As a result, electron density decays exponentially, rather than a physically correct decay of 1/r (r is the distance of the electron from the nucleus). For anionic systems, which contain an additional electron, the self-interaction error is more severe and is reflected as the HOMO energy increases to become positive in the Kohn-Sham scheme of DFT.

Since the Schaefer group discussed the positive HOMO energy calculated with DFT for anionic systems in 1996, [69] an extended investigation on whether DFT is applicable to these systems has been carried out by several groups. Galbraith and Schaefer examined the F and F_2 electron affinities and HOMO energies at the complete basis set limit using several density functionals with the augmented correlation consistent basis sets. [76] It was found that the extra electron in F^- did show tendency to remain bound even though the HOMO energy was positive. They concluded that Koopmans' theorem may not be applied to DFT in determining the electron affinity for anionic systems. In a later study by Jarecki and Davidson, [77] a negative HOMO energy for F^- was obtained by utilizing very large diffuse basis sets with LDA and BLYP functionals. From this study, it is evident that the positive HOMO energies of F^- obtained with DFT functionals is caused by using too incomplete of a basis set.

Furthermore, other calculations have shown that the positive HOMO energies cannot be obtained in every calculation, and have a strong dependence on the system studied and density functionals used. For example, with B3LYP the correct electron affinity and negative HOMO energy can be obtained, [78] since mixing in a portion of the HF exchange energy alleviates the self-interaction error. In a DFT electron affinity study by Curtiss *et al*., [79] larger deviations from experiment were noted for 10 molecules, whose neutral species are closed-shell molecules.

In a recent benchmark study by the Schaefer group, a total of 110 atomic and molecular electron affinities were obtained using B3LYP, B3P86, BHLYP, BLYP, BP86, and LSDA density functionals with DZP++ basis sets. [80] Among all functionals, B3LYP and BLYP perform best with an average absolute error of 0.19 eV. When the data set was refined to a smaller set with accurate experimental electron affinities, the absolute average error is reduced to 0.16 and 0.15 eV for B3LYP and BLYP, respectively. Overall, despite the deficiencies in predicting the HOMO energies, DFT can provide reasonable estimates of electron affinities.

While the reasonable description of electron affinities requires diffuse functions to be present in a basis set, our focus here is upon a possible improvement in basis set convergence behavior with respect to increasing basis set size of properties such as atomization energy. We examine how different angular momentum diffuse functions affect this convergence. This idea is from our earlier observations that additional diffuse functions may play an important role in improving the unexpected convergence problem. [62]

5.2 Methodology

All DFT calculations were carried out using the Gaussian 98 software suite. [35] Optimization and frequency calculations were performed for each functional and basis set

combination. Zero-point energy corrections were obtained from frequency calculations and included in the calculations of atomization energies. In order to achieve the same accuracy for the calculations of atoms and molecules, the tight convergence criteria on the density were requested.

The Kohn-Sham (KS) limits were obtained for atomization energies by using an empirical exponential scheme, [36] which has already been addressed in previous chapters.

$$D_e(x) = D_e(\infty) + Ae^{-Bx} \tag{5-1}$$

Besides using cc-pV*x*Z and aug-cc-pV*x*Z in the calculations of the atomization energy of 17 molecules, two truncated series of basis sets were constructed by truncating the aug-cc-pV*x*Z sets. The first basis sets are denoted as cc-pV*x*Z+*sp*, which are constructed by removing all diffuse functions but the *s* and *p* functions, and the second basis sets are cc-pV*x*Z+*spd*, which are constructed by removing all diffuse functions but the *s*, *p*, and *d* functions. Likewise, other truncated basis sets are constructed by removing the higher angular momentum functions like *g* and *h* functions. For the hydrogen atom, the same procedure is taken to remove higher angular momentum diffuse functions from aug-cc-pV*x*Z to form cc-pV*x*Z+*sp* and cc-pV*x*Z+*spd* except for aug-cc-pVDZ, which only has diffuse *s* and *p* functions. For the basis set of hydrogen, diffuse functions from aug-cc-pVDZ are used to construct cc-pVDZ+*sp* and cc-pVDZ+*spd*. Throughout this chapter, these truncated basis sets are used to evaluate the impact of diffuse functions with different angular momentum on the convergence of energy and structure.

5.3 Results and Discussion

5.3.1 Geometry

The optimized geometries using B3LYP and BLYP with four series of basis sets are listed in Table 5.1. The diffuse *s*, *p*, and *d* functions have a small impact at the double- and triple-zeta basis set levels and almost no impact beyond the triple-zeta level. In general, the additional diffuse *sp* functions have little impact on the bond lengths (<0.01 angstrom) and on the bond angles (<1^{o}). The most remarkable effect is observed for dihedral angles. The additional *d* function reduces the dihedral angle of HOOH from 117.70 to 113.18^{0} at the double-zeta level and 114.16 to 113.33^{0} at the triple-zeta level. The cc-pV*x*Z+*sp* and cc-pV*x*Z+*spd* have a similar effect on the dihedral angle of HOOH.

5.3.2 Atomic Energy

Table 5.2 contains the atomic energies for hydrogen and four first-row atoms calculated using B3LYP and BLYP with the four series of basis sets. The addition of diffuse *s* and *p* functions amounts to most of the energy change between cc-pV*x*Z and aug-cc-pV*x*Z. For the total energies of the atoms, the diffuse *d* function is less important than the diffuse *s* and *p* functions, and only makes a difference of ~0.06 mhartree. Similar to the effect on geometry, diffuse *s* and *p* functions only have an impact on total energies at the lower level basis sets.

Table 5.1 Optimized bond lengths and angles. Bond lengths are given in angstroms, and bond angles are given in degrees.

Molecules, Experiment	Basis set	B3LYP cc-pV*x*Z	B3LYP cc-pV*x*Z+*sp*	B3LYP cc-pV*x*Z+*spd*	B3LYP aug-cc-pV*x*Z	BLYP cc-pV*x*Z	BLYP cc-pV*x*Z+*sp*	BLYP cc-pV*x*Z+*spd*	BLYP aug-cc-pV*x*Z
O_3									
r(OO) =	D	1.2597	1.2566	1.2566	1.2565	1.2953	1.2914	1.2907	1.2908
1.278 Å[a]	T	1.2563	1.2548	1.2547	1.2549	1.2919	1.2898	1.2895	1.2901
	Q	1.2531	1.2525	1.2525	1.2522	1.2881	1.2871	1.2870	1.2868
	5	1.2524	1.2522	1.2522	1.2520	1.2873	1.2867	1.2866	1.2866
a(OOO) =	D	117.95	118.36	118.07	118.07	117.90	118.22	117.94	117.97
116.8°[a]	T	118.14	118.34	118.31	118.28	118.00	118.18	118.14	118.14
	Q	118.26	118.35	118.34	118.35	118.10	118.20	118.19	118.20
	5	118.30	118.34	118.34	118.35	118.11	118.19	118.19	118.19
H_2									
r(HH) =	D	0.7617	0.7609	0.7609	0.7609	0.7674	0.7664	0.7664	0.7662
0.741 Å[b]	T	0.7429	0.7431	0.7430	0.7429	0.7468	0.7468	0.7468	0.7468
	Q	0.7420	0.7421	0.7421	0.7420	0.7457	0.7457	0.7457	0.7458
	5	0.7418	0.7419	0.7419	0.7418	0.7455	0.7455	0.7455	0.7455
H_2O									
r(HO) =	D	0.9687	0.9686	0.9649	0.9649	0.9798	0.9793	0.9751	0.9751
0.956 Å[a]	T	0.9614	0.9619	0.9619	0.9621	0.9715	0.9723	0.9723	0.9719
	Q	0.9603	0.9606	0.9606	0.9606	0.9703	0.9708	0.9708	0.9707
	5	0.9603	0.9604	0.9604	0.9604	0.9703	0.9703	0.9703	0.9705
a(HOH) =	D	102.74	103.89	104.73	104.76	101.77	103.27	104.15	104.16
105.2°[a]	T	104.50	105.02	105.09	104.95	103.75	104.41	104.47	104.48
	Q	104.88	105.11	105.13	105.12	104.20	104.51	104.53	104.52

-continue-

-continue-

Molecules, Experiment	Basis set	B3LYP cc-pV*x*Z	B3LYP cc-pV*x*Z+*sp*	B3LYP cc-pV*x*Z+*spd*	B3LYP aug-cc-pV*x*Z	BLYP cc-pV*x*Z	BLYP cc-pV*x*Z+*sp*	BLYP cc-pV*x*Z+*spd*	BLYP aug-cc-pV*x*Z
	5	105.10	105.12	105.13	105.13	104.48	104.48	104.48	104.54
HF									
r(HF) =	D	0.9268	0.9294	0.9257	0.9256	0.9384	0.9406	0.9369	0.9367
0.917 Å[b]	T	0.9225	0.9238	0.9240	0.9242	0.9330	0.9345	0.9347	0.9350
	Q	0.9214	0.9222	0.9222	0.9224	0.9320	0.9329	0.9329	0.9330
	5	0.9220	0.9220	0.9220	0.9222	0.9325	0.9328	0.9328	0.9328
HCN									
r(HC) =	D	1.0772	1.0770	1.0742	1.0744	1.0836	1.0838	1.0806	1.0808
1.064 Å[a]	T	1.0654	1.0659	1.0655	1.0656	1.0711	1.0719	1.0711	1.0714
	Q	1.0655	1.0655	1.0655	1.0656	1.0712	1.0712	1.0712	1.0713
	5	1.0656	1.0656	1.0656	1.0656	1.0714	1.0714	1.0714	1.0714
r(CN) =	D	1.1579	1.1584	1.1569	1.1568	1.1697	1.1704	1.1685	1.1684
1.156 Å[a]	T	1.1462	1.1463	1.1461	1.1460	1.1575	1.1577	1.1575	1.1573
	Q	1.1450	1.1451	1.1451	1.1451	1.1565	1.1565	1.1565	1.1566
	5	1.1450	1.1450	1.1450	1.1450	1.1565	1.1565	1.1565	1.1565
CO									
r(CO) =	D	1.1345	1.1345	1.1341	1.1340	1.1471	1.1471	1.1463	1.1463
1.128 Å[b]	T	1.1262	1.1262	1.1260	1.1258	1.1379	1.1379	1.1378	1.1376
	Q	1.1237	1.1238	1.1238	1.1238	1.1355	1.1355	1.1355	1.1356
	5	1.1236	1.1236	1.1236	1.1236	1.1354	1.1354	1.1354	1.1354
N_2									
r(NN) =	D	1.1044	1.1041	1.1044	1.1044	1.1172	1.1167	1.1168	1.1168

-continue-

-continue-

Molecules, Experiment	Basis set	B3LYP cc-pV*x*Z	B3LYP cc-pV*x*Z+*sp*	B3LYP cc-pV*x*Z+*spd*	B3LYP aug-cc-pV*x*Z	BLYP cc-pV*x*Z	BLYP cc-pV*x*Z+*sp*	BLYP cc-pV*x*Z+*spd*	BLYP aug-cc-pV*x*Z
1.098 Å[b]	T	1.0914	1.0914	1.0914	1.0912	1.1032	1.1033	1.1032	1.1030
	Q	1.0902	1.0902	1.0902	1.0901	1.1022	1.1021	1.1021	1.1021
	5	1.0900	1.0899	1.0899	1.0899	1.1019	1.1019	1.1019	1.1019
HNO									
r(HN) =	D	1.0776	1.0719	1.0673	1.0674	1.1002	1.0909	1.0853	1.0855
1.09 Å[c]	T	1.0628	1.0616	1.0612	1.0613	1.0813	1.0789	1.0785	1.0786
	Q	1.0613	1.0608	1.0608	1.0610	1.0792	1.0781	1.0781	1.0783
	5	1.0607	1.0607	1.0607	1.0608	1.0781	1.0779	1.0779	1.0781
r(NO) =	D	1.2028	1.2035	1.2051	1.2051	1.2193	1.2209	1.2222	1.2221
1.209 Å[c]	T	1.1984	1.1979	1.1980	1.1978	1.2153	1.2149	1.2149	1.2149
	Q	1.1970	1.1967	1.1967	1.1964	1.2139	1.2136	1.2135	1.2135
	5	1.1966	1.1964	1.1964	1.1962	1.2137	1.2133	1.2133	1.2133
a(HNO) =	D	108.35	108.64	108.63	108.65	108.30	108.53	108.53	108.53
108.047°[c]	T	108.68	108.87	108.87	108.86	108.55	108.73	108.74	108.74
	Q	108.81	108.92	108.92	108.92	108.68	108.78	108.79	108.81
	5	108.87	108.93	108.93	108.92	108.73	108.79	108.79	108.80
H_2O_2									
r(HO) =	D	0.9734	0.9744	0.9701	0.9700	0.9853	0.9866	0.9817	0.9817
0.965 Å[d]	T	0.9659	0.9667	0.9668	0.9667	0.9773	0.9781	0.9781	0.9781
	Q	0.9650	0.9655	0.9655	0.9654	0.9763	0.9766	0.9767	0.9767
	5	0.9654	0.9653	0.9654	0.9652	0.9764	0.9764	0.9766	0.9766
r(OO) =	D	1.4525	1.4543	1.4507	1.4507	1.4915	1.4946	1.4897	1.4897

-continue-

-continue-

Molecules, Experiment	Basis set	B3LYP cc-pV*x*Z	B3LYP cc-pV*x*Z+*sp*	B3LYP cc-pV*x*Z+*spd*	B3LYP aug-cc-pV*x*Z	BLYP cc-pV*x*Z	BLYP cc-pV*x*Z+*sp*	BLYP cc-pV*x*Z+*spd*	BLYP aug-cc-pV*x*Z
1.464 Å[d]	T	1.4517	1.4507	1.4507	1.4512	1.4920	1.4915	1.4916	1.4916
	Q	1.4489	1.4480	1.4485	1.4483	1.4891	1.4890	1.4885	1.4885
	5	1.4489	1.4474	1.4472	1.4480	1.4888	1.4883	1.4883	1.4883
a(HOO) =	D	99.87	100.37	100.75	100.79	98.60	99.31	99.71	99.71
99.4°[d]	T	100.43	100.70	100.75	100.74	99.19	99.58	99.59	99.59
	Q	100.69	100.80	100.82	100.81	99.50	99.65	99.68	99.68
	5	100.78	100.82	100.83	100.81	99.63	99.67	99.69	99.69
d(HOOH) =	D	117.68	117.70	113.18	113.23	119.37	117.69	114.29	114.29
111.8°[d]	T	113.91	114.16	113.33	113.39	115.04	115.04	114.28	114.28
	Q	113.00	113.53	113.40	113.37	113.89	114.55	114.42	114.42
	5	113.35	113.49	113.33	113.43	114.49	114.59	114.44	114.44
HOF									
r(HO) =	D	0.9775	0.9791	0.9746	0.9747	0.9898	0.9914	0.9864	0.9866
0.96 Å[e]	T	0.9700	0.9713	0.9712	0.9715	0.9817	0.9828	0.9828	0.9829
	Q	0.9693	0.9699	0.9699	0.9698	0.9809	0.9814	0.9814	0.9819
	5	0.9694	0.9697	0.9697	0.9696	0.9811	0.9811	0.9811	0.9814
r(OF) =	D	1.4349	1.4378	1.4324	1.4328	1.4706	1.4763	1.4700	1.4699
1.442 Å[e]	T	1.4301	1.4295	1.4296	1.4310	1.4675	1.4679	1.4680	1.4684
	Q	1.4291	1.4285	1.4286	1.4288	1.4669	1.4673	1.4673	1.4668
	5	1.4286	1.4280	1.4280	1.4284	1.4667	1.4667	1.4667	1.4666
a(HOF) =	D	97.87	98.18	98.47	98.56	96.96	97.33	97.61	97.65

-continue-

-continue-

Molecules, Experiment	Basis set	B3LYP cc-pV*x*Z	B3LYP cc-pV*x*Z+*sp*	B3LYP cc-pV*x*Z+*spd*	B3LYP aug-cc-pV*x*Z	BLYP cc-pV*x*Z	BLYP cc-pV*x*Z+*sp*	BLYP cc-pV*x*Z+*spd*	BLYP aug-cc-pV*x*Z
97.2 Å[e]	T	98.48	98.66	98.64	98.59	97.43	97.69	97.68	97.68
	Q	98.63	98.67	98.67	98.72	97.58	97.76	97.75	97.66
	5	98.71	98.69	98.69	98.74	97.68	97.68	97.68	97.73
F_2									
r(FF) =	D	1.4102	1.4111	1.4034	1.4034	1.4435	1.4481	1.4386	1.4386
1.412 Å[b]	T	1.3976	1.3966	1.3965	1.3971	1.433	1.4330	1.4330	1.4331
	Q	1.3968	1.3962	1.3962	1.3961	1.4328	1.4328	1.4328	1.4324
	5	1.3962	1.3957	1.3957	1.3957	1.4326	1.4321	1.4321	1.4320
CO_2									
r(CO) =	D	1.1673	1.1678	1.1674	1.1673	1.1815	1.1819	1.1811	1.1811
1.162 Å[a]	T	1.1604	1.1606	1.1605	1.1605	1.1736	1.1738	1.1736	1.1737
	Q	1.1588	1.1589	1.1589	1.1589	1.1720	1.1720	1.1720	1.1722
	5	1.1587	1.1588	1.1588	1.1587	1.1721	1.1721	1.1721	1.1721
H_2CO									
r(CO) =	D	1.2040	1.2077	1.2075	1.2073	1.2156	1.2202	1.2195	1.2196
1.205 Å[a]	T	1.1992	1.2005	1.2004	1.2004	1.2105	1.2122	1.2122	1.2122
	Q	1.1982	1.1986	1.1987	1.1987	1.2096	1.2106	1.2106	1.2106
	5	1.1984	1.1985	1.1985	1.1985	1.2102	1.2103	1.2103	1.2103
r(CH) =	D	1.1203	1.1162	1.1138	1.1139	1.1309	1.1256	1.1230	1.1228
1.111 Å[a]	T	1.1065	1.1056	1.1056	1.1057	1.1155	1.1143	1.1143	1.1143
	Q	1.1056	1.1053	1.1053	1.1054	1.1145	1.1141	1.1141	1.1141
	5	1.1053	1.1053	1.1053	1.1053	1.1141	1.1141	1.1141	1.1141

-continue-

-continue-

Molecules, Experiment	Basis set	B3LYP cc-pV*x*Z	B3LYP cc-pV*x*Z+*sp*	B3LYP cc-pV*x*Z+*spd*	B3LYP aug-cc-pV*x*Z	BLYP cc-pV*x*Z	BLYP cc-pV*x*Z+*sp*	BLYP cc-pV*x*Z+*spd*	BLYP aug-cc-pV*x*Z
a(HCO) =	D	122.47	121.78	121.81	121.84	122.66	121.89	121.92	122.00
121.9°[a]	T	122.10	121.90	121.91	121.93	122.19	122.03	122.03	122.03
	Q	122.01	121.93	121.94	121.94	122.09	122.04	122.04	122.04
	5	121.95	121.94	121.93	121.94	122.06	122.04	122.04	122.04
CH_3NH_2									
r(HC) =	D	1.1120	1.1076	1.1057	1.1057	1.1207	1.1152	1.1129	1.1130
1.093 Å[a]	T	1.0980	1.0971	1.0970	1.0970	1.1053	1.1041	1.1040	1.1040
	Q	1.0968	1.0965	1.0966	1.0966	1.1039	1.1035	1.1035	1.1035
	5	1.0964	1.0965	1.0965	1.0965	1.1036	1.1035	1.1035	1.1033
r(NH) =	D	1.0228	1.0206	1.0175	1.0175	1.0327	1.0299	1.0261	1.0259
1.011 Å[a]	T	1.0127	1.0124	1.0122	1.0122	1.0216	1.0207	1.0206	1.0206
	Q	1.0116	1.0113	1.0113	1.0113	1.0203	1.0199	1.0199	1.0199
	5	1.0114	1.0113	1.0112	1.0112	1.0203	1.0199	1.0199	1.0200
r(CN) =	D	1.4640	1.4667	1.4669	1.4669	1.4779	1.4825	1.4822	1.4818
1.474 Å[a]	T	1.4641	1.4644	1.4645	1.4645	1.4793	1.4793	1.4795	1.4796
	Q	1.4634	1.4632	1.4632	1.4632	1.4783	1.4786	1.4786	1.4786
	5	1.4635	1.4632	1.4630	1.4631	1.4788	1.4786	1.4786	1.4790
a(HNC) =	D	109.34	110.40	110.84	110.84	108.67	109.87	110.34	110.38
112.1°[a]	T	110.37	110.95	110.96	110.96	109.73	110.53	110.55	110.51
	Q	110.69	111.04	111.04	111.04	110.13	110.55	110.55	110.55
	5	110.91	111.04	111.05	111.03	110.37	110.55	110.55	110.53
CH_3OH									

-continue-

-continue-

Molecules, Experiment	Basis set	B3LYP cc-pV*x*Z	B3LYP cc-pV*x*Z+*sp*	B3LYP cc-pV*x*Z+*spd*	B3LYP aug-cc-pV*x*Z	BLYP cc-pV*x*Z	BLYP cc-pV*x*Z+*sp*	BLYP cc-pV*x*Z+*spd*	BLYP aug-cc-pV*x*Z
r(OH) =	D	0.9677	0.9673	0.9639	0.9639	0.9788	0.9783	0.9744	0.9747
0.956 Å[a]	T	0.9606	0.9609	0.9609	0.9608	0.9712	0.9711	0.9711	0.9714
	Q	0.9594	0.9595	0.9596	0.9596	0.9699	0.9701	0.9701	0.9701
	5	0.9593	0.9595	0.9594	0.9596	0.9697	0.9701	0.9701	0.9694
a(HOC) =	D	107.49	108.47	108.89	108.89	106.79	107.85	108.28	108.27
108.87°[a]	T	108.51	108.99	109.01	109.01	107.77	108.39	108.41	108.35
	Q	108.86	109.06	109.05	109.05	108.17	108.41	108.41	108.41
	5	109.01	109.06	109.06	109.05	108.42	108.41	108.41	108.49
N_2H_4									
r(HN) =	D	1.0266	1.0236	1.0201	1.0202	1.0378	1.0336	1.0298	1.0299
1.016 Å[f]	T	1.0152	1.0146	1.0145	1.0145	1.0249	1.0240	1.0238	1.0239
	Q	1.0140	1.0138	1.0138	1.0138	1.0235	1.0231	1.0232	1.0233
	5	1.0137	1.0137	1.0136	1.0137	1.0232	1.0230	1.0231	1.0233
r(NN) =	D	1.4356	1.4361	1.4353	1.4355	1.4613	1.4620	1.4603	1.4606
1.446 Å[f]	T	1.4357	1.4330	1.4331	1.4334	1.4625	1.4588	1.4590	1.4594
	Q	1.4327	1.4310	1.4310	1.4311	1.4585	1.4561	1.4561	1.4561
	5	1.4313	1.4307	1.4307	1.4309	1.4567	1.4557	1.4558	1.4561
a(HNN) =	D	106.67	107.32	107.66	107.66	105.48	106.27	106.65	106.66
108.85°[f]	T	107.42	107.91	107.92	107.92	106.23	106.85	106.85	106.84
	Q	107.74	108.02	108.02	108.04	106.61	106.99	106.99	106.99
	5	107.97	108.03	108.04	108.05	106.89	107.01	107.00	106.99
CH_3F									

-continue-

-continue-

Molecules, Experiment	Basis set	B3LYP cc-pV*x*Z	B3LYP cc-pV*x*Z+*sp*	B3LYP cc-pV*x*Z+*spd*	B3LYP aug-cc-pV*x*Z	BLYP cc-pV*x*Z	BLYP cc-pV*x*Z+*sp*	BLYP cc-pV*x*Z+*spd*	BLYP aug-cc-pV*x*Z
r(HC) =	D	1.1037	1.0994	1.0979	1.0979	1.1119	1.1068	1.1048	1.1048
1.087 Å[g]	T	1.0903	1.0895	1.0894	1.0895	1.0971	1.0959	1.0959	1.0959
	Q	1.0892	1.0889	1.0889	1.0890	1.0958	1.0954	1.0954	1.0953
	5	1.0889	1.0889	1.0889	1.0889	1.0954	1.0953	1.0953	1.0953
r(CF) =	D	1.3847	1.3989	1.4017	1.4014	1.4001	1.4200	1.4223	1.4223
1.383 Å[g]	T	1.3865	1.3915	1.3917	1.3921	1.4050	1.4119	1.4119	1.4119
	Q	1.3884	1.3904	1.3904	1.3906	1.4071	1.4107	1.4107	1.4102
	5	1.3898	1.3900	1.3900	1.3902	1.4092	1.4098	1.4098	1.4098
a(HCF) =	D	109.55	108.53	108.41	108.43	109.69	108.31	108.20	108.20
108.73°[g]	T	109.07	108.68	108.67	108.68	108.99	108.55	108.55	108.55
	Q	108.90	108.73	108.73	108.73	108.82	108.53	108.53	108.60
	5	108.77	108.74	108.74	108.73	108.66	108.60	108.60	108.60

[a] Ref. [38].
[b] Ref. [39].
[c] Ref. [40].
[d] Ref. [41].
[e] Ref. [42].
[f] Ref. [43].
[g] Ref. [44].

Table 5.2 Total energies for atoms in hartrees.

Atoms, Exact.[a]	Basis set	B3LYP cc-pV*x*Z	B3LYP cc-pV*x*Z+*sp*	B3LYP cc-pV*x*Z+*spd*	B3LYP aug-cc-pV*x*Z	BLYP cc-pV*x*Z	BLYP cc-pV*x*Z+*sp*	BLYP cc-pV*x*Z+*spd*	BLYP aug-cc-pV*x*Z
H	D	-0.501258	-0.501657	-0.501657	-0.501657	-0.496403	-0.497007	-0.497007	-0.497007
-0.5000	T	-0.502156	-0.502260	-0.502260	-0.502260	-0.497555	-0.497722	-0.497722	-0.497722
	Q	-0.502346	-0.502392	-0.502392	-0.502392	-0.497781	-0.497860	-0.497860	-0.497860
	5	-0.502428	-0.502438	-0.502438	-0.502436	-0.497889	-0.497908	-0.497908	-0.497905
C	D	-37.851975	-37.854138	-37.854196	-37.854196	-37.837836	-37.840798	-37.840849	-37.840848
-37.8450	T	-37.858575	-37.859054	-37.859061	-37.859061	-37.845501	-37.846232	-37.846237	-37.845313
	Q	-37.860592	-37.860783	-37.860784	-37.860785	-37.847806	-37.848133	-37.848134	-37.848135
	5	-37.861508	-37.861540	-37.861540	-37.861541	-37.849077	-37.849139	-37.849139	-37.849140
N	D	-54.589136	-54.593843	-54.593843	-54.593843	-54.572571	-54.578765	-54.578765	-54.578765
-54.5893	T	-54.601781	-54.602891	-54.602891	-54.602891	-54.586935	-54.588525	-54.588525	-54.588525
	Q	-54.605328	-54.605735	-54.605735	-54.605735	-54.590896	-54.591546	-54.591546	-54.591546
	5	-54.606704	-54.606773	-54.606773	-54.606773	-54.592689	-54.592811	-54.592811	-54.592811
O	D	-75.068499	-75.077084	-75.077164	-75.077164	-75.054526	-75.065527	-75.065596	-75.065596
-75.067	T	-75.091864	-75.094055	-75.094063	-75.094180	-75.080286	-75.083302	-75.083305	-75.083421
	Q	-75.098201	-75.099017	-75.099019	-75.099049	-75.087251	-75.088479	-75.088479	-75.088511
	5	-75.100485	-75.100607	-75.100608	-75.100614	-75.090069	-75.090280	-75.090280	-75.090288
F	D	-99.726602	-99.739386	-99.739496	-99.739496	-99.713359	-99.729672	-99.729776	-99.729776
-99.734	T	-99.762867	-99.766004	-99.766011	-99.766141	-99.752932	-99.757261	-99.757265	-99.757394
	Q	-99.772527	-99.773605	-99.773607	-99.773645	-99.763470	-99.765110	-99.765110	-99.765151
	5	-99.775818	-99.775958	-99.775959	-99.775969	-99.767416	-99.767669	-99.767669	-99.767680

[a] Davidson estimates of the atomic energies, which are from reference [45].

5.3.3 Atomization Energy

The atomization energies from B3LYP and BLYP with the different basis sets are given in Table 5.3. In terms of previous studies, BLYP with the correlation consistent basis sets performs poorly in determining energies for the molecules tested, while B3LYP improves the accuracy greatly (but they are still not close to "chemical accuracy"). In this section, the focus is on the convergence behavior, as the accuracy will be discussed in a later part.

The convergence problem is evident for atomization energies determined by using BLYP and B3LYP with standard correlation consistent basis sets. For several molecules, both functionals do not converge smoothly, suffering from a small dip at the quintuple-zeta level. Using cc-pV*x*Z+*sp* remedies the convergence problem. Relative to the atomization energy with cc-pV*x*Z, the energy change due to the additional diffuse *s* and *p* functions is greater at lower-level basis sets, compared with the higher-level basis sets. For example in CO_2, as compared with the cc-pV*x*Z atomization energy, the changes of the atomization energy due to diffuse *s* and *p* functions are 4.58 kcal/mol, 1.65 kcal/mol, 0.76 kcal/mol, and 0.13 kcal/mol for BLYP with the double-, triple-, quadruple-, and quintuple-zeta level, respectively. It is the energy change which occurs for low-level basis sets that helps improve the convergence behavior. Improved convergence behavior is also observed for cc-pV*x*Z+*spd*. It is not surprising considering the fact that cc-pV*x*Z+*spd* and aug-cc-pV*x*Z have similar performance in determining energy and that aug-cc-pV*x*Z improves the convergence behavior (already noted in the preceding study). However, improved convergence behavior is not evident for all molecules, the exceptions being O_3 and F_2. The dependence of the atomization energy of CO_2 on the different basis sets is plotted in Figure 5.1.

Figure 5.1 Comparison of the BLYP atomization energies of CO_2 with four sets of basis sets. (note that cc-pVDZ+*spd* is identical to aug-cc-pVDZ.)

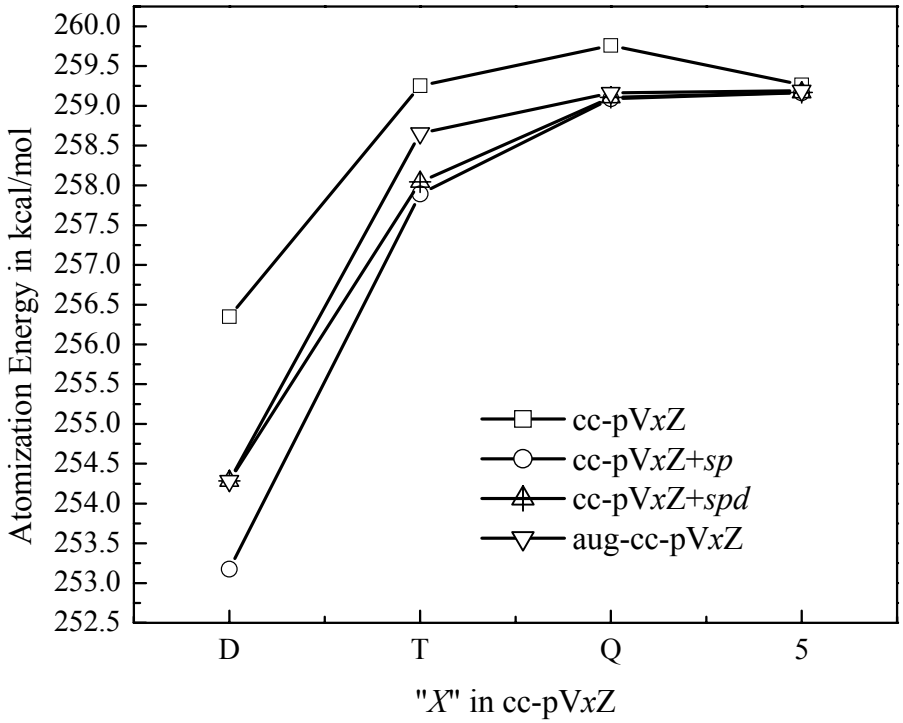

The convergent behavior of CO_2 is somewhat surprising. What was expected was that the cc-pV*x*Z+*sp* or cc-pV*x*Z+*spd* atomization energy would converge between the atomization energies from the standard and augmented correlation consistent basis sets, based on their respective size. However, the cc-pV*x*Z+*spd* and cc-pV*x*Z+*sp* atomization energies do not fall in between the atomization energy with cc-pV*x*Z and aug-cc-pV*x*Z, although the cc-pV*x*Z+*spd* atomization energies are closer to those with the aug-cc-pV*x*Z set. Compared with cc-pV*x*Z atomization energies, the energy changes due to additional *s* and *p* (cc-pV*x*Z+*sp*) and additional *s*, *p*, and *d* (cc-pV*x*Z+*spd*) have larger impacts at the double-, triple-, and, in particular, the quadruple-zeta levels, but only a slight impact at the quintuple-zeta level. These effects directly result in the

improvement of convergence by lowering the atomization energies at double-, triple-, and quadruple-zeta levels. Also, we noticed for this case that the diffuse *f* function has a larger effect on the energy at the triple-zeta level than the diffuse *d* function.

More attention is paid to two "difficult" molecules, F_2 and O_3, whose DFT atomization energies have problematic convergence when standard and augmented correlation consistent basis sets are used. Interestingly, when the two new series of basis sets are used, cc-pV*x*Z+*sp* improves the convergence and results in smooth convergence, while cc-pV*x*Z+*spd* does not. The atomization energies of F_2 and O_3 calculated with four sets of basis sets are compared in Figure 5.2 and Figure 5.3 for the BLYP functional, respectively. The most pronounced energy difference between cc-pV*x*Z and cc-pV*x*Z+*sp* is observed at the double-zeta level with a 7 kcal/mol reduction for both F_2 and O_3. With increasing basis set size, the energy difference decreases. As a result, atomization energies of these two molecules can converge smoothly when combined with cc-pV*x*Z+*sp*. Unlike the diffuse *s* and *p* functions, the diffuse *d* functions cannot improve the convergence behavior, they only reduce the atomization energy at the double-zeta level. The large reduction of atomization energy at the double-zeta level is related to the different convergence patterns of total energies of atoms and molecules. It is found that the total energies of atoms, when using cc-pV*x*Z+*sp*, are almost the same as those when using aug-cc-pV*x*Z, while the total energies of the molecules are between those obtained with standard and augmented correlation consistent basis sets.

Besides the diffuse *s* and *p* functions, functions with higher angular momentum were also considered. Comparing the slight converge dip in aug-cc-pV*x*Z with the smooth convergent behavior in cc-pV*x*Z+*sp*, it is obvious that the convergence behavior deteriorates with the high angular momentum diffuse functions. The BLYP CO_2 atomization energies for quadruple- and

Figure 5.2 Comparison of the BLYP atomization energies of F_2 with four sets of basis sets

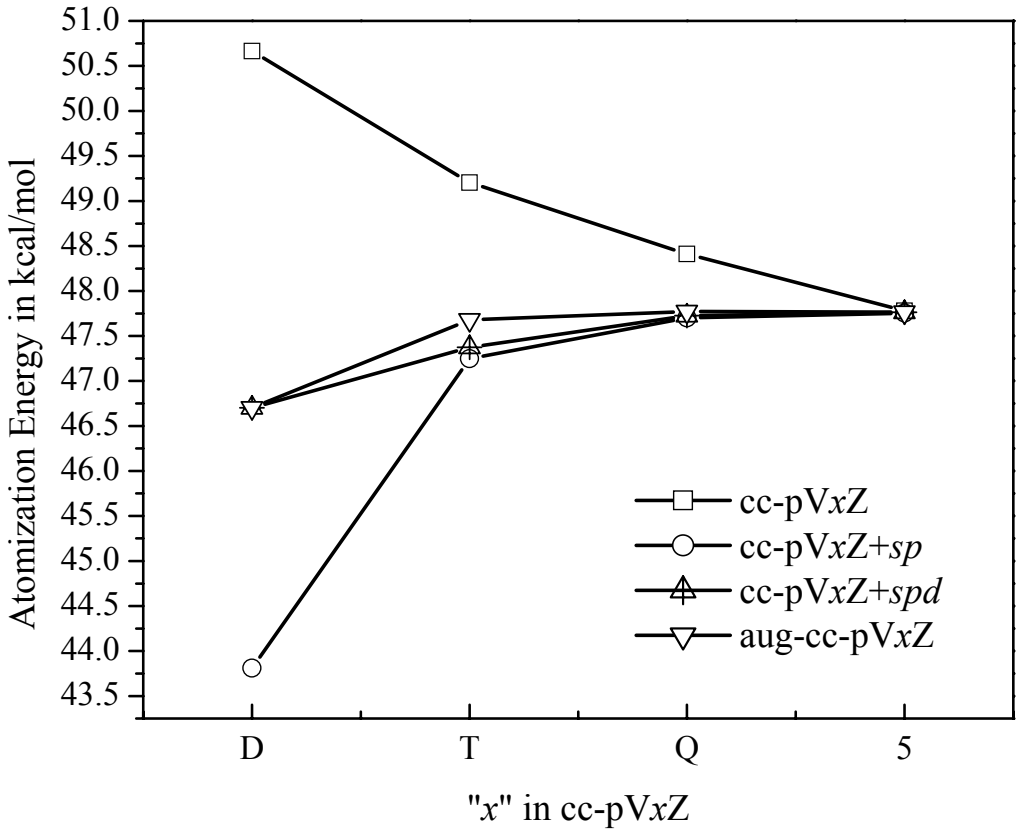

Figure 5.3 Comparison of the BLYP atomization energies of O_3 with four sets of basis sets

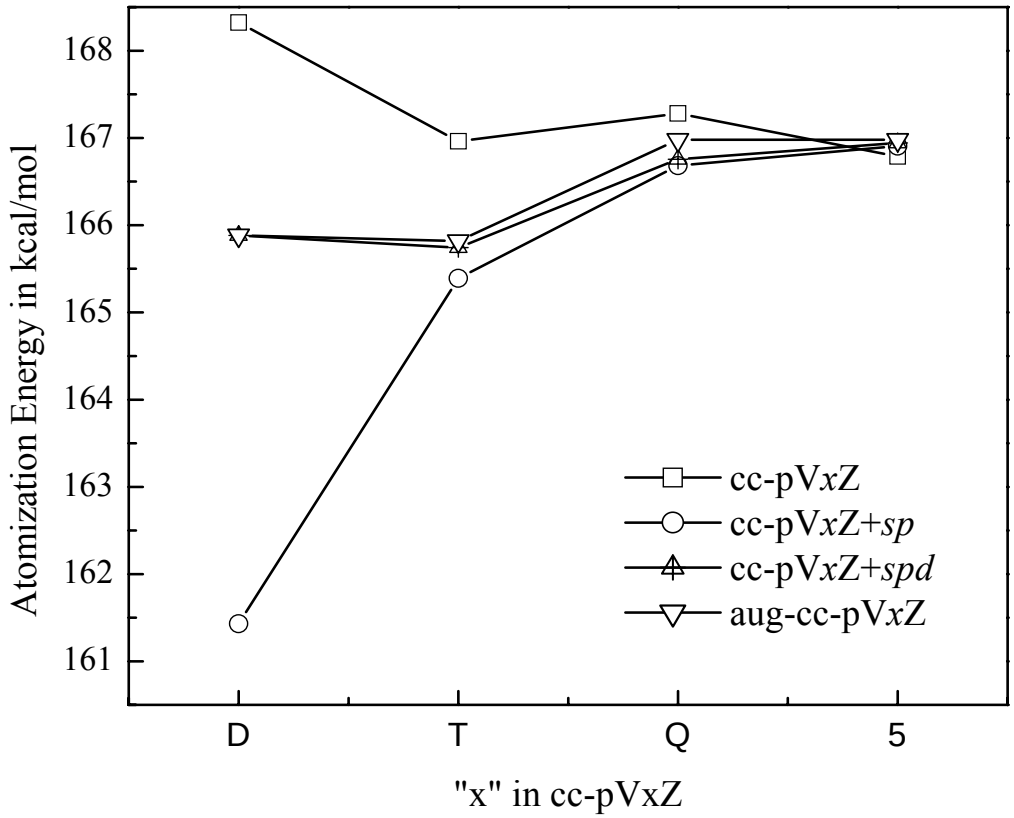

quintuple-zeta level basis sets with different high angular momentum diffuse functions are listed in Table 5.4. As seen in the table, using cc-pV*x*Z+*sp* sets decreases the cc-pV*x*Z atomization energy. However, relative to cc-pV*x*Z+*sp* atomization energy, adding higher angular momentum functions *d*, *f*, *g,* and *h* increases the atomization energy. Although the increase is small, the energy change for quadruple-zeta level is more than that of quintuple-zeta level when the higher angular momentum functions are added to cc-pV*x*Z+*sp*. As a result, aug-cc-pV*x*Z cannot converge smoothly due to a slight dip at the quintuple-zeta level. In this case, among all energy contributions, the diffuse *g* function has the biggest impact on the quadruple-zeta level basis set and results in the convergence dip for the aug-cc-pV*x*Z.

Table 5.3 Calculated atomization energies in kcal/mol.

Molecules, Experiment.[a]	Basis set	B3LYP cc-pV*x*Z	B3LYP cc-pV*x*Z+*sp*	B3LYP cc-pV*x*Z+*spd*	B3LYP aug-cc-pV*x*Z	BLYP cc-pV*x*Z	BLYP cc-pV*x*Z+*sp*	BLYP cc-pV*x*Z+*spd*	BLYP aug-cc-pV*x*Z
O_3	D	133.76	129.33	134.42	134.41	168.32	161.43	165.88	165.88
142.4	T	135.68	134.92	135.33	135.39	166.96	165.39	165.74	165.82
	Q	136.58	136.37	136.45	136.67	167.28	166.68	166.76	166.98
	5	136.45	136.63	136.67	136.70	166.79	166.91	166.94	166.98
	∞		136.78				167.10		
H_2	D	101.11	100.90	100.90	100.90	100.17	99.86	99.86	99.86
103.3	T	103.93	103.81	103.82	103.82	103.27	103.08	103.08	103.08
	Q	104.03	103.98	103.98	103.98	103.35	103.25	103.25	103.25
	5	104.02	104.01	104.01	104.01	103.31	103.28	103.28	103.29
	∞		104.00				103.27		
H_2O	D	206.14	213.37	215.20	215.20	207.84	215.63	217.53	217.53
219.4	T	214.85	217.22	217.34	217.29	216.81	219.53	219.65	219.59
	Q	216.78	217.78	217.82	217.83	218.91	220.13	220.16	220.17
	5	217.57	217.84	217.85	217.86	219.81	220.16	220.18	220.20
	∞		217.86				220.20		
HF	D	124.58	130.80	132.00	132.00	126.08	132.97	134.18	134.17
135.4	T	131.30	133.24	133.34	133.28	133.07	135.37	135.47	135.41
	Q	132.78	133.53	133.56	133.57	134.74	135.67	135.71	135.72
	5	133.37	133.54	133.56	133.56	135.43	135.69	135.70	135.71
	∞		133.55				135.70		

-continue-

-continue-

Molecules, Experiment.[a]	Basis set	B3LYP cc-pV*x*Z	B3LYP cc-pV*x*Z+*sp*	B3LYP cc-pV*x*Z+*spd*	B3LYP aug-cc-pV*x*Z	BLYP cc-pV*x*Z	BLYP cc-pV*x*Z+*sp*	BLYP cc-pV*x*Z+*spd*	BLYP aug-cc-pV*x*Z
HCN	D	295.79	294.72	295.68	295.68	303.84	302.04	303.12	303.12
302.5	T	302.78	302.36	302.52	302.60	310.36	309.63	309.79	310.46
	Q	303.74	303.49	303.51	303.58	311.21	310.78	310.80	310.89
	5	303.63	303.58	303.58	303.60	310.92	310.82	310.83	310.85
	∞		303.63				310.89		
CO	D	248.42	246.19	247.20	247.20	256.35	253.17	254.28	254.29
256.2	T	252.12	251.18	251.33	251.36	259.25	257.89	258.04	258.66
	Q	252.84	252.41	252.43	252.47	259.76	259.09	259.11	259.16
	5	252.56	252.51	252.51	252.53	259.26	259.16	259.17	259.19
	∞		252.64				259.30		
N_2	D	219.32	218.68	219.36	219.36	231.22	229.89	230.53	230.53
225.1	T	225.45	225.25	225.33	225.42	236.49	236.06	236.13	236.25
	Q	226.38	226.42	226.44	226.52	237.27	237.21	237.23	237.33
	5	226.43	226.57	226.58	226.60	237.19	237.35	237.36	237.38
	∞		226.63				237.42		
HNO	D	192.98	192.87	194.64	194.64	206.22	205.17	206.87	206.87
196.9	T	196.94	197.05	197.21	197.27	209.05	208.86	209.01	209.08
	Q	198.00	198.11	198.16	198.26	209.98	209.95	210.00	210.12
	5	198.13	198.25	198.27	198.29	209.96	210.08	210.10	210.14
	∞		198.36				210.22		
H_2O_2	D	241.65	243.87	247.65	247.65	252.29	254.26	258.02	258.02
252.3	T	249.23	249.87	250.10	250.16	259.28	259.87	260.09	260.14

-continue-

-continue-

Molecules, Experiment.[a]	Basis set	B3LYP cc-pV*x*Z	B3LYP cc-pV*x*Z+*sp*	B3LYP cc-pV*x*Z+*spd*	B3LYP aug-cc-pV*x*Z	BLYP cc-pV*x*Z	BLYP cc-pV*x*Z+*sp*	BLYP cc-pV*x*Z+*spd*	BLYP aug-cc-pV*x*Z
	Q	250.48	250.74	250.79	250.87	260.51	260.75	260.80	260.89
	5	250.74	250.85	250.87	250.89	260.72	260.85	260.87	260.89
	∞		250.87				260.88		
HOF	D	144.19	143.06	146.71	146.71	156.42	154.64	158.09	158.10
151.6	T	148.35	148.08	148.33	148.50	159.55	159.04	159.29	159.44
	Q	148.77	148.70	148.75	148.83	159.85	159.67	159.73	159.80
	5	148.75	148.79	148.81	148.82	159.73	159.75	159.77	159.79
	∞		148.80				159.77		
F_2	D	36.32	30.74	33.94	33.94	50.67	43.81	46.70	46.70
36.9	T	36.54	35.15	35.26	35.59	49.21	47.25	47.37	47.68
	Q	36.04	35.61	35.62	35.68	48.41	47.70	47.73	47.77
	5	35.63	35.68	35.68	35.68	47.78	47.75	47.76	47.77
	∞		35.67				47.77		
CO_2	D	375.18	370.60	372.82	372.82	390.46	383.74	386.01	386.01
381.9	T	380.63	378.98	379.17	379.21	394.00	391.49	391.67	392.31
	Q	381.49	380.73	380.74	380.85	394.46	393.23	393.25	393.38
	5	380.95	380.82	380.83	380.86	393.52	393.28	393.29	393.32
	∞		380.98				393.46		
H_2CO	D	350.33	349.67	351.05	351.05	356.37	354.56	356.16	356.16
357.3	T	356.51	356.20	356.33	356.36	361.85	361.08	361.21	361.83
	Q	357.47	357.23	357.25	357.34	362.64	362.13	362.17	362.27
	5	357.38	357.34	357.35	357.37	362.31	362.21	362.22	362.25

-continue-

-continue-

Molecules, Experiment.[a]	Basis set	B3LYP cc-pV*x*Z	B3LYP cc-pV*x*Z+*sp*	B3LYP cc-pV*x*Z+*spd*	B3LYP aug-cc-pV*x*Z	BLYP cc-pV*x*Z	BLYP cc-pV*x*Z+*sp*	BLYP cc-pV*x*Z+*spd*	BLYP aug-cc-pV*x*Z
	∞		357.39				362.27		
CH_3NH_2	D	531.57	533.58	535.91	535.91	530.87	532.28	535.02	535.02
542.5	T	542.83	543.45	543.60	543.68	542.14	542.48	542.65	543.33
	Q	544.51	544.76	544.80	544.91	543.79	543.89	543.94	544.08
	5	544.87	544.93	544.94	544.98	543.98	544.02	544.03	
	∞		544.96				544.07		
CH_3OH	D	468.45	470.40	472.85	472.85	469.32	470.63	473.36	473.36
480.9	T	478.25	478.87	479.04	479.08	478.88	479.24	479.42	480.04
	Q	479.76	479.92	479.96	480.06	480.34	480.35	480.40	480.53
	5	480.00	480.07	480.08	480.10	480.40	480.46	480.47	480.51
	∞		480.08				480.49		
N_2H_4	D	395.93	401.00	404.07	404.08	400.79	405.55	408.98	408.98
405.5	T	408.17	409.80	410.00	410.10	412.83	414.41	414.61	414.72
	Q	410.57	411.26	411.30	411.42	415.28	415.96	416.01	416.15
	5	411.31	411.44	411.46	411.49	415.96	416.12	416.13	416.17
	∞		411.51				416.20		
CH_3F	D	389.44	389.48	391.51	391.51	390.93	390.06	392.24	392.24
402.4	T	397.11	397.18	397.36	397.45	398.04	397.72	397.90	398.58
	Q	397.95	397.89	397.93	398.04	398.75	398.48	398.52	398.65
	5	397.99	398.02	398.03	398.05	398.56	398.56	398.56	398.60
	∞		398.00				398.56		

[a] Experimental values are obtained from reference [46]

Table 5.4 The CO_2 atomization energies in kcal/mol determined by BLYP with different truncated basis sets. The atomization energies calculated with cc-pV*x*Z are listed in the first row, and the energy differences due to the addition of diffuse *s* and *p* functions to cc-pV*x*Z are listed in the second row. Likewise, the energy differences due to the addition of *s*, *p*, and *d* diffuse functions are listed in the third row……

	cc-pVDZ	cc-pVTZ	cc-pVQZ	cc-pV5Z
cc-pV*x*Z	390.4553	394.0023	394.4626	393.5171
sp+	-6.7178	-2.5143	-1.2366	-0.2413
spd+	-4.4475	-2.3297	-1.2168	-0.2285
spdf+		-1.6875	-1.1790	-0.2276
spdfg+			-1.0870	-0.2160
spdfgh+				-0.1925

5.3.4 Statistical Analysis

The MEs and MAEs of atomization energy (relative to experiment) are calculated for BLYP and B3LYP in combination with all levels of basis sets and are listed in Table 5.5. The MEs and MAEs of extrapolated atomization energies are also included in the table. Overall, the best results, in terms of mean absolute error, are found with the B3LYP functional with aug-cc-pV*x*Z, with deviations of 5.69 kcal/mol for double-zeta, 2.34 kcal/mol for triple-zeta, 2.19 kcal/mol for quadruple-zeta, and 2.19 kcal/mol for quintuple-zeta. Except at the double-zeta level, the other levels of cc-pV*x*Z+*sp* basis sets perform slightly worse than the standard and augmented correlation consistent basis sets. However, considering the strong basis set dependence of many larger systems, the basis sets, which enable to smooth convergence behavior, are recommended. For BLYP, since it overestimates the atomization energies for most

of molecules, the reduction of energy due to the use of cc-pV*x*Z+*sp* slightly improves the accuracy, in particular at the low-level basis sets. As compared with MAE at the quintuple-zeta level basis set, the extrapolation decreases the MAE for B3LYP and increases MAE for BLYP slightly.

Interestingly, the mean errors of cc-pV*x*Z+*sp* are between those of cc-pV*x*Z and aug-cc-pV*x*Z for B3LYP. The absolute values of ME are decreased from 7.84 to 0.68 kcal/mol with respect to increasing basis set size. On the contrary, the MEs increase for BLYP as the basis sets increase, with the smallest error at double-zeta level (2.01 kcal/mol). The smallest ME at the double-zeta level may be attributed to fortuitous cancellation of errors, which is reflected in the large difference between MEs and MAEs at the double-zeta level.

Table 5.5 Mean absolute errors (MAE) and mean errors (ME) for the atomization energies in kcal/mol.

Basis set	B3LYP cc-pV*x*Z	B3LYP cc-pV*x*Z+*sp*	B3LYP aug-cc-pV*x*Z	BLYP cc-pV*x*Z	BLYP cc-pV*x*Z+*sp*	BLYP aug-cc-pV*x*Z
MAE						
D	8.09	7.84	5.69	7.91	5.56	6.12
T	2.36	2.47	2.34	7.18	6.42	6.67
Q	2.19	2.24	2.19	7.32	7.14	7.22
5	2.22	2.22	2.19	7.15	7.21	7.22
∞		2.21			7.27	
ME						
D	-8.09	-7.84	-5.69	0.33	-0.17	2.01
T	-1.88	-1.76	-1.53	5.79	5.64	6.11
Q	-0.85	-0.80	-0.69	6.70	6.61	6.74
5	-0.76	-0.68	-0.66	6.65	6.70	6.73
∞		-0.63			6.77	

5.4 Conclusions

In the present study, a set of truncated correlation consistent basis sets, cc-pV*x*Z+*sp*, are proposed. Using these truncated basis sets in combination with BLYP and B3LYP reduces the convergence problem observed with the standard correlation consistent basis sets, and does not cause a significant deterioration of the structures and atomization energy for the molecules tested. A detailed analysis has shown that use of lower angular momentum diffuse *s* and *p* functions is important in order to improve the convergence of molecular properties with respect to increasing basis set size for DFT, even for molecules such as O_3 and F_2, where the standard and augmented correlation consistent basis sets can not converge smoothly at all. The improvement is reflected in a large reduction of atomization energy at the double-, triple-, and quadruple-zeta levels. Compared with the standard correlation consistent basis sets, cc-pV*x*Z+*sp* is more desirable as it provides smooth convergence needed to achieve Kohn-Sham limits, especially for the strongly basis set dependent systems, without the additional computational expense of using the fully augmented basis sets.

CHAPTER 6

THE PERFORMANCE OF DENSITY FUNCTIONALS WITH RESPECT TO BASIS SETS: THE BASIS SET SUPERPOSITION ERROR (BSSE)

6.1 Introduction

Basis set superposition error (BSSE) originates from the finite size of the basis sets used in the calculation of interaction energy between monomers, where the interaction energy is obtained by taking the difference between the energy of the complex and the sum of the energies of the monomers. The energy of the complex benefits from the basis sets of the monomers, but the monomers only make use of their own basis set, which leads to the overestimation of the interaction energy between monomers. This effect is called the basis set superposition error (BSSE), which was first proposed by Liu and Mclean [81]. In particular, basis set superposition error plays an important role in the computation of interaction energies of weakly bound systems. Usually, two kinds of approaches are used to correct BSSE, the counterpoise approach or the use of a very large basis set. In the counterpoise approach by Boys and Bernardi, [82] the energies of the individual monomers and the complex are evaluated using the basis set of the complex. Even though debates about the appropriateness of the counterpoise approach continue, as it is thought to overcorrect the interaction energy, [83] this approach is the only practical method to correct BSSE. Other alternatives [84-91] to the counterpoise method were found to

produce unsatisfactory results. [83, 92] Another approach in correcting BSSE is to use a very large basis set. There is little or no BSSE if the basis set is saturated, or near the complete basis sets limit. However, it is not always practical to perform calculations with very large basis sets.

In addition to its use in determining accurate interaction energy in weakly bound systems, accounting for BSSE also plays an important role in improving the convergence of molecular properties with respect to the correlation consistent basis sets. A number of calculations of weakly bound systems have demonstrated that energies corrected and uncorrected for BSSE energies will converge to the same basis set limit when using the correlation consistent basis sets. [36, 93-98] However, for the low-level basis sets, the effect of BSSE on energy is very significant. Some previous studies [36, 93-99] on weakly bound systems using *ab initio* correlated methods with the correlation consistent basis sets have shown that uncorrected results do not converge smoothly, and the irregular convergence of computed results with increasing basis set size was observed. This convergence problem can be remedied by correcting BSSE. As compared with uncorrected results, the corrected results provide better convergence behavior. Most the previous studies have used correlated *ab initio* methods like MP2 and CCSD(T). There have only been a few reported studies on the effect of BSSE in DFT calculations (due to the deficiency of DFT in predicting weakly bound systems). In a paper by Rappe and Bernstein, [100] the binding energies for several non-bonded systems were investigated using a series of theoretical approaches including HF, MP2, CCSD(T), and B3LYP with the correlation consistent and Pople basis sets. Even though DFT methods are inadequate at predicting the energetics of non-bonded systems, correcting BSSE improves the convergent behavior of the binding energies computed with the correlation consistent basis sets. Correcting BSSE not only improves the convergence behavior of molecular properties for weakly bounded systems, but also for the

strongly bound systems. van Mourik *et al.* have investigated the effect of BSSE on strongly bound systems using correlated *ab initio* methods with correlation consistent basis sets. [49, 95, 101] They found that the effect of BSSE on the strongly bound systems is not insignificant, especially for the low-level basis sets.

In the previous section, an unexpected convergence problem was reported in prior chapters when several density functionals combined with the standard and augmented correlation consistent basis sets were used to determine the structures and energies of 17 strongly bound systems. Moreover, in Chapter 3, which focused upon basis set uncontraction, the convergence problem was improved by using contracted and uncontracted basis sets to calculate molecule and atoms separately. Considering the definition of BSSE and the effect of BSSE on the convergence behavior reported in previous sections of this dissertation, it is natural to assume that correcting BSSE might also help to reduce the convergence problem.

In this section, we examine the effect of BSSE on the convergence behavior of atomization energy computed from several density functionals with standard and augmented correlation consistent basis sets. Also, the effect of BSSE on the structures and frequencies is investigated in particular for the small basis sets.

6.2 Methodology

BSSE was corrected using the counterpoise methods, as implemented in the Gaussian 98 package suite.[35] The molecular property examined in this study is atomization energy, which is defined as Equation (6-1),

$$\Delta E(R) = E_{AB}(R) - (E_A + E_B) \tag{6-1}$$

where $E_{AB}(R)$ is the total energy of molecule at a distance R, and E_A and E_B are the total energies of the two atoms. According to the counterpoise method, the overestimation of the interaction energy can be corrected by the use of Equation (6-2):

$$\Delta E^{\bullet}(R) = E_{AB}(R) - (E_{A(B)}(R) + E_{B(A)}(R)) \tag{6-2}$$

Where $E_{A(B)}(R)$ is the total energy of atom A calculated using the basis sets on both A and B, and $E_{B(A)}(R)$ is the total energy of atom B calculated using both A and B basis sets. The difference between $\Delta E^{\bullet}(R)$ and $\Delta E(R)$ is considered the BSSE when the counterpoise method is used, as shown in Equation (6-3).

$$\boldsymbol{E_{CP}(R) = \Delta E^{\bullet}(R) - \Delta E(R) = E_A(R) - E_{A(B)}(R) + E_B(R) - E_{B(A)}(R)} \tag{6-3}$$

Furthermore, BSSE can impact not only the interaction energy, but also the geometries, zero-point energy, and vibrational frequencies. Thus, optimization and frequency calculations correcting BSSE were performed for each combination of density functional and basis set using the counterpoise scheme. These results are compared with those obtained from calculations which did not include the BSSE correction. BSSE corrected and uncorrected zero-point energies were obtained from the corresponding frequency calculations and included in the BSSE corrected and uncorrected atomization energies, respectively.

6.3 Result and Discussions

6.3.1 The Effect of BSSE on Structures and Frequencies

Table 6.1 lists the BSSE uncorrected and corrected geometries calculated using six density functionals with cc-pV*x*Z and aug-cc-pV*x*Z for eight molecules, H_2O, HF, HCN, CO, N_2, HNO, HOF, and CO_2, which were chosen due to the convergence behavior of their atomization energies with respect to increasing basis set size observed in our earlier studies Overall, for the molecules studied, the effect of BSSE on geometries is small, even at the double-zeta basis set level. The impact of BSSE upon bond length is less than 0.001Å, and upon bond angle is less than 0.2^o, with the exception of the HOH angle, where the impact is ~0.5 ^{o} for all functionals. When the aug-cc-pV*x*Z basis sets is used, the effect of BSSE on geometries is insignificant. With increasing basis set size, both BSSE uncorrected and corrected geometries converge to the same basis set limit.

Table 6.2 gives the uncorrected and corrected harmonic frequencies. Analogous to the geometries, in general, the harmonic frequencies are only slightly affected by the counterpoise correction. The corrected frequencies are ~10 cm^{-1} less than the uncorrected results at the double-zeta level for most of the functionals. The most substantial differences in the frequencies was noted when using BP86 and B3P86. The variation of frequencies for several molecules is more than ~100 cm^{-1}. Examples include ω_1 and ω_2 for H_2O, ω_1 and ω_2 for HCN, and ω_2 for HNO. Overall, at the quintuple-zeta level, there is very little difference, if any, in the corrected and uncorrected frequencies.

Table 6.1 The BSSE uncorrected (no corr.) and corrected (corr.) optimized geometries using DFT with the correlation consistent basis sets.

Molecules, Experiment	Basis set	B3LYP		B3PW91		B3P86		BLYP		BPW91		BP86	
H_2O		no corr.	corr.	no corr.	corr.	no corr.	corr.	no corr.	corr.	no corr.	corr.	no corr.	corr.
r(HO) =	cc-pVDZ	0.9687	0.9694	0.9663	0.9668	0.9659	0.9665	0.9798	0.9812	0.9762	0.9767	0.9779	0.9786
0.956 Å[a]	T	0.9614	0.9613	0.9596	0.9597	0.9594	0.9595	0.9715	0.9717	0.9687	0.9689	0.9707	0.9708
	Q	0.9603	0.9603	0.9587	0.9587	0.9584	0.9584	0.9703	0.9703	0.9677	0.9677	0.9697	0.9697
	5	0.9603	0.9603	0.9587	0.9586	0.9584	0.9584	0.9703	0.9701	0.9677	0.9676	0.9697	0.9697
	aug-cc-pVDZ	0.9649	0.9650	0.9631	0.9633	0.9629	0.9630	0.9751	0.9753	0.9724	0.9725	0.9744	0.9744
	T	0.9621	0.9620	0.9601	0.9603	0.9599	0.9601	0.9719	0.9721	0.9692	0.9694	0.9712	0.9714
	Q	0.9606	0.9607	0.9590	0.9590	0.9587	0.9588	0.9707	0.9707	0.9680	0.9680	0.9700	0.9700
	5	0.9604	0.9604	0.9588	0.9587	0.9586	0.9585	0.9705	0.9703	0.9679	0.9677	0.9698	0.9697
a(HOH) =	cc-pVDZ	102.74	102.25	102.68	102.27	102.74	102.34	101.77	101.14	101.78	101.24	101.74	101.18
105.2°[a]	T	104.50	104.63	104.34	104.24	104.38	104.29	103.75	103.57	103.60	103.46	103.57	103.43
	Q	104.88	104.84	104.66	104.64	104.70	104.68	104.20	104.12	103.97	103.92	103.94	103.89
	5	105.10	105.10	104.84	104.85	104.87	104.89	104.48	104.45	104.18	104.22	104.16	104.18
	aug-cc-pVDZ	104.76	104.73	104.42	104.47	104.44	104.50	104.16	104.04	103.80	103.74	103.81	103.71
	T	104.95	105.08	104.83	104.84	104.86	104.86	104.48	104.40	104.17	104.15	104.15	104.12
	Q	105.12	105.12	104.86	104.87	104.88	104.90	104.52	104.48	104.20	104.21	104.19	104.18
	5	105.13	105.14	104.87	104.89	104.90	104.92	104.54	104.51	104.22	104.24	104.21	104.21
HF													
r(HF) =	cc-pVDZ	0.9268	0.9264	0.9244	0.9239	0.9241	0.9236	0.9384	0.9379	0.9344	0.9346	0.9358	0.9361
0.917 Å[b]	T	0.9225	0.9221	0.9198	0.9198	0.9197	0.9197	0.9330	0.933	0.9293	0.9294	0.9311	0.9311
	Q	0.9214	0.9215	0.9189	0.9189	0.9189	0.9189	0.9320	0.9322	0.9282	0.9286	0.9302	0.9302
	5	0.9220	0.9219	0.9192	0.9192	0.9191	0.9191	0.9325	0.9325	0.9288	0.9290	0.9306	0.9306
	aug-cc-pVDZ	0.9256	0.9257	0.9235	0.9235	0.9232	0.9232	0.9367	0.9372	0.9333	0.9336	0.9349	0.9352
	T	0.9242	0.9242	0.9216	0.9216	0.9216	0.9216	0.9350	0.9351	0.9311	0.9311	0.9329	0.9329
	Q	0.9224	0.9223	0.9196	0.9196	0.9195	0.9195	0.9330	0.9333	0.9293	0.9293	0.9311	0.9311
	5	0.9222	0.9221	0.9194	0.9194	0.9193	0.9193	0.9328	0.9329	0.9290	0.9290	0.9308	0.9308

-continue-

-continue-

Molecules, Experiment	Basis set	B3LYP		B3PW91		B3P86		BLYP		BPW91		BP86	
HCN													
r(HC) =	cc-pVDZ	1.0772	1.0776	1.0775	1.0776	1.0769	1.0771	1.0836	1.0848	1.0833	1.0840	1.0852	1.0861
1.064 Å[a]	T	1.0654	1.0656	1.0672	1.0674	1.0663	1.0665	1.0711	1.0718	1.0729	1.0735	1.0744	1.0750
	Q	1.0655	1.0656	1.0673	1.0673	1.0664	1.0665	1.0712	1.0718	1.0730	1.0735	1.0746	1.0749
	5	1.0656	1.0655	1.0673	1.0672	1.0665	1.0664	1.0714	1.0717	1.0731	1.0734	1.0747	1.0748
	aug-cc-pVDZ	1.0744	1.0747	1.0752	1.0754	1.0746	1.0748	1.0808	1.0813	1.0811	1.0815	1.0831	1.0834
	T	1.0656	1.0658	1.0674	1.0676	1.0665	1.0667	1.0714	1.0721	1.0730	1.0736	1.0746	1.0752
	Q	1.0656	1.0656	1.0673	1.0673	1.0665	1.0665	1.0713	1.0718	1.0731	1.0736	1.0747	1.0749
	5	1.0656	1.0655	1.0673	1.0673	1.0665	1.0664	1.0714	1.0717	1.0732	1.0735	1.0747	1.0748
r(CN) =	cc-pVDZ	1.1579	1.1584	1.1578	1.1582	1.1571	1.1575	1.1697	1.1703	1.1692	1.1695	1.1703	1.1707
1.156 Å[a]	T	1.1462	1.1464	1.1468	1.1469	1.1459	1.1460	1.1575	1.1577	1.1576	1.1578	1.1585	1.1588
	Q	1.1450	1.1451	1.1455	1.1456	1.1446	1.1447	1.1565	1.1564	1.1565	1.1565	1.1574	1.1576
	5	1.1450	1.1450	1.1454	1.1454	1.1445	1.1445	1.1565	1.1563	1.1564	1.1563	1.1573	1.1574
	aug-cc-pVDZ	1.1568	1.1572	1.1569	1.1572	1.1561	1.1564	1.1684	1.1689	1.1680	1.1684	1.1691	1.1695
	T	1.1460	1.1462	1.1464	1.1466	1.1455	1.1458	1.1573	1.1577	1.1573	1.1577	1.1582	1.1586
	Q	1.1451	1.1452	1.1456	1.1457	1.1447	1.1448	1.1566	1.1566	1.1566	1.1566	1.1575	1.1577
	5	1.1450	1.1450	1.1454	1.1454	1.1445	1.1445	1.1565	1.1563	1.1564	1.1563	1.1573	1.1574
CO													
r(CO) =	cc-pVDZ	1.1345	1.1350	1.1340	1.1342	1.1334	1.1336	1.1471	1.1478	1.1459	1.1462	1.1469	1.1473
1.128 Å[b]	T	1.1262	1.1262	1.1260	1.1262	1.1253	1.1254	1.1379	1.1381	1.1373	1.1375	1.1382	1.1384
	Q	1.1237	1.1238	1.1236	1.1237	1.1229	1.1229	1.1355	1.1357	1.1349	1.1351	1.1358	1.1360
	5	1.1236	1.1236	1.1235	1.1235	1.1227	1.1227	1.1354	1.1354	1.1347	1.1348	1.1356	1.1356
	aug-cc-pVDZ	1.1340	1.1343	1.1337	1.1339	1.1330	1.1332	1.1463	1.1466	1.1453	1.1455	1.1463	1.1465
	T	1.1258	1.1259	1.1257	1.1257	1.1249	1.1251	1.1376	1.1379	1.1369	1.1371	1.1378	1.1380
	Q	1.1238	1.1239	1.1237	1.1237	1.1230	1.1230	1.1356	1.1357	1.1350	1.1350	1.1359	1.1359
	5	1.1236	1.1236	1.1235	1.1235	1.1227	1.1227	1.1354	1.1354	1.1347	1.1347	1.1356	1.1356

-continue-

-continue-

Molecules, Experiment	Basis set	B3LYP		B3PW91		B3P86		BLYP		BPW91		BP86	
N_2													
r(NN) =	cc-pVDZ	1.1044	1.1048	1.1036	1.1038	1.1032	1.1033	1.1172	1.1178	1.1154	1.1158	1.1166	1.117
1.098 Å[b]	T	1.0914	1.0915	1.0912	1.0913	1.0906	1.0906	1.1032	1.1034	1.1025	1.1027	1.1034	1.1036
	Q	1.0902	1.0903	1.0901	1.0902	1.0895	1.0895	1.1022	1.1023	1.1016	1.1017	1.1025	1.1026
	5	1.0900	1.0899	1.0899	1.0899	1.0892	1.0892	1.1019	1.1020	1.1013	1.1013	1.1022	1.1022
	aug-cc-pVDZ	1.1044	1.1048	1.1036	1.1039	1.1032	1.1035	1.1168	1.1173	1.1152	1.1155	1.1163	1.1167
	T	1.0912	1.0913	1.0910	1.0912	1.0904	1.0905	1.1030	1.1032	1.1023	1.1025	1.1032	1.1034
	Q	1.0901	1.0902	1.0901	1.0901	1.0894	1.0894	1.1021	1.1022	1.1015	1.1015	1.1024	1.1024
	5	1.0899	1.0899	1.0898	1.0899	1.0892	1.0892	1.1019	1.1019	1.1012	1.1012	1.1021	1.1021
HNO													
r(HN) =	cc-pVDZ	1.0776	1.0779	1.0758	1.0759	1.0746	1.0746	1.1002	1.1014	1.0967	1.0968	1.0997	1.0996
1.09 Å[c]	T	1.0628	1.0633	1.0630	1.0637	1.0620	1.0626	1.0813	1.0813	1.0805	1.0809	1.0829	1.0833
	Q	1.0613	1.0614	1.0619	1.0622	1.0610	1.0615	1.0792	1.0792	1.0793	1.0793	1.0815	1.0816
	5	1.0607	1.0610	1.0614	1.0616	1.0605	1.0609	1.0781	1.0782	1.0783	1.0783	1.0808	1.0807
	aug-cc-pVDZ	1.0674	1.0678	1.0673	1.0672	1.0664	1.0665	1.0855	1.0862	1.0845	1.0850	1.0871	1.0876
	T	1.0613	1.0619	1.0618	1.0626	1.0610	1.0617	1.0786	1.0786	1.0785	1.0791	1.0810	1.0815
	Q	1.0610	1.0614	1.0616	1.0617	1.0607	1.0612	1.0783	1.0783	1.0784	1.0785	1.0810	1.0813
	5	1.0608	1.0611	1.0615	1.0615	1.0606	1.0610	1.0781	1.0779	1.0783	1.0782	1.0809	1.0808
r(NO) =	cc-pVDZ	1.2028	1.2033	1.1985	1.1989	1.1983	1.1986	1.2193	1.2200	1.2130	1.2136	1.2145	1.2153
1.209 Å[c]	T	1.1984	1.1984	1.1945	1.1945	1.1939	1.1939	1.2153	1.2154	1.2091	1.2090	1.2106	1.2105
	Q	1.1970	1.1970	1.1932	1.1933	1.1926	1.1926	1.2139	1.2140	1.2081	1.2080	1.2093	1.2093
	5	1.1966	1.1968	1.1927	1.1929	1.1922	1.1922	1.2137	1.2137	1.2078	1.2076	1.2092	1.2090
	aug-cc-pVDZ	1.2051	1.2057	1.2006	1.2012	1.2002	1.2008	1.2221	1.2230	1.2155	1.2159	1.2172	1.2177
	T	1.1978	1.1981	1.1939	1.1941	1.1934	1.1936	1.2149	1.2152	1.2088	1.2088	1.2103	1.2102
	Q	1.1964	1.1968	1.1926	1.1927	1.1921	1.1921	1.2135	1.2135	1.2076	1.2075	1.2090	1.2087
	5	1.1962	1.1965	1.1924	1.1924	1.1918	1.1919	1.2133	1.2132	1.2074	1.2071	1.2088	1.2086

-continue-

-continue-

Molecules, Experiment	Basis set	B3LYP		B3PW91		B3P86		BLYP		BPW91		BP86	
a(HNO) =	cc-pVDZ	108.35	108.49	108.36	108.42	108.32	108.39	108.30	108.45	108.29	108.42	108.28	108.38
108.047°[c]	T	108.68	108.72	108.67	108.70	108.65	108.68	108.55	108.57	108.53	108.58	108.50	108.54
	Q	108.81	108.81	108.79	108.75	108.77	108.77	108.68	108.69	108.68	108.66	108.63	108.59
	5	108.87	108.89	108.85	108.86	108.83	108.84	108.73	108.74	108.72	108.66	108.70	108.75
	aug-cc-pVDZ	108.65	108.58	108.61	108.65	108.57	108.56	108.53	108.51	108.52	108.49	108.48	108.47
	T	108.86	108.89	108.84	108.81	108.82	108.86	108.74	108.74	108.72	108.72	108.69	108.69
	Q	108.92	108.94	108.89	108.89	108.87	108.82	108.81	108.80	108.78	108.79	108.75	108.76
	5	108.92	108.94	108.89	108.89	108.87	108.88	108.80	108.80	108.78	108.80	108.75	108.76
HOF													
r(HO) =	cc-pVDZ	0.9775	0.9773	0.9754	0.9752	0.9751	0.9750	0.9898	0.9899	0.9864	0.9860	0.9883	0.9881
0.96 Å[e]	T	0.9700	0.9700	0.9685	0.9685	0.9683	0.9683	0.9817	0.9814	0.9790	0.9786	0.9811	0.9806
	Q	0.9693	0.9695	0.9677	0.9678	0.9676	0.9676	0.9809	0.9809	0.9782	0.9780	0.9803	0.9800
	5	0.9694	0.9696	0.9679	0.9679	0.9677	0.9677	0.9811	0.9811	0.9783	0.9781	0.9804	0.9802
	aug-cc-pVDZ	0.9747	0.9750	0.9725	0.9731	0.9726	0.9729	0.9866	0.9872	0.9836	0.9839	0.9857	0.9860
	T	0.9715	0.9715	0.9694	0.9694	0.9692	0.9692	0.9829	0.9830	0.9799	0.9799	0.9820	0.9820
	Q	0.9698	0.9698	0.9682	0.9682	0.9680	0.9680	0.9819	0.9814	0.9786	0.9786	0.9808	0.9808
	5	0.9696	0.9696	0.9680	0.9680	0.9678	0.9678	0.9814	0.9814	0.9785	0.9785	0.9806	0.9806
r(OF) =	cc-pVDZ	1.4349	1.4366	1.4240	1.4248	1.4219	1.4226	1.4706	1.4729	1.4543	1.4557	1.4551	1.4566
1.442 Å[e]	T	1.4301	1.4300	1.4164	1.4164	1.4145	1.4145	1.4675	1.4677	1.4480	1.4489	1.4489	1.4500
	Q	1.4291	1.4289	1.4152	1.4154	1.4132	1.4132	1.4669	1.4673	1.4475	1.4479	1.4487	1.4490
	5	1.4286	1.4287	1.4146	1.4145	1.4126	1.4126	1.4667	1.4672	1.4471	1.4471	1.4483	1.4483
	aug-cc-pVDZ	1.4328	1.4342	1.4196	1.4212	1.4179	1.4192	1.4699	1.4715	1.4516	1.4530	1.4526	1.4540
	T	1.4310	1.4310	1.4166	1.4166	1.4147	1.4147	1.4684	1.4688	1.4489	1.4489	1.4502	1.4502
	Q	1.4288	1.4288	1.4148	1.4148	1.4127	1.4127	1.4668	1.4667	1.4473	1.4473	1.4484	1.4484

-continue-

-continue-

Molecules, Experiment	Basis set	B3LYP		B3PW91		B3P86		BLYP		BPW91		BP86	
	5	1.4284	1.4284	1.4144	1.4144	1.4124	1.4124	1.4666	1.4667	1.4469	1.4469	1.4481	1.4481
a(HOF) =	cc-pVDZ	97.87	98.02	97.99	98.17	98.00	98.18	96.96	97.10	97.13	97.32	97.11	97.30
97.2 Å[e]	T	98.48	98.40	98.68	98.68	98.68	98.68	97.43	97.45	97.67	97.72	97.64	97.69
	Q	98.63	98.53	98.80	98.80	98.81	98.81	97.58	97.60	97.89	97.82	97.85	97.79
	5	98.71	98.71	98.88	98.87	98.88	98.88	97.68	97.72	97.97	97.90	97.93	97.86
	aug-cc-pVDZ	98.56	98.56	98.76	98.70	98.67	98.74	97.65	97.58	97.85	97.87	97.83	97.84
	T	98.59	98.59	98.84	98.84	98.84	98.84	97.68	97.66	97.95	97.95	97.91	97.91
	Q	98.72	98.72	98.90	98.90	98.90	98.90	97.66	97.72	98.00	98.00	97.96	97.96
	5	98.74	98.74	98.91	98.91	98.91	98.91	97.73	97.72	98.01	98.01	97.97	97.97
CO_2													
r(CO) =	cc-pVDZ	1.1673	1.1681	1.1656	1.1660	1.1650	1.6530	1.1815	1.1827	1.1784	1.1792	1.1797	1.1805
1.162 Å[a]	T	1.1604	1.1608	1.1592	1.1594	1.1584	1.1586	1.1736	1.1740	1.1714	1.1718	1.1725	1.1728
	Q	1.1588	1.1589	1.1576	1.1577	1.1568	1.1570	1.1720	1.1722	1.1699	1.1701	1.1710	1.1712
	5	1.1587	1.1588	1.1575	1.1576	1.1567	1.1568	1.1721	1.1722	1.1699	1.1699	1.1709	1.1710
	aug-cc-pVDZ	1.1673	1.1677	1.1659	1.1661	1.1652	1.1654	1.1811	1.1817	1.1783	1.1788	1.1795	1.1800
	T	1.1605	1.1609	1.1592	1.1595	1.1585	1.1587	1.1737	1.1741	1.1715	1.1719	1.1725	1.1729
	Q	1.1589	1.1590	1.1577	1.1578	1.1569	1.1570	1.1722	1.1724	1.1700	1.1702	1.1711	1.1712
	5	1.1587	1.1588	1.1575	1.1576	1.1568	1.1568	1.1721	1.1721	1.1699	1.1699	1.1709	1.1710

Table 6.2 The BSSE uncorrected (no corr.) and corrected (corr.) frequencies using DFT with the correlation consistent basis sets.

Molecules, Experiment	Basis set	B3LYP		B3PW91		B3P86		BLYP		BPW91		BP86	
		no corr.	corr.	no corr.	corr.	no corr.	corr.	no corr.	corr.	no corr.	corr.	no corr.	corr.
H_2O	cc-pVDZ	1659	1657	1660	1661	1659	1623	1630	1631	1632	1630	1626	1559

-continue-

-continue-

Molecules, Experiment	Basis set	B3LYP		B3PW91		B3P86		BLYP		BPW91		BP86	
ω_1	T	1640	1638	1640	1641	1639	1617	1611	1605	1612	1607	1606	1559
1595 cm^{-1}	Q	1635	1635	1636	1635	1635	1602	1605	1602	1607	1603	1601	1533
	5	1630	1631	1632	1628	1631	1615	1599	1593	1603	1601	1596	1561
	aug-cc-pVDZ	1619	1619	1623	1620	1623	1545	1584	1583	1592	1588	1585	1484
	T	1629	1627	1629	1628	1628	1676	1596	1597	1600	1598	1593	1662
	Q	1629	1628	1632	1630	1630	1677	1598	1597	1602	1598	1595	1662
	5	1629	1630	1632	1627	1631	1737	1598	1596	1602	1597	1595	1798
ω_2	cc-pVDZ	3751	3751	3795	3794	3803	3785	3592	3586	3653	3656	3637	3611
3657 cm^{-1}	T	3800	3803	3834	3835	3838	3832	3656	3660	3706	3709	3686	3673
	Q	3806	3806	3837	3838	3841	3833	3664	3667	3710	3713	3691	3672
	5	3808	3809	3839	3842	3843	3839	3668	3671	3713	3715	3693	3678
	aug-cc-pVDZ	3794	3797	3826	3825	3831	3793	3649	3654	3693	3699	3675	3631
	T	3793	3797	3829	3828	3832	3844	3655	3658	3702	3705	3681	3702
	Q	3804	3804	3836	3836	3840	3857	3664	3666	3709	3712	3689	3718
	5	3807	3807	3838	3841	3842	3883	3667	3666	3712	3714	3692	3777
ω_3	cc-pVDZ	3853	3846	3900	3893	3908	3899	3694	3680	3759	3754	3743	3732
3756 cm^{-1}	T	3900	3904	3937	3937	3942	3945	3756	3757	3808	3810	3789	3792
	Q	3906	3906	3940	3941	3945	3944	3764	3765	3813	3816	3794	3791
	5	3909	3911	3943	3947	3947	3948	3769	3772	3817	3820	3797	3792
	aug-cc-pVDZ	3904	3797	3937	3938	3943	3902	3759	3764	3805	3811	3787	3733
	T	3895	3899	3934	3934	3937	3949	3757	3760	3806	3810	3785	3804
	Q	3906	3906	3940	3941	3944	3957	3765	3768	3813	3817	3794	3811
	5	3909	3910	3943	3947	3947	3950	3768	3772	3816	3821	3797	3816
HF	cc-pVDZ	4021	4027	4065	4072	4075	4075	3846	3855	3912	3907	3902	3882
ω_1	T	4085	4091	4129	4128	4132	4132	3930	3930	3986	3984	3968	3964

-continue-

-continue-

Molecules, Experiment	Basis set	B3LYP		B3PW91		B3P86		BLYP		BPW91		BP86	
4138 cm^{-1}	Q	4086	4085	4125	4126	4129	4127	3930	3927	3987	3981	3965	3960
	5	4078	4080	4122	4122	4126	4120	3926	3925	3980	3977	3962	3949
	aug-cc-pVDZ	4061	4052	4093	4085	4100	4057	3898	3883	3947	3933	3933	3873
	T	4069	4069	4108	4109	4111	4094	3913	3914	3969	3971	3950	3940
	Q	4073	4076	4117	4118	4121	4110	3920	3918	3975	3975	3957	3953
	5	4076	4077	4120	4119	4124	4133	3922	3921	3977	3977	3956	3995
HCN	cc-pVDZ	773	765	774	767	774	667	740	730	742	735	738	546
ω_1	T	762	761	764	765	764	654	724	722	727	726	723	551
712 cm^{-1}	Q	762	752	764	757	764	701	723	722	728	728	724	667
	5	759	749	762	755	762	936	718	718	725	725	720	1047
	aug-cc-pVDZ	728	725	736	733	736	704	688	681	698	693	693	572
	T	760	759	763	763	763	918	718	719	725	725	720	914
	Q	758	778	761	755	761	720	717	725	724	733	720	652
	5	757	748	761	754	762	891	717	714	724	722	720	858
ω_2	cc-pVDZ	774	765	774	767	774	667	741	732	742	737	738	548
712 cm^{-1}	T	762	761	764	765	764	654	724	722	727	726	723	551
	Q	762	752	764	757	764	701	723	722	728	728	724	667
	5	759	749	762	755	762	936	719	719	725	725	720	1047
	aug-cc-pVDZ	729	727	737	733	736	704	689	682	698	693	693	573
	T	760	759	763	763	763	918	718	719	725	725	720	914
	Q	758	778	762	755	762	720	717	725	724	734	720	652
	5	757	748	761	754	762	891	717	716	724	722	720	859
ω_3	cc-pVDZ	2200	2197	2207	2205	2210	2211	2107	2104	2119	2120	2112	2114
2089 cm^{-1}	T	2201	2199	2205	2200	2209	2211	2114	2112	2122	2121	2116	2120
	Q	2202	2199	2206	2204	2210	2215	2113	2113	2122	2122	2116	2123

-continue-

-continue-

Molecules, Experiment	Basis set	B3LYP		B3PW91		B3P86		BLYP		BPW91		BP86	
	5	2201	2202	2205	2206	2210	2213	2112	2113	2121	2122	2116	2120
	aug-cc-pVDZ	2187	2185	2194	2193	2198	2193	2095	2093	2108	2107	2100	2092
	T	2200	2198	2204	2200	2209	2210	2111	2109	2121	2119	2115	2116
	Q	2200	2197	2205	2203	2210	2208	2111	2112	2121	2123	2115	2113
	5	2200	2202	2205	2206	2210	2212	2111	2113	2121	2122	2115	2116
ω_4	cc-pVDZ	3464	2197	3475	3472	3478	3448	3378	3366	3398	3393	3381	3326
3312 cm^{-1}	T	3450	3450	3452	3450	3458	3430	3369	3366	3378	3373	3364	3322
	Q	3441	3438	3442	3443	3449	3431	3360	3356	3368	3364	3354	3333
	5	3442	3441	3443	3444	3449	3485	3360	3358	3368	3366	3355	3429
	aug-cc-pVDZ	3451	3446	3457	3454	3461	3460	3366	3360	3380	3376	3363	3348
	T	3444	3446	3447	3446	3453	3497	3363	3361	3371	3370	3358	3411
	Q	3439	3437	3442	3443	3448	3447	3360	3357	3368	3367	3354	3345
	5	3441	3441	3443	3443	3449	3482	3359	3358	3367	3366	3355	3387
CO	cc-pVDZ	2201	2198	2210	2210	2225	2213	2098	2093	2113	2110	2107	2104
ω_1	T	2211	2211	2219	2218	2213	2222	2114	2112	2126	2124	2120	2119
2170 cm^{-1}	Q	2214	2214	2221	2221	2223	2226	2117	2115	2129	2127	2123	2122
	5	2213	2213	2221	2220	2225	2225	2115	2115	2128	2128	2122	2122
	aug-cc-pVDZ	2186	2186	2194	2194	2198	2198	2086	2086	2101	2100	2095	2094
	T	2207	2207	2215	2216	2220	2220	2109	2107	2123	2121	2117	2115
	Q	2212	2212	2220	2220	2224	2224	2114	2114	2127	2127	2121	2121
	5	2213	2213	2220	2220	2224	2225	2115	2115	2128	2128	2122	2089
N_2	cc-pVDZ	2455	2451	2468	2466	2470	2469	2332	2327	2354	2352	2345	2343
ω_1	T	2450	2450	2461	2461	2465	2466	2335	2334	2353	2353	2346	2345
2359 cm^{-1}	Q	2448	2447	2458	2458	2463	2463	2333	2333	2350	2351	2343	2344
	5	2449	2450	2459	2460	2464	2464	2333	2335	2351	2353	2344	2346

-continue-

-continue-

Molecules, Experiment	Basis set	B3LYP		B3PW91		B3P86		BLYP		BPW91		BP86	
	aug-cc-pVDZ	2444	2442	2457	2457	2460	2460	2325	2324	2347	2351	2339	2341
	T	2448	2447	2458	2458	2462	2462	2333	2332	2351	2351	2344	2343
	Q	2448	2447	2458	2459	2463	2463	2333	2333	2351	2352	2344	2846
	5	2449	2450	2460	2460	2464	2464	2334	2336	2352	2354	2345	2347
HNO	cc-pVDZ	1555	1553	1563	1563	1563	1534	1480	1479	1500	1500	1492	1440
ω_1	T	1567	1567	1571	1571	1572	1555	1492	1493	1511	1509	1503	1484
1501 cm^{-1}	Q	1566	1566	1569	1570	1570	1530	1496	1495	1510	1510	1503	1438
	5	1564	1564	1567	1568	1568	1575	1493	1492	1508	1508	1500	1512
	aug-cc-pVDZ	1551	1549	1556	1553	1557	1511	1483	1478	1497	1497	1490	1417
	T	1560	1559	1564	1564	1564	1640	1487	1487	1504	1504	1495	1563
	Q	1562	1561	1565	1566	1566	1588	1491	1492	1506	1506	1498	1519
	5	1562	1562	1566	1566	1567	1641	1491	1493	1506	1506	1499	1573
ω_2	cc-pVDZ	1683	1680	1714	1712	1717	1715	1566	1565	1605	1604	1597	1440
1565 cm^{-1}	T	1665	1665	1695	1695	1698	1698	1560	1561	1593	1594	1586	1587
	Q	1668	1668	1696	1696	1700	1699	1562	1563	1594	1595	1588	1584
	5	1668	1666	1697	1696	1700	1699	1562	1561	1595	1596	1587	1589
	aug-cc-pVDZ	1673	1673	1705	1703	1707	1706	1563	1559	1601	1599	1593	1588
	T	1663	1662	1692	1692	1696	1696	1558	1558	1591	1593	1583	1617
	Q	1669	1667	1697	1697	1700	1701	1562	1563	1595	1596	1588	1593
	5	1669	1667	1697	1697	1701	1701	1562	1564	1596	1597	1588	1631
ω_3	cc-pVDZ	2744	2747	2779	2782	2792	2783	2491	2486	2543	2546	2520	2502
2684 cm^{-1}	T	2844	2841	2859	2854	2871	2857	2625	2627	2656	2652	2636	2619
	Q	2854	2854	2868	2863	2878	2852	2642	2643	2662	2663	2646	2615
	5	2867	1666	2875	2872	2884	2880	2657	2657	2674	2676	2657	2659
	aug-cc-pVDZ	2855	2856	2867	2872	2877	2860	2638	2639	2663	2662	2645	2606

-continue-

-continue-

Molecules, Experiment	Basis set	B3LYP		B3PW91		B3P86		BLYP		BPW91		BP86	
	T	2866	2862	2877	2870	2887	2925	2658	2662	2680	2675	2657	2715
	Q	2864	2861	2873	2873	2884	2897	2657	2659	2675	2677	2657	2678
	5	2866	2863	2875	2875	2884	2916	2660	2661	2677	2680	2658	2716
HOF	cc-pVDZ	967	960	984	981	991	986	890	860	914	911	917	911
ω_1	T	988	987	1016	1015	1022	1021	904	907	939	936	940	935
886 cm^{-1}	Q	982	983	1011	1011	1017	1016	897	897	932	932	932	929
	5	981	982	1011	1011	1017	1016	896	895	931	932	932	930
	aug-cc-pVDZ	973	967	998	992	1004	994	891	888	921	917	923	911
	T	984	984	1014	1014	1020	1022	900	900	935	935	935	938
	Q	981	981	1010	1010	1016	1018	895	896	930	931	931	934
	5	981	981	1010	1011	1017	1022	896	895	930	932	931	940
ω_2	cc-pVDZ	1386	1393	1400	1409	1401	1382	1307	1316	1329	1336	1323	1274
1393 cm^{-1}	T	1405	1398	1422	1417	1423	1409	1332	1331	1356	1347	1349	1311
	Q	1408	1408	1425	1424	1425	1397	1334	1330	1356	1353	1350	1289
	5	1409	1408	1425	1425	1426	1412	1334	1333	1357	1356	1350	1308
	aug-cc-pVDZ	1408	1406	1423	1424	1425	1350	1334	1310	1355	1352	1349	1237
	T	1407	1405	1423	1419	1424	1471	1332	1327	1355	1353	1348	1420
	Q	1408	1407	1425	1424	1426	1455	1335	1332	1356	1355	1350	1394
	5	1409	1408	1425	1425	1426	1526	1335	1334	1357	1356	1351	1534
ω_3	cc-pVDZ	3681	3692	3721	3729	3728	3727	3512	3522	3568	3581	3552	3548
3537 cm^{-1}	T	3737	3736	3767	3766	3769	3768	3578	3582	3624	3629	3602	3602
	Q	3735	3731	3764	3763	3767	3759	3578	3580	3623	3626	3603	3590
	5	3733	3733	3761	3763	3767	3761	3575	3579	3622	3627	3603	3593
	aug-cc-pVDZ	3717	3720	3750	3750	3753	3725	3556	3553	3601	3605	3583	3543
	T	3718	3719	3752	3754	3756	3778	3564	3569	3611	3614	3590	3622

-continue-

-continue-

Molecules, Experiment	Basis set	B3LYP		B3PW91		B3P86		BLYP		BPW91		BP86	
	Q	3729	3731	3760	3760	3763	3780	3569	3577	3620	3621	3598	3622
	5	3733	3732	3763	3763	3766	3799	3577	3576	3622	3622	3602	3664
CO_2	cc-pVDZ	655	654	662	660	663	660	617	618	626	625	623	623
ω_1	T	672	665	676	675	677	677	634	631	641	638	639	637
667 cm^{-1}	Q	675	674	679	668	680	680	637	635	643	646	641	644
	5	675	675	679	679	679	680	637	635	643	643	641	641
	aug-cc-pVDZ	666	662	673	671	674	672	628	622	637	631	635	622
	T	674	673	678	677	679	677	636	635	642	641	640	639
	Q	675	675	680	679	680	680	638	637	644	642	642	641
	5	674	675	679	679	680	679	636	636	643	643	641	641
ω_2	cc-pVDZ	655	655	662	660	663	661	617	619	626	625	623	623
667 cm^{-1}	T	672	665	676	676	677	677	634	631	641	638	639	637
	Q	675	675	679	681	680	691	637	636	643	646	641	645
	5	675	675	679	679	679	680	637	635	643	644	641	645
	aug-cc-pVDZ	666	663	673	671	674	672	628	623	637	632	635	640
	T	674	674	678	677	679	678	636	635	642	641	640	639
	Q	675	675	680	679	680	680	638	637	644	644	642	642
	5	674	675	679	679	680	680	636	636	643	643	641	641
ω_3	cc-pVDZ	1363	1360	1374	1373	1376	1376	1294	1291	1312	1311	1307	1305
1333 cm^{-1}	T	1372	1370	1381	1380	1384	1383	1307	1306	1321	1320	1317	1316
	Q	1372	1371	1381	1380	1384	1383	1307	1307	1321	1319	1317	1317
	5	1371	1371	1380	1380	1383	1383	1306	1306	1320	1320	1316	1316
	aug-cc-pVDZ	1355	1354	1365	1365	1368	1368	1289	1288	1306	1305	1301	1300
	T	1369	1368	1378	1377	1381	1380	1304	1303	1318	1317	1314	1313
	Q	1371	1371	1380	1380	1383	1383	1306	1306	1320	1319	1316	1316

-continue-

-continue-

Molecules, Experiment	Basis set	B3LYP		B3PW91		B3P86		BLYP		BPW91		BP86	
	5	1371	1371	1380	1380	1383	1383	1306	1306	1320	1320	1316	1316
ω_4	cc-pVDZ	2423	2416	2449	2447	2453	2451	2329	2322	2369	2366	2360	2355
2349 cm^{-1}	T	2417	2414	2441	2440	2446	2444	2329	2326	2363	2361	2355	2353
	Q	2408	2407	2433	2433	2438	2437	2320	2320	2356	2351	2346	2348
	5	2405	2404	2430	2430	2435	2435	2315	2316	2352	2351	2343	2340
	aug-cc-pVDZ	2389	2387	2417	2416	2421	2421	2299	2297	2340	2338	2331	2329
	T	2400	2397	2426	2424	2431	2429	2311	2309	2348	2345	2339	2337
	Q	2404	2403	2430	2429	2435	2434	2315	2315	2352	2350	2343	2343
	5	2405	2404	2430	2430	2434	2435	2315	2315	2351	2351	2343	2343

Generally, molecular properties, that are less related to energy, do not necessarily converge with increasing basis set size. For geometries, the bond lengths and angles converge to the basis set limit, but the convergence is not best described by an exponential function. The variation of frequencies with increasing basis set size is more involved. No general trend was observed for the BSSE uncorrected and corrected frequencies.

6.3.2 Basis Set Superposition Error in Atomization Energy

It is assumed that, for strongly bound molecules, the effect of BSSE on energy is trivial for *ab initio* and DFT methods, and that BSSE plays a much smaller role in DFT than in *ab initio* correlated methods, due to the faster convergence of DFT energy with respect to basis set size. However, earlier work by Wilson *et al*. [49] has found that, for advanced correlated *ab initio* methods with small basis sets, BSSE is not insignificant in calculating the energy of strongly bound systems. For example, a BSSE of 5 kcal/mol for the N_2 binding energy at the CCSD(T)/cc-pVDZ level was observed. In the present study, the effect of BSSE on strongly bound systems using density functional methods were investigated. The BSSE for atomization energies of eight strongly bound molecules using six density functionals and the standard and augmented correlation consistent basis sets are presented in Table 6.3.

As shown in the table, the largest BSSE was observed at the double-zeta level, and the BSSE decreases with increasing basis set size. For example, with the BLYP/cc-pVDZ, the BSSE of CO_2 is 7.11 kcal/mol, and it rapidly drops to 2.25 kcal/mol at the triple-zeta level, 1.36 kcal/mol at the quadruple-zeta level, and finally to 0.28 kcal/mol at the quintuple-zeta level. It has been stated in previous *ab initio* studies that the effectiveness of the counterpoise correction approach at the self-consistent-field level mainly relies on the quality of the basis sets.[102] For example, BSSE is larger when using cc-pV*x*Z, as compared with aug-cc-pV*x*Z basis sets. Like

for *ab initio* methods, DFT in combination with aug-cc-pV*x*Z shows less BSSE as compared with cc-pV*x*Z, especially with the low-level basis sets. For example, the BSSE is reduced to 1.86 kcal/mol for CO_2 with aug-cc-pVDZ, as compared to the BSSE (7.11 kcal/mol) with cc-pVDZ. In general, the BSSE does decrease as the basis set size increases. For several cases, similar amounts of BSSE were achieved at the triple- and quadruple-zeta level basis sets like B3LYP/cc-pV*x*Z BSSE for H_2O, all functionals/cc-pV*x*Z BSSE for N_2, while the BSSE at the quintuple-zeta level is trivial (<0.2 kcal/mol). For all molecules but HF, pure functionals, BLYP, BPW91, and BP86, result in a larger BSSE at the double-zeta level, as compared with hybrid functionals, B3LYP, B3PW91, and B3P86, respectively. For HF, BLYP predicts a larger BSSE than B3LYP, while BPW91 and BP86 give smaller BSSE than B3PW91 and B3P86.

Table 6.3 The basis set superposition error for eight molecules using DFT with the correlation consistent basis sets

Molecules	Basis Sets	B3LYP	B3PW91	B3P86	BLYP	BPW91	BP86
H_2O	cc-pVDZ	3.51	2.84	2.73	4.47	3.44	3.48
	T	0.46	0.84	0.77	1.34	1.05	1.02
	Q	0.46	0.39	0.34	0.67	0.54	0.50
	5	0.08	0.07	0.06	0.14	0.12	0.11
	aug-cc-pVDZ	0.49	0.50	0.48	0.59	0.53	0.50
	T	0.18	0.25	0.25	0.18	0.26	0.24
	Q	0.12	0.12	0.13	0.15	0.15	0.16
	5	0.03	0.03	0.03	0.05	0.04	0.04
HF	cc-pVDZ	1.75	1.43	1.38	2.26	0.96	0.97
	T	0.40	0.32	0.29	0.24	0.19	0.18
	Q	0.20	0.16	0.14	0.16	0.13	0.12
	5	0.04	0.03	0.03	0.04	0.03	0.03
	aug-cc-pVDZ	0.25	0.25	0.24	0.46	0.45	0.43
	T	0.14	0.18	0.17	0.09	0.12	0.12
	Q	0.08	0.09	0.10	0.10	0.10	0.10
	5	0.02	0.02	0.02	0.03	0.03	0.03

-continue-

-continue-

Molecules	Basis Sets	B3LYP	B3PW91	B3P86	BLYP	BPW91	BP86
HCN	cc-pVDZ	1.58	1.19	1.17	2.43	1.65	1.75
	T	0.44	0.39	0.36	0.65	0.54	0.52
	Q	0.34	0.30	0.26	0.55	0.45	0.41
	5	0.08	0.06	0.05	0.12	0.10	0.09
	aug-cc-pVDZ	0.91	0.99	0.92	1.26	1.14	1.05
	T	0.34	0.43	0.44	0.45	0.57	0.55
	Q	0.26	0.23	0.24	0.38	0.32	0.67
	5	0.05	0.04	0.04	0.08	0.05	0.06
CO	cc-pVDZ	2.68	2.15	2.10	2.67	2.13	2.20
	T	0.74	0.62	0.57	0.82	0.66	0.64
	Q	0.42	0.35	0.30	0.54	0.44	0.41
	5	0.08	0.07	0.06	0.13	0.11	0.09
	aug-cc-pVDZ	0.71	0.78	0.73	0.70	0.83	0.79
	T	0.27	0.36	0.35	0.30	0.43	0.40
	Q	0.18	0.17	0.18	0.24	0.21	0.22
	5	0.04	0.03	0.04	0.06	0.05	0.05
N_2	cc-pVDZ	1.17	0.89	0.90	1.54	1.12	1.18
	T	0.26	0.22	0.21	0.38	0.31	0.31
	Q	0.21	0.18	0.16	0.33	0.27	0.25
	5	0.06	0.04	0.04	0.09	0.07	0.06
	aug-cc-pVDZ	0.87	0.91	0.87	1.02	1.03	0.97
	T	0.24	0.30	0.30	0.30	0.38	0.38
	Q	0.18	0.16	0.17	0.24	0.21	0.22
	5	0.04	0.03	0.03	0.07	0.05	0.05
HNO	cc-pVDZ	2.34	1.85	1.81	3.02	2.26	2.33
	T	0.59	0.48	0.45	0.79	0.61	0.60
	Q	0.36	0.40	0.35	0.53	0.43	0.52
	5	0.11	0.10	0.08	0.16	0.11	0.11
	aug-cc-pVDZ	0.97	1.06	1.00	1.00	1.06	0.98
	T	0.27	0.37	0.37	0.28	0.40	0.38
	Q	0.20	0.19	0.21	0.26	0.24	0.25
	5	0.05	0.04	0.04	0.08	0.06	0.06
HOF	cc-pVDZ	4.42	3.70	3.57	5.52	4.42	4.45
	T	1.21	1.01	0.94	1.57	1.24	1.22
	Q	0.52	0.46	0.40	0.69	0.64	0.59
	5	0.09	0.09	0.09	0.18	0.16	0.12
	aug-cc-pVDZ	0.87	0.95	0.90	0.86	0.92	0.86
	T	0.31	0.42	0.41	0.24	0.40	0.37

-continue-

-continue-

Molecules	Basis Sets	B3LYP	B3PW91	B3P86	BLYP	BPW91	BP86
	Q	0.18	0.19	0.21	0.21	0.22	0.24
	5		0.05	0.06	0.08	0.07	0.08
CO_2	cc-pVDZ	5.60	4.52	4.41	7.11	5.44	5.58
	T	1.69	1.41	1.31	2.25	1.77	1.73
	Q	0.92	0.77	0.67	1.36	1.09	1.01
	5	0.17	0.16	0.13	0.28	0.25	0.21
	aug-cc-pVDZ	1.65	1.80	1.71	1.86	1.93	1.81
	T	0.60	0.77	0.76	0.67	0.88	0.84
	Q	0.38	0.36	0.38	0.50	0.46	0.48
	5	0.09	0.07	0.07	0.13	0.10	0.10

6.3.3 The Effect of BSSE on the Convergence of Atomization Energy

The BSSE corrected and uncorrected atomization energies for eight molecules are presented in Table 6.4. The previous section discussed that, for DFT, the BSSE is non-negligible at the double-zeta level, even for strongly bound systems. However, relative to the energy change due to the basis set effect (difference between energies calculated at the double and quintuple zeta levels), the energy change arising from BSSE is small. For the B3LYP/cc-pVDZ atomization energy of H_2O, the energy change due to the basis set effect is about 11 kcal/mol, while the BSSE results in an energy change of 3.51 kcal/mol. It must be noted that these two effects are in opposite directions. The basis sets effect increases the atomization energy, whereas the BSSE effect decreases the atomization energy.

Another effect of BSSE on the atomization energy is that the convergence behavior of atomization energy is improved for most of the molecules. As compared with the irregular convergence behavior of the uncorrected energies, which have a slight dip at the quintuple-zeta level, the corrected atomization energies generally converge smoothly to the complete basis set limit. However, this improvement is not applicable to all molecules and functionals. In general,

the convergence problem with hybrid functionals has been improved for almost all molecules. For pure functionals, the convergence behavior of some of the molecules like HCN for BLYP and BP86 with cc-pV*x*Z and CO for BLYP, BPW91, and BP86 with cc-pV*x*Z is not improved at all, and even gets worse.

The uncorrected and corrected B3LYP/cc-pV*x*Z atomization energies for CO_2 with increasing basis set size are provided in Figure 6.1. Among all of the molecules studied, CO_2 shows the largest dip (~0.5 kcal/mol) for the uncorrected atomization energies. To be expected, both uncorrected and corrected atomization energies converge to the same basis set limit. The main difference resulting from the BSSE corrections occurs for energies at the double-, triple-, and quadruple-zeta levels. These corrections lead to improved convergence behavior of the energies.

6.4 Conclusions

For DFT methods, the effect of BSSE on the geometries and harmonic frequencies is small, which indicates that computed geometries and harmonic frequencies are not sensitive to BSSE corrections. For strongly bound systems, the BSSE is not insignificant, with the largest error occuring at the double-zeta level, and decreasing with increasing basis set size. As expected, both uncorrected and corrected energies converge to the same basis set limit. In a number of cases, the unexpected convergence problem observed in previous studies is improved when using the counterpoise correction. For HCN and CO, addressing the BSSE did not resolve the convergence problem, especially using pure density functionals. The improvement is mainly attributed to the energy changes at the triple- and quadruple-zeta levels.

Figure 6.1 The comparison of BSSE corrected and uncorrected atomization energies for CO_2 in kcal/mol.

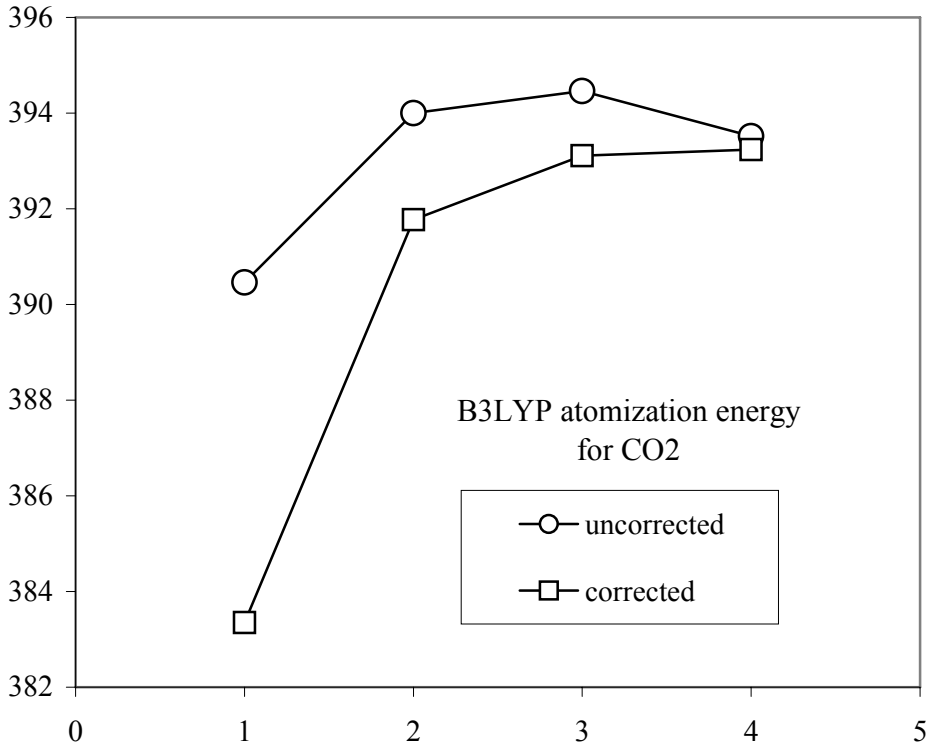

Table 6.4 The BSSE uncorrected (no corr.) and corrected (corr.) atomization energies (in kcal/mol)

Molecules		B3LYP		B3PW91		B3P86		BLYP		BPW91		BP86	
E_o	Basis Sets	no corr.	corr.	no corr.	corr.	no corr.	corr.	no corr.	corr.	no corr.	corr.	no corr.	corr.
H_2O	cc-pVDZ	206.14	202.64	205.40	202.56	214.10	211.46	207.84	203.40	207.40	203.96	215.95	212.61
219.3	T	214.85	214.38	213.37	212.53	222.22	221.49	216.81	215.48	215.59	214.54	224.29	223.35
	Q	216.78	216.32	215.02	214.63	223.87	223.59	218.91	218.24	217.33	216.79	226.08	225.71
	5	217.57	217.49	215.66	215.58	224.51	224.48	219.81	219.67	218.03	217.90	226.81	226.78
	aug-cc-pVDZ	215.20	214.70	213.56	213.06	222.36	222.11	217.53	216.93	215.99	215.45	224.74	224.52
	T	217.29	217.10	215.47	215.22	224.31	223.96	219.59	219.39	217.91	217.64	226.69	226.29
	Q	217.83	217.71	215.89	215.77	224.73	224.49	220.17	220.02	218.34	218.19	227.12	226.80
	5	217.86	217.82	215.91	215.88	224.74	224.50	220.20	220.15	218.35	218.31	227.12	226.64
HF	cc-pVDZ	124.58	122.82	124.61	123.17	129.11	127.73	126.08	123.81	126.34	125.38	130.60	129.66
135.2	T	131.30	130.89	130.80	130.48	135.35	135.06	133.07	132.83	132.76	132.58	137.11	136.93
	Q	132.78	132.58	132.06	131.89	136.59	136.45	134.74	134.59	134.13	134.01	138.49	138.38
	5	133.37	133.33	132.53	132.49	137.04	137.02	135.43	135.39	134.68	134.65	139.04	139.03
	aug-cc-pVDZ	132.00	131.77	131.35	131.11	135.82	135.65	134.17	133.74	133.57	133.14	137.89	137.55
	T	133.28	133.15	132.52	132.34	137.04	136.89	135.41	135.32	134.73	134.60	139.10	138.99
	Q	133.57	133.48	132.72	132.62	137.22	137.14	135.72	135.62	134.93	134.83	139.30	139.20
	5	133.56	133.54	132.70	132.68	137.20	137.16	135.71	135.71	134.91	134.88	139.27	139.18
HCN	cc-pVDZ	295.79	294.25	294.45	293.29	303.84	303.02	303.84	302.50	303.43	301.80	311.77	310.64
301.8	T	302.78	302.35	300.73	300.35	310.36	310.35	310.36	310.75	309.19	308.66	317.62	317.65
	Q	303.74	303.43	301.65	301.37	311.29	311.22	311.21	311.70	309.99	309.55	318.42	318.19
	5	303.63	303.58	301.59	301.55	311.26	310.66	310.92	310.80	309.80	309.70	318.25	317.11
	aug-cc-pVDZ	295.68	294.79	294.42	293.44	303.92	303.10	303.12	302.87	302.88	301.76	311.19	310.53
	T	302.60	302.26	300.68	300.25	310.39	309.44	310.46	311.04	308.93	308.36	317.40	316.21
	Q	303.58	303.27	301.51	301.30	311.22	311.10	310.89	311.54	309.73	309.38	318.21	317.70
	5	303.60	303.57	301.58	301.55	311.25	310.79	310.85	310.78	309.73	309.68	318.20	317.69

-continue-

-continue-

Molecules		B3LYP		B3PW91		B3P86		BLYP		BPW91		BP86	
E_o	Basis Sets	no corr.	corr.	no corr.	corr.	no corr.	corr.	no corr.	corr.	no corr.	corr.	no corr.	corr.
CO	cc-pVDZ	295.79	294.25	248.77	246.62	254.18	252.08	256.35	253.69	257.70	255.58	261.90	259.71
256.2	T	302.78	302.35	252.23	251.61	257.84	257.26	259.25	258.44	260.43	259.77	264.71	264.06
	Q	303.74	303.43	252.97	252.63	258.61	258.30	259.76	259.22	260.99	260.55	265.25	264.84
	5	303.63	303.58	252.76	252.69	258.43	258.37	259.26	259.14	260.63	260.52	264.90	264.81
	aug-cc-pVDZ	295.68	294.79	247.79	247.01	253.33	252.59	254.29	253.59	256.05	255.22	260.22	259.43
	T	302.60	302.26	251.68	251.32	257.36	257.01	258.66	258.36	259.60	259.17	263.88	263.48
	Q	303.58	303.27	252.66	252.49	258.36	258.18	259.16	258.92	260.51	260.30	264.81	264.59
	5	303.60	303.57	252.73	252.70	258.42	258.38	259.19	259.13	260.55	260.51	264.85	264.85
N_2	cc-pVDZ	248.42	245.74	215.60	214.71	223.51	222.62	231.22	229.69	228.07	226.95	235.22	234.04
225.1	T	252.12	251.38	221.50	221.28	229.52	229.31	236.49	236.11	233.12	232.81	240.24	239.94
	Q	252.84	252.42	222.40	222.22	230.46	230.30	237.27	236.94	233.87	233.60	241.03	240.78
	5	252.56	252.47	222.46	222.41	230.55	230.51	237.19	237.10	233.83	233.76	241.00	240.93
	aug-cc-pVDZ	247.20	246.49	215.88	214.97	223.84	222.97	230.53	229.51	227.71	226.67	234.80	233.83
	T	251.36	251.09	221.48	221.19	229.58	229.27	236.25	235.94	232.93	232.54	240.10	239.72
	Q	252.47	252.28	222.50	222.34	230.60	230.43	237.33	237.09	233.90	233.68	241.08	240.14
	5	252.53	252.48	222.60	222.56	230.68	230.65	237.38	237.31	233.98	233.92	241.14	241.09
HNO	cc-pVDZ	192.98	190.63	190.78	188.93	200.74	198.99	206.22	203.21	204.55	202.29	213.96	211.74
198.7	T	196.94	196.35	194.78	194.30	204.91	204.50	209.05	208.25	207.57	206.97	217.00	216.45
	Q	198.00	197.64	195.78	195.39	205.94	205.69	209.98	209.44	208.47	208.03	217.91	217.53
	5	198.13	198.03	195.92	195.83	206.11	206.03	209.96	209.81	208.49	208.37	217.95	217.82
	aug-cc-pVDZ	194.64	193.67	192.76	191.69	202.86	201.95	206.87	205.87	205.69	204.64	215.10	214.29
	T	197.27	197.01	195.17	194.81	205.37	204.84	209.08	208.80	207.73	207.34	217.22	216.61
	Q	198.26	198.07	196.04	195.85	206.24	205.98	210.12	209.86	208.62	208.38	218.11	217.79
	5	198.29	198.25	196.07	196.03	206.26	206.06	210.14	210.05	208.63	208.57	218.11	217.80
HOF	cc-pVDZ	144.19	139.75	142.49	138.77	150.51	146.97	156.42	150.92	154.70	150.26	162.29	157.92
151.9	T	148.35	147.15	147.16	146.16	155.33	154.42	159.55	157.97	158.52	157.29	166.15	164.99

-continue-

-continue-

Molecules		B3LYP		B3PW91		B3P86		BLYP		BPW91		BP86	
E_o	Basis Sets	no corr.	corr.	no corr.	corr.	no corr.	corr.	no corr.	corr.	no corr.	corr.	no corr.	corr.
	Q	148.77	148.25	147.59	147.14	155.80	155.45	159.85	159.17	158.85	158.21	166.49	166.01
	5	148.75	148.66	147.57	147.48	155.81	155.75	159.73	159.54	158.72	158.55	166.39	166.35
	aug-cc-pVDZ	146.71	145.85	145.52	144.58	153.73	152.99	158.10	157.28	157.05	156.14	164.70	164.08
	T	148.50	148.19	147.42	147.01	155.68	155.17	159.44	159.20	158.58	158.18	166.27	165.75
	Q	148.83	148.64	147.66	147.47	155.92	155.64	159.80	159.58	158.81	158.58	166.50	166.16
	5	148.82	148.77	147.63	147.59	155.88	155.63	159.79	159.71	158.77	158.70	166.45	166.01
CO_2	cc-pVDZ	375.18	369.60	378.49	373.98	387.69	383.30	390.46	383.35	395.87	390.43	402.33	396.76
381.9	T	380.63	378.97	383.85	382.44	393.37	392.07	394.00	391.77	399.60	397.84	406.14	404.41
	Q	381.49	380.57	384.74	383.99	394.30	393.61	394.46	393.11	400.18	399.09	406.67	405.65
	5	380.95	380.78	384.34	384.18	393.98	393.85	393.52	393.24	399.48	399.23	406.02	406.73
	aug-cc-pVDZ	372.82	371.18	376.99	375.20	386.43	384.72	386.01	384.17	392.80	390.89	399.17	397.37
	T	379.21	378.62	382.80	382.03	392.49	391.73	392.31	391.65	397.98	397.10	404.55	403.72
	Q	380.85	380.47	384.22	383.87	393.92	393.53	393.38	392.88	399.33	398.88	405.92	405.45
	5	380.86	380.77	384.25	384.18	393.92	393.85	393.32	393.20	399.30	399.20	405.88	359.43

CHAPTER 7

THE PERFORMANCE OF DENSITY FUNCTIONALS WITH RESPECT TO BASIS SETS: THE CORE-VALENCE EFFECT

7.1 Introduction

The chemical properties of atoms and molecules are mainly determined by the valence electrons. So in general, most theoretical studies largely focus on the description of valence electrons. Furthermore, this preference is also reflected in theoretical models, such as the frozen-core approximation, in which the orbitals occupied by core electrons are constrained to remain doubly occupied in all configurations. This approximation assumes that the correlation effect arising from the core electrons can be neglected, since the error resulting from the frozen-core approximation is smaller than other errors, such as from an incomplete basis set or an inadequate description of electron correlation. From the basis set perspective, most popular basis sets were developed to better describe the valence electrons than the core electrons. Typically, basis functions used to describe core orbitals were optimized for Hartree-Fock and may not describe the core-core and core-valence correlation effects.

In order to describe molecular properties accurately or to understand properties that involve core electrons, basis functions accounting for the core correlation must be included in a basis set. The most widely used basis sets for the description of core correlation are the polarized

core-valence correlation consistent basis sets by Dunning and co-workers. [48, 53] Two series of core-valence correlation consistent basis sets are available: cc-pCV*x*Z [48] and cc-pwCV*x*Z. [53] The cc-pCV*x*Z was optimized to recover the core-core and core-valence correlation energy. A set of optimized functions was added to the cc-pV*x*Z sets, i.e., (1*s*1*p*) to cc-pVDZ to form the cc-pCVDZ set, (2*s*2*p*1*d*) to cc-pVTZ to form the cc-pCVTZ set, and so on. Atomic calculations show that using cc-pCV*x*Z sets recovers the core-core and core-valence correlation energy effectively. As for the cc-pV*x*Z, calculations with the cc-pCV*x*Z sets enable systematical convergence to the complete basis set limit. However, it was noted that the core correlation energy including core-core and core-valence correlation energy can not converge very well.[53] The basis set of cc-pwCV*x*Z was developed based on a different strategy, which was motivated by the observation that the core-valence correlation is the dominant effect of the core correlation effects. Properties described using these basis sets can converge more quickly and smoothly than for the cc-pV*x*Z sets, as only core-valence correlation and a small amount of core-core correlation were considered. Since the contribution of core-core correlation energy is controlled by a weighting factor, the basis sets are named weighted core-valence sets. The success of cc-pwCV*x*Z sets was expressed in the number of calculations of molecular properties including dissociation energies, geometries, and harmonic frequencies for a set of homonuclear diatomic molecules. These two types of basis sets have been applied extensively to investigate molecular properties including energies and spectroscopic constants. [48, 53, 103-110] However, almost all calculations with the core-valence correlation consistent basis sets involved correlated *ab initio* methods like CCSD(T). Systematic studies on the dependence of DFT used in combination with core-valence sets are rarely reported. Some studies related to our research are discussed below briefly.

Helgaker *et al*. investigated the performance of B3LYP for the calculation of indirect nuclear spin-spin coupling constants in substituted hydrocarbons. [111] They observed that coupling constants show a severe basis-set dependence, and do not converge smoothly with respect to cc-pV*x*Z and cc-pCV*x*Z. Uncontracting the original *s* functions and adding tight *s* functions to each level of basis set can remedy this irregular convergence problem. B3LYP and core-valence sets were also utilized in the work by Carmichael *et al*., who studied the geometries, frequencies and anharmonic correction of HPO_2 and HOPO. [112] Erratic and slow convergence of the Fermi contact terms for ^{31}P with respect to increasing basis set size was noted. Adding energy optimized and high-exponent *s* functions to aug-cc-pCV*x*Z improve the convergence, but the converged result was still far from the experiment. This deviation may be attributed to the deficiency of the functional, since B3LYP was parameterized mainly from thermochemical data.

Kupka *et al*. used B3PW91 and HF with cc-pV*x*Z, aug-cc-pV*x*Z, cc-pCV*x*Z, and aug-cc-pCV*x*Z to calculate the NMR parameters for a set of first-row element compounds. [113] The results were extrapolated to the complete basis set limits for each series of basis set, and compared with experimental and *ab initio* results. They found that the core-valence basis sets yield slightly lower total energies than the valence sets at the low-level basis sets. For the NMR parameters, the core-valence sets converge more rapidly than the valence set, but this faster convergence was only observed for the heavy nuclei (non-hydrogen). The effect of core electrons on the geometries was examined by Swart *et al*. for a set of small and several large metallocene molecules. [114] As seen in this study, using all-electron and frozen-core basis sets made little difference, and the former performs slightly better than the latter for the smaller basis sets.

As seen in the above work, the use of core-valence sets was centered on accurate determination of spectroscopic parameters due to their strong dependence on core electrons. The effect of using core-valence sets in combination with DFT on energies is not very clear. The convergence of the core-valence sets has not been studied systematically. In this study, the performance of two popular density functionals, BLYP and B3LYP, used with the core-valence basis sets are evaluated for a number of molecules. We focus on the convergence behavior of structures and atomization energies with respect to increasing the basis set size. The convergence behavior is compared with that of the standard correlation consistent basis sets. The accuracy of these two functionals in combination with the core-valence sets has been assessed using several means of statistical analysis.

7.2 Computational Methodology

Two density functionals, BLYP [6, 8] and B3LYP, [10] were combined with six series of basis sets, the polarized core-valence (cc-pCV*x*Z), [48] the polarized core-valence +*sp* (cc-pCV*x*Z+*sp*), the augmented polarized core-valence (aug-cc-pCV*x*Z), the polarized weighted core-valence (cc-pwCV*x*Z), [53] the polarized weighted core-valence +*sp* (cc-pwCV*x*Z+*sp*) and the augmented polarized weighted core-valence (aug-cc-pwCV*x*Z) correlation consistent basis sets, where *x*=D, T, Q and 5, to determine the structures and atomization energies of a number of molecules, which were chosen due to their typical convergence behaviors in the earlier studies. The cc-pCV*x*Z and cc-pwCV*x*Z basis sets were obtained from the online EMSL Gaussian Basis Set Library (www.emsl.pnl.gov/forms/basisform.html). The aug-cc-pCV*x*Z and aug-cc-pwCV*x*Z basis sets were derived from the cc-pCV*x*Z and cc-pwCV*x*Z sets, respectively, by addition of a set of diffuse functions, which were taken from the augmented correlation consistent basis sets

(aug-cc-pV*x*Z). The cc-pCV*x*Z+*sp* and cc-pwCV*x*Z+*sp* were constructed by adding only diffuse *s* and *p* functions to cc-pCV*x*Z and cc-pwCV*x*Z, respectively.

All calculations were carried out utilizing the G98 package. [35] The geometries and energies were optimized using each combination of density functional and basis set. The atomization energies listed in the tables consider the contribution from the zero-point energy, which was obtained from frequency calculations. As done in the previous study, the tight convergence criteria on density were requested for atomic calculations.

7.3 Results and Discussion

7.3.1 Structures

The optimized structures are summarized in Table 7.1. Overall, the bond lengths and angles are not sensitive to the type of basis sets used, and different compositions of basis sets cause only a slight change in geometries. The geometries are nearly converged at the triple-zeta level for all basis sets studied. The polarized core-valence and weighted core-valence basis sets have a similar performance at the triple-zeta level for both functionals. Beyond the triple-zeta level, the polarized core-valence and the polarized valence basis sets converge to the same limits. The largest difference in bond lengths between the polarized valence and the polarized core-valence basis sets arises from the double-zeta level, with a difference of 0.001 Å.

7.3.2 Atomic Energy

The total energies of the H, C, N, O, and F atoms calculated using BLYP and B3LYP with the six series of core-valence basis sets are listed in Table 7.2. The results with the standard and augmented basis sets (cc-pV*x*Z, cc-pV*x*Z+*sp* and aug-cc-pV*x*Z) and accurate Davidson atomic energies [45] are also listed for comparison. Overall, the total energies decrease with increasing the basis set size. The basis sets of cc-pCV*x*Z and cc-pwCV*x*Z predict nearly the same

Table 7.1 Optimized bond lengths and angles. Bond lengths are given in angstroms, and bond angles are given in degree

BLYP						B3LYP					
CO r(CO) 1.128 Å											
cc-pV*x*Z		cc-pCV*x*Z		cc-pwCV*x*Z		cc-pV*x*Z		cc-pCV*x*Z		cc-pwCV*x*Z	
D	1.1471	D	1.1461	D	1.1444	D	1.1345	D	1.1335	D	1.1321
T	1.1379	T	1.1370	T	1.1366	T	1.1262	T	1.1252	T	1.1248
Q	1.1355	Q	1.1355	Q	1.1355	Q	1.1237	Q	1.1237	Q	1.1236
5	1.1354	5	1.1354	5	1.1354	5	1.1236	5	1.1236	5	1.1236
cc-pV*x*Z+sp		cc-pCV*x*Z+sp		cc-pwCV*x*Z+sp		cc-pV*x*Z+sp		cc-pCV*x*Z+sp		cc-pwCV*x*Z+sp	
D	1.1471	D	1.1462	D	1.1449	D	1.1345	D	1.1336	D	1.1325
T	1.1379	T	1.1375	T	1.1370	T	1.1262	T	1.1256	T	1.1251
Q	1.1355	Q	1.1355	Q	1.1355	Q	1.1238	Q	1.1237	Q	1.1237
5	1.1354	5	1.1354	5	1.1354	5	1.1236	5	1.1236	5	1.1236
aug-cc-pV*x*Z		aug-cc-pCV*x*Z		aug-cc-pwCV*x*Z		aug-cc-pV*x*Z		aug-cc-pCV*x*Z		aug-cc-pwCV*x*Z	
D	1.1463	D	1.1450	D	1.1443	D	1.134	D	1.1328	D	1.1322
T	1.1376	T	1.1375	T	1.1371	T	1.1258	T	1.1257	T	1.1252
Q	1.1356	Q	1.1355	Q	1.1355	Q	1.1238	Q	1.1237	Q	1.1237
5	1.1354	5	1.1354	5	1.1354	5	1.1236	5	1.1236	5	1.1236
HCN r(HC) 1.064 Å											
cc-pV*x*Z		cc-pCV*x*Z		cc-pwCV*x*Z		cc-pV*x*Z		cc-pCV*x*Z		cc-pwCV*x*Z	
D	1.0836	D	1.0838	D	1.0834	D	1.0772	D	1.0770	D	1.0765
T	1.0711	T	1.072	T	1.0720	T	1.0654	T	1.0660	T	1.0660
Q	1.0712	Q	1.0712	Q	1.0712	Q	1.0655	Q	1.0656	Q	1.0656
5	1.0714	5	1.0714	5	1.0714	5	1.0656	5	1.0655	5	1.0655
cc-pV*x*Z+sp		cc-pCV*x*Z+sp		cc-pwCV*x*Z+sp		cc-pV*x*Z+sp		cc-pCV*x*Z+sp		cc-pwCV*x*Z+sp	
D	1.0838	D	1.0837	D	1.0832	D	1.0770	D	1.0770	D	1.0764
T	1.0719	T	1.0722	T	1.0722	T	1.0659	T	1.0662	T	1.0661
Q	1.0712	Q	1.0712	Q	1.0712	Q	1.0655	Q	1.0656	Q	1.0657
5	1.0714	5	1.0714	5	1.0714	5	1.0656	5	1.0655	5	1.0656

-continue-

-continue-

BLYP						B3LYP					
aug-cc-pV*x*Z		aug-cc-pCV*x*Z		aug-cc-pwCV*x*Z		aug-cc-pV*x*Z		aug-cc-pCV*x*Z		aug-cc-pwCV*x*Z	
D	1.0808	D	1.0808	D	1.0806	D	1.0744	D	1.0742	D	1.0740
T	1.0714	T	1.0721	T	1.0721	T	1.0656	T	1.0661	T	1.0661
Q	1.0713	Q	1.0712	Q	1.0712	Q	1.0656	Q	1.0656	Q	1.0657
5	1.0714	5	1.0714	5	1.0714	5	1.0656	5	1.0655	5	1.0656
R(CN) 1.156 Å											
cc-pV*x*Z		cc-pCV*x*Z		cc-pwCV*x*Z		cc-pV*x*Z		cc-pCV*x*Z		cc-pwCV*x*Z	
D	1.1697	D	1.1689	D	1.1674	D	1.1579	D	1.1570	D	1.1556
T	1.1575	T	1.1570	T	1.1568	T	1.1462	T	1.1456	T	1.1454
Q	1.1565	Q	1.1565	Q	1.1565	Q	1.1450	Q	1.1450	Q	1.1450
5	1.1565	5	1.1565	5	1.1565	5	1.1450	5	1.1450	5	1.1449
cc-pV*x*Z+sp		cc-pCV*x*Z+sp		cc-pwCV*x*Z+sp		cc-pV*x*Z+sp		cc-pCV*x*Z+sp		cc-pwCV*x*Z+sp	
D	1.1704	D	1.1695	D	1.1681	D	1.1584	D	1.1575	D	1.1563
T	1.1577	T	1.1574	T	1.1572	T	1.1463	T	1.1459	T	1.1457
Q	1.1565	Q	1.1565	Q	1.1565	Q	1.1451	Q	1.1451	Q	1.1451
5	1.1565	5	1.1565	5	1.1565	5	1.1450	5	1.1450	5	1.1449
aug-cc-pV*x*Z		aug-cc-pCV*x*Z		aug-cc-pwCV*x*Z		aug-cc-pV*x*Z		aug-cc-pCV*x*Z		aug-cc-pwCV*x*Z	
D	1.1684	D	1.1678	D	1.1669	D	1.1568	D	1.1561	D	1.1553
T	1.1573	T	1.1573	T	1.1571	T	1.1460	T	1.1459	T	1.1456
Q	1.1566	Q	1.1565	Q	1.1565	Q	1.1451	Q	1.1451	Q	1.1451
5	1.1565	5	1.1565	5	1.1565	5	1.1450	5	1.1450	5	1.1449
HNO r(HN) 1.090 Å											
cc-pV*x*Z		cc-pCV*x*Z		cc-pwCV*x*Z		cc-pV*x*Z		cc-pCV*x*Z		cc-pwCV*x*Z	
D	1.1002	D	1.1000	D	1.0995	D	1.0776	D	1.0775	D	1.0768
T	1.0813	T	1.0813	T	1.0814	T	1.0628	T	1.0629	T	1.0628
Q	1.0792	Q	1.0792	Q	1.0792	Q	1.0613	Q	1.0614	Q	1.0614
5	1.0781	5	1.0781	5	1.0778	5	1.0607	5	1.0606	5	1.0606
cc-pV*x*Z+sp		cc-pCV*x*Z+sp		cc-pwCV*x*Z+sp		cc-pV*x*Z+sp		cc-pCV*x*Z+sp		cc-pwCV*x*Z+sp	

-continue-

-continue-

BLYP						B3LYP					
D	1.0909	D	1.0906	D	1.0902	D	1.0719	D	1.0719	D	1.0715
T	1.0789	T	1.0788	T	1.0787	T	1.0616	T	1.0615	T	1.0613
Q	1.0781	Q	1.0782	Q	1.0782	Q	1.0608	Q	1.0609	Q	1.0609
5	1.0779	5	1.0779	5	1.0779	5	1.0607	5	1.0607	5	1.0607
aug-cc-pV*x*Z		aug-cc-pCV*x*Z		aug-cc-pwCV*x*Z		aug-cc-pV*x*Z		aug-cc-pCV*x*Z		aug-cc-pwCV*x*Z	
D	1.0855	D	1.0848	D	1.0844	D	1.0674	D	1.0674	D	1.0672
T	1.0786	T	1.0787	T	1.0787	T	1.0613	T	1.0614	T	1.0613
Q	1.0783	Q	1.0782	Q	1.0782	Q	1.0610	Q	1.0609	Q	1.0609
5	1.0781	5	1.0779	5	1.0779	5	1.0608	5	1.0607	5	1.0607
R(NO) 1.209 Å											
cc-pV*x*Z		cc-pCV*x*Z		cc-pwCV*x*Z		cc-pV*x*Z		cc-pCV*x*Z		cc-pwCV*x*Z	
D	1.2193	D	1.2185	D	1.2181	D	1.2028	D	1.202	D	1.2020
T	1.2153	T	1.2153	T	1.2152	T	1.1984	T	1.1983	T	1.1984
Q	1.2139	Q	1.2139	Q	1.2137	Q	1.1970	Q	1.197	Q	1.1971
5	1.2137	5	1.2137	5	1.2135	5	1.1966	5	1.1968	5	1.1968
cc-pV*x*Z+sp		cc-pCV*x*Z+sp		cc-pwCV*x*Z+sp		cc-pV*x*Z+sp		cc-pCV*x*Z+sp		cc-pwCV*x*Z+sp	
D	1.2209	D	1.2198	D	1.2195	D	1.2035	D	1.2025	D	1.2024
T	1.2149	T	1.2147	T	1.2148	T	1.1979	T	1.1977	T	1.1977
Q	1.2136	Q	1.2134	Q	1.2134	Q	1.1967	Q	1.1965	Q	1.1965
5	1.2133	5	1.2134	5	1.2134	5	1.1964	5	1.1964	5	1.1964
aug-cc-pV*x*Z		aug-cc-pCV*x*Z		aug-cc-pwCV*x*Z		aug-cc-pV*x*Z		aug-cc-pCV*x*Z		aug-cc-pwCV*x*Z	
D	1.2221	D	1.2213	D	1.2211	D	1.2051	D	1.2044	D	1.2043
T	1.2149	T	1.2147	T	1.2147	T	1.1978	T	1.1976	T	1.1977
Q	1.2135	Q	1.2134	Q	1.2134	Q	1.1964	Q	1.1965	Q	1.1965
5	1.2133	5	1.2135	5	1.2135	5	1.1962	5	1.1964	5	1.1964
A(HNO) 108.047 ^{o}											
cc-pV*x*Z		cc-pCV*x*Z		cc-pwCV*x*Z		cc-pV*x*Z		cc-pCV*x*Z		cc-pwCV*x*Z	
D	108.30	D	108.30	D	108.33	D	108.35	D	108.38	D	108.38
T	108.55	T	108.55	T	108.53	T	108.68	T	108.68	T	108.68

-continue-

-continue-

BLYP						B3LYP					
Q	108.68	Q	108.68	Q	108.68	Q	108.81	Q	108.82	Q	108.82
5	108.73	5	108.73	5	108.74	5	108.87	5	108.88	5	108.88
cc-pV*x*Z+sp		cc-pCV*x*Z+sp		cc-pwCV*x*Z+sp		cc-pV*x*Z+sp		cc-pCV*x*Z+sp		cc-pwCV*x*Z+sp	
D	108.53	D	108.54	D	108.55	D	108.64	D	108.65	D	108.65
T	108.73	T	108.72	T	108.72	T	108.87	T	108.86	T	108.86
Q	108.78	Q	108.79	Q	108.79	Q	108.92	Q	108.92	Q	108.92
5	108.79	5	108.83	5	108.83	5	108.93	5	108.93	5	108.93
aug-cc-pV*x*Z		aug-cc-pCV*x*Z		aug-cc-pwCV*x*Z		aug-cc-pV*x*Z		aug-cc-pCV*x*Z		aug-cc-pwCV*x*Z	
D	108.53	D	108.54	D	108.55	D	108.65	D	108.64	D	108.64
T	108.74	T	108.74	T	108.74	T	108.86	T	108.87	T	108.87
Q	108.81	Q	108.80	Q	108.80	Q	108.92	Q	108.93	Q	108.93
5	108.80	5	108.84	5	108.84	5	108.92	5	108.93	5	108.93
HOF r(HO) 0.960 Å											
cc-pV*x*Z		cc-pCV*x*Z		cc-pwCV*x*Z		cc-pV*x*Z		cc-pCV*x*Z		cc-pwCV*x*Z	
D	0.9898	D	0.9897	D	0.9898	D	0.9775	D	0.9772	D	0.9773
T	0.9817	T	0.9821	T	0.9822	T	0.9700	T	0.9703	T	0.9703
Q	0.9809	Q	0.9812	Q	0.9813	Q	0.9693	Q	0.9693	Q	0.9697
5	0.9811	5	0.9812	5	0.9814	5	0.9694	5	0.9694	5	0.9698
cc-pV*x*Z+sp		cc-pCV*x*Z+sp		cc-pwCV*x*Z+sp		cc-pV*x*Z+sp		cc-pCV*x*Z+sp		cc-pwCV*x*Z+sp	
D	0.9914	D	0.9916	D	0.9914	D	0.9791	D	0.979	D	0.9793
T	0.9828	T	0.9831	T	0.9831	T	0.9713	T	0.9711	T	0.9715
Q	0.9814	Q	0.9818	Q	0.9818	Q	0.9699	Q	0.9699	Q	0.9703
5	0.9811	5	0.9815	5	0.9815	5	0.9697	5	0.9694	5	0.9700
aug-cc-pV*x*Z		aug-cc-pCV*x*Z		aug-cc-pwCV*x*Z		aug-cc-pV*x*Z		aug-cc-pCV*x*Z		aug-cc-pwCV*x*Z	
D	0.9866	D	0.9865	D	0.9864	D	0.9747	D	0.9744	D	0.9743
T	0.9829	T	0.9831	T	0.9832	T	0.9715	T	0.9711	T	0.9716
Q	0.9819	Q	0.9818	Q	0.9818	Q	0.9698	Q	0.9699	Q	0.9703
5	0.9814	5	0.9815	5	0.9815	5	0.9696	5	0.9694	5	0.9700

-continue-

-continue-

BLYP						B3LYP					
R(OF) 1.442 Å											
cc-pV*x*Z		cc-pCV*x*Z		cc-pwCV*x*Z		cc-pV*x*Z		cc-pCV*x*Z		cc-pwCV*x*Z	
D	1.4706	D	1.4716	D	1.4729	D	1.4349	D	1.4358	D	1.4372
T	1.4675	T	1.4663	T	1.4660	T	1.4301	T	1.4292	T	1.4292
Q	1.4669	Q	1.4665	Q	1.4661	Q	1.4291	Q	1.4291	Q	1.4288
5	1.4667	5	1.4666	5	1.4662	5	1.4286	5	1.4286	5	1.4287
cc-pV*x*Z+sp		cc-pCV*x*Z+sp		cc-pwCV*x*Z+sp		cc-pV*x*Z+sp		cc-pCV*x*Z+sp		cc-pwCV*x*Z+sp	
D	1.4763	D	1.4778	D	1.4791	D	1.4378	D	1.4387	D	1.4395
T	1.4679	T	1.4672	T	1.4673	T	1.4295	T	1.4297	T	1.4295
Q	1.4673	Q	1.4668	Q	1.4667	Q	1.4285	Q	1.4287	Q	1.4286
5	1.4667	5	1.4664	5	1.4664	5	1.4280	5	1.4286	5	1.4285
aug-cc-pV*x*Z		aug-cc-pCV*x*Z		aug-cc-pwCV*x*Z		aug-cc-pV*x*Z		aug-cc-pCV*x*Z		aug-cc-pwCV*x*Z	
D	1.4699	D	1.4708	D	1.4718	D	1.4328	D	1.4339	D	1.4338
T	1.4684	T	1.4679	T	1.4680	T	1.4310	T	1.4303	T	1.4303
Q	1.4668	Q	1.4666	Q	1.4666	Q	1.4288	Q	1.4286	Q	1.4286
5	1.4666	5	1.4664	5	1.4664	5	1.4284	5	1.4286	5	1.4285
A(HOF) 97.2 ^{o}											
cc-pV*x*Z		cc-pCV*x*Z		cc-pwCV*x*Z		cc-pV*x*Z		cc-pCV*x*Z		cc-pwCV*x*Z	
D	96.96	D	96.90	D	96.89	D	97.87	D	97.89	D	97.74
T	97.43	T	97.47	T	97.47	T	98.48	T	98.43	T	98.47
Q	97.58	Q	97.60	Q	97.60	Q	98.63	Q	98.63	Q	98.49
5	97.68	5	97.69	5	97.69	5	98.71	5	98.71	5	98.57
cc-pV*x*Z+sp		cc-pCV*x*Z+sp		cc-pwCV*x*Z+sp		cc-pV*x*Z+sp		cc-pCV*x*Z+sp		cc-pwCV*x*Z+sp	
D	97.33	D	97.28	D	97.24	D	98.18	D	98.23	D	98.19
T	97.69	T	97.74	T	97.73	T	98.66	T	98.76	T	98.65
Q	97.76	Q	97.73	Q	97.73	Q	98.67	Q	98.71	Q	98.63
5	97.68	5	97.74	5	97.74	5	98.69	5	98.71	5	98.62
aug-cc-pV*x*Z		aug-cc-pCV*x*Z		aug-cc-pwCV*x*Z		aug-cc-pV*x*Z		aug-cc-pCV*x*Z		aug-cc-pwCV*x*Z	
D	97.65	D	97.61	D	97.57	D	98.56	D	98.47	D	98.53

-continue-

-continue-

BLYP						B3LYP					
T	97.68	T	97.70	T	97.70	T	98.59	T	98.74	T	98.60
Q	97.66	Q	97.73	Q	97.73	Q	98.72	Q	98.70	Q	98.63
5	97.73	5	97.74	5	97.74	5	98.74	5	98.71	5	98.61
N_2 r(NN) 1.098 Å											
cc-pV*x*Z		cc-pCV*x*Z		cc-pwCV*x*Z		cc-pV*x*Z		cc-pCV*x*Z		cc-pwCV*x*Z	
D	1.1172	D	1.1165	D	1.1150	D	1.1044	D	1.1037	D	1.1025
T	1.1032	T	1.1029	T	1.1027	T	1.0914	T	1.0908	T	1.0906
Q	1.1022	Q	1.1022	Q	1.1022	Q	1.0902	Q	1.0901	Q	1.0902
5	1.1019	5	1.1019	5	1.1019	5	1.0900	5	1.0899	5	1.0899
cc-pV*x*Z+sp		cc-pCV*x*Z+sp		cc-pwCV*x*Z+sp		cc-pV*x*Z+sp		cc-pCV*x*Z+sp		cc-pwCV*x*Z+sp	
D	1.1167	D	1.1159	D	1.1145	D	1.1041	D	1.1034	D	1.1022
T	1.1033	T	1.1028	T	1.1027	T	1.0914	T	1.0907	T	1.0905
Q	1.1021	Q	1.1021	Q	1.1021	Q	1.0902	Q	1.0901	Q	1.0901
5	1.1019	5	1.1019	5	1.1019	5	1.0899	5	1.0899	5	1.0899
aug-cc-pV*x*Z		aug-cc-pCV*x*Z		aug-cc-pwCV*x*Z		aug-cc-pV*x*Z		aug-cc-pCV*x*Z		aug-cc-pwCV*x*Z	
D	1.1030	D	1.1159	D	1.1148	D	1.1044	D	1.1036	D	1.1026
T	1.1021	T	1.1027	T	1.1025	T	1.0912	T	1.0906	T	1.0905
Q	1.1019	Q	1.1021	Q	1.1021	Q	1.0901	Q	1.0901	Q	1.0901
5		5	1.1019	5	1.1019	5	1.0899	5	1.0899	5	1.0899
O_3 r(OO) 1.2780 Å											
cc-pV*x*Z		cc-pCV*x*Z		cc-pwCV*x*Z		cc-pV*x*Z		cc-pCV*x*Z		cc-pwCV*x*Z	
D	1.2953	D	1.2953	D	1.2962	D	1.2597	D	1.2598	D	1.2602
T	1.2919	T	1.2913	T	1.2915	T	1.2563	T	1.2558	T	1.2561
Q	1.2881	Q	1.2877	Q	1.2877	Q	1.2531	Q	1.2528	Q	1.2528
5	1.2873	5	1.2871	5	1.2871	5	1.2524	5	1.2523	5	1.2523
cc-pV*x*Z+sp		cc-pCV*x*Z+sp		cc-pwCV*x*Z+sp		cc-pV*x*Z+sp		cc-pCV*x*Z+sp		cc-pwCV*x*Z+sp	
D	1.2914	D	1.2918	D	1.2925	D	1.2566	D	1.2566	D	1.2566

-continue-

-continue-

BLYP						B3LYP					
T	1.2898	T	1.2895	T	1.2898	T	1.2548	T	1.2545	T	1.2548
Q	1.2871	Q	1.2867	Q	1.2867	Q	1.2525	Q	1.2522	Q	1.2522
5	1.2867	5	1.2865	5	1.2865	5	1.2522	5	1.2522	5	1.2522
aug-cc-pV*x*Z		aug-cc-pCV*x*Z		aug-cc-pwCV*x*Z		aug-cc-pV*x*Z		aug-cc-pCV*x*Z		aug-cc-pwCV*x*Z	
D	1.2908	D	1.2909	D	1.2913	D	1.2565	D	1.2565	D	1.2566
T	1.2901	T	1.2897	T	1.2899	T	1.2549	T	1.2547	T	1.2548
Q	1.2868	Q	1.2866	Q	1.2866	Q	1.2522	Q	1.2522	Q	1.2522
5	1.2866	5	1.2865	5	1.2865	5	1.252	5	1.2522	5	1.2522
A(OOO) 116.8 ^{o}											
cc-pV*x*Z		cc-pCV*x*Z		cc-pwCV*x*Z		cc-pV*x*Z		cc-pCV*x*Z		cc-pwCV*x*Z	
D	117.90	D	117.91	D	117.90	D	117.95	D	118.01	D	117.99
T	118.00	T	118.04	T	118.04	T	118.14	T	118.18	T	118.18
Q	118.10	Q	118.10	Q	118.10	Q	118.26	Q	118.25	Q	118.25
5	118.11	5	118.12	5	118.12	5	118.30	5	118.28	5	118.28
cc-pV*x*Z+sp		cc-pCV*x*Z+sp		cc-pwCV*x*Z+sp		cc-pV*x*Z+sp		cc-pCV*x*Z+sp		cc-pwCV*x*Z+sp	
D	118.22	D	118.25	D	118.25	D	118.36	D	118.36	D	118.36
T	118.18	T	118.19	T	118.19	T	118.34	T	118.31	T	118.34
Q	118.20	Q	118.21	Q	118.20	Q	118.35	Q	118.33	Q	118.33
5	118.19	5	118.20	5	118.20	5	118.34	5	118.34	5	118.34
aug-cc-pV*x*Z		aug-cc-pCV*x*Z		aug-cc-pwCV*x*Z		aug-cc-pV*x*Z		aug-cc-pCV*x*Z		aug-cc-pwCV*x*Z	
D	117.97	D	117.97	D	117.96	D	118.07	D	118.06	D	118.06
T	118.14	T	118.15	T	118.15	T	118.28	T	118.29	T	118.29
Q	118.20	Q	118.20	Q	118.19	Q	118.35	Q	118.31	Q	118.30
5	118.19	5	118.19	5	118.19	5	118.35	5	118.34	5	118.34
F_2 r(FF) 1.412 Å											
cc-pV*x*Z		cc-pCV*x*Z		cc-pwCV*x*Z		cc-pV*x*Z		cc-pCV*x*Z		cc-pwCV*x*Z	
D	1.4435	D	1.4446	D	1.4460	D	1.4102	D	1.4111	D	1.4119
T	1.4330	T	1.4317	T	1.4318	T	1.3976	T	1.3966	T	1.3966

-continue-

-continue-

BLYP						B3LYP					
Q	1.4328	Q	1.4325	Q	1.4325	Q	1.3968	Q	1.3962	Q	1.3962
5	1.4326	5	1.4325	5	1.4325	5	1.3962	5	1.3961	5	1.3961
cc-pV*x*Z+sp		cc-pCV*x*Z+sp		cc-pwCV*x*Z+sp		cc-pV*x*Z+sp		cc-pCV*x*Z+sp		cc-pwCV*x*Z+sp	
D	1.4481	D	1.4492	D	1.4503	D	1.4111	D	1.4118	D	1.4123
T	1.4330	T	1.4321	T	1.4322	T	1.3966	T	1.3961	T	1.3962
Q	1.4328	Q	1.4323	Q	1.4323	Q	1.3962	Q	1.3962	Q	1.3962
5	1.4321	5	1.4320	5	1.4320	5	1.3957	5	1.3957	5	1.3957
aug-cc-pV*x*Z		aug-cc-pCV*x*Z		aug-cc-pwCV*x*Z		aug-cc-pV*x*Z		aug-cc-pCV*x*Z		aug-cc-pwCV*x*Z	
D	1.4386	D	1.4397	D	1.4406	D	1.4034	D	1.4042	D	1.4048
T	1.4331	T	1.4327	T	1.4328	T	1.3971	T	1.3966	T	1.3966
Q	1.4324	Q	1.4322	Q	1.4322	Q	1.3961	Q	1.3962	Q	1.3962
5	1.4320	5	1.4320	5	1.4320	5	1.3957	5	1.3957	5	1.3957
CO_2 r(CO) 1.162 Å											
cc-pV*x*Z		cc-pCV*x*Z		cc-pwCV*x*Z		cc-pV*x*Z		cc-pCV*x*Z		cc-pwCV*x*Z	
D	1.1815	D	1.1800	D	1.1798	D	1.1673	D	1.1669	D	1.1661
T	1.1736	T	1.1730	T	1.1729	T	1.1604	T	1.1600	T	1.1597
Q	1.1720	Q	1.1720	Q	1.1720	Q	1.1588	Q	1.1589	Q	1.1589
5	1.1721	5	1.1721	5	1.1720	5	1.1587	5	1.1588	5	1.1588
cc-pV*x*Z+sp		cc-pCV*x*Z+sp		cc-pwCV*x*Z+sp		cc-pV*x*Z+sp		cc-pCV*x*Z+sp		cc-pwCV*x*Z+sp	
D	1.1819	D	1.1812	D	1.1803	D	1.1678	D	1.1672	D	1.1665
T	1.1738	T	1.1735	T	1.1733	T	1.1606	T	1.1602	T	1.1600
Q	1.1720	Q	1.1721	Q	1.1722	Q	1.1589	Q	1.1589	Q	1.1589
5	1.1721	5	1.1720	5	1.1720	5	1.1588	5	1.1588	5	1.1588
aug-cc-pV*x*Z		aug-cc-pCV*x*Z		aug-cc-pwCV*x*Z		aug-cc-pV*x*Z		aug-cc-pCV*x*Z		aug-cc-pwCV*x*Z	
D	1.1811	D	1.1804	D	1.1800	D	1.1673	D	1.1669	D	1.1665
T	1.1737	T	1.1736	T	1.1734	T	1.1605	T	1.1603	T	1.1601
Q	1.1722	Q	1.1722	Q	1.1722	Q	1.1589	Q	1.1589	Q	1.1589
5	1.1721	5	1.1720	5	1.1722	5	1.1587	5	1.1588	5	1.1588

Table 7.2 Total energies for atoms in hartrees.

BLYP						B3LYP					
C -37.8450 hartree											
cc-pV*x*Z		cc-pCV*x*Z		cc-pwCV*x*Z		cc-pV*x*Z		cc-pCV*x*Z		cc-pwCV*x*Z	
D	-37.837836	D	-37.838790	D	-37.839156	D	-37.851975	D	-37.852624	D	-37.852873
T	-37.845501	T	-37.846623	T	-37.846577	T	-37.858575	T	-37.859263	T	-37.859234
Q	-37.847806	Q	-37.848767	Q	-37.848783	Q	-37.860592	Q	-37.861204	Q	-37.861210
5	-37.849077	5	-37.849328	5	-37.849330	5	-37.861508	5	-37.861663	5	-37.861664
cc-pV*x*Z+sp		cc-pCV*x*Z+sp		cc-pwCV*x*Z+sp		cc-pV*x*Z+sp		cc-pCV*x*Z+sp		cc-pwCV*x*Z+sp	
D	-37.840798	D	-37.841806	D	-37.842056	D	-37.854138	D	-37.854817	D	-37.854991
T	-37.846232	T	-37.847435	T	-37.847386	T	-37.859054	T	-37.859792	T	-37.859762
Q	-37.848133	Q	-37.849052	Q	-37.849064	Q	-37.860783	Q	-37.861369	Q	-37.861373
5	-37.849139	5	-37.849390	5	-37.849393	5	-37.861540	5	-37.861694	5	-37.861696
aug-cc-pV*x*Z		aug-cc-pCV*x*Z		aug-cc-pwCV*x*Z		aug-cc-pV*x*Z		aug-cc-pCV*x*Z		aug-cc-pwCV*x*Z	
D	-37.840848	D	-37.841857	D	-37.842107	D	-37.854196	D	-37.854875	D	-37.855048
T	-37.845313	T	-37.847440	T	-37.847391	T	-37.859061	T	-37.859799	T	-37.859768
Q	-37.848135	Q	-37.849054	Q	-37.849066	Q	-37.860785	Q	-37.861371	Q	-37.861374
5	-37.849140	5	-37.849392	5	-37.849394	5	-37.861541	5	-37.861695	5	-37.861697
N -54.5893 hartree											
cc-pV*x*Z		cc-pCV*x*Z		cc-pwCV*x*Z		cc-pV*x*Z		cc-pCV*x*Z		cc-pwCV*x*Z	
D	-54.572571	D	-54.573835	D	-54.574474	D	-54.589136	D	-54.590011	D	-54.590441
T	-54.586935	T	-54.588122	T	-54.588026	T	-54.601781	T	-54.602526	T	-54.602453
Q	-54.590896	Q	-54.591878	Q	-54.591881	Q	-54.605328	Q	-54.605962	Q	-54.605958
5	-54.592689	5	-54.592967	5	-54.592968	5	-54.606704	5	-54.606876	5	-54.606878
cc-pV*x*Z+sp		cc-pCV*x*Z+sp		cc-pwCV*x*Z+sp		cc-pV*x*Z+sp		cc-pCV*x*Z+sp		cc-pwCV*x*Z+sp	
D	-54.578765	D	-54.580033	D	-54.580466	D	-54.593843	D	-54.594710	D	-54.595003
T	-54.588525	T	-54.589806	T	-54.589706	T	-54.602891	T	-54.603691	T	-54.603615

-continue-

-continue-

BLYP						B3LYP					
Q	-54.591546	Q	-54.592479	Q	-54.592479	Q	-54.605735	Q	-54.606338	Q	-54.606332
5	-54.592811	5	-54.593089	5	-54.593091	5	-54.606773	5	-54.606945	5	-54.606946
aug-cc-pV*x*Z		aug-cc-pCV*x*Z		aug-cc-pwCV*x*Z		aug-cc-pV*x*Z		aug-cc-pCV*x*Z		aug-cc-pwCV*x*Z	
D	-54.578765	D	-54.580033	D	-54.580466	D	-54.593843	D	-54.594710	D	-54.595003
T	-54.588525	T	-54.589806	T	-54.589706	T	-54.602891	T	-54.603691	T	-54.603615
Q	-54.591546	Q	-54.592479	Q	-54.592479	Q	-54.605735	Q	-54.606338	Q	-54.606332
5	-54.592811	5	-54.593089	5	-54.593091	5	-54.606773	5	-54.606945	5	-54.606946
O -75.067 hartree											
cc-pV*x*Z		cc-pCV*x*Z		cc-pwCV*x*Z		cc-pV*x*Z		cc-pCV*x*Z		cc-pwCV*x*Z	
D	-75.054526	D	-75.056165	D	-75.056961	D	-75.068499	D	-75.069651	D	-75.070176
T	-75.080286	T	-75.081595	T	-75.081424	T	-75.091864	T	-75.092706	T	-75.092573
Q	-75.087251	Q	-75.088273	Q	-75.088268	Q	-75.098201	Q	-75.098871	Q	-75.098858
5	-75.090069	5	-75.090385	5	-75.090390	5	-75.100485	5	-75.100683	5	-75.100686
cc-pV*x*Z+sp		cc-pCV*x*Z+sp		cc-pwCV*x*Z+sp		cc-pV*x*Z+sp		cc-pCV*x*Z+sp		cc-pwCV*x*Z+sp	
D	-75.065527	D	-75.067084	D	-75.067562	D	-75.077084	D	-75.078167	D	-75.078474
T	-75.083302	T	-75.084744	T	-75.084571	T	-75.094055	T	-75.094985	T	-75.094852
Q	-75.088479	Q	-75.089436	Q	-75.089429	Q	-75.099017	Q	-75.099646	Q	-75.099631
5	-75.090280	5	-75.090602	5	-75.090608	5	-75.100607	5	-75.100808	5	-75.100811
aug-cc-pV*x*Z		aug-cc-pCV*x*Z		aug-cc-pwCV*x*Z		aug-cc-pV*x*Z		aug-cc-pCV*x*Z		aug-cc-pwCV*x*Z	
D	-75.065596	D	-75.067153	D	-75.067632	D	-75.077164	D	-75.078247	D	-75.078554
T	-75.083421	T	-75.084863	T	-75.084691	T	-75.094180	T	-75.095111	T	-75.094977
Q	-75.088511	Q	-75.089468	Q	-75.089460	Q	-75.099049	Q	-75.099678	Q	-75.099662
5	-75.090288	5	-75.090610	5	-75.090616	5	-75.100614	5	-75.100815	5	-75.100819
F -99.734 hartree											
cc-pV*x*Z		cc-pCV*x*Z		cc-pwCV*x*Z		cc-pV*x*Z		cc-pCV*x*Z		cc-pwCV*x*Z	
D	-99.713359	D	-99.715429	D	-99.716465	D	-99.726602	D	-99.728059	D	-99.728726
T	-99.752932	T	-99.754387	T	-99.754138	T	-99.762867	T	-99.763820	T	-99.763621

-continue-

-continue-

BLYP						B3LYP					
Q	-99.763470	Q	-99.764550	Q	-99.764523	Q	-99.772527	Q	-99.773245	Q	-99.773209
5	-99.767416	5	-99.767748	5	-99.767754	5	-99.775818	5	-99.776026	5	-99.776030
cc-pV*x*Z+sp		cc-pCV*x*Z+sp		cc-pwCV*x*Z+sp		cc-pV*x*Z+sp		cc-pCV*x*Z+sp		cc-pwCV*x*Z+sp	
D	-99.729672	D	-99.731566	D	-99.732163	D	-99.739386	D	-99.740706	D	-99.741070
T	-99.757261	T	-99.758880	T	-99.758630	T	-99.766004	T	-99.767072	T	-99.766874
Q	-99.765110	Q	-99.766115	Q	-99.766089	Q	-99.773605	Q	-99.774274	Q	-99.774239
5	-99.767669	5	-99.768010	5	-99.768017	5	-99.775958	5	-99.776171	5	-99.776175
aug-cc-pV*x*Z		aug-cc-pCV*x*Z		aug-cc-pwCV*x*Z		aug-cc-pV*x*Z		aug-cc-pCV*x*Z		aug-cc-pwCV*x*Z	
D	-99.729776	D	-99.731671	D	-99.732267	D	-99.739496	D	-99.740816	D	-99.741181
T	-99.757394	T	-99.759014	T	-99.758764	T	-99.766141	T	-99.767210	T	-99.767011
Q	-99.765151	Q	-99.766156	Q	-99.766129	Q	-99.773645	Q	-99.774313	Q	-99.774277
5	-99.767680	5	-99.768021	5	-99.768028	5	-99.775969	5	-99.776182	5	-99.776186

energy at the quintuple-zeta level. A similar observation can be made on cc-pCV*x*Z+*sp* and the cc-pwCV*x*Z+*sp* as well as on the aug-cc-pCV*x*Z and aug-cc-pwCV*x*Z basis sets. For each level of correlation consistent basis set, the total energy decreases in the following sequence: cc-pCV*x*Z > cc-pCV*x*Z+*sp* > aug-cc-pCV*x*Z (or cc-pwCV*x*Z > cc-pwCV*x*Z+*sp* > aug-cc-pwCV*x*Z). This sequence is in accord with the number of basis functions. The additional diffuse *sp* functions account for most of the energy difference between the standard core-valence and augmented core-valence sets. For example, at the double-zeta level, the energy difference of the O atom between cc-pwCV*x*Z and aug-cc-pwCV*x*Z is 0.01067 hartree, while the difference between cc-pwCV*x*Z and cc-pwCV*x*Z+*sp* is 0.01060 hartree. As compared with Davidson energies, all calculated results are underestimated at the quintuple–zeta level for BLYP and B3LYP.

7.3.3 Atomization Energy

The computed atomization energies and experimental results are presented in Table 7.3. The atomization energies are nearly converged at the triple-zeta level. The atomization energies with the polarized core-valence, the polarized weighted core-valence, and standard correlation consistent basis sets converge to the same limit, as expected. This seems to indicate that the basis set limit has been reached, at least for atomization energy. Although the additional functions for core correlation did not affect the basis set limit, the atomization energy at the double-zeta level was affected slightly. For example, the BLYP atomization energy of HCN with cc-pVDZ is 303.84 kcal/mol, about 1 kcal/mol lower than that with cc-pCVDZ, and about 2 kcal/mol lower than that with cc-pwCVDZ. The impact is decreased as the basis set size is increased. In general, the impact is insignificant at the triple- and higher basis set level.

The unexpected convergence problem was also observed for the polarized core-valence and the polarized weighted core-valence basis sets (cc-pCV*x*Z and cc-pwCV*x*Z). For CO, CO_2, and HOF, a slight energy dip occurs when the pure functional BLYP was used with both the cc-pCV*x*Z and cc-pwCV*x*Z basis sets. However, unlike for cc-pV*x*Z where the energy dip was observed at the quintuple-zeta level, the energy dip occurs at the quadruple-zeta level, which is due to the substantial increase on energy at the triple-zeta level. For example, the BLYP/cc-pCV*x*Z atomization energies of CO are 257.10, 259.91, 259.80, and 259.31 kcal/mol for the double-, triple-, quadruple-, and quintuple-zeta levels, respectively. An energy dip is observed at the quadruple-zeta level with the largest energy, 259.91 kcal/mol, at the triple-zeta level. When B3LYP was used, the polarized core-valence and the polarized weighted core-valence sets result in an energy dip at the quintuple-zeta level as for cc-pV*x*Z, but differ from the cc-pV*x*Z, the B3LYP/cc-pCV*x*Z or B3LYP/cc-pwCV*x*Z atomization energy at the quintuple-zeta level which is lower than the energy at the triple-zeta level. It appears that additional core-correlation functions have a larger effect on the quintuple zeta level than the triple-zeta level. The non-convergent behavior of the polarized core-valence and the polarized weighted core-valence sets can be alleviated through the use of additional diffuse functions (aug-cc-pCV*x*Z and aug-cc-pwCV*x*Z) for both density functionals. An example is the atomization energies of CO. For the other two molecules, the dip still exists at the quintuple-zeta level, but is less pronounced (~0.05 kcal/mol). According to the difference in construction between cc-pV*x*Z and cc-pCV*x*Z or cc-pwCV*x*Z, the energy dip occurred earlier in core-valence sets may be caused by the additional core correlated functions, especially high angular momentum functions. In the previous chapter, how the convergence deteriorates with such functions has been addressed.

Among all molecules studied, O_3 and F_2 have an irregular convergence behavior of their atomization energies with respect to increasing basis set size, which has already been observed in our previous studies. For F_2, the BLYP/cc-pCV*x*Z and BLYP/cc-pwCV*x*Z atomization energies decrease as the basis set size increases, but the atomization energies can not converge exponentially. When B3LYP was used, an energy dip occurs at the triple-zeta level for both the cc-pCV*x*Z and cc-pwCV*x*Z sets. As compared with the cc-pV*x*Z sets, the addition of core correlation functions does not improve the convergence behavior of BLYP and B3LYP atomization energies, but the addition of diffuse functions can affect the convergence behavior for BLYP and B3LYP with the cc-pV*x*Z set. Unfortunately, the dip still exists for the augmented polarized core-valence and the polarized weighted core-valence sets (aug-cc-pCV*x*Z and aug-cc-pwCV*x*Z). For O_3, the BLYP/cc-pV*x*Z results in an energy fluctuation with increasing basis set size: 168.32, 166.96, 167.28 and 166.79 kcal/mol for double-, triple-, quadruple- and quintuple-zeta level, respectively. BLYP/cc-pCV*x*Z results in an increase of the atomization energy at the triple-zeta level, but the convergence of atomization energies are still not smooth. BLYP/cc-pwCV*x*Z decreases the atomization energy at the double-zeta level and increases the atomization energy at the triple-zeta level, as compared with BLYP/cc-pV*x*Z results. As a result, an energy dip occurs at the quadruple-zeta level. For B3LYP, all three types of basis sets (cc-pV*x*Z, cc-pCV*x*Z and cc-pwCV*x*Z) result in similar convergence behavior with an energy dip at the quintuple-zeta level. The convergence problem can not be alleviated by the addition of diffuse functions for BLYP, whereas B3LYP/aug-cc-pCV*x*Z and B3LYP/aug-cc-pwCV*x*Z improve the irregular convergence behavior. Although the dip still exists, it was reduced to ~0.03 kcal/mol for the aug-cc-pwCV*x*Z and aug-cc-pCV*x*Z sets.

Table 7.3 Calculated atomization energies in kcal/mol.

BLYP						B3LYP					
CO 256.2 kcal/mol											
cc-pV*x*Z		cc-pCV*x*Z		cc-pwCV*x*Z		cc-pV*x*Z		cc-pCV*x*Z		cc-pwCV*x*Z	
D	256.35	D	257.10	D	257.60	D	248.42	D	249.09	D	249.53
T	259.25	T	259.91	T	259.99	T	252.12	T	252.75	T	252.86
Q	259.76	Q	259.80	Q	259.79	Q	252.84	Q	252.92	Q	252.91
5	259.26	5	259.31	5	259.31	5	252.56	5	252.60	5	252.60
cc-pV*x*Z+sp		cc-pCV*x*Z+sp		cc-pwCV*x*Z+sp		cc-pV*x*Z+sp		cc-pCV*x*Z+sp		cc-pwCV*x*Z+sp	
D	253.17	D	253.74	D	254.20	D	246.19	D	246.71	D	247.08
T	257.89	T	258.42	T	258.48	T	251.18	T	251.71	T	251.81
Q	259.09	Q	259.19	Q	259.17	Q	252.41	Q	252.52	Q	252.51
5	259.16	5	259.21	5	259.21	5	252.51	5	252.55	5	252.55
aug-cc-pV*x*Z		aug-cc-pCV*x*Z		aug-cc-pwCV*x*Z		aug-cc-pV*x*Z		aug-cc-pCV*x*Z		aug-cc-pwCV*x*Z	
D	254.29	D	254.84	D	255.10	D	247.20	D	247.74	D	247.95
T	258.66	T	258.46	T	258.52	T	251.36	T	251.74	T	251.84
Q	259.16	Q	259.19	Q	259.17	Q	252.47	Q	252.53	Q	252.52
5	259.19	5	259.21	5	259.21	5	252.53	5	252.55	5	252.55
HCN 302.5 kcal/mol											
cc-pV*x*Z		cc-pCV*x*Z		cc-pwCV*x*Z		cc-pV*x*Z		cc-pCV*x*Z		cc-pwCV*x*Z	
D	303.84	D	304.82	D	305.74	D	295.79	D	296.68	D	297.46
T	310.36	T	310.97	T	310.94	T	302.78	T	303.37	T	303.38
Q	311.21	Q	311.17	Q	311.15	Q	303.74	Q	303.75	Q	303.74
5	310.92	5	310.95	5	310.95	5	303.63	5	303.66	5	303.66
cc-pV*x*Z+sp		cc-pCV*x*Z+sp		cc-pwCV*x*Z+sp		cc-pV*x*Z+sp		cc-pCV*x*Z+sp		cc-pwCV*x*Z+sp	
D	302.04	D	302.84	D	303.72	D	294.72	D	295.48	D	296.20
T	309.63	T	310.13	T	310.10	T	302.36	T	302.87	T	302.88
Q	310.78	Q	310.78	Q	310.76	Q	303.49	Q	303.53	Q	303.52
5	310.82	5	310.85	5	310.85	5	303.58	5	303.61	5	303.61

-continue-

-continue-

BLYP						B3LYP					
aug-cc-pV*x*Z		aug-cc-pCV*x*Z		aug-cc-pwCV*x*Z		aug-cc-pV*x*Z		aug-cc-pCV*x*Z		aug-cc-pwCV*x*Z	
D	303.12	D	303.87	D	304.56	D	295.68	D	296.39	D	296.96
T	310.46	T	310.23	T	310.20	T	302.60	T	302.98	T	302.98
Q	310.89	Q	310.80	Q	310.78	Q	303.58	Q	303.56	Q	303.55
5	310.85	5	310.86	5	310.85	5	303.60	5	303.62	5	303.62
HNO 196.9 kcal/mol											
cc-pV*x*Z		cc-pCV*x*Z		cc-pwCV*x*Z		cc-pV*x*Z		cc-pCV*x*Z		cc-pwCV*x*Z	
D	206.22	D	206.79	D	206.81	D	192.98	D	193.46	D	193.48
T	209.05	T	209.62	T	209.54	T	196.94	T	197.43	T	197.38
Q	209.98	Q	210.05	Q	210.04	Q	198.00	Q	198.09	Q	198.09
5	209.96	5	210.00	5	209.99	5	198.13	5	198.17	5	198.17
cc-pV*x*Z+sp		cc-pCV*x*Z+sp		cc-pwCV*x*Z+sp		cc-pV*x*Z+sp		cc-pCV*x*Z+sp		cc-pwCV*x*Z+sp	
D	205.17	D	205.56	D	205.67	D	192.87	D	193.22	D	193.30
T	208.86	T	209.38	T	209.31	T	197.05	T	197.51	T	197.46
Q	209.95	Q	210.05	Q	210.05	Q	198.11	Q	198.22	Q	198.21
5	210.08	5	210.12	5	210.12	5	198.25	5	198.29	5	198.29
aug-cc-pV*x*Z		aug-cc-pCV*x*Z		aug-cc-pwCV*x*Z		aug-cc-pV*x*Z		aug-cc-pCV*x*Z		aug-cc-pwCV*x*Z	
D	206.87	D	207.24	D	207.37	D	194.64	D	194.99	D	195.09
T	209.08	T	209.53	T	209.45	T	197.27	T	197.69	T	197.63
Q	210.12	Q	210.13	Q	210.12	Q	198.26	Q	198.30	Q	198.29
5	210.14	5	210.14	5	210.14	5	198.29	5	198.31	5	198.31
HOF 151.6 kcal/mol											
cc-pV*x*Z		cc-pCV*x*Z		cc-pwCV*x*Z		cc-pV*x*Z		cc-pCV*x*Z		cc-pwCV*x*Z	
D	156.42	D	156.70	D	156.72	D	144.19	D	144.40	D	144.42
T	159.55	T	160.02	T	159.98	T	148.35	T	148.77	T	148.74
Q	159.85	Q	159.86	Q	159.85	Q	148.77	Q	148.79	Q	148.78
5	159.73	5	159.71	5	159.71	5	148.75	5	148.74	5	148.74

-continue-

-continue-

BLYP						B3LYP					
cc-pV*x*Z+sp		cc-pCV*x*Z+sp		cc-pwCV*x*Z+sp		cc-pV*x*Z+sp		cc-pCV*x*Z+sp		cc-pwCV*x*Z+sp	
D	154.64	D	154.86	D	154.94	D	143.06	D	143.24	D	143.30
T	159.04	T	159.43	T	159.40	T	148.08	T	148.44	T	148.42
Q	159.67	Q	159.70	Q	159.69	Q	148.70	Q	148.73	Q	148.73
5	159.75	5	159.74	5	159.74	5	148.79	5	148.79	5	148.79
aug-cc-pV*x*Z		aug-cc-pCV*x*Z		aug-cc-pwCV*x*Z		aug-cc-pV*x*Z		aug-cc-pCV*x*Z		aug-cc-pwCV*x*Z	
D	158.10	D	158.29	D	158.36	D	146.71	D	146.89	D	146.92
T	159.44	T	159.73	T	159.68	T	148.50	T	148.76	T	148.72
Q	159.80	Q	159.77	Q	159.75	Q	148.83	Q	148.81	Q	148.81
5	159.79	5	159.76	5	159.76	5	148.82	5	148.81	5	148.81
N_2 225.1 kcal/mol											
cc-pV*x*Z		cc-pCV*x*Z		cc-pwCV*x*Z		cc-pV*x*Z		cc-pCV*x*Z		cc-pwCV*x*Z	
D	231.22	D	232.21	D	232.81	D	219.32	D	220.19	D	220.70
T	236.49	T	237.07	T	237.02	T	225.45	T	226.03	T	226.01
Q	237.27	Q	237.37	Q	237.36	Q	226.38	Q	226.49	Q	226.49
5	237.19	5	237.24	5	237.25	5	226.43	5	226.48	5	226.48
cc-pV*x*Z+sp		cc-pCV*x*Z+sp		cc-pwCV*x*Z+sp		cc-pV*x*Z+sp		cc-pCV*x*Z+sp		cc-pwCV*x*Z+sp	
D	229.89	D	230.72	D	231.41	D	218.68	D	219.42	D	220.00
T	236.06	T	236.66	T	236.62	T	225.25	T	225.87	T	225.86
Q	237.21	Q	237.32	Q	237.31	Q	226.42	Q	226.54	Q	226.53
5	237.35	5	237.40	5	237.40	5	226.57	5	226.62	5	226.62
aug-cc-pV*x*Z		aug-cc-pCV*x*Z		aug-cc-pwCV*x*Z		aug-cc-pV*x*Z		aug-cc-pCV*x*Z		aug-cc-pwCV*x*Z	
D	230.53	D	231.33	D	231.99	D	219.36	D	220.08	D	220.64
T	236.25	T	236.75	T	236.70	T	225.42	T	225.97	T	225.96
Q	237.33	Q	237.36	Q	237.34	Q	226.52	Q	226.57	Q	226.56
5	237.38	5	237.41	5	237.41	5	226.60	5	226.63	5	226.63
O_3 142.4 kcal/mol											

-continue-

-continue-

BLYP						B3LYP					
cc-pV*x*Z		cc-pCV*x*Z		cc-pwCV*x*Z		cc-pV*x*Z		cc-pCV*x*Z		cc-pwCV*x*Z	
D	168.32	D	168.47	D	167.96	D	133.76	D	133.87	D	133.46
T	166.96	T	168.09	T	168.03	T	135.68	T	136.67	T	136.62
Q	167.28	Q	167.43	Q	167.42	Q	136.58	Q	136.75	Q	136.75
5	166.79	5	166.83	5	166.82	5	136.45	5	136.49	5	136.49
cc-pV*x*Z+sp		cc-pCV*x*Z+sp		cc-pwCV*x*Z+sp		cc-pV*x*Z+sp		cc-pCV*x*Z+sp		cc-pwCV*x*Z+sp	
D	161.43	D	161.55	D	161.31	D	129.33	D	129.42	D	129.21
T	165.39	T	166.18	T	166.11	T	134.92	T	135.62	T	135.56
Q	166.68	Q	166.87	Q	166.86	Q	136.37	Q	136.57	Q	136.56
5	166.91	5	166.95	5	166.94	5	136.63	5	136.68	5	136.67
aug-cc-pV*x*Z		aug-cc-pCV*x*Z		aug-cc-pwCV*x*Z		aug-cc-pV*x*Z		aug-cc-pCV*x*Z		aug-cc-pwCV*x*Z	
D	165.88	D	165.94	D	165.78	D	134.41	D	134.48	D	134.34
T	165.82	T	166.45	T	166.35	T	135.39	T	135.97	T	135.87
Q	166.98	Q	167.02	Q	167.00	Q	136.67	Q	136.75	Q	136.73
5	166.98	5	166.98	5	166.98	5	136.70	5	136.72	5	136.72
F_2 36.9 kcal/mol											
cc-pV*x*Z		cc-pCV*x*Z		cc-pwCV*x*Z		cc-pV*x*Z		cc-pCV*x*Z		cc-pwCV*x*Z	
D	50.67	D	50.72	D	50.58	D	36.32	D	36.35	D	36.24
T	49.21	T	49.65	T	49.64	T	36.54	T	36.96	T	36.97
Q	48.41	Q	48.41	Q	48.40	Q	36.04	Q	36.04	Q	36.04
5	47.78	5	47.77	5	47.76	5	35.63	5	35.62	5	35.62
cc-pV*x*Z+sp		cc-pCV*x*Z+sp		cc-pwCV*x*Z+sp		cc-pV*x*Z+sp		cc-pCV*x*Z+sp		cc-pwCV*x*Z+sp	
D	43.81	D	43.91	D	43.90	D	30.74	D	30.82	D	30.80
T	47.25	T	47.55	T	47.54	T	35.15	T	35.42	T	35.42
Q	47.70	Q	47.71	Q	47.70	Q	35.61	Q	35.62	Q	35.62
5	47.75	5	47.74	5	47.74	5	35.68	5	35.67	5	35.66
aug-cc-pV*x*Z		aug-cc-pCV*x*Z		aug-cc-pwCV*x*Z		aug-cc-pV*x*Z		aug-cc-pCV*x*Z		aug-cc-pwCV*x*Z	
D	46.70	D	46.75	D	46.74	D	33.94	D	33.98	D	33.96

-continue-

-continue-

BLYP						B3LYP					
T	47.68	T	47.90	T	47.87	T	35.59	T	35.79	T	35.77
Q	47.77	Q	47.74	Q	47.73	Q	35.68	Q	35.66	Q	35.65
5	47.77	5	47.74	5	47.74	5	35.68	5	35.67	5	35.67
CO_2 381.9 kcal/mol											
cc-pV*x*Z		cc-pCV*x*Z		cc-pwCV*x*Z		cc-pV*x*Z		cc-pCV*x*Z		cc-pwCV*x*Z	
D	390.46	D	391.62	D	392.04	D	375.18	D	376.19	D	376.56
T	394.00	T	394.98	T	395.00	T	380.63	T	381.52	T	381.60
Q	394.46	Q	394.48	Q	394.45	Q	381.49	Q	381.59	Q	381.57
5	393.52	5	393.58	5	393.58	5	380.95	5	381.02	5	381.02
cc-pV*x*Z+sp		cc-pCV*x*Z+sp		cc-pwCV*x*Z+sp		cc-pV*x*Z+sp		cc-pCV*x*Z+sp		cc-pwCV*x*Z+sp	
D	383.74	D	384.62	D	385.13	D	370.60	D	371.41	D	371.81
T	391.49	T	392.27	T	392.28	T	378.98	T	379.73	T	379.80
Q	393.23	Q	393.34	Q	393.31	Q	380.73	Q	380.89	Q	380.87
5	393.28	5	393.34	5	393.34	5	380.82	5	380.89	5	380.89
aug-cc-pV*x*Z		aug-cc-pCV*x*Z		aug-cc-pwCV*x*Z		aug-cc-pV*x*Z		aug-cc-pCV*x*Z		aug-cc-pwCV*x*Z	
D	386.01	D	386.77	D	387.09	D	372.82	D	373.53	D	373.78
T	392.31	T	392.38	T	392.39	T	379.21	T	379.85	T	379.92
Q	393.38	Q	393.36	Q	393.32	Q	380.85	Q	380.91	Q	380.89
5	393.32	5	393.34	5	393.34	5	380.86	5	380.90	5	380.90

Table 7.4 Mean absolute errors (MAE) and mean errors (ME) for the atomization energies in kcal/mol.

ME	BLYP	BLYP	BLYP	B3LYP	B3LYP	B3LYP
cc-pV*x*Z	cc-pCV*x*Z	cc-pwCV*x*Z	cc-pV*x*Z	cc-pCV*x*Z	cc-pwCV*x*Z	
D 8.75	D 9.37	D 9.59	D -5.94	D -5.41	D	-5.21

-continue-

-continue-

ME	BLYP		BLYP		BLYP		B3LYP		B3LYP		B3LYP
T	11.42	T	12.10	T	12.08	T	-1.88	T	-1.25	T	-1.24
Q	11.84	Q	11.89	Q	11.87	Q	-1.21	Q	-1.13	Q	-1.14
5	11.46	5	11.49	5	11.48	5	-1.37	5	-1.34	5	-1.34
cc-pV*x*Z+sp		cc-pCV*x*Z+sp		cc-pwCV*x*Z+sp		cc-pV*x*Z+sp		cc-pCV*x*Z+sp		cc-pwCV*x*Z+sp	
D	5.05	D	5.54	D	5.85	D	-8.41	D	-7.97	D	-7.73
T	10.27	T	10.81	T	10.79	T	-2.57	T	-2.04	T	-2.04
Q	11.35	Q	11.43	Q	11.42	Q	-1.46	Q	-1.36	Q	-1.37
5	11.45	5	11.48	5	11.48	5	-1.33	5	-1.30	5	-1.30
aug-cc-pV*x*Z		aug-cc-pCV*x*Z		aug-cc-pwCV*x*Z		aug-cc-pV*x*Z		aug-cc-pCV*x*Z		aug-cc-pwCV*x*Z	
D	7.25	D	7.69	D	7.94	D	-6.09	D	-5.68	D	-5.48
T	10.77	T	10.99	T	10.96	T	-2.27	T	-1.85	T	-1.85
Q	11.49	Q	11.48	Q	11.46	Q	-1.33	Q	-1.30	Q	-1.31
5	11.49	5	11.49	5	11.49	5	-1.30	5	-1.29	5	-1.29

MAE	BLYP		BLYP		BLYP				B3LYP		B3LYP
cc-pV*x*Z		cc-pCV*x*Z		cc-pwCV*x*Z		cc-pV*x*Z		cc-pCV*x*Z		cc-pwCV*x*Z	
D	8.75	D	9.37	D	9.59	D	5.94	D	5.41	D	5.21
T	11.42	T	12.10	T	12.08	T	2.05	T	1.85	T	1.83
Q	11.84	Q	11.89	Q	11.87	Q	2.11	Q	2.09	Q	2.10
5	11.46	5	11.49	5	11.48	5	2.29	5	2.29	5	2.29
cc-pV*x*Z+sp		cc-pCV*x*Z+sp		cc-pwCV*x*Z+sp		cc-pV*x*Z+sp		cc-pCV*x*Z+sp		cc-pwCV*x*Z+sp	
D	5.05	D	6.15	D	6.35	D	8.41	D	7.97	D	7.73
T	10.27	T	10.81	T	10.79	T	2.64	T	2.48	T	2.46
Q	11.35	Q	11.43	Q	11.42	Q	2.34	Q	2.31	Q	2.31
5	11.45	5	11.48	5	11.48	5	2.31	5	2.31	5	2.31
aug-cc-pV*x*Z		aug-cc-pCV*x*Z		aug-cc-pwCV*x*Z		aug-cc-pV*x*Z		aug-cc-pCV*x*Z		aug-cc-pwCV*x*Z	
D	7.73	D	8.03	D	8.21	D	6.09	D	5.68	D	5.48
T	10.77	T	10.99	T	10.96	T	2.47	T	2.38	T	2.37
Q	11.49	Q	11.48	Q	11.46	Q	2.30	Q	2.28	Q	2.29
5	11.49	5	11.49	5	11.49	5	2.30	5	2.30	5	2.30

On the other hand, the convergence problem can be avoided by using cc-pCV*x*Z+*sp* sets. This can be applied to all molecules studied in this study. This observation is in accord with our earlier investigations (Chapter 5), which has shown the impact of additional diffuse *sp* functions on the convergence behavior.

For the other molecules, the convergence dip observed for the cc-pV*x*Z sets also occurs for the polarized core-valence and the polarized weighted core-valence sets. The augmented sets (aug-cc-pCVxZ and aug-cc-pwCVxZ) improved the convergence behavior.

7.3.4 Statistical Analysis

The statistical results including mean error (ME) and mean absolute error (MAE) are listed in Table 7.4. As shown by the mean errors, B3LYP underestimates the atomization energy, while BLYP overestimates the atomization energy.

Based on the MAE of the atomization energy as compared with experiment, the best result comes from using B3LYP with the cc-pwCVTZ and cc-pCVTZ basis sets, which give MAE of 1.83 and 1.85 kcal/mol, respectively. These smallese deviations (relative to the MAE for BLYP) may be attributed to that the triple-zeta set produces the largest atomization energies for most of molecules, and to the fact that almost all atomization energies were underestimated by B3LYP. In contrast to B3LYP, BLYP/cc-pCVTZ and BLYP/cc-pwCVTZ result in the largest MAE, with deviations of 12.10 and 12.08 kcal/mol, respectively. This deviation corresponds to the largest atomization energies at the triple-zeta level and the overestimation of the atomization energies by BLYP.

The aug-cc-pCV*x*Z and aug-cc-pwCV*x*Z basis sets improve the convergence behavior of the non-augmented corresponding sets. Accordingly, for these two sets, the mean absolute errors

deviate further from experiment for BLYP, and get closer to experiment for B3LYP with respect to increasing basis set size, which is also the case for cc-pCV*x*Z+*sp* and cc-pwCV*x*Z+sp.

7.4 Conclusion

Overall, the core correlation functions have a small effect on the calculated geometries, atomic energies, and atomization energies, due to the small number of core electrons for first-row elements. For atomization energies with the polarized core-valence and the polarized weighted core-valence sets, unexpected convergence problems occur for a number of molecules and functionals studied. As compared with standard correlation consistent basis sets, the convergence behavior deteriorates with the additional functions for core correlation. The possible reasons include: the additional core-correlation sets were optimized using the CISD method and the core-valence sets include too many high angular momentum functions, which have been proven in this study as a potential factor corresponding to the non-convengence problem The fact is exemplified by an earlier occurrence of the energy dip for the core-valence sets as compared to the standard sets. The inclusion of additional diffuse functions to core-valence sets (cc-pCV*x*Z and cc-pwCV*x*Z) can help alleviate the unexpected behavior, but not for all molecules. However, the convergence problem observed in the core-valence sets can be avoided completely by just adding diffuse *sp* functions to cc-pCV*x*Z and cc-pwCV*x*Z. This agrees with the observations made in Chapter 5.

CHAPTER 8

THE PERFORMANCE OF DENSITY FUNCTIONALS WITH RESPECT TO BASIS SETS: THE TIGHT *d* EFFECT ON SO_2, CCl, AND ClO_2

8.1 Introduction

Since the development of correlation consistent basis sets, [15] there have been thousands of successful studies using them. Using CCSD(T) with the correlation consistent basis sets has become a standard approach to provide some of the most accurate information on molecular properties. However, these basis sets are not without questions. The weakness of the correlation consistent basis sets was observed first in the work of Bauschlicher and Patridge in 1995. [115] They found the dissociation energy of SO_2 was underestimated by 6.2 kcal/mol with results obtained from CCSD(T) calculations. The addition of a tight *d* function (high exponent) in the sulfur basis sets reduces the error significantly to -1.9 kcal/mol. Other studies have shown this problem also exists in SO and other systems containing second-row atoms. [116, 117]

The means to alleviate this problem has been proposed. Martin suggested a systematic procedure to add higher angular momentum functions for sulfur: a (1*d*) set to the cc-pVTZ set, a (2*d*1*f*) set to the cc-pVQZ set, and a (3*d*2*f*1*g*) set to the cc-pV5Z set. [116] These functions result in significant improvements in the extrapolated binding energies. Bauschlicher and Ricca also added the additional higher-angular momentum functions to the correlation consistent basis sets

for sulfur. [118] They suggested an optimal adding of (2*d*) set to each level of basis set. Dunning, Peterson and Wilson reinvestigated the basis set deficiencies, [52] and found that the cause of these errors in the standard sets arise from near duplication of the exponents in two of the *d* sets and a lack of high-exponent functions. A strategy was developed to revise the standard correlation consistent basis sets: adding a high-exponent function to each level of basis set, and higher basis sets (cc-pVQZ and cc-pV5Z) required reexamination of the basis set convergence. The key to this revision is that systematic behavior to provide extrapolations to the CBS limit is preserved. As a consequence, an improved family of the correlation consistent basis set, denoted as cc-pV(*x*+*d*)Z, where *x*=D(2), T(3), Q(4), and 5, was formulated. To date, these newly developed correlation consistent basis sets have been used in a number of *ab initio* studies on the second row atoms, [52, 119-125] and the significant improvements in energies have been observed.

So far, extensive studies using tight *d*-augmented correlation consistent basis sets predominantly have been done by our group, and more recently by the Denis group. Studies to date have primarily focused on the thermodynamic properties, energies, and structures of sulfur species of importance in atmospheric chemistry. Wilson and Dunning investigated structures and energetics of the HSO/HOS isomers and their relative stability using CCSD(T) with the tight *d*-augmented correlation consistent basis sets. [119] As compared with standard correlation consistent basis sets, the impact of the tight *d* functions is most important at the double- and triple-zeta levels. The energy difference between the two isomers converges faster for tight *d* sets over the standard sets. The detailed discussion can be seen in the next chapter. The conclusion that tight *d*-augmented sets have an important effect on energy at the low level basis sets was also observed in other studies such as Bell and Wilson, who investigated the effect of tight *d*

functions on the atomization energy of SO_3. [121] Furthermore, for species with strong basis set dependence, the impact of the tight *d*-augmented sets is not limited to low-level basis sets. Denis *et al* determined enthalpies of formation for a series of thionitroso and thiazyl isomers using CCSD(T)/cc-pV*x*Z, aug-cc-pV(*x*+*d*)Z, and B3LYP/6-311+G(3*df*,2*p*).[123] They found that for species, which include second-row atoms, CCSD(T) enthalpies of formations have essentially converged with the aug-cc-pV(5+*d*)Z basis set. However, for the cc-pV*x*Z basis sets, even the results with cc-pV6Z are not fully converged. This observation demonstrates the significance of tight *d* functions on energy at the higher-level basis sets.

Advanced *ab initio* correlated methods like CCSD(T) coupled with tight *d* sets or tight *d*-augmented correlation consistent basis sets have been used as a reliable approach to predict molecular properties accurately. Peterson and Dixon used CCSD(T) with tight *d* correlation consistent basis sets through sextuple-zeta to calculate the heats of formation of CCl and CCl_2. [126] The results, after an additional correction for several relativistic effects, are in excellent agreement with the latest experiments. The CCSD(T) with tight *d*-augmented sets was also applied to predict the heat of formation of HSO and the enthalpies of formation of a series of sulfur molecules. [124, 125]

In this chapter, density functionals are combined with the newly revised tight *d*-augmented correlation consistent basis sets to investigate the atomization energy of several molecules consisting of second-row atoms. The molecules, SO_2, CCl, and ClO_2, are derived from a study by Martell *et al.* of the impact of functional and basis set choice on the atomization energies of a series of 44 molecules. [27] For the dissociation energy, the errors of these molecules, as compared with experiment, were most severe: -19.4 for SO_2, -11.9 for ClO_2, and

14.4 kcal/mol for CCl at the B3LYP/cc-pVTZ//cc-pVDZ level. However, it must be noted that the largest basis sets used in this study were of triple-zeta quality.

Two density functionals, B3LYP and B3PW91, are coupled with the standard and revised correlation consistent basis sets, to examine the impact of the additional *d* functions on the structures and energies of SO_2, CCl, and ClO_2. Additionally, as a result of their systematic construction, results obtained for each level of basis set with a given method can be extrapolated to the Kohn-Sham (KS) limit. This enables a better understanding of the performance of computational methods due to elimination of the basis set error. In this study, two schemes often used to estimate complete basis set limits were utilized to determine KS limits for each DFT approach.

8.2 Methodology

In this study, four series of the correlation consistent basis sets were used in combination with B3LYP [7, 10] and B3PW91 [8]: the standard correlation consistent basis sets, cc-pV*x*Z; the tight *d*-augmented sets, cc-pV(*x*+*d*)*Z*; the augmented correlation consistent basis sets, aug-cc-pV*x*Z; and the augmented tight *d*-augmented sets, which include diffuse functions, aug-cc-pV(*x*+*d*)Z (*x* = D(2), T(3), Q(4), 5). Geometry optimizations and frequency calculations were carried out for each combination of density functional and basis set. The zero-point energy correction was taken from the frequency calculations and was included in the atomization energies. All calculations were performed using the Gaussian 98 package.

Two empirical extrapolation schemes were used to estimate the Kohn-Sham limit: an exponential and a two-point extrapolation scheme. Both schemes have been discussed in the previous chapter.

8.3 Results and Discussion

8.3.1 SO_2

All calculated structures and atomization energies of SO_2 using B3LYP and B3PW91 with four series of basis sets are given in Table 8.1. For both functionals, the bond length decreases as the basis set size increases. The difference in bond lengths between double- and the quintuple- zeta level basis sets is ~0.05Å for cc-pV*x*Z and aug-cc-pV*x*Z, while the difference is reduced to ~0.02Å for cc-pV(*x*+*d*)Z and aug-cc-pV(*x*+*d*)Z). For the bond angles, the impact of tight *d* functions is more evident. The difference of bond angle between double- and quintuple-zeta level basis sets is reduced from ~1.5 ° to ~0.2° when tight *d* functions were included in cc-pV*x*Z or aug-cc-pV*x*Z.

As shown in Table 8.1, B3LYP and B3PW91 atomization energies increase with respect to basis set size. For cc-pV*x*Z, the atomization energy converges slowly for both B3LYP and B3PW91, compared with the tight *d* sets. B3LYP/cc-pV5Z and B3PW91/cc-pV5Z still result in an increase in energy, 5.23 and 4.95 kcal/mol, respectively, over that of cc-pVQZ. The convergence of energies is dramatically affected by the tight *d* functions. In comparison with cc-pV*x*Z basis sets, the cc-pV(*x*+*d*)Z sets reach convergence more quickly. The difference in energy between quadruple- and quintuple- zeta level basis sets drops to 0.52 kcal/mol for B3LYP and 0.58 kcal/mol for B3PW91. In addition, substantial improvement in energy was observed at the low-level basis sets. For example, the tight *d* basis set improves the atomization energy by 17.3 and 10.24 kcal/mol at the B3LYP/cc-pVDZ and B3LYP/cc-pVTZ levels, respectively, while the tight *d* basis set results in an improvement of 5.79 kcal/mol at the cc-pVQZ level and 1.08 kcal/mol at the cc-pV5Z level.

For augmented correlation consistent basis sets, the effect of the tight *d* functions on the convergence of atomization energy is similar to that of the standard correlation consistent basis sets. Compared with non-augmented correlation consistent basis sets (cc-pV*x*Z and cc-pV(*x*+*d*)Z), the additional diffuse functions in augmented sets (aug-cc-pV*x*Z and aug-cc-pV(*x*+*d*)Z) causes less of an improvement than the tight *d* functions. At the double zeta level for B3LYP, the augmented basis sets result in an increase of 5.67 kcal/mol in atomization energy, which is less substantial than the improvement arising from the tight *d* functions (17.30 kcal/mol).

We compared the convergence behavior of atomization energy with both B3LYP/cc-pV*x*Z and B3LYP/cc-pV(*x*+*d*)Z, as shown in Figure 8.1. The atomization energies at the double-, triple- and quadruple-zeta levels are significantly affected by tight *d* functions, which result in a faster convergence for the tight *d* sets than the standard correlation consistent basis sets. However, we note that both series of atomization energies converge to nearly the same limit. The same behavior was observed for the augmented sets, shown in Figure 8.2, which is also for the B3LYP functional.

Figure 8.1 The comparison of the atomization energy of SO2 obtained with BLYP/cc-pV*x*Z and BLYP/cc-pV(*x*+*d*)Z

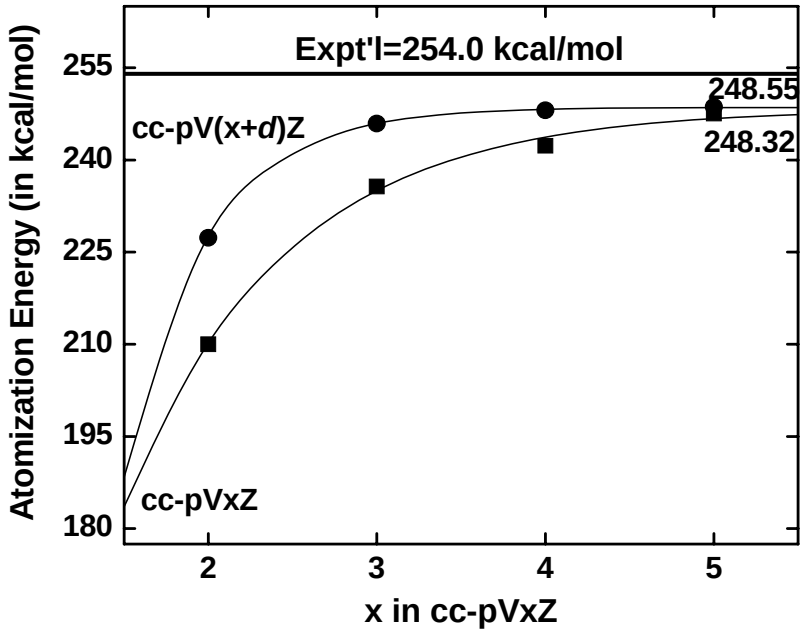

Figure 8.2 The comparison of the atomization energy of SO2 obtained with BLYP/cc-pV*x*Z and BLYP/cc-pV(*x*+*d*)Z

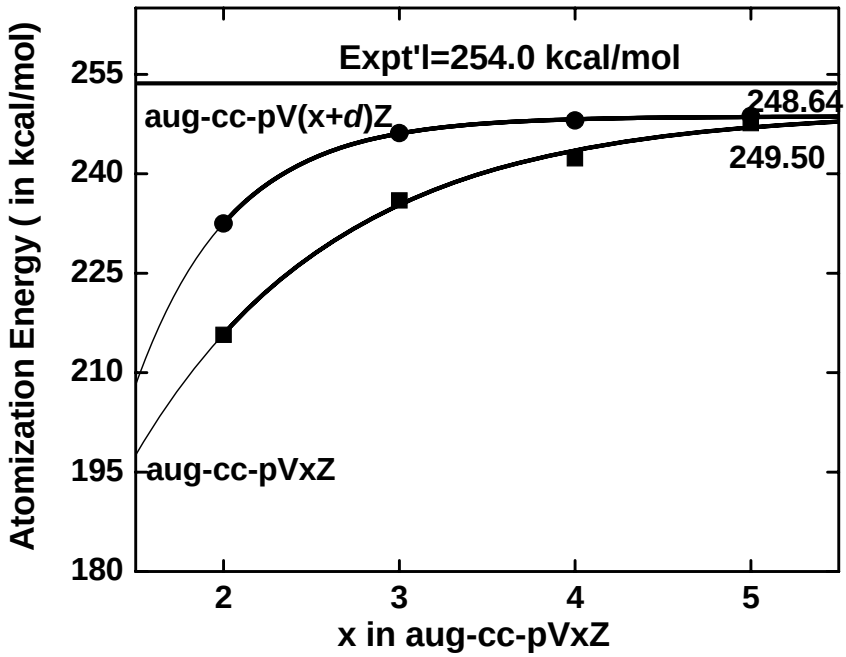

An interesting phenomenon was noted when comparing the results with tight *d* sets (cc-pV(*x*+*d*)Z, aug-cc-pV(*x*+*d*)Z) and standard sets (cc-pV*x*Z and aug-cc-pV*x*Z). For each level of basis set, the effect of adding a tight *d* function on the atomization energy of SO_2 is similar for the B3LYP and B3PW91. For example, at the double-zeta level, the B3LYP energy difference due to tight *d* functions is 17.3 kcal/mol, while the B3PW91 energy difference is 17.46 kcal/mol. This is also the case for augmented correlation consistent basis sets. This similarity suggests that there exists an additivity arising from the density functional effect and tight *d* function effect. For each level of correlation consistent basis set, the energy of a given functional/tight *d* set can be determined approximately by combining the energy at a same functional/standard set and energy

difference due to tight *d* functions from another density functional. This can be expressed in equation below:

$$D_e(\text{B3LYP/cc-pV}(x+d)\text{Z}) = D_e(\text{B3LYP/cc-pV}x\text{Z}) + D_e(\text{B3PW91/cc-pV}(x+d)\text{Z}) - D_e(\text{B3PW91/cc-pV}x\text{Z}))$$

We used results at the cc-pVDZ level as an example. The B3LYP/cc-pV(D+*d*)Z atomization energy derived from the above approximate approach is 227.48 kcal/mol, which is in excellent agreement with the computed result, with a small difference of 0.16 kcal/mol. Since B3LYP and B3PW91 have similar performance and computational costs, the improvement of computational expense is not substantial. This approach can also be applied to *ab initio* methods like HF and CCSD(T). The reliability of this approach has been proven by earlier calculations of Wilson and Dunning, [119] where the atomization energy of SO_2 was determined using CCSD(T) with tight *d* and standard correlation consistent basis sets:

$$D_e(\text{CCSD(T)/cc-pV}(x+d)\text{Z}) = D_e(\text{CCSD(T)/cc-pV}x\text{Z}) + D_e(\text{HF/cc-pV}(x+d)\text{Z}) - D_e(\text{HF/cc-pV}x\text{Z}))$$

Using the above equation results in the values of 148.68, 170.55, 177.33, and 179.89 kcal/mol for the CCSD(T)/cc-pV(D+*d*)Z, CCSD(T)/cc-pV(T+*d*)Z, CCSD(T)/cc-pV(Q+*d*)Z and CCSD(T)/ cc-pV(5+*d*)Z atomization energies of HSO, respectively. These derived results are within 0.12 kcal/mol of the computed results. As a consequence, the additional cost due to tight *d* functions can be avoided using the additivity property of tight *d* functions in the correlation consistent basis sets.

The Kohn-Sham limits are obtained by extrapolating the results from a series of calculations with the correlation consistent basis sets and the tight *d* revised sets. Results from the exponential scheme and from a two-point scheme are listed in Tables 8.1 and 8.2, respectively. For the exponential scheme, the B3PW91/aug-cc-pV*x*Z Kohn-Sham limit results in 1.79 kcal/mol improvement over the atomization energy at the aug-cc-pVQZ level, and provides

Table 8.1 Atomization energy of SO_2 (kcal/mol) using B3LYP and B3PW91 with the correlation consistent basis sets.

Method	basis set	D_0	r (Å)	*A* (°)
Experiment [a]		254.0	1.4321	119.50
B3LYP	cc-pVDZ	210.02	1.4808	117.71
	cc-pVTZ	235.69	1.4505	118.25
	cc-pVQZ	242.30	1.4419	118.65
	cc-pV5Z	247.53	1.4355	119.13
	cc-pV∞Z[b]	248.32		
	cc-pV(D+d)Z	227.32	1.4525	119.33
	cc-pV(T+d)Z	245.93	1.4370	119.23
	cc-pV(Q+d)Z	248.09	1.4349	119.18
	cc-pV(5+d)Z	248.61	1.4340	119.20
	cc-pV∞+Z[b]	248.55		
	aug-cc-pVDZ	215.69	1.4842	117.46
	aug-cc-pVTZ	235.98	1.4514	118.15
	aug-cc-pVQZ	242.33	1.4420	118.63
	aug-cc-pV5Z	247.64	1.4355	119.14
	aug-cc-pV∞Z[b]	249.50		
	aug-cc-pV(D+d)Z	232.52	1.4567	119.17
	aug-cc-pV(T+d)Z	246.13	1.4381	119.12
	aug-cc-pV(Q+d)Z	248.05	1.4350	119.15
	aug-cc-pV(5+d)Z	248.71	1.4340	119.20
	aug-cc-pV∞+Z[b]	248.64		
B3PW91	cc-pVDZ	212.02	1.4758	117.80

-continue-

-continue-

Method	basis set	D_0	r (Å)	*A* (°)
	cc-pVTZ	238.00	1.4468	118.28
	cc-pVQZ	244.46	1.4385	118.68
	cc-pV5Z	249.41	1.4322	119.10
	cc-pV∞Z[b]	250.01		
	cc-pV(D+d)Z	229.48	1.4483	119.39
	cc-pV(T+d)Z	248.26	1.4337	119.23
	cc-pV(Q+d)Z	250.30	1.4317	119.16
	cc-pV(5+d)Z	250.88	1.4308	119.19
	cc-pV∞+Z[b]	250.78		
	aug-cc-pVDZ	218.27	1.4796	117.53
	aug-cc-pVTZ	238.34	1.4475	118.20
	aug-cc-pVQZ	244.45	1.4385	118.67
	aug-cc-pV5Z	249.84	1.4320	119.13
	aug-cc-pV∞Z[b]	251.63		
	aug-cc-pV(D+d)Z	235.28	1.4527	119.21
	aug-cc-pV(T+d)Z	248.53	1.4347	119.15
	aug-cc-pV(Q+d)Z	250.23	1.4317	119.15
	aug-cc-pV(5+d)Z	250.93	1.4309	119.20
	aug-cc-pV∞+Z[b]	250.81		

[a] Experimental data were obtained from Reference [46].

[b] Kohn-Sham limits were obtained using the exponential extrapolation scheme (Equation (1)).

Table 8.2 Extrapolation of the calculated atomization energy of SO_2 to the Kohn-Sham limit using several two-parameter extrapolation schemes and the exponential scheme. The atomization energy from experiment is 254.0 kcal/mol.

method	extrapolation scheme [a]	cc-pVxZ	cc-pV(x+d)Z	aug-cc-pVxZ	aug-cc-pV(x+d)Z
B3LYP	DT	246.50	253.77	244.52	251.86
	DQ	246.91	251.06	246.14	250.27
	D5	250.09	250.07	249.82	249.82
	TQ	247.12	249.67	246.96	249.45
	T5	250.79	249.35	250.85	249.42
	Q5	253.02	249.16	253.21	249.40
	∞	248.32	248.55	249.50	248.64
B3PW91	DT	248.94	256.17	246.79	254.11
	DQ	249.09	253.27	248.19	252.37
	D5	251.97	252.34	252.00	252.00
	TQ	249.17	251.79	248.91	251.47
	T5	252.55	251.60	253.01	251.59
	Q5	254.60	251.49	255.50	251.66
	∞	250.01	250.78	251.63	250.81

[a] DT represents extrapolation using cc-pVDZ and cc-pVTZ, TQ represent extrapolation using cc-pVTZ and cc-pVQZ, . . . ∞ represents the extrapolated Kohn-Sham limit

the best agreement with experiment, with a deviation of 2.37 kcal/mol. The tight *d* sets have little impact on the Kohn-Sham limit, although a dramatic impact on the atomization energy at the low-level basis sets was observed. In Table 8.2, several extrapolation methods based on the two-point scheme are compared. For the standard correlation consistent basis sets (cc-pVxZ and aug-cc-pVxZ), the extrapolated B3LYP Kohn-Sham limit using results at the quadruple- and quintuple-zeta basis sets give the best agreement with experiment, with errors of 0.98 kcal/mol

for cc-pV*x*Z and 0.79 kcal/mol for aug-cc-pV*x*Z. Decreasing the number of basis sets included in the extrapolation of the Kohn-Sham limit leads to a lowering of Kohn-Sham limit. To contrast, for the tight *d* revised sets (cc-pV(*x*+*d*)Z and aug-cc-pV(*x*+*d*)Z), Increasing basis set levels results in a lowering of Kohn-Sham limit. As a consequence, the best B3LYP Kohn-Sham limit, as compared with experiment, was obtained by using the results at the cc-pV(D+*d*)Z (aug-cc-pV(*x*+*d*)Z) and cc-pV(T+*d*)Z (aug-pV(T+*d*)Z), with errors of 0.23 kcal/mol and 2.14 kcal/mol, respectively.

8.3.2 CCl

Optimized geometries and atomization energies are presented for CCl in Table 8.3. In general, bond lengths are predicted to within 0.01Å at the quintuple-zeta level, compared with experiment. Bond lengths are nearly converged at the triple-zeta level for tight *d* revised sets (cc-pV(*x*+*d*)Z and aug-cc-pV(*x*+*d*)Z), while bond lengths reach near convergence at the quadruple-zeta level for the standard sets (cc-pV*x*Z and aug-cc-pV*x*Z).

The reason that theoretical chemists pay more attention to CCl is the large deviation in atomization energy between experiment and theoretical studies. The G2 scheme predicted an atomization energy of 95.9 kcal/mol for CCl, [127] with a difference of ~10 kcal/mol from previous experiment (80 ± 5 kcal/mol).[128] Considering that the atomization energies obtained using G2 methods are usually accurate to within 2-3 kcal/mol, a doubt was cast on the reliability of the experimental value. Recently, other experimental atomization energies have been reported. Jesinger *et al* gives a atomization energy of 93.8 kcal/mol which is derived from an accurate experimental determination of the heat of formation of CCl and known heats of formation of C(g) and Cl(g)[129] Also, the NIST reports a value of 94.4 kcal/mol. [46] These values are in better agreement with the G2 result. A recent high-level *ab initio* study by Dixon and

Peterson[126] also supports the new experimental results. An atomization energy of 95.5 ± 0.3 kcal/mol was obtained using a CBS limit of CCSD(T) with aug-cc-pVxZ plus several relativistic effect corrections including: core valence, scalar relativity, and spin-orbit.

In analogy to SO_2, the tight *d* sets improve the atomization energy of CCl especially for the low-level basis sets, as compared with the standard correlation consistent basis sets. The diffuse functions in augmented sets also improve the atomization energy, but with less of an impact than from the tight *d* sets. For example, for B3LYP with the double-zeta basis set, the augmented sets increase the atomization energy by 0.48 kcal/mol, and the tight *d* sets increase the atomization energy by 1.72 kcal/mol. Overall, the tight *d* sets lead to a faster convergence to the Kohn-Sham limit than standard sets. In contrast to SO_2, the atomization energies of CCl, as compared with experiment, were overestimated at the basis set limit, with ~2 kcal/mol and ~5 kcal/mol greater than experiment for B3LYP and B3PW91, respectively.

Estimated Kohn-Sham limits for two extrapolation schemes are given in Tables 8.3 and 8.4. The improvement in energy due to the extrapolation to Kohn-Sham limit is less substantial. For the two-point extrapolation, a ~2 kcal/mol energy change was observed according to the selected two points in the extrapolation for the standard sets, while very little energy fluctuation occurs for tight *d* sets.

Table 8.3 Atomization energy of CCl (kcal/mol) using B3LYP and B3PW91 with the correlation consistent basis sets.

Method	basis set	D_0	r (Å)
Experiment [a]		94.4	1.65
B3LYP	cc-pVDZ	92.42	1.6897
	cc-pVTZ	94.56	1.6666

-continue-

-continue-

Method	basis set	D_0	r (Å)
	cc-pVQZ	95.44	1.6594
	cc-pV5Z	96.06	1.6541
	cc-pV∞Z[b]	96.49	
	cc-pV(D+d)Z	94.14	1.6760
	cc-pV(T+d)Z	95.66	1.6577
	cc-pV(Q+d)Z	96.14	1.6542
	cc-pV(5+d)Z	96.20	1.6531
	cc-pV∞+Z[b]	96.27	
	aug-cc-pVDZ	92.90	1.6832
	aug-cc-pVTZ	94.77	1.6638
	aug-cc-pVQZ	95.60	1.6581
	aug-cc-pV5Z	96.42	1.6533
	aug-cc-pV∞Z[b]	97.30	
	aug-cc-pV(D+d)Z	94.76	1.6686
	aug-cc-pV(T+d)Z	95.88	1.6549
	aug-cc-pV(Q+d)Z	96.30	1.6530
	aug-cc-pV(5+d)Z	96.55	1.6523
	aug-cc-pV∞+Z[b]	96.68	
B3PW91	cc-pVDZ	94.76	1.6795
	cc-pVTZ	97.39	1.6577
	cc-pVQZ	98.26	1.6521
	cc-pV5Z	98.90	1.6471
	cc-pV∞Z[b]	99.15	
	cc-pV(D+d)Z	96.53	1.6661
	cc-pV(T+d)Z	98.53	1.6498
	cc-pV(Q+d)Z	98.97	1.6471
	cc-pV(5+d)Z	99.05	1.6460
	cc-pV∞+Z[b]	99.08	
	aug-cc-pVDZ	95.62	1.6740
	aug-cc-pVTZ	97.64	1.6556
	aug-cc-pVQZ	98.55	1.6510
	aug-cc-pV5Z	99.18	1.6464
	aug-cc-pV∞Z[b]	99.72	
	aug-cc-pV(D+d)Z	97.54	1.6593
	aug-cc-pV(T+d)Z	98.78	1.6476
	aug-cc-pV(Q+d)Z	99.25	1.6461

-continue-

-continue-

Method	basis set	D_0	r (Å)
	aug-cc-pV(5+d)Z	99.32	1.6453
	aug-cc-pV∞+Z[b]	99.41	

[a] Experimental data were obtained from Reference [46].
[b] Kohn-Sham limits were obtained using the exponential extrapolation scheme (Equation (1))

Table 8.4 Extrapolation of the calculated atomization energy of CCl to the Kohn-Sham limit using several two-parameter extrapolation schemes and the exponential scheme. The atomization energy from experiment is 94.4 kcal/mol.

Method	extrapolation scheme [a]	cc-pVxZ	cc-pV(x+d)Z	aug-cc-pVxZ	aug-cc-pV(x+d)Z
B3LYP	DT	95.46	96.30	95.56	96.35
	DQ	95.87	96.43	95.99	96.52
	D5	96.31	96.34	96.66	96.67
	TQ	96.08	96.49	96.21	96.61
	T5	96.47	96.35	96.87	96.73
	Q5	96.71	96.26	97.28	96.81
	∞	96.49	96.27	97.30	96.68
B3PW91	DT	98.50	99.37	98.49	99.30
	DQ	98.76	99.32	98.97	99.49
	D5	99.18	99.22	99.42	99.44
	TQ	98.89	99.29	99.21	99.59
	T5	99.32	99.19	99.60	99.47
	Q5	99.57	99.13	99.84	99.30
	∞	99.15	99.08	99.72	99.41

[a] DT represents extrapolation using cc-pVDZ and cc-pVTZ, TQ represent extrapolation using cc-pVTZ and cc-pVQZ, . . . ∞ represents the extrapolated Kohn-Sham limit.

8.3.3 ClO_2

The optimized structures for ClO_2 at the quintuple zeta level are in good agreement with experiment. Bond lengths are within 0.01 Å and bond angles are within 0.3°, as shown in Table

8.5. Atomization energies are also listed in Table 8.5. Both impacts of additional diffuse and tight *d* functions on the atomization energy are significant. At the B3LYP/cc-pVDZ level, the augmented set increases the atomization energy by 9.16 kcal/mol, while the tight *d* sets increase the atomization energy by 13.26 kcal/mol. Overall, an increase of 22.42 kcal/mol in energy was obtained by including the tight *d* and diffuse functions in the standard sets. The improvement in energy due to tight *d* and diffuse functions decreases when the basis set size increases. At the quintuple-zeta level, the energy change arising from tight *d* and diffuse functions are reduced to 1.14 kcal/mol and 0.5 kcal/mol, respectively.

Estimated Kohn-Sham limits from the exponential scheme are listed in Table 8.5, and the limits from the two-point extrapolation are listed in Table 8.6. For the Kohn-Sham limits from the exponential scheme, B3LYP overestimates the atomization energy by ~0.5 kcal/mol for all basis sets but aug-cc-pV*x*Z, compared with experiment. B3PW91 overestimates the atomization energy by 4.0-6.0 kcal/mol for all basis sets. For standard sets, the two-point extrapolation scheme results in a large energy fluctuation (~10 kcal/mol) due to the selected two basis sets, but results in a relative small fluctuation (~2 kcal/mol) for the tight *d* sets.

Table 8.5 Atomization energy of ClO_2 (kcal/mol) using B3LYP and B3PW91 in combination with the correlation consistent basis sets.

Method	basis set	D_0	r (Å)	A (°)
Experiment [a]		122.9	1.47	117.6
B3LYP	cc-pVDZ	88.10	1.5405	117.79
	cc-pVTZ	110.74	1.4992	116.97
	cc-pVQZ	116.87	1.4880	117.08
	cc-pV5Z	122.05	1.4780	117.35
	cc-pV∞Z[b]	123.10		

-continue-

-continue-

Method	basis set	D_0	r (Å)	A (°)
	cc-pV(D+d)Z	101.36	1.5036	118.89
	cc-pV(T+d)Z	119.64	1.4797	117.54
	cc-pV(Q+d)Z	122.39	1.4767	117.42
	cc-pV(5+d)Z	123.19	1.4757	117.36
	cc-pV∞+Z[b]	123.15		
	aug-cc-pVDZ	97.26	1.5407	116.80
	aug-cc-pVTZ	112.32	1.4998	116.77
	aug-cc-pVQZ	117.36	1.4881	116.98
	aug-cc-pV5Z	122.55	1.4778	117.31
	aug-cc-pV∞Z[b]	125.23		
	aug-cc-pV(D+d)Z	110.52	1.5058	117.85
	aug-cc-pV(T+d)Z	121.11	1.4803	117.36
	aug-cc-pV(Q+d)Z	122.79	1.4768	117.33
	aug-cc-pV(5+d)Z	123.63	1.4757	117.36
	aug-cc-pV∞+Z[b]	123.53		
B3PW91	cc-pVDZ	91.15	1.5272	117.82
	cc-pVTZ	115.37	1.4892	116.99
	cc-pVQZ	121.50	1.4788	117.11
	cc-pV5Z	126.84	1.4692	117.41
	cc-pV∞Z[b]	127.63		
	cc-pV(D+d)Z	105.11	1.4922	118.85
	cc-pV(T+d)Z	124.61	1.4707	117.54
	cc-pV(Q+d)Z	127.24	1.4679	117.45
	cc-pV(5+d)Z	128.03	1.4668	117.41
	cc-pV∞+Z[b]	127.95		
	aug-cc-pVDZ	101.29	1.5286	116.89
	aug-cc-pVTZ	116.91	1.4898	116.83
	aug-cc-pVQZ	122.07	1.4788	117.04
	aug-cc-pV5Z	127.22	1.4689	117.36
	aug-cc-pV∞Z[b]	129.70		
	aug-cc-pV(D+d)Z	115.23	1.4952	117.89
	aug-cc-pV(T+d)Z	126.05	1.4712	117.40
	aug-cc-pV(Q+d)Z	127.72	1.4679	117.39
	aug-cc-pV(5+d)Z	128.37	1.4668	117.41
	aug-cc-pV∞+Z[b]	128.31		

[a] Experimental data were obtained from Reference [46].

[b] Kohn-Sham limits were obtained using the exponential extrapolation scheme (Equation (1)).

Table 8.6 Extrapolation of the calculated atomization energy of ClO_2 to the Kohn-Sham limit using several two-parameter extrapolation schemes and the exponential scheme. The atomization energy from experiment is 122.9 kcal.mol.

method	extrapolation scheme [a]	cc-pVxZ	cc-pV(x+d)Z	aug-cc-pVxZ	aug-cc-pV(x+d)Z
B3LYP	DT	120.27	127.34	118.66	125.57
	DQ	120.98	125.39	120.23	124.54
	D5	124.37	124.68	124.28	124.53
	DQ	121.34	124.40	121.04	124.02
	T5	125.17	124.17	125.37	124.32
	Q5	127.48	124.03	128.00	124.51
	∞	123.10	123.15	125.23	123.53
B3PW91	DT	125.57	132.82	123.49	130.61
	DQ	125.84	130.40	125.04	129.50
	D5	129.28	129.60	128.99	129.27
	DQ	125.97	129.16	125.84	128.94
	T5	130.00	128.97	130.06	129.01
	Q5	132.44	128.86	132.62	129.05
	∞	127.63	127.95	129.70	128.31

[a] DT represents extrapolation using cc-pVDZ and cc-pVTZ, TQ represent extrapolation using cc-pVTZ and cc-pVQZ, . . . ∞ represents the extrapolated Kohn-Sham limit.

8.4 Conclusions

For the three molecules studied, all show smooth convergence towards a limit as the basis set size increases. The newly developed tight *d* correlation consistent basis sets have a significant impact on the convergence of the structures and energies. This impact decreases with respect to increasing basis set size for both density functionals. Though the rate of convergence is increased, the convergence limits undergoes little change. Substantial improvement due to the tight *d* functions was observed at the double- and triple-zeta levels. The revised tight *d* sets are recommended in future calculations using basis sets no larger than double- and triple-zeta.

CHAPTER 9

THE PERFORMANCE OF DENSITY FUNCTIONALS WITH RESPECT TO BASIS SETS: THE TIGHT *d* EFFECT ON HSO and HOS

9.1 Introduction

The correlation consistent basis sets have been shown in thousands of studies reported in the literature to be important in the high accuracy description of molecular properties and energetics. [15, 47-51, 53-55, 130, 131] One of the early successes of the correlation consistent basis sets was for the HSO and HOS isomers. Prior theoretical studies all had predicted that HOS was the more stable of the two isomers, [132-135] while experiments had predicted the HSO isomer to be more stable. [136, 137] In 1993, Xantheas and Dunning carried out two studies on these species, [138, 139] and by using more advanced methodology (CASSCF) in combination with correlation consistent basis sets of at least triple-zeta quality, correctly predicted HSO to be the more stable isomer. They also found that the HSO-HOS energy difference converged slowly as the basis set size increases, and with small basis sets (cc-pVDZ and cc-pVTZ) they predicted HOS to be the more stable isomer. This observation also shed light on the results of previous computational studies of HSO/HOS, considering that these previous calculations only used small basis sets.

After Xantheas and Dunning's work, a number of additional computational studies on these isomers were carried out. [32, 140-146] All calculations made the correct prediction that HSO is the more stable isomer. In general, a large basis set and a high-level correlated *ab initio* method like MP4, QCISD(T) etc. is needed to result in a correct prediction. However, none of the studies discussed the slow convergence behavior of the HSO/HOS energy difference, even though a similar problem was noted in a study of the enthalpy of formation of HSO by Denis and Ventura using DFT (B3LYP and B3PW91) with the correlation consistent basis sets. [147]

Recently, Wilson and Dunning revisited the HSO and HOS isomers using CCSD(T) with the newly developed tight *d*-augmented correlation consistent basis sets. [119] They found that the correct prediction about the stability of the isomers occurs with lower level basis sets of tight *d*-augmented sets compared to that of the regular sets. The relative energy difference converges more rapidly for tight *d* sets than for regular sets, and the impact of tight *d* sets on the dissociation energy is most significant at the double- and triple-zeta levels.

Another property worthy being mentioned is the enthalpy of formation of HSO. A number of theoretical studies give varied results. Xantheas and Dunning reported a value of –6.1 ± 1.3 kcal/mol by extrapolating the results of MRCI with a series of correlation consistent basis sets. [139] Essefar *et al*. [142] and Marshall *et al* [141] used similar G2 approachs to derive a value of –4.9 ± 1.3 and –4.8 kcal/mol, respectively. Wilson and Hurst predicted a value of –4.8 kcal/mol using modified G2 calculations. [143] Using different theoretical methods, B3LYP and B3PW91, Denis and Ventura determined a value of –6.6 kcal/mol. [147] However, these results are in sharp contrast with the latest experimental results, -3.0 kcal/mol, which was measured in a crossed beam study by Balucani *et al*. [148] More recently, Denis employed the CCSD(T) with aug-cc-pV(*x*+*d*)Z and determined a value of –5.2 ± 0.5 kcal/mol.[125] But, this is still 2.2

kcal/mol away from experimental result. In Denis paper, the difference between the calculation and experiment is attributed to the very elongated transition state of the reaction $O + H_2S \rightarrow H + HSO$, which was used to determine the experimental result.

This chapter covers the second part of the performance of DFT with respect to tight *d* correlation consistent basis sets on the structure and energies of molecules with second row atoms. In this study, we are not focused on the accurate determination of HSO enthalpy of formation. We aim to examine the impact of tight *d* functions on the convergence behavior of HSO/HOS energy difference and enthalpy of formation of HSO in density functional theory. To our knowledge, this is the first density functional benchmark study on the impact of the tight *d* species upon the enthalpies of formation of sulfur species. Two density functionals, B3LYP and B3PW91, with the tight *d* sets are used to determine the relative energies of the two isomers and the enthalpy of formation of HSO for several reactions. By comparing with the results with standard sets, a better understanding of the impact of tight *d* functions on energy and thermodynamic properties are expected.

9.2 Computational Details

Three functionals, B3LYP,[7, 149] B3PW91,[150] and PBE[151, 152] were used in the calculations and were combined with the two new families of correlation consistent basis sets: cc-pV(*x*+*d*)Z and aug-cc-pV(*x*+*d*)Z. For the PBE functional, calculations were also performed using the cc-pV*x*Z and aug-cc-pV*x*Z basis sets. All calculations were performed using the Gaussian 98 and Gaussian 03 program suites.[35, 153]Geometry optimizations and frequency calculations were done for each functional and basis set combination. Zero point energy corrections were taken directly from the frequency calculations without scaling and were

included in the final energies reported. To evaluate the density functional integrals, the default numerical grid (75,302) provided in the Gaussian program was used. This grid includes 75 radial shells and 302 angular points per shell, resulting in approximately 7000 quadrature points per atom. In general, this grid is known to provide energies accurate to five places past the decimal.

The Gaussian 03 program suite was used to determine the vibrational averaged structures and anharmonic frequencies via numerical differentiation along the normal modes.[154-157] Calculations to obtain the anharmonic properties were done for all three density functionals in combination with both the standard and tight *d*-augmented correlation consistent basis sets. The SURFIT program [158] was used to confirm the anharmonic frequencies obtained. For each molecule, a total of 125 points was calculated in a range of $0.4a_o \geq \Delta r \geq -0.4a_o$ and $40^o \geq \theta \geq -40^o$. Spectroscopic parameters were determined from the potential curve generated by these points. The anharmonic frequencies obtained are similar to those determined using Gaussian 03, with slight differences of no more than a few wavenumbers.

Two schemes have been used to extrapolate the energetic results obtained from calculations using a series of the correlation consistent basis sets to the Kohn-Sham limit. The first approach is the exponential scheme:

$$D_e(x) = D_e(\infty) + Ae^{-Bx} \qquad (1)$$

This approach has been used extensively to approximate CBS limits for *ab initio* methods such as HF, MP2, CISD, and CCSD(T) since Feller first introduced the scheme in 1992. [36] More recently, the scheme has been used successfully to approximate Kohn-Sham (KS) limits for a number of density functional methods. [31, 113, 159] Within the extrapolation scheme, *x* is the

cardinal number of the basis set (*i.e.* for cc-pVDZ, x=2; for cc-pVTZ, x=3), $D_e(x)$ represents the energy at the "x" level, and $D_e(\infty)$ represents the extrapolated energy at the CBS limit, or KS limit in the case of DFT. A and B are parameters that are determined in the fit. Using this scheme, at least three data points are necessary. In this study, two exponential fits were used to obtain the KS limits. The first, denoted KS_{DTQ5}, includes four data points, where "D" represents the data obtained using a double-zeta level basis set, "T" represents the triple-zeta level, "Q" represents the quadruple-zeta level, and "5" represents the quintuple-zeta level. The second, denoted KS_{DTQ}, includes results from double-, triple-, and quadruple-zeta level basis sets.

Another commonly used extrapolation scheme is a two-point extrapolation approach introduced by Halkier, *et al.* [37] The formulation is as follows:

$$D_e(\infty) = \frac{\left(D_e(x) \times x^3\right) - \left(D_e(x-1) \times (x-1)^3\right)}{x^3 - (x-1)^3} \qquad (2)$$

For this scheme, three extrapolations were done: KS_{DT}, KS_{TQ}, and KS_{Q5} where "DT" refers to the inclusion of double- and triple-zeta level results in the fit, and, similarly for the other pairings. Again, x represents the cardinal number of the basis set.

9.3 Results and Discussion

9.3.1 Structures of the HSO and HOS Isomers

Optimized structures and vibrationally averaged structures obtained using B3LYP, B3PW91, and PBE in combination with the cc-pV(x+d)Z and aug-cc-pV(x+d)Z basis sets are provided in Tables 9.1 and 9.2. In order to examine the overall impact of the tight d-augmented basis sets, results from Denis and Ventura's earlier study [32] using the standard correlation

consistent basis sets are included in Table 1 for comparison for B3LYP and B3PW91. As shown in the tables, the bond lengths of H-S and S-O for HSO and S-O for HOS converge more rapidly when the tight *d*-augmented basis sets are used than for the standard correlation consistent basis sets. For example, the bond length of S-O in HSO, which experiences the greatest impact, is nearly converged at the cc-pV(T+*d*)Z level, while with the standard basis sets, the bond length does not approach convergence until the cc-pVQZ or cc-pV5Z level. The effect upon the S-H bond length in HSO is minimal, with the greatest difference of 0.004 Å at the double-zeta level for PBE. Additional diffuse functions (aug-cc-pV(*x*+*d*)Z) result in a small difference in the bond lengths as compared with those obtained using the regular tight *d*-augmented basis sets (cc-pV(*x*+*d*)Z), with differences ranging from 0.001-0.007 Å. In general, cc-pV(T+*d*)Z structures are similar to those obtained using the cc-pVQZ or cc-pV5Z basis sets.

Overall, the bond angles are affected very slightly (< 1.0º) by the tight *d* functions, with the greater impact occurring for the smaller basis sets. Interestingly, the HSO bond angle increases for the cc-pV*x*Z series as the basis set size increases, while it decreases for cc-pV(*x*+*d*)Z when the basis set size increases. The opposite trend occurs for the HOS angle.

In comparing B3LYP and B3PW91, both result in nearly identical structures. Both methods are in good agreement with experimental geometries for HSO, [160] with a converged bond distance for S-H in error from experiment by 0.015 Å for B3LYP and for B3PW91, and the S-O bond distance differing by 0.006 Å for B3LYP and in agreement with experiment for B3PW91. The bond angle differs from experiment by ~2.0º. In comparing previous studies shown in Table 9.1, such as work by Wilson and Dunning which used CCSD(T) in combination with regular and tight *d* correlation consistent basis sets, [119] the calculated bond angle of the present study is in near agreement, just slightly below 105º. PBE predicts slightly longer bond

lengths for S-H and S-O, differing by 0.003 Å and 0.018 Å, respectively, from experiment. The bond angle of H-S-O is underestimated by ~1.6º.

The vibrationally averaged structures of HSO and HOS have also been determined and are provided in Table 9.2. When the dynamic correction is considered, the error as compared with experiment for the S-H bond distance is decreased to 0.001 Å for B3LYP and B3PW91, while the error of the S-O bond distance is increased to 0.01 Å for B3LYP and 0.005 Å for B3PW91. The error in the bond angle is decreased to ~1.7º. For PBE, the dynamic correction increases the error of the S-H and S-O bond distances to 0.021 Å and 0.022 Å, respectively, while it decreases the error of the bond angle to ~1.4º.

Table 9.1 Optimized geometries for HSO and HOS. Bond angles are in degrees and bond lengths are in angstroms.

		HSO			HOS		
Method	basis set	r(SH),Å	r(SO),Å	θ(HSO),°	r(SO),Å	r(OH),Å	θ(HOS),°
B3LYP	cc-pVDZ	1.393	1.554	103.91	1.673	0.974	106.92
	cc-pVTZ [a]	1.379	1.518	104.24	1.648	0.967	108.42
	cc-pVQZ [a]	1.376	1.509	104.47	1.642	0.966	108.89
	cc-pV5Z [a]	1.375	1.502	104.60	1.638	0.966	109.20
	cc-pV(D+*d*)Z	1.390	1.527	104.79	1.657	0.974	107.49
	cc-pV(T+*d*)Z	1.376	1.504	104.77	1.640	0.967	108.74
	cc-pV(Q+*d*)Z	1.374	1.502	104.68	1.638	0.966	109.08
	cc-pV(5+*d*)Z	1.374	1.500	104.57	1.637	0.965	109.25
	aug-cc-pV(D+*d*)Z	1.383	1.528	103.93	1.661	0.971	108.60
	aug-cc-pV(T+*d*)Z	1.374	1.505	104.45	1.640	0.967	109.15
	aug-cc-pV(Q+*d*)Z	1.374	1.501	104.50	1.638	0.966	109.25
	aug-cc-pV(5+*d*)Z	1.374	1.500	104.54	1.637	0.966	109.29
B3PW91	cc-pVDZ	1.390	1.546	103.92	1.663	0.973	106.77
	cc-pVTZ [a]	1.378	1.512	104.29	1.639	0.965	108.16

-continue-

-continue-

Method	basis set	HSO			HOS		
		r(SH),Å	r(SO),Å	θ(HSO),°	r(SO),Å	r(OH),Å	θ(HOS),°
	cc-pVQZ [a]	1.376	1.503	104.47	1.633	0.964	108.60
	cc-pV5Z [a]	1.375	1.496	104.69	1.629	0.964	108.88
	cc-pV(D+*d*)Z	1.387	1.520	104.76	1.648	0.973	107.25
	cc-pV(T+*d*)Z	1.376	1.498	104.70	1.630	0.966	108.44
	cc-pV(Q+*d*)Z	1.375	1.495	104.73	1.629	0.965	108.72
	cc-pV(5+*d*)Z	1.374	1.494	104.73	1.628	0.965	108.86
	aug-cc-pV(D+*d*)Z	1.382	1.521	104.10	1.651	0.969	108.29
	aug-cc-pV(T+*d*)Z	1.375	1.500	104.60	1.631	0.966	108.77
	aug-cc-pV(Q+*d*)Z	1.374	1.495	104.67	1.629	0.965	108.86
	aug-cc-pV(5+*d*)Z	1.374	1.494	104.71	1.628	0.965	108.89
PBE	cc-pVDZ	1.412	1.560	104.83	1.687	0.984	105.49
	cc-pVTZ	1.398	1.528	104.79	1.662	0.977	106.97
	cc-pVQZ	1.395	1.520	104.87	1.656	0.976	107.46
	cc-pV5Z	1.393	1.513	105.01	1.652	0.976	107.79
	cc-pV(D+*d*)Z	1.408	1.535	105.59	1.671	0.984	106.08
	cc-pV(T+*d*)Z	1.395	1.515	105.18	1.653	0.977	107.38
	cc-pV(Q+*d*)Z	1.393	1.512	105.08	1.652	0.976	107.65
	cc-pV(5+*d*)Z	1.392	1.512	105.04	1.651	0.976	107.83
	aug-cc-pV(D+*d*)Z	1.399	1.538	104.36	1.674	0.980	107.24
	aug-cc-pV(T+*d*)Z	1.392	1.516	104.87	1.653	0.977	107.81
	aug-cc-pV(Q+*d*)Z	1.392	1.513	104.95	1.652	0.976	107.87
	aug-cc-pV(5+*d*)Z	1.392	1.512	105.00	1.651	0.976	107.89
CASSCF [b]	aug-cc-pVDZ	1.361	1.571	103.40	1.690	0.973	105.50
	cc-pVTZ	1.355	1.528	104.69	1.656	0.969	106.34
	cc-pVQZ	1.354	1.519	104.86	1.650	0.968	106.79
CASSCF+1+2 [b]	cc-pVTZ	1.363	1.518	104.75	1.655	0.965	105.81
	cc-pVQZ	1.361	1.506	104.95	1.645	0.963	106.37
CCSD(T) [c]	cc-pVDZ	1.383	1.559	103.53	1.683	0.972	105.65
	cc-pVTZ	1.371	1.517	104.32	1.648	0.965	106.94
	cc-pVQZ	1.369	1.504	104.47	1.639	0.964	107.82
	cc-pV(D+*d*)Z	1.379	1.532	104.42	1.668	0.972	106.14
	cc-pV(T+*d*)Z	1.369	1.504	104.82	1.641	0.965	107.21
	cc-pV(Q+*d*)Z	1.369	1.498	104.69	1.635	0.964	107.83

-continue-

-continue-

Method	basis set	HSO			HOS		
		r(SH),Å	r(SO),Å	θ(HSO),°	r(SO),Å	r(OH),Å	θ(HOS),°
exp [d]		1.389±	1.494±	106.6±			
		0.005	0.005	0.5			
exp [e]		1.35	1.54	102			

[a] Ref. [32]. [b] Ref. [139] [c] Ref. [119] [d] Ref. [160] [e] Ref. [161].

Table 9.2 Vibrationally averaged geometries for HSO and HOS. Bond angles are in degrees and bond lengths are in angstroms.

method	basis set	HSO			HOS		
		r(SH),Å	r(SO),Å	θ(HSO),°	r(SO),Å	r(OH),Å	θ(HOS),°
B3LYP	cc-pVDZ	1.409	1.559	104.10	1.678	0.985	107.27
	cc-pVTZ	1.395	1.523	104.38	1.653	0.978	108.70
	cc-pVQZ	1.392	1.514	104.58	1.647	0.976	109.16
	cc-pV5Z	1.390	1.506	104.80	1.642	0.976	109.56
	cc-pV(D+*d*)Z	1.405	1.532	105.01	1.663	0.985	107.81
	cc-pV(T+*d*)Z	1.392	1.509	104.95	1.645	0.978	109.01
	cc-pV(Q+*d*)Z	1.391	1.506	104.83	1.643	0.976	109.34
	cc-pV(5+*d*)Z	1.390	1.505	104.85	1.642	0.976	109.52
	aug-cc-pV(D+*d*)Z	1.398	1.533	104.17	1.666	0.982	108.82
	aug-cc-pV(T+*d*)Z	1.390	1.509	104.64	1.646	0.978	109.44
	aug-cc-pV(Q+*d*)Z	1.390	1.505	104.85	1.643	0.977	109.52
	aug-cc-pV(5+*d*)Z	1.390	1.505	104.85	1.642	0.976	109.52
B3PW91	cc-pVDZ	1.406	1.551	104.14	1.653	0.984	107.54
	cc-pVTZ	1.395	1.516	104.47	1.635	0.977	108.68
	cc-pVQZ	1.392	1.507	104.70	1.633	0.975	108.95
	cc-pV5Z	1.390	1.500	104.88	1.633	0.975	109.09
	cc-pV(D+*d*)Z	1.402	1.525	104.93	1.653	0.984	107.52
	cc-pV(T+*d*)Z	1.391	1.503	104.89	1.635	0.977	108.67
	cc-pV(Q+*d*)Z	1.390	1.500	104.93	1.634	0.975	108.95
	cc-pV(5+*d*)Z	1.390	1.499	104.93	1.633	0.975	109.09
	aug-cc-pV(D+*d*)Z	1.397	1.525	104.32	1.656	0.980	108.47
	aug-cc-pV(T+*d*)Z	1.390	1.503	104.79	1.636	0.977	109.00
	aug-cc-pV(Q+*d*)Z	1.390	1.500	104.87	1.633	0.976	109.09
	aug-cc-pV(5+*d*)Z	1.390	1.499	104.91	1.633	0.975	109.13

-continue-

-continue-

		HSO			HOS		
method	basis set	r(SH),Å	r(SO),Å	θ(HSO),°	r(SO),Å	r(OH),Å	θ(HOS),°
PBE	cc-pVDZ	1.431	1.565	105.01	1.692	0.996	105.76
	cc-pVTZ	1.416	1.533	104.98	1.667	0.988	107.19
	cc-pVQZ	1.413	1.524	105.08	1.662	0.987	107.66
	cc-pV5Z	1.410	1.518	105.21	1.657	0.987	108.01
	cc-pV(D+*d*)Z	1.427	1.539	105.77	1.677	0.996	106.34
	cc-pV(T+*d*)Z	1.412	1.520	105.37	1.658	0.988	107.60
	cc-pV(Q+*d*)Z	1.410	1.517	105.29	1.657	0.987	107.86
	cc-pV(5+*d*)Z	1.410	1.516	105.24	1.656	0.987	108.05
	aug-cc-pV(D+*d*)Z	1.416	1.542	104.58	1.679	0.992	107.39
	aug-cc-pV(T+*d*)Z	1.409	1.521	105.06	1.658	0.988	108.03
	aug-cc-pV(Q+*d*)Z	1.409	1.517	105.16	1.657	0.987	108.08
	aug-cc-pV(5+*d*)Z	1.409	1.516	105.20	1.656	0.987	108.10

As shown in Table 9.3, the tight *d*-augmented basis sets result in very little change in the computed vibrational frequencies as compared with the standard correlation consistent basis sets. For example, the frequency corresponding to the S-O stretch of HSO results in a value of 944 cm^{-1} with the cc-pVDZ basis set, while it is 973 cm^{-1} with the cc-pV(D+*d*)Z basis set for B3LYP. The convergence, however, is faster with the tight *d*-augmented basis sets. As shown for the S-O stretch of HSO, the B3LYP/cc-pV5Z frequency is identical to that of the B3LYP/cc-pV(T+*d*)Z frequency (which is essentially converged).

As compared to experiment, the converged B3LYP/cc-pV(*x*+*d*)Z S-O stretch frequencies (generally occurring at the triple-zeta level) are within a few wavenumbers of experiment (1013, 1026 cm^{-1}).[160, 161] For B3PW91, the calculated value of 1033 cm^{-1} is just slightly above the two experimental predictions, whereas PBE predicts a value of 998 cm^{-1}, which is lower than experiment. The H-S-O bend has been calculated as 1092 cm^{-1} (B3LYP/cc-pV(T+*d*)Z) and 1106 cm^{-1} (B3PW91/cc-pV(T+*d*)Z), falling between the experimental frequencies (1063,1164 cm^{-}

[1]),[160, 161] while the PBE/cc-pV(T+*d*)Z result of 1057 cm^{-1} is slightly below the experimental values. For the S-H stretch of HSO, the B3LYP/cc-pV(T+*d*)Z, B3PW91/cc-pV(T+*d*)Z, and PBE/cc-pV(T+*d*)Z predictions of 2408, 2430, and 2301 cm^{-1}, respectively, are within the experimental values (2271, 2570 cm^{-1}).[160, 161] For the anharmonic frequencies reported in Table 9.4, all were decreased by ~10 cm^{1} for the S-O stretch and the H-S-O bend and ~150 cm^{-1} for the S-H stretch as compared with the harmonic frequencies.

Overall, as shown by the comparison of frequencies given in Table 9.3, there is little fluctuation in the values obtained from B3LYP, B3PW91, and CCSD(T).

Table 9.3 Harmonic vibrational frequencies (in cm^{-1}) for HSO and HOS.

method	basis set	HSO			HOS		
		ω_1 (SO str)	ω_2 (HSO bend)	ω_3 (HS str)	ω_1 (SO str)	ω_2 (HOS bend)	ω_3 (OH str)
B3LYP	cc-pVDZ	944	1049	2394	828	1148	3702
	cc-pVTZ [a]	999	1080	2399	841	1176	3746
	cc-pVQZ [a]	1010	1088	2404	841	1174	3746
	cc-pV5Z [a]	1018	1093	2418	842	1170	3749
	cc-pV(D+*d*)Z	973	1068	2388	830	1150	3697
	cc-pV(T+*d*)Z	1018	1092	2408	845	1176	3745
	cc-pV(Q+*d*)Z	1019	1093	2419	843	1173	3747
	cc-pV(5+*d*)Z	1021	1095	2419	842	1169	3750
	aug-cc-pV(D+*d*)Z	977	1066	2426	824	1159	3737
	aug-cc-pV(T+*d*)Z	1016	1092	2424	840	1168	3741
	aug-cc-pV(Q+*d*)Z	1019	1095	2419	841	1168	3746
	aug-cc-pV(5+*d*)Z	1020	1096	2420	841	1169	3750
B3PW91	cc-pVDZ	966	1059	2428	849	1150	3736
	cc-pVTZ [a]	1016	1092	2422	865	1179	3776
	cc-pVQZ [a]	1025	1099	2423	864	1176	3775
	cc-pV5Z [a]	1032	1106	2437	864	1173	3777

-continue-

-continue-

method	basis set	HSO			HOS		
		ω_1 (SO str)	ω_2 (HSO bend)	ω_3 (HS str)	ω_1 (SO str)	ω_2 (HOS bend)	ω_3 (OH str)
	cc-pV(D+*d*)Z	994	1078	2422	851	1153	3728
	cc-pV(T+*d*)Z	1033	1106	2430	867	1181	3770
	cc-pV(Q+*d*)Z	1033	1106	2435	866	1178	3768
	cc-pV(5+*d*)Z	1034	1108	2438	866	1175	3771
	aug-cc-pV(D+*d*)Z	996	1077	2452	846	1164	3762
	aug-cc-pV(T+*d*)Z	1030	1105	2442	864	1174	3764
	aug-cc-pV(Q+*d*)Z	1033	1107	2438	864	1175	3768
	aug-cc-pV(5+*d*)Z	1033	1108	2439	865	1175	3770
PBE	cc-pVDZ	947	1014	2266	800	1102	3574
	cc-pVTZ	984	1045	2295	814	1136	3625
	cc-pVQZ	990	1051	2302	814	1133	3623
	cc-pV5Z	996	1058	2313	815	1130	3625
	cc-pV(D+*d*)Z	973	1032	2272	802	1103	3572
	cc-pV(T+*d*)Z	998	1057	2301	819	1137	3621
	cc-pV(Q+*d*)Z	998	1059	2313	817	1133	3622
	cc-pV(5+*d*)Z	998	1060	2315	816	1130	3625
	aug-cc-pV(D+*d*)Z	963	1031	2329	799	1116	3610
	aug-cc-pV(T+*d*)Z	993	1056	2322	816	1129	3616
	aug-cc-pV(Q+*d*)Z	996	1059	2319	815	1129	3622
	aug-cc-pV(5+*d*)Z	997	1060	2317	815	1129	3624
CASSCF [b]	aug-cc-pVDZ	941	1094	2634	795	1220	3692
	cc-pVTZ	959	1121	2620	820	1230	3723
	cc-pVQZ	939	1115	2651	802	1226	3713
CASSCF+1+2 [b]	cc-pVTZ	1013	1099	2525	844	1220	3806
	cc-pVQZ	966	1078	2620	821	1202	3729
CCSD(T) [c]	cc-pVDZ	918	1054	2464	807	1172	3768
	cc-pVTZ	1008	1089	2452	847	1200	3792
	cc-pV(D+*d*)Z	948	1075	2458	811	1175	3766
	cc-pV(T+*d*)Z	1027	1102	2448	851	1200	3791
exp [d]		1026	1164	2271			
exp [e]		1013	1063	2570			

[a] Ref. [32]. [b] Ref. [139] [c] Ref. [119] [d] Ref. [160] [e] Ref. [161].

Table 9.4 Anharmonic vibrational frequencies (in cm^{-1}) for HSO and HOS.

method	basis set	HSO			HOS		
		ν_1 (SO str)	ν_2 (HSO bend)	ν_3 (HS str)	ν_1 (SO str)	ν_2 (HOS bend)	ν_3 (OH str)
B3LYP	cc-pVDZ	929	1028	2218	815	1123	3501
	cc-pVTZ	985	1062	2254	829	1146	3551
	cc-pVQZ	996	1071	2271	828	1138	3549
	cc-pV5Z	1008	1079	2283	832	1133	3549
	cc-pV(D+*d*)Z	956	1048	2223	818	1123	3496
	cc-pV(T+*d*)Z	1003	1075	2263	833	1145	3547
	cc-pV(Q+*d*)Z	1007	1078	2279	832	1137	3549
	cc-pV(5+*d*)Z	1010	1080	2286	831	1133	3551
	aug-cc-pV(D+*d*)Z	965	1050	2275	811	1128	3533
	aug-cc-pV(T+*d*)Z	1003	1076	2283	829	1137	3543
	aug-cc-pV(Q+*d*)Z	1009	1079	2284	830	1132	3547
	aug-cc-pV(5+*d*)Z	1009	1080	2287	830	1132	3552
B3PW91	cc-pVDZ	954	1045	2251	871	1135	3532
	cc-pVTZ	1006	1078	2270	872	1154	3574
	cc-pVQZ	1016	1085	2284	862	1145	3573
	cc-pV5Z	1027	1094	2297	856	1140	3574
	cc-pV(D+*d*)Z	981	1065	2251	838	1129	3533
	cc-pV(T+*d*)Z	1023	1092	2285	856	1150	3574
	cc-pV(Q+*d*)Z	1026	1093	2297	855	1143	3573
	cc-pV(5+*d*)Z	1028	1095	2300	854	1140	3575
	aug-cc-pV(D+*d*)Z	988	1065	2295	833	1132	3562
	aug-cc-pV(T+*d*)Z	1021	1091	2301	853	1143	3568
	aug-cc-pV(Q+*d*)Z	1025	1093	2302	853	1139	3571
	aug-cc-pV(5+*d*)Z	1028	1095	2302	853	1139	3573
PBE	cc-pVDZ	929	991	2067	784	1084	3368
	cc-pVTZ	963	1025	2091	799	1110	3421
	cc-pVQZ	973	1033	2097	798	1105	3415
	cc-pV5Z	981	1041	2104	800	1099	3413
	cc-pV(D+*d*)Z	949	1004	2059	786	1084	3362
	cc-pV(T+*d*)Z	975	1037	2095	805	1110	3412
	cc-pV(Q+*d*)Z	981	1041	2106	801	1103	3412
	cc-pV(5+*d*)Z	982	1043	2105	800	1099	3412

-continue-

-continue-

method	basis set	HSO			HOS		
		ν_1 (SO str)	ν_2 (HSO bend)	ν_3 (HS str)	ν_1 (SO str)	ν_2 (HOS bend)	ν_3 (OH str)
	aug-cc-pV(D+*d*)Z	950	1015	2116	783	1090	3398
	aug-cc-pV(T+*d*)Z	975	1038	2119	801	1101	3407
	aug-cc-pV(Q+*d*)Z	980	1041	2114	800	1098	3409
	aug-cc-pV(5+*d*)Z	982	1043	2108	800	1098	3411

9.3.3 Relative Energies of HSO and HOS

In Table 9.5, relative energy differences between the HSO and HOS isomers calculated with B3LYP, B3PW91, and PBE in combination with the cc-pV(*x*+*d*)Z and aug-cc-pV(*x*+*d*)Z basis set series are provided. Additionally, for comparison, previous B3LYP and B3PW91 results of Dennis and Ventura, [32] CASSCF results of Xantheas and Dunning, [139] and CCSD(T) results of Wilson and Dunning, [119] have been given.

For the zero-point corrected relative energy, ΔE_o, B3LYP, B3PW91, and PBE incorrectly predict that HOS is the more stable isomer when a cc-pVDZ basis set is used. Using a cc-pVTZ basis set or larger results in the prediction that HSO is the more stable isomer. Combining these methods with a cc-pV(*x*+*d*)Z level of basis sets results in the correct prediction, even at the double-zeta level, that HSO is the more stable isomer. In earlier work by Wilson and Dunning with CCSD(T), even the tight *d*-augmented sets did not result in the correct qualitative picture at the double-zeta level.

The tight *d* functions have a significant impact on the small basis sets, in particular. For example, B3LYP/cc-pVDZ yields an ΔE_o of –2.41 kcal/mol, while cc-pV(D+*d*)Z results in 1.36 kcal/mol – an energy difference of 3.77 kcal/mol, which also results in a change in qualitative picture. The diffuse functions (aug-cc-pV(*x*+*d*)Z) increase this difference by another 1.29 kcal/mol to an ΔE_o of 2.65 kcal/mol. For the larger basis sets, the differences are less

pronounced with differences of 1.41 kcal/mol between B3LYP/cc-pVQZ (ΔE_o of 3.20 kcal/mol) and B3LYP/cc-pV(Q+*d*)Z (ΔE_o of 4.61 kcal/mol) and 0.28 kcal/mol between B3LYP/cc-pV5Z (ΔE_o of 4.64 kcal/mol) and B3LYP/cc-pV(5+*d*)Z (ΔE_o of 4.92 kcal/mol).

The tight *d*-augmented sets result in much faster convergence towards a limit, as shown in Table 9.5. For B3LYP, the difference in the ΔE_o obtained occurring between the cc-pVQZ (3.20 kcal/mol) and cc-pV5Z (4.64 kcal/mol) basis sets is still 1.44 kcal/mol (31% of the cc-pV5Z ΔE_o), where the tight *d*-augmented sets result in a difference in the ΔE_o of only 0.31 kcal/mol (6% of the cc-pV(5+*d*)Z ΔE_o), between the cc-pV(Q+*d*)Z (4.61 kcal/mol) and cc-pV(5+*d*)Z (4.92 kcal/mol) basis sets. The B3PW91 and PBE results are very similar to these B3LYP results. In comparing previous results, similar improvement in convergence behavior is noted for CCSD(T) in combination with the correlation consistent basis sets, [119] though with overall slower convergence (49% and 17% using the types of comparisons discussed above).

Our best results for ΔE_o, 5.59 kcal/mol for B3PW91/aug-cc-pV(5+*d*)Z and 4.98 kcal/mol for B3LYP/aug-cc-pV(5+*d*)Z can be compared with the CASSCF+1+2 and then extrapolated result of 5.4 kcal/mol by Xantheas and Dunning. [139] PBE/aug-cc-pV(5+*d*) provides an ΔE_o of 6.99 kcal/mol, which is 1.59 kcal/mol larger than the CASSCF+1+2. A more recent theoretical ΔE_o has been reported by Wilson and Dunning using CCSD(T) with the tight *d*-augmented sets. [119] They reported a CBS limit of 4.2 kcal/mol, which is 1.2 kcal/mol lower than that estimated by Xantheas and Dunning and is 1.7 kcal/mol higher than that (2.5 kcal/mol) determined by Esseffar using QCISD(T)/6-311+G(5*d*2*f*, 2*p*). [142] In contrasting these methods, DFT may not be an ideal choice of methodology due to the multi-reference character of HSO. However, the current results are comparable with a number of previous results using advanced *ab initio* methods. [119, 138, 142]

As discussed in Section 9.2, several extrapolation methods have been used to estimate Kohn-Sham limits for ΔE_o, and the results are listed in Table 9.6. For the standard correlation consistent basis sets, the KS limits are inconsistent, depending highly upon the extrapolation scheme chosen. When the tight *d*-augmented sets are used, the KS limits show much less dependence upon the extrapolation scheme. The largest deviation occurs for the KS_{DT} extrapolation, which is to be expected. Similar KS limits are obtained whether the exponential KS_{DTQ5} or KS_{DTQ} fits, or the two-point KS_{TQ} fit are used. The KS limits from the KS_{Q5} fit are slightly (~0.2-0.5 kcal/mol) higher than those obtained using the KS_{DTQ5}, KS_{DTQ}, and KS_{TQ} extrapolation schemes. As compared with the CBS limits of 5.41 and 5.42 kcal/mol for CASSCF and CASSCF+1+2, respectively, reported by Xantheas and Dunning, the B3PW91 KS_{DTQ5}, KS_{DTQ}, and KS_{TQ} limits for aug-cc-pV(*x*+*d*)Z are in good agreement (5.54, 5.45, and 5.55 kcal/mol), while B3LYP underestimates (4.94, 4.86, and 4.97 kcal/mol) them. The KS limits for PBE overestimate these previous results. However, all of the KS limits greatly overestimate the CBS limit of 4.2 kcal/mol predicted using CCSD(T).

In Figure 9.1, the calculated ΔE_o for B3PW91 with respect to cc-pV(*x*+*d*)Z and aug-cc-pV(*x*+*d*)Z basis sets is shown. Included in this figure are previous cc-pV*x*Z results from Denis and Ventura. [32] The tight *d* functions greatly improved the convergence behavior with respect to increasing basis set as shown.

Table 9.5 Energy differences (with respect to HSO) of HSO and HOS. ΔE_e represents the energy difference without including the zero point correction while ΔE_o represents the energy difference including the zero point correction. A positive value indicates that the HSO isomer is more stable.

method	basis set	ΔE_e(HOS-HSO) kcal/mol	ΔE_o(HOS-HSO) kcal/mol
B3LYP	cc-pVDZ	-4.25	-2.41
	cc-pVTZ [a]	-0.26	1.55
	cc-pVQZ [a]	1.41	3.20
	cc-pV5Z [a]	2.87	4.64
	cc-pV(D+*d*)Z	-0.42	1.36
	cc-pV(T+*d*)Z	2.21	3.99
	cc-pV(Q+*d*)Z	2.85	4.61
	cc-pV(5+*d*)Z	3.17	4.92
	aug-cc-pV(D+*d*)Z	0.86	2.65
	aug-cc-pV(T+*d*)Z	2.92	4.66
	aug-cc-pV(Q+*d*)Z	3.09	4.84
	aug-cc-pV(5+*d*)Z	3.23	4.98
B3PW91	cc-pVDZ	-3.65	-1.82
	cc-pVTZ [a]	-0.41	2.34
	cc-pVQZ [a]	2.01	3.82
	cc-pV5Z [a]	3.47	5.23
	cc-pV(D+*d*)Z	0.24	2.01
	cc-pV(T+*d*)Z	2.90	4.68
	cc-pV(Q+*d*)Z	3.48	5.24
	cc-pV(5+*d*)Z	3.78	5.54
	aug-cc-pV(D+*d*)Z	1.66	3.44
	aug-cc-pV(T+*d*)Z	3.52	5.27
	aug-cc-pV(Q+*d*)Z	3.67	5.43
	aug-cc-pV(5+*d*)Z	3.83	5.59
PBE	cc-pVDZ	-1.94	-0.15
	cc-pVTZ	1.77	3.56
	cc-pVQZ	3.38	5.14
	cc-pV5Z	4.90	6.62

-continue-

-continue-

method	basis set	ΔE_e(HOS-HSO) kcal/mol	ΔE_o(HOS-HSO) kcal/mol
	cc-pV(D+*d*)Z	1.88	3.59
	cc-pV(T+*d*)Z	4.20	5.95
	cc-pV(Q+*d*)Z	4.83	6.55
	cc-pV(5+*d*)Z	5.21	6.92
	aug-cc-pV(D+*d*)Z	3.39	5.11
	aug-cc-pV(T+*d*)Z	4.98	6.68
	aug-cc-pV(Q+*d*)Z	5.13	6.83
	aug-cc-pV(5+*d*)Z	5.28	6.99
CASSCF [b]	aug-cc-pVDZ	-3.3	-1.9
	cc-pVTZ	0.4	1.9
	cc-pVQZ	2.2	3.7
	cc-pV5Z	3.1	4.6
	CBS limit [c]		5.41
CASSCF+1+2 [b]	aug-cc-pVDZ	-4.4	-3.0
	cc-pVTZ	-0.8	1.0
	cc-pVQZ	1.5	3.1
	cc-pV5Z	2.6	4.2
	CBS limit [c]		5.42
CCSD(T) [d]	cc-pVDZ	-6.37	-4.49
	cc-pVTZ	-2.26	-0.41
	cc-pVQZ	-0.15	1.70
	cc-pV5Z	1.49	3.34
	cc-pV(D+*d*)Z	-2.76	-0.95
	cc-pV(T+*d*)Z	0.01	1.82
	cc-pV(Q+*d*)Z	1.16	2.97
	cc-pV(5+*d*)Z	1.76	3.57
	CBS limit	2.4	4.2

[a] Ref. [32] [b] Ref. [139] [c] A cc-pVQZ geometry was used. [d] Ref. [119].

Table 9.6 Kohn-Sham limits of the energy differences (with respect to HSO) of HSO and HOS. ΔE_o represents the energy difference including zero point correction. A positive value indicates that the HSO isomer is more stable than HOS.

Method	Extrapolation	ΔE_o(HOS-HSO) kcal/mol		
		cc-pVxZ	cc-pV(*x*+*d*)Z	aug-cc-pV(*x*+*d*)Z
B3LYP	KS_{DTQ5}	5.81	4.95	4.94
	KS_{DTQ}	4.38	4.80	4.86
	KS_{DT}	3.22	5.70	6.15
	KS_{TQ}	4.40	5.06	4.97
	KS_{Q5}	6.15	5.25	5.13
B3PW91	KS_{DTQ5}	6.04	5.55	5.54
	KS_{DTQ}	4.64	5.39	5.45
	KS_{DT}	4.09	6.49	6.75
	KS_{TQ}	4.90	5.65	5.55
	KS_{Q5}	6.71	5.85	5.76
PBE	KS_{DTQ5}	7.97	6.97	6.94
	KS_{DTQ}	6.31	6.75	6.85
	KS_{DT}	5.12	7.76	8.20
	KS_{TQ}	4.55	6.99	6.94
	KS_{Q5}	6.49	7.31	7.16

Figure 9.1 Relative energies of the HSO and HOS isomers obtained from B3PW91 calculations with the cc-pV(*x*+d)Z and aug-cc-pV(*x*+d)Z basis sets. cc-pV*x*Z results from Denis and Ventura**[32]** (represented by the □ - though the cc-pVDZ result is from the present study) have been included for comparison.

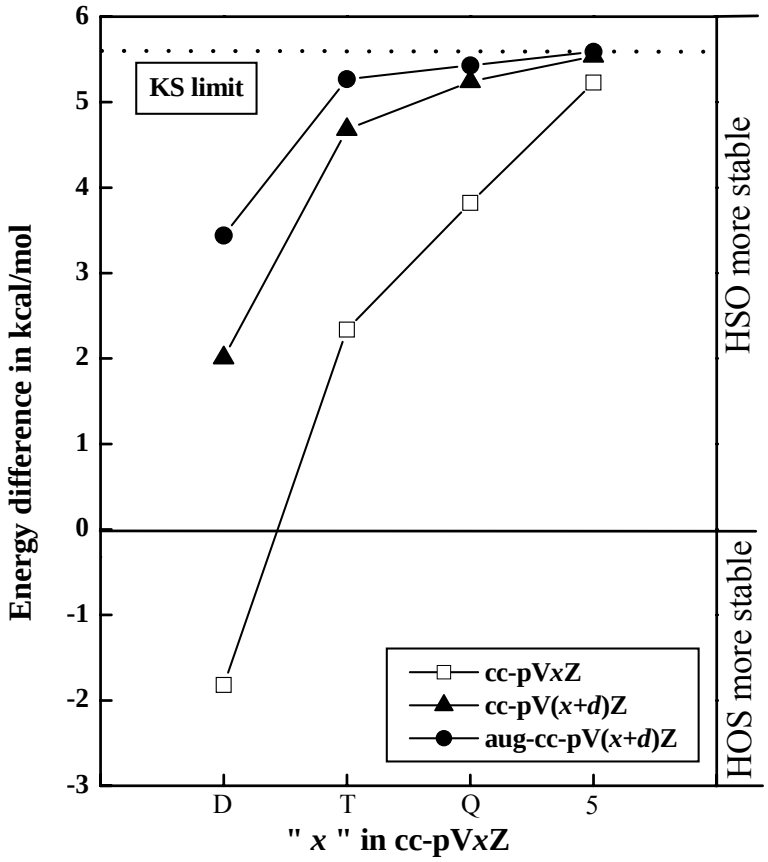

9.3.4 Enthalpy of Formation of HSO

For purposes of this study, our interest in examining the enthalpy of formation is in order to assess the potential impact of the tight *d* functions upon calculated enthalpies of formation, rather than provide a recommended route or full discussion of possible means to determine the enthalpy of formation. We have simply selected a series of reactions used (and discussed fully) in previous work, most notably the work by Denis and Ventura using B3LYP and B3PW91 in combination with the cc-pV*x*Z basis sets, [32] as this provides us with a means for comparison for the tight *d*-augmented basis sets.

The seven reactions evaluated include the following:

$$H_2S + SO \rightarrow HSO + HS \quad [1]$$

$$H + SO \rightarrow HSO \quad [2]$$

$$H_2 + 2SO \rightarrow 2HSO \quad [3]$$

$$HS + O \rightarrow HSO \quad [4]$$

$$2HS + O_2 \rightarrow 2HSO \quad [5]$$

$$H + S + O \rightarrow HSO \quad [6]$$

$$H_2 + 2S + O_2 \rightarrow 2HSO \quad [7]$$

In Table 9.7, the HSO enthalpy of formation determined for each reaction, method, and basis set combination is reported, along with results from previous calculations. For each combination, the enthalpy of formation has been determined by combining enthalpies of reaction with accurately known enthalpies of formation.

Reactions [4] through [7] are more greatly impacted by the tight *d*-augmented basis sets than reactions [1] through [3]. For example, at the aug-cc-pVDZ level, the tight *d* set results in an overall reduction of the enthalpies of formation of 5 kcal/mol (or greater), as well as a change

in sign of the enthalpy (in all cases but reaction [5]). In reaction [6] with B3LYP, tight *d* functions result in reduction of the enthalpy of formation by 6.27, 3.86, 2.3 and 0.51 kcal/mol energy at the aug-cc-pVDZ, cc-pVTZ, cc-pVQZ, and cc-pV5Z levels, respectively. Overall, at the quadruple-zeta level, for reactions [4] through [7], the tight *d* set results in a reduction of ~2-3 kcal/mol in the enthalpy. This marks a change in the value of cc-pVQZ relative to cc-pV(Q+*d*)Z of 48%, 70%, 36%, and 57% for reactions [4], [5], [6], and [7], respectively.

Reactions [1] through [3] are not impacted as significantly by the tight *d* functions. At the B3LYP/aug-cc-pVDZ level, the tight *d* drops the enthalpy of formation determined by reaction [1] by only 0.17 kcal/mol. The changes for reactions [2] and [3] are slightly higher, with differences of 1.37 and 1.33 kcal/mol, respectively. At the quadruple-zeta level, the impact of the tight *d* function is reduced to 0.06, 0.58, and 0.54 kcal/mol for reactions [1], [2], and [3]. As compared with the cc-pV(Q+*d*)Z enthalpy of formation, this marks percentage differences of 1%, 13%, and 13% for the three reactions, indicating the smaller impact of the tight *d* functions.

Though the tight *d* functions do have an impact upon the overall convergence rate of the enthalpy of formation and also can have a dramatic impact upon the value of the enthalpy when lower level basis sets (through quadruple-zeta for reactions [4] through [7]) are used, at the quintuple-zeta level, the conclusions reached in the earlier study by Denis and Ventura regarding the magnitude of enthalpies of formation calculated via reactions [1] through [7] remain the same. The calculated enthalpies of formation overall result in two different ranges of values. From reactions [1], [4], and [6], B3LYP/aug-cc-pV(5+*d*)Z values of –6.29, -6.36, and –7.06 kcal/mol emerge, while for reactions [2], [3], [5], and [7], values of –4.83, -4.42, -4.49, and -4.73 kcal/mol result. For B3PW91, all predicted enthalpies of formation fall in three ranges, ~-4

kcal/mol for reaction [2] and [5], ~-6 kcal/mol for reaction [1], [3] and [7] and ~-7 kcal/mol for reaction [4] and [6]. Interestingly, the enthalpies of formation determined using PBE differ

Table 9.7 Estimated enthalpies of formation for HSO in kcal/mol.

method/ basis set	reaction [1] $H_2S+SO \rightarrow$ HSO+HS	reaction [2] $H+SO \rightarrow$ HSO	reaction [3] $H_2+2SO \rightarrow$ 2HSO	reaction [4] $HS+O \rightarrow$ HSO	reaction [5] $2HS+O_2 \rightarrow$ 2HSO	reaction [6] $H+S+O \rightarrow$ HSO	reaction [7] $H_2+2S+O_2 \rightarrow$ 2HSO
B3LYP/							
aug-cc-pVDZ [a]	-6.05	-2.39	-3.59	5.33	6.48	6.00	5.98
cc-pVTZ [a]	-5.43	-3.04	-2.70	-0.41	1.31	-1.00	1.05
cc-pVQZ [a]	-5.98	-3.97	-3.59	-3.06	-1.17	-4.13	-1.74
cc-pV5Z [a]	-6.38	-4.61	-4.23	-5.02	-3.23	-6.38	-4.21
cc-pV(D+*d*)Z	-4.50	-1.71	-2.75	3.48	5.14	4.64	5.31
cc-pV(T+*d*)Z	-5.62	-3.99	-3.63	-4.49	-2.76	-4.86	-2.72
cc-pV(Q+*d*)Z	-6.04	-4.55	-4.13	-5.84	-3.95	-6.43	-4.08
cc-pV(5+*d*)Z	-6.23	-4.75	-4.34	-6.26	-4.47	-6.89	-4.64
aug-cc-pV(D+*d*)Z	-6.22	-3.76	-4.92	-0.64	0.51	-0.27	-0.22
aug-cc-pV(T+*d*)Z	-6.25	-4.67	-4.36	-5.35	-3.92	-6.00	-4.21
aug-cc-pV(Q+*d*)Z	-6.27	-4.78	-4.39	-6.12	-4.27	-6.84	-4.56
aug-cc-pV(5+*d*)Z	-6.29	-4.83	-4.42	-6.36	-4.49	-7.06	-4.73
B3PW91/							
aug-cc-pVDZ [a]	-5.81		-4.54	4.25	6.02		4.90
cc-pVTZ [a]	-5.26		-3.92	-1.53	0.81		-0.24
cc-pVQZ [a]	-5.76		-4.68	-4.13	-1.58		-2.99
cc-pV5Z [a]	-6.12		-5.28	-6.09	-3.61		-5.31
cc-pV(D+*d*)Z	-4.41	-1.70	-3.88	2.80	4.63	4.47	4.10
cc-pV(T+*d*)Z	-5.46	-3.71	-4.82	-5.66	-3.31	-5.34	-4.10
cc-pV(Q+*d*)Z	-5.84	-4.16	-5.22	-6.95	-4.39	-6.79	-5.30
cc-pV(5+*d*)Z	-5.99	-4.33	-5.40	-7.36	-4.87	-7.24	-5.82
aug-cc-pV(D+*d*)Z	-6.01	-3.58	-5.88	-1.84	-0.08	-0.85	-1.39
aug-cc-pV(T+*d*)Z	-5.98	-4.26	-5.41	-6.52	-4.37	-6.37	-5.38
aug-cc-pV(Q+*d*)Z	-6.01	-4.34	-5.42	-7.19	-4.66	-7.08	-5.64

-continue-

-continue-

method/ basis set	reaction [1] $H_2S+SO \rightarrow HSO+HS$	reaction [2] $H+SO \rightarrow HSO$	reaction [3] $H_2+2SO \rightarrow 2HSO$	reaction [4] $HS+O \rightarrow HSO$	reaction [5] $2HS+O_2 \rightarrow 2HSO$	reaction [6] $H+S+O \rightarrow HSO$	reaction [7] $H_2+2S+O_2 \rightarrow 2HSO$
aug-cc-pV(5+*d*)Z PBE/	-6.04	-4.40	-5.46	-7.44	-4.88	-7.36	-5.88
cc-pVDZ	-2.39	0.56	-2.91	-6.54	5.75	-4.74	4.08
cc-pVTZ	-3.81	-2.12	-4.44	-15.33	-3.30	-15.11	-5.40
cc-pVQZ	-4.46	-3.02	-5.35	-17.75	-5.70	-17.90	-8.18
cc-pV5Z	-4.93	-3.72	-6.07	-19.58	-7.72	-19.99	-10.50
cc-pV(D+*d*)Z	-3.03	-1.00	-4.46	-11.33	0.96	-10.47	-1.65
cc-pV(T+*d*)Z	-4.31	-3.12	-5.44	-18.47	-6.44	-18.79	-9.08
cc-pV(Q+*d*)Z	-4.77	-3.62	-5.95	-19.66	-7.61	-20.12	-10.40
cc-pV(5+*d*)Z	-4.98	-3.83	-6.18	-19.96	-8.10	-20.45	-10.95
aug-cc-pV(D+*d*)Z	-4.85	-3.05	-6.73	-15.15	-3.80	-14.88	-7.21
aug-cc-pV(T+*d*)Z	-4.96	-3.77	-6.19	-19.14	-7.61	-19.61	-10.52
aug-cc-pV(Q+*d*)Z	-5.01	-3.86	-6.23	-19.83	-7.93	-20.34	-10.82
aug-cc-pV(5+*d*)Z	-5.05	-3.92	-6.28	-20.04	-8.12	-20.57	-11.03
QCISD(T)/6-311++G(5d2f,2p)[b]	-4.71	-4.71		-4.40		-4.30	
CASSCF+1+2/cc-pV5Z [c]		-4.11					
CASSCF+1+2/CBS limit [c]		-4.21					
CI/CBS limit [c]		-5.40					
G2 [b]	-5.40	-5.62		-3.11		-3.01	
G2* [b]	-5.62	-5.90		-2.51		-2.41	
G2** [d]	-5.40	-5.90		-5.90		-4.57	
Experimental	$\Delta_{H^o_{f,o}}$						
Exp. [e]	14.9						
Exp. [f]	-3.0						
Exp. [g]	-1.4 ± 2.0						
Exp. [h]	-1.6 ± 0.7						
Exp. [i]	< -3.7						

[a] Ref. [32]. [b] Ref. [142]. [c] Ref. [139]. [d] Ref. [143]. [e] Ref. [160]. [f] Ref. [136]. [g] Ref. [162] [h] Ref. [163] [i] Ref. [148]

substantially, based upon the reaction used in the determination. A very large enthalpy of formation (~-20 kcal/mol) is obtained based upon reactions [4] and [6], while reactions [1] and [2] result in similar enthalpies as those determined by B3PW91. These values are not surprising, as PBE has been shown to perform poorly in predicting thermochemical data, including enthalpies of formation, for a large range of molecular systems. [164, 165] Xantheas and Dunning suggest a value of –4.2 kcal/mol based upon their CASSCF results, which were obtained using the standard correlation consistent basis sets. [138] Esseffar also suggests a value of –4.2 kcal/mol, using QCISD(T). [142] Recently, Denis determined a value of –5.2 kcal/mol using CCSD(T) with the aug-cc-pV(*x*+*d*)Z basis sets. [125] All above theoretical results are larger than a recently experimental enthalpy of formation (-3.0 kcal/mol) by Balucani. [148]

9.3.5 Reaction barrier to HSO→ HOS

In a previous study, CASSCF+1+2 was used in combination with cc-pVTZ and cc-pVQZ to determine the reaction barrier for the HSO/HOS isomerization. [138] A substantial barrier was observed, which helps to explain why only HSO has been observed experimentally. In this study, DFT was used with the standard and tight *d*-augmented correlation consistent basis sets in order to assess the usefulness and impact of DFT and tight *d* functions in determining the barrier to isomerization, which is reported in Table 9.8. Additionally, the structure and harmonic frequencies for the transition state are shown in Table 8, and are compared with previous CASSCF+1+2 calculations.

The tight *d*-augmented functions have an expected effect upon the barrier to isomerization – convergence in the barrier occurs more quickly than for the standard basis sets. For all three functionals, the barrier has nearly reached convergence at the quadruple-zeta level when the tight *d*-augmented sets are used, whereas this does not occur until the quintuple-zeta

level for the standard basis sets. The bond S-O and H-S bond distances determined for the transition state are slightly longer than those shown by CASSCF+1+2/cc-pVQZ. The bond angle is ~1-2^{o} larger using DFT.

Table 9.8 Structure of the transition state and the barrier for the HSO → HOS isomerization with respect to HSO.

method	basis set	R (S-O) Å	R (H-S) Å	Φ (H-S-O) deg	ΔE kcal/mol
B3LYP	cc-pVDZ	1.703	1.435	51.03	40.77
	cc-pVTZ	1.665	1.435	50.99	45.59
	cc-pVQZ	1.657	1.437	50.89	46.93
	cc-pV5Z	1.650	1.438	50.84	48.00
	cc-pV(D+*d)*Z	1.684	1.432	51.04	43.83
	cc-pV(T+*d)*Z	1.655	1.434	50.96	47.52
	cc-pV(Q+*d)*Z	1.651	1.436	50.88	48.02
	cc-pV(5+*d)*Z	1.649	1.438	50.83	48.22
	aug-cc-pV(D+*d)*Z	1.678	1.447	50.59	45.06
	aug-cc-pV(T+*d)*Z	1.653	1.439	50.78	47.71
	aug-cc-pV(Q+*d)*Z	1.650	1.438	50.81	48.05
	aug-cc-pV(5+*d)*Z	1.649	1.438	50.81	48.22
B3PW91	cc-pVDZ	1.689	1.429	51.40	40.46
	cc-pVTZ	1.653	1.429	51.32	45.00
	cc-pVQZ	1.645	1.431	51.22	46.23
	cc-pV5Z	1.639	1.431	51.16	47.26
	cc-pV(D+*d)*Z	1.672	1.426	51.41	43.52
	cc-pV(T+*d)*Z	1.643	1.428	51.28	46.90
	cc-pV(Q+*d)*Z	1.639	1.430	51.19	47.31
	cc-pV(5+*d)*Z	1.638	1.431	51.15	47.49
	aug-cc-pV(D+*d)*Z	1.666	1.440	50.89	44.58
	aug-cc-pV(T+*d)*Z	1.641	1.432	51.11	46.99
	aug-cc-pV(Q+*d)*Z	1.639	1.432	51.13	47.31
	aug-cc-pV(5+*d)*Z	1.638	1.432	51.13	47.49
PBE	cc-pVDZ	1.716	1.436	52.11	35.26
	cc-pVTZ	1.681	1.440	51.51	39.78
	cc-pVQZ	1.674	1.442	51.31	41.04
	cc-pV5Z	1.669	1.443	51.15	42.12

-continue-

-continue-

method	basis set	R (S-O) Å	R (H-S) Å	Φ (H-S-O) deg	ΔE kcal/mol
	cc-pV(D+*d)*Z	1.700	1.434	51.96	38.20
	cc-pV(T+*d)*Z	1.672	1.439	51.42	41.64
	cc-pV(Q+*d)*Z	1.668	1.441	51.24	42.12
	cc-pV(5+*d)*Z	1.667	1.443	51.13	42.34
	aug-cc-pV(D+*d)*Z	1.694	1.452	50.94	39.61
	aug-cc-pV(T+*d)*Z	1.670	1.444	51.07	41.90
	aug-cc-pV(Q+*d)*Z	1.668	1.444	51.09	42.20
	aug-cc-pV(5+*d)*Z	1.667	1.444	51.09	42.37
CASSCF+1+2 [a]	cc-pVTZ	1.677	1.355	54.92	44.5
	cc-pVQZ	1.630	1.426	49.88	46.3

[a] Ref. [139].

9.3.6 Spectroscopic Constants for the HSO

Tables 9.9, 9.10, and 9.11 list calculated spectroscopic constants for HSO including rotational constants, anharmonicity constants, and rotational-vibrational coupling. The results were calculated using three density functionals in combination with cc-pV*x*Z, cc-pV(*x*+*d*)Z, and aug-cc-pV(*x*+*d*)Z. Though experimental spectroscopic constants for HSO are not available to date, in this section, we aim to investigate the effect of tight *d* sets on the calculated DFT spectroscopic constants.

As expected, tight *d* sets have an impact on almost all of the spectroscopic constants. The impact is greatest at the double- and triple-zeta levels. For example, the B3PW91/cc-pVDZ and B3PW91/cc-pV(D+*d*)Z results for A_e differ by 0.13 cm^{-1}. The difference decreases to 0.1 cm^{-1} at the triple zeta level, 0.05 cm^{-1} at the quadruple zeta level , and 0.02 cm^{-1} at the quintuple zeta level. Comparision of the results from cc-pV(*x*+*d*)Z and aug-cc-pV(*x*+*d*)Z shows that the addition of extra diffuse functions contributes little to the spectroscopic constants of HSO. As for the other properties described above, B3LYP and B3PW91 result in similar performance in

determining the spectroscopic constants of HSO. However, PBE results are quite different particularly for the anharmonicity constants, as compared with B3LYP and B3PW91.

Table 9.9 Calculated spectroscopic constants for HSO using B3LYP in combination with cc-pV*x*Z, cc-pV(*x*+*d*)Z, and aug-cc-pV(*x*+*d*)Z.

	cc-pV*x*Z				cc-pV(*x*+*d*)Z				aug-cc-pV(*x*+*d*)Z			
B3LYP	D	T	Q	5	D	T	Q	5	D	T	Q	5
X_{11}	-85.5	-75.6	-69.8	-68.7	-83.3	-72.1	-68.4	-67.8	-78.8	-70.3	-67.6	-67.9
X_{12}	-15.7	-9.7	-6.8	-4.2	-13.3	-7.0	-5.4	-3.8	-9.1	-6.5	-5.3	-3.9
X_{13}	7.5	6.6	7.9	9.4	7.5	6.7	8.1	9.5	7.7	6.8	8.2	9.5
X_{22}	-3.8	-3.6	-3.6	-3.4	-3.4	-3.7	-3.6	-3.4	-3.2	-3.6	-3.6	-3.4
X_{23}	-11.2	-12.4	-12.7	-11.4	-11.0	-12.9	-12.6	-11.3	-10.4	-12.3	-12.6	-11.2
X_{33}	-6.5	-5.8	-5.6	-5.0	-6.9	-5.7	-5.4	-5.0	-5.3	-5.3	-5.3	-4.9
A_e	9.62	9.84	9.91	9.95	9.77	9.95	9.96	9.97	9.76	9.95	9.96	9.96
B_e	0.64	0.67	0.67	0.68	0.66	0.68	0.68	0.68	0.66	0.68	0.68	0.68
C_e	0.60	0.62	0.63	0.64	0.62	0.63	0.64	0.64	0.62	0.63	0.64	0.64
A_o	9.54	9.77	9.83	9.88	9.70	9.88	9.89	9.90	9.69	9.88	9.88	9.89
B_o	0.63	0.66	0.67	0.68	0.66	0.68	0.68	0.68	0.66	0.68	0.68	0.68
C_o	0.59	0.62	0.63	0.63	0.61	0.63	0.63	0.63	0.61	0.63	0.63	0.63
α_1^A	0.3167	0.3090	0.3045	0.3026	0.3094	0.3069	0.3057	0.3016	0.2993	0.3040	0.3048	0.3016
α_2^A	-0.1358	-0.1116	-0.1066	-0.1002	-0.1367	-0.1022	-0.1001	-0.0985	-0.1194	-0.0984	-0.0986	-0.0973
α_3^A	-0.0231	-0.0481	-0.0547	-0.0638	-0.0270	-0.0616	-0.0630	-0.0663	-0.0434	-0.0649	-0.0644	-0.0668
α_1^B	-0.0021	-0.0017	-0.0016	-0.0015	-0.0019	-0.0015	-0.0015	-0.0014	-0.0016	-0.0015	-0.0015	-0.0014
α_2^B	0.0004	0.0011	0.0013	0.0015	0.0004	0.0015	0.0015	0.0016	0.0008	0.0016	0.0016	0.0016
α_3^B	0.0054	0.0045	0.0042	0.0039	0.0055	0.0041	0.0039	0.0038	0.0045	0.0039	0.0039	0.0038
α_1^C	-0.0008	-0.0005	-0.0004	-0.0003	-0.0007	-0.0004	-0.0003	-0.0003	-0.0005	-0.0003	-0.0003	-0.0003
α_2^C	0.0014	0.0013	0.0013	0.0014	0.0012	0.0013	0.0013	0.0014	0.0014	0.0015	0.0014	0.0014
α_3^C	0.0065	0.0066	0.0066	0.0066	0.0069	0.0067	0.0066	0.0066	0.0063	0.0065	0.0065	0.0065

Table 9.10 Calculated spectroscopic constants for HSO using B3PW91 in combination with cc-pV*x*Z, cc-pV(*x*+*d*)Z, and aug-cc-pV(*x*+*d*)Z.

	cc-pV*x*Z				cc-pV(*x*+*d*)Z				aug-cc-pV(*x*+*d*)Z			
B3PW91	D	T	Q	5	D	T	Q	5	D	T	Q	5
X_{11}	-86.4	-76.4	-71.6	-70.2	-84.0	-72.2	-69.3	-69.6	-78.4	-70.6	-68.6	-69.5
X_{12}	-14.0	-7.5	-5.3	-3.1	-11.2	-4.6	-3.7	-2.9	-7.5	-4.3	-3.7	-2.9
X_{13}	6.0	3.0	4.5	6.5	6.2	3.7	5.0	6.3	5.5	3.6	5.2	6.3
X_{22}	-1.6	-3.2	-3.3	-3.5	-1.5	-3.6	-3.6	-3.6	-2.4	-3.7	-3.6	-3.6
X_{23}	-7.9	-9.8	-9.0	-7.2	-7.8	-9.2	-8.2	-7.4	-6.8	-8.5	-8.2	-7.3
X_{33}	-5.7	-4.3	-3.6	-2.4	-6.0	-3.7	-3.1	-2.4	-3.6	-3.1	-3.0	-2.4
A_e	9.67	9.85	9.92	9.96	9.80	9.95	9.97	9.98	9.80	9.96	9.97	9.98
B_e	0.64	0.67	0.68	0.68	0.66	0.68	0.69	0.69	0.66	0.68	0.69	0.69
C_e	0.60	0.63	0.64	0.64	0.62	0.64	0.64	0.64	0.62	0.64	0.64	0.64
A_o	9.59	9.78	9.85	9.90	9.73	9.88	9.91	9.91	9.74	9.90	9.91	9.91
B_o	0.64	0.67	0.68	0.68	0.66	0.68	0.68	0.68	0.66	0.68	0.68	0.68
C_o	0.60	0.62	0.63	0.64	0.62	0.64	0.64	0.64	0.62	0.63	0.64	0.64
α_1^A	0.3073	0.3013	0.2966	0.2943	0.3018	0.2984	0.2969	0.2935	0.2889	0.2955	0.2962	0.2933
α_2^A	-0.1256	-0.0860	-0.0792	-0.0710	-0.1219	-0.0729	-0.0707	-0.0686	-0.0977	-0.0694	-0.0701	-0.0682
α_3^A	-0.0365	-0.0761	-0.0856	-0.0960	-0.0429	-0.0923	-0.0961	-0.0990	-0.0697	-0.0971	-0.0969	-0.0994
α_1^B	-0.0019	-0.0015	-0.0014	-0.0014	-0.0017	-0.0014	-0.0014	-0.0013	-0.0015	-0.0013	-0.0013	-0.0013
α_2^B	0.0007	0.0020	0.0023	0.0026	0.0008	0.0025	0.0026	0.0027	0.0016	0.0026	0.0026	0.0027
α_3^B	0.0049	0.0033	0.0030	0.0026	0.0048	0.0028	0.0026	0.0025	0.0035	0.0025	0.0026	0.0025
α_1^C	-0.0007	-0.0004	-0.0003	-0.0002	-0.0006	-0.0003	-0.0002	-0.0002	-0.0004	-0.0002	-0.0002	-0.0002
α_2^C	0.0014	0.0016	0.0016	0.0018	0.0012	0.0017	0.0017	0.0018	0.0015	0.0018	0.0018	0.0018
α_3^C	0.0065	0.0062	0.0061	0.0060	0.0068	0.0061	0.0060	0.0059	0.0060	0.0059	0.0059	0.0059

Table 9.11 Calculated spectroscopic constants for HSO using PBE in combination with cc-pV*x*Z, cc-pV(*x*+*d*)Z, and aug-cc-pV(*x*+*d*)Z.

	cc-pV*x*Z				cc-pV(*x*+*d*)Z				aug-cc-pV(*x*+*d*)Z			
PBE	D	T	Q	5	D	T	Q	5	D	T	Q	5
X_{11}	-90.6	-95.2	-96.7	-98.8	-96.9	-96.4	-97.4	-99.3	-99.6	-96.1	-96.8	-99.1
X_{12}	-31.8	-15.3	-12.6	-10.7	-31.5	-12.3	-10.6	-10.3	-18.4	-11.6	-10.5	-10.2
X_{13}	-4.7	-11.5	-11.1	-11.8	-7.4	-14.5	-13.1	-12.4	-8.6	-12.4	-11.7	-12.2
X_{22}	-1.5	-3.6	-3.6	-3.9	-2.8	-4.3	-4.1	-4.1	-2.2	-4.0	-4.0	-4.1
X_{23}	-8.3	-10.7	-8.5	-7.5	-12.4	-11.2	-8.3	-7.9	-4.7	-9.1	-8.0	-7.7
X_{33}	-5.7	-5.0	-3.6	-2.7	-7.1	-5.1	-3.2	-2.9	-3.1	-3.8	-2.9	-2.7
A_e	9.45	9.65	9.70	9.74	9.59	9.74	9.76	9.75	9.58	9.74	9.76	9.75
B_e	0.63	0.66	0.66	0.67	0.65	0.67	0.67	0.67	0.65	0.67	0.67	0.67
C_e	0.59	0.61	0.62	0.63	0.61	0.62	0.63	0.63	0.61	0.62	0.63	0.63
A_o	9.35	9.55	9.61	9.66	9.50	9.65	9.67	9.67	9.50	9.66	9.67	9.67
B_o	0.63	0.65	0.66	0.67	0.65	0.66	0.67	0.67	0.65	0.66	0.67	0.67
C_o	0.59	0.61	0.62	0.62	0.60	0.62	0.62	0.62	0.60	0.62	0.62	0.62
α_1^A	0.3663	0.3468	0.3374	0.3330	0.3561	0.3401	0.3340	0.3321	0.3335	0.3335	0.3316	0.3311
α_2^A	-0.1179	-0.0786	-0.0721	-0.0652	-0.1136	-0.0668	-0.0634	-0.0633	-0.0917	-0.0670	-0.0645	-0.0629
α_3^A	-0.0394	-0.0816	-0.0912	-0.1006	-0.0466	-0.0966	-0.1023	-0.1028	-0.0749	-0.0978	-0.1017	-0.1034
α_1^B	-0.0019	-0.0015	-0.0014	-0.0013	-0.0016	-0.0014	-0.0013	-0.0013	-0.0015	-0.0014	-0.0013	-0.0013
α_2^B	0.0009	0.0023	0.0026	0.0028	0.0010	0.0028	0.0029	0.0029	0.0019	0.0028	0.0029	0.0029
α_3^B	0.0047	0.0030	0.0027	0.0023	0.0045	0.0025	0.0022	0.0022	0.0034	0.0024	0.0023	0.0022
α_1^C	-0.0005	-0.0002	-0.0001	-0.0001	-0.0003	-0.0001	-0.0001	-0.0001	-0.0002	-0.0001	-0.0001	-0.0001
α_2^C	0.0010	0.0014	0.0015	0.0016	0.0007	0.0015	0.0016	0.0016	0.0015	0.0017	0.0016	0.0017
α_3^C	0.0069	0.0064	0.0063	0.0061	0.0073	0.0063	0.0061	0.0061	0.0061	0.0061	0.0061	0.0060

9.4. Conclusions

The use of the cc-pV(*x*+*d*)Z and aug-cc-pV(*x*+*d*)Z basis sets in combination with B3LYP, B3PW91, and PBE for sulfur species such as HSO and HOS can be important, particularly for the lower level basis sets. For structures, the impact upon the bond lengths and angles of these structures is slight. However, the sets do enable a converged geometry to be ascertained using a lower level basis set. In terms of a description of the relative energies of the isomers, the tight *d* functions enable the correct prediction that HSO is more stable than HOS to occur with simply a double-zeta level basis set and yield a relative energy of HSO and HOS that is in good agreement with previous MRCI calculations by Xantheas and Dunning. For the enthalpy of formation, the tight *d*-augmented basis sets can have a significant impact upon the enthalpies, even for a quadruple-zeta level basis set. The level of impact seems to be heavily based upon reaction used to determine the enthalpy. Overall, the use of the cc-pV(*x*+*d*)Z and aug-cc-pV(*x*+*d*)Z basis sets is important in the determination of energetics, including thermochemical properties such as enthalpies, and is recommended, particularly when lower level basis sets will be employed.

REFERENCES

[1] THOMAS, L. H., 1927, *Proc. Camb. Phil. Soc.*, 23, 542.

[2] FERMI, E., 1927, *PRend. Accad. Lincei*, 6, 602.

[3] KOHN, W. and SHAM, L. J., 1965, *Phys. Rev. A*, 140, 1133.

[4] SLATER, J. C., 1951, *Phys. Rev.*, 81, 385.

[5] VOSKO, S. H., WILK, L. and NUSAIR, M., 1980, *Can. J. Phys.*, 58, 1200.

[6] BECKE, A. D., 1988, *Phys. Rev. A*, 38, 3098.

[7] LEE, C., YANG, W. and PARR, R. G., 1988, *Phys. Rev. B*, 37, 785.

[8] PERDEW, J. P., CHEVARY, J. A., VOSKO, S. H., JACKSON, K. A., PEDERSON, M. R., SINGH, D. J. and FIOLHAIS, C., 1992, *Phys. Rev. B*, 46

[9] PERDEW, J. P., 1986, *Phys. Rev. B*, 33, 8822.

[10] BECKE, A. D., 1993, *J. Chem. Phys.*, 98, 5648.

[11] HOHENBERG, P. and KOHN, W., 1964, *Phys. Rev. B*, 136, 864.

[12] ZHANG, Y. and YANG, W., 1998, *J. Chem. Phys.*, 109, 2604.

[13] GILL, P. M. W., JOHNSON, B. G., GONZALES, C. A. and POPLE, J. A., 1994, *Chem. Phys. Lett.*, 221, 100.

[14] POREZAG, D. and PEDERSON, M. R., 1995, *J. Chem. Phys.*, 102, 9345.

[15] DUNNING JR., T. H., 1989, *J. Chem. Phys.*, 90, 1007.

[16] PETERSON, K. A., 1997, *Spectrochim. Acta Part A*, 53, 1051.

[17] DUNNING JR., T. H., 2000, *J. Phys. Chem. A*, 104, 9062.

[18] FELLER, D., DIXON, D. A. and FRANCISCO, J. S., 2003, *J. Phys. Chem. A*, 107, 1064.

[19] KEMENY, A. E., FRANCISCO, J. S., DIXON, D. A. and FELLER, D., 2003, *J. Chem. Phys.*, 118, 8290.

[20] PAK, C., SARI, L., RIENSTRA-KIRACOFE, J. C., WESOLOWSKI, S. S., HORNY, L., YAMAGUCHI, Y. and SCHAEFER III, H. F., 2003, *J. Chem. Phys.*, 118, 7256.

[21] PERDEW, J. P., BURKE, K. and WANG, Y., 1996, *Phys. Rev. B*, 54, 16533.

[22] PERDEW, J. P., KURTH, S., ZUPAN, A. and BLAHA, P., 1999, *Phys. Rev. Lett.*, 82, 2544.

[23] PROFT, F. D., TIELENS, F. and GEERLINGS, P., 2000, *J. Mol. Struct. (Theochem)*, 506, 1.

[24] PROFT, F. D., MARTIN, J. M. and GEERLINGS, P., 1996, *Chem. Phys. Lett.*, 256, 400.

[25] SCHEINER, A. C., BAKER, J. and ANDZELM, J. W., 1997, *J. Comput. Chem.*, 18, 775.

[26] MARTIN, J. M., EL-YAZAL, J. and FRANCOIS, J. P., 1995, *Mol. Phys.*, 86, 1437.

[27] MARTELL, J. M. and GODDARD, J. D., 1997, *J. Phys. Chem.*, 101, 1927.

[28] GILL, P. M. W., JOHNSON, B. G., POPLE, J. A. and FRISCH, M. J., 1992, *Chem. Phys. Lett.*, 197, 499.

[29] MARTIN, J. M. L., 2000, In *Density Functional Theory: A Bridge Between Chemistry and Physics*, ed. P. Geerlings, F. De Proft and W. Langenaeker, pp. 111. Brussels: VUB Press

[30] GILL, P. M. W., JOHNSON, B. G., POPLE, J. A. and FRISCH, M. J., 1992, *Int. J. Quantum Chem. Symp.*, 26, 319.

[31] RAYMOND, K. S. and WHEELER, R. A., 1999, *J. Comp. Chem.*, 20, 207.

[32] DENIS, P. A. and VENTURA, O. N., 2000, *Int. J. Quantum Chem.*, 80, 439.

[33] SEKUSAK, S. and FRENKING, G., 2001, *J. Mol. Struct. (Theochem)*, 541, 17.

[34] BECKE, A. D., 1993, *J. Chem. Phys.*, 98, 1372.

[35] Gaussian 98, Revision A. 11, FRISCH, M. J., TRUCKS, G. W., SCHLEGEL, H. B., SCUSERIA, G. E., ROBB, M. A., CHEESEMAN, J. R., ZAKRZEWSKI, V. G., MONTGOMERY JR., J. A., STRATMANN, R. E., BURANT, J. C., DAPPRICH, S., MILLAM, J. M., DANIELS, A. D., KUDIN, K. N., STRAIN, M. C., FARKAS, O., TOMASI, J., BARONE, V., COSSI, M., CAMMI, R., MENNUCCI, B., POMELLI, C., ADAMO, C., CLIFFORD, S., OCHTERSKI, J., PETERSSON, G. A., AYALA, P. Y., CUI, Q., MOROKUMA, K., SALVADOR, P., DANNENBERG, J. J., MALICK, D. K., RABUCK, A. D., RAGHAVACHARI, K., FORESMAN, J. B., CIOSLOWSKI, J., ORTIZ, J. V., BABOUL, A. G., STEFANOV, B. B., LIU, G., LIASHENKO, A., PISKORZ, P., KOMAROMI, I., GOMPERTS, R., MARTIN, R. L., FOX, D. J., KEITH, T., AL-LAHAM, M. A., PENG, C. Y., NANAYAKKARA, A., CHALLACOMBE, M., GILL, P. M. W., JOHNSON, B., CHEN, M., WONG, M. W., ANDRES, J. L., GONZALEZ, C., HEAD-GORDON, M., REPLOGLE, E. S. and POPLE, J. A., Gaussian, Inc, Pittsburgh PA, 2001.

[36] FELLER, D., 1992, *J. Chem. Phys.*, 96, 6104.

[37] HALKIER, A., HELGAKER, T., JOGENSEN, P., KLOPPER, W., KOCH, H., OLSEN, J. and WILSON, A. K., 1998, *Chem. Phys. Lett.*, 286, 243.

[38] HERZBERG, G., 1966, *Electronic spectra and electronic structure of polyatomic molecules* (New York: Van Nostrand).

[39] HUBER, K. P. and HERZBERG, G., 1979, *Molecular Spectra and Molecular Structure. IV. Constants of Diatomic Molecules* (New York: Van Nostrand).

[40] OGILVIE, J. F., 1976, *J. Mol. Struct. (Theochem)*, 31, 407.

[41] KOPUT, J., 1986, *J. Mol. Spectrosc.*, 115, 438.

[42] GURVICH, L. V., VEYTS, I. V. and ALCOCK, C. B., 1989, *Thermodynamics Properties of Individual Substances* (New York: Hemisphere).

[43] TSUBOI, M. and OVEREND, J., 1974, *J. Mol. Spectrosc.*, 52, 256.

[44] DEMAISON, J., BREIDUNG, J., THIEL, W. and PAPOUSEK, D., 1999, *Struct. Chem.*, 10, 129.

[45] DAVIDSON, E. R., HAGSTROM, S. A., CHAKRAVORTY, S. J., UMAR, V. M. and FROESE, C., 1991, *Phys. Rev. A*, 44, 7071.

[46] 1998, *NIST-JANAF Thermochemical Tables, 4th Ed. J. Phys. Chem. Ref. Data Monograph 9*).

[47] WOON, D. E. and DUNNING JR., T. H., 1993, *J. Chem. Phys.*, 98, 1358.

[48] WOON, D. E. and DUNNING JR., T. H., 1995, *J. Chem. Phys.*, 103, 4572.

[49] WILSON, A. K., VAN MOURIK, T. and DUNNING JR., T. H., 1996, *J. Mol. Struct. (Theochem)*, 388, 339.

[50] WILSON, A. K., WOON, D. E., PETERSON, K. A. and DUNNING JR., T. H., 1999, *J. Chem. Phys.*, 110, 7667.

[51] VAN MOURIK, T. and DUNNING JR., T. H., 2000, *Int. J. Quantum Chem.*, 76, 205.

[52] DUNNING JR., T. H., PETERSON, K. A. and WILSON, A. K., 2001, *J. Chem. Phys.*, 114, 9244.

[53] PETERSON, K. A. and DUNNING JR., T. H., 2002, *J. Chem. Phys.*, 117, 10548.

[54] KENDALL, R. A., DUNNING JR., T. H. and HARRISON, R. J., 1992, *J. Chem. Phys.*, 96, 6796.

[55] PETERSON, K. A., FIGGEN, D., GOLL, E., STOLL, H. and DOLG, M., 2003, *J. Chem. Phys.*, 119, 11113.

[56] JENSEN, F., 2001, *J. Chem. Phys.*, 115, 9113.

[57] JENSEN, F., 2000, *Theor. Chim. Acta*, 104, 484.

[58] JENSEN, F., 2002, *J. Chem. Phys.*, 116, 7372.

[59] JENSEN, F., 2002, *J. Chem. Phys.*, 117, 9234.

[60] JENSEN, F., 2003, *J. Chem. Phys.*, 118, 2459.

[61] JENSEN, F. and HELGAKER, T., 2004, *J. Chem. Phys.*, 121, 3462.

[62] WANG, N. X. and WILSON, A. K., 2004, *J. Chem. Phys.*, 121, 7632.

[63] RAFFENETTI, R. C., 1973, *J. Chem. Phys.*, 58, 4452.

[64] DUIJNEVELDT, F. B., 1971, *IBM Tech. Res. Rep.*, RJ945.

[65] CLARK, T., CHANDRASEKHAR, J., SPITZNAGEL, G. W. and V. R. SCHLEYER, P., 1983, *J. Comput. Chem.*, 4, 294.

[66] DUNNING, T. H., 1970, *J. Chem. Phys.*, 53, 2823.

[67] COLE, L. A. and PERDEW, J. P., 1982, *Phys. Rev. A*, 25, 1265.

[68] ZIEGLER, T. and GUTSEV, G. L., 1992, *J. Comput. Chem.*, 13, 70.

[69] MILLER, D. M., ALLEN, W. D. and SCHAEFER III, H. F., 1996, *Molecular Physics*, 88, 727.

[70] GILL, P. M. W., JOHNSON, B. G., POPLE, J. A. and FRISCH, M. J., 1992, *Int. J. Quantum Chem., Quantum Chem. Symp*, 26, 319.

[71] SCHWARZ, K., 1978, *J. Phys. B*, 11, 1339.

[72] SCHWARZ, K., 1978, *Chem. Phys. Lett.*, 57, 605.

[73] SHORE, H. B., ROSE, J. H. and ZAREMBA, E., 1977, *Phys. Rev. B*, 15, 2858.

[74] PERDEW, J. P., 1979, *Chem. Phys. Lett.*, 64, 127.

[75] ZUNGER, A., PERDEW, J. P. and OLIVER, G. L., 1980, *Solid State Commun.*, 34, 933.

[76] GALBRAITH, J. M. and SCHAEFER III, H. F., 1996, *J. Chem. Phys.*, 105, 862.

[77] JARECKI, A. A. and DAVIDSON, E. R., 1999, *Chem. Phys. Lett.*, 300, 44.

[78] RIENSTRA-KIRACOFE, J. C., GRAHAM, R. G. and SCHAEFER III, H. F., 1998, *Mol. Phys.*, 94, 767.

[79] CURTISS, L. A., REDFERN, P. C., RAGHAVACHARI, K. and POPLE, J. A., 1998, *J. Chem. Phys.*, 109, 42.

[80] RIENSTRA-KIRACOFE, J. C., TSCHUMPER, G. S., SCHAEFER III, H. F., NANADI, S. and ELLISON, G. B., 2002, *Chem. Rev.*, 102, 231.

[81] LIU, B. and MCLEAN, A. D., 1973, *J. Chem. Phys.*, 59, 4557.

[82] BOYS, S. F. and BERNARDI, F., 1970, *Mol. Phys.*, 19, 553.

[83] VAN DUIJNEVELDT, F. B., VAN DUIJNEVELDT-VAN DE RIJDT, J. G. C. M. and VAN LENTHE, J. H., 1994, *Chem. Rev.*, 94, 1873.

[84] CULLEN, J. M., 1991, *Int. J. Quant. Chem. Symp.*, 23, 193.

[85] MAYER, I., SURJAN, P. J. and VIBOK, A., 1989, *Int. J. Quant. Chem. Symp.*, 23, 281.

[86] MAYER, I. and SURJAN, P. R., 1989, *Int. J. Quant. Chem.*, 36, 225.

[87] MAYER, I. and VIBOK, A., 1991, *Int. J. Quant. Chem.*, 40, 139.

[88] NOGA, J. and VIBOK, A., 1991, *Chem. Phys. Lett.*, 180, 114.

[89] SADLEJ, A. J., 1991, *J. Chem. Phys.*, 95, 6707.

[90] VALIRON, P., VIBOK, A. and MAYER, I., 1993, *J. Comput. Chem.*, 14, 401.

[91] VIBOK, A. and MAYER, I., 1992, *Int. J. Quant. Chem.*, 43, 801.

[92] GUTOWSKI, M. and CHALASINSKI, G., 1993, *J. Chem. Phys.*, 98, 5540.

[93] FEYEREISEN, M. W., FELLER, D. and DIXON, D. A., 1996, *J. Phys. Chem.*, 100, 2993.

[94] JENSEN, F., 1996, *Chem. Phys. Lett.*, 261, 633.

[95] PETERSON, K. A. and DUNNING JR., T. H., 1995, *J. Chem. Phys.*, 102, 2032.

[96] WOON, D. E., 1993, *Chem. Phys. Lett.*, 204, 29.

[97] WOON, D. E., 1994, *J. CHem. Phys.*, 100, 2838.

[98] WOON, D. E., DUNNING JR., T. H. and PETERSON, K. A., 1996, *J. Chem. Phys.*, 104, 5883.

[99] XANTHEAS, S. S., 1996, *J. Chem. Phys.*, 104, 8821.

[100] RAPPE, A. K. and BERNSTEIN, E. R., 2000, *J. Phys. Chem. A*, 104, 6117.

[101] VAN MOURIK, T. and DUNNING JR., T. H., 1997, *J. Chem. Phys.*, 107, 2451.

[102] VAN MOURIK, T., WILSON, A. K., PETERSON, K. A., WOON, D. E. and DUNNING JR., T. H., 1999, *Adv. Quantum Chem.*, 31, 105.

[103] DEMAISON, J., MARGULES, L. and BOGGS, J. E., 2003, *Phys. Chem. Chem. Phys.*, 5, 3359.

[104] WANG, D., SHI, Q. and ZHU, Q.-S., 2000, *J. Chem. Phys.*, 112, 9624.

[105] KUCHARSKI, S., KOLASKI, M. and BARTLETT, R. J., 2001, *J. Chem. Phys.*, 114, 692.

[106] WHEELER, S. E., SATTELMEYER, K. W., SCHLEYER, P. R. and SCHAEFER III, H. F., 2004, *J. Chem. Phys.*, 120, 4683.

[107] MARENICH, A. V. and BOGGS, J. E., 2003, *J. Phys. Chem. A*, 107, 2343.

[108] BRINKMANN, N. R., RICHARDSON, N. A., WESOLOWSKI, S. S., YAMAGUCHI, Y. and SCHAEFER III, H. F., 2002, *Chem. Phys. Lett.*, 352, 505.

[109] KUPKA, T., KOLASKI, M., PASTERNA, G. and RUUD, K., 1999, *Journal of Molecular Structure (Theochem)*, 467, 63.

[110] LEE, J. S., 2003, *Phys. Rev. A*, 68, 043201.

[111] LUTNAES, O. B., RUDEN, T. A. and HELGAKER, T., 2004, *Magn. Reson. Chem.*, 42, S117.

[112] BRINKMANN, N. R. and CARMICHAEL, I., 2004, *J. Phys. Chem. A*, 108, 9390.

[113] KUPKA, T., RUSCIC, B. and BOTTO, R., 2003, *Solid State Nucl. Magn. Reson.*, 23, 145.

[114] SWART, M. and SNIJDERS, J. G., 2003, *Theor. Chem. Acc.*, 110, 34.

[115] BAUSCHLICHER, C. W. and PARTRIDGE, H., 1995, *Chem. Phys. Lett.*, 240, 533.

[116] MARTIN, J. M. L., 1998, *J. Chem. Phys.*, 108, 2791.

[117] MARTIN, J. M. L. and UZAN, O., 1998, *Chem. Phys. Lett.*, 282, 16.

[118] BAUSCHLICHER, C. W. and RICCA, A., 1998, *J. Phys. Chem. A*, 102, 8044.

[119] WILSON, A. K. and DUNNING JR., T. H., 2004, *J. Phys. Chem. A*, 108, 3129.

[120] WILSON, A. K. and DUNNING JR., T. H., 2003, *J. Chem. Phys.*, 119, 11712.

[121] BELL, R. D. and WILSON, A. K., 2004, *Chem. Phys. Lett.*, 394, 105.

[122] YOCKEL, S., MINTZ, B. and WILSON, A. K., 2004, *Journal of Chemical Physics*, 121, 60.

[123] DENIS, P. A., VENTURA, O. N., MAI, H. T. and NGUYEN, M. T., 2004, *J. Phys. Chem. A*, 108, 5073.

[124] DENIS, P. A., 2003, *Chemical Physics Letters*, 382, 65.

[125] DENIS, P. A., 2005, *Chem. Phys. Lett.*, 402, 289.

[126] DIXON, D. A. and PETERSON, K. A., 2001, *J. Chem. Phys.*, 115, 6327.

[127] CURTISS, L. A., RAGHAVACHARI, K., TRUCKS, G. W. and POPLE, J. A., 1991, *J. Chem. Phys.*, 94, 7221.

[128] CHASE JR., M. W., DAVIES, C. A., DOWNEY JR., J. R., FRURIP, D. J., MCDONALD, R. A. and SYVERUD, A. N., 1985, *J. Phys. Chem. Ref. Data 14, Suppl. No. 1 (1985)*,

[129] JESINGER, R. A. and SQUIRES, R. R., 1999, *Int. J. Mass. Spectrom.*, 185, 745.

[130] PETERSON, K. A., 2003, *J. Chem. Phys.*, 119, 11099.

[131] DUNNING JR., T. H., PETERSON, K. A. and WILSON, A. K., 2001, *J. Chem. Phys.*, 114, 9244.

[132] LUKE, B. T. and MCLEAN, A. D., 1985, *J. Phys. Chem.*, 89, 4592.

[133] MOORE PLUMMER, P. L., 1990, *J. Chem. Phys.*, 92, 6627.

[134] SANNIGRAHI, A. B., THUNEMANN, K. H., PEYERIMHOFF, S. D. and BUENKER, R. J., 1977, *J. Chem. Phys.*, 20, 55.

[135] SANNIGRAHI, A. B., PEYERIMHOFF, S. D. and BUENKER, R. J., 1977, *J. Chem. Phys.*, 20, 381.

[136] SLAGLE, I. R., GRAHAM, R. G. and GUTMAN, D., 1976, *Int. J. Chem. Kinet.*, 8, 451.

[137] KAWASAKI, M., KASATANI, K., TANAHASHI, S., SATO, H. and FUJIMURA, Y., 1983, *J. Chem. Phys.*, 78, 7146.

[138] XANTHEAS, S. S. and DUNNING JR., T. H., 1993, *J. Phys. Chem.*, 97, 18.

[139] XANTHEAS, S. S. and DUNNING JR., T. H., 1993, *J. Phys. Chem.*, 97, 6616.

[140] DECKER, B. K., ADAMS, N. G., BABCOCK, L. M., CRAWFORD, T. D. and SCHAEFER III, H. F., 2000, *J. Phys. Chem. A*, 104, 4636.

[141] GOUMRI, A., LAAKSO, D., ROCHA, J. R., SMITH, C. E. and MARSHALL, P., 1995, *J. Chem. Phys.*, 102, 161.

[142] ESSEFFAR, M., MO, O. and YANEZ, M., 1994, *J. Chem. Phys.*, 101, 2175.

[143] WILSON, C. and HIRST, D. M., 1994, *J. Chem. Soc. Faraday Trans.*, 90, 3051.

[144] MARTINEZ-NUNEZ, E., VAZQUEZ, S. A. and VARANDAS, A. J. C., 2002, *Phys. Chem. Chem. Phys.*, 4, 279.

[145] MARTINEZ-NUNEZ, E. and VARANDAS, A. J. C., 2001, *J. Phys. Chem. A*, 105, 5923.

[146] BADENES, M. P., TUCCERI, M. E. and COBOS, C. J. Z., 2000, *Phys. Chem.*, 214, 1193.

[147] DENIS, P. A. and VENTURA, O. N., 2001, *Chem. Phys. Lett.*, 344, 221.

[148] BALUCANI, N., STRANGES, D., CASAVECCHIA, P. and VOLPI, G. G., 2004, *J. Chem. Phys.*, 120, 9571.

[149] BECKE, A. D., 1993, *J. Chem. Phys.*, 98, 5648.

[150] PERDEW, J. P., CHEVARY, J. A., VOSKO, S. H., JACKSON, K. A., PEDERSON, M. R., SINGH, D. J. and FIOLHAS, C., 1992, *Phys. Rev. B*, 46, 6671.

[151] PERDEW, J. P., BURKE, K. and ERNZERHOF, M., 1996, *Phys. Rev. Lett.*, 77, 3865.

[152] PERDEW, J. P., BURKE, K. and ERNZERHOF, M., 1997, *Phys. Rev. Lett.*, 78, 1396.

[153] Gaussian 03, Revison C.02, FRISCH, M. J., TRUCKS, G. W., SCHLEGEL, H. B., SCUSERIA, G. E., ROBB, M. A., CHEESEMAN, J. R., MONTGOMERY, J., J. A., VREVEN, T., KUDIN, K. N., BURANT, J. C., MILLAM, J. M., IYENGAR, S. S., TOMASI, J., BARONE, V., MENNUCCI, B., COSSI, M., SCALMANI, G., REGA, N., PETERSSON, G. A., NAKATSUJI, H., HADA, M., EHARA, M., TOYOTA, K., FUKUDA, R., HASEGAWA, J., ISHIDA, M., NAKAJIMA, T., HONDA, Y., KITAO, O., NAKAI, H., KLENE, M., LI, X., KNOX, J. E., HRATCHIAN, H. P., CROSS, J. B., BAKKEN, V., ADAMO, C., JARAMILLO, J., GOMPERTS, R., STRATMANN, R. E., YAZYEV, O., AUSTIN, A. J., CAMMI, R., POMELLI, C., OCHTERSKI, J. W., AYALA, P. Y., MOROKUMA, K., VOTH, G. A., SALVADOR, P., DANNENBERG, J. J., ZAKRZEWSKI, V. G., DAPPRICH, S., DANIELS, A. D., STRAIN, M. C., FARKAS, O., MALICK, D. K., RABUCK, A. D., RAGHAVACHARI, K., FORESMAN, J. B., ORTIZ, J. V., CUI, Q., BABOUL, A. G., CLIFFORD, S., CIOSLOWSKI, J., STEFANOV, B. B., LIU, G., LIASHENKO, A., PISKORZ, P., KOMAROMI, I., MARTIN, R. L., FOX, D. J., KEITH, T., AL-LAHAM, M. A., PENG, C. Y., NANAYAKKARA, A., CHALLACOMBE, M., GILL, P. M. W., JOHNSON, B., CHEN, W., WONG, M. W., GONZALEZ, C. and POPLE, J. A., Gaussian, Inc., Wallingford CT, 2004.

[154] CLABO, D. A., ALLEN, W. D., REMINGTON, R. B., YAMAGUCHI, Y. and SCHAEFER III, H. F., 1988, *Chem. Phys.*, 123, 187.

[155] MILLER, W. H., HANDY, N. C. and ADAMS, J. E., 1980, *J. Chem. Phys.*, 72, 99.

[156] PAGE, M. and MCIVER JR., J. W., 1988, *J. Chem. Phys.*, 88, 922.

[157] PAGE, M., DOUBLEDAY, C. and MCIVER JR., J. W., 1990, *J. Chem. Phys.*, 93, 5634.

[158] SENEKOWITSCH, J., 1988: Ph.D. thesis, Universität Frankfurt, Germany

[159] KUPKA, T., RUSCIC, B. and BOTTO, R. E., 2002, *J. Phys. Chem. A*, 106, 10396.

[160] OHASHI, N., KAKIMOTO, M., SAITO, S. and HIROTA, E., 1980, *J. Mol. Spectrosc.*, 84, 204.

[161] SCHURATH, U., WEBER, M. and BECKER, K. H., 1977, *J. Chem. Phys.*, 67, 110.

[162] DAVIDSON, F. E., CLEMO, A. R., DUNCAN, D. L., BROWET, R. J., HOBSON, J. H. and GRICE, R., 1985, *Mol. Phys.*, 46, 33.

[163] BALUCANI, N., CASAVECCHIA, P., STRANGES, D. and VOLPI, G. G., 1993, *Chem. Phys. Lett.*, 211, 469.

[164] XU, X. and GODDARD, W. A., 2004, *J. Chem. Phys.*, 121, 4068.

[165] RABUCK, A. D. and SCUSERIA, G. E., 1999, *Chem. Phys. Lett.*, 309, 450.